2016

Engine Vibration of a Compressed Natural Gas Engine as an effect of Combustion

Scott Hunt
University of Windsor

Engine Vibration of a Compressed Natural Gas Engine as an Effect of Combustion

By

Scott Hunt

A Thesis
Submitted to the Faculty of Graduate Studies
through the Department of Mechanical, Automotive and Materials Engineering
in Partial Fulfillment of the Requirements for
the Degree of Master of Applied Science
at the University of Windsor

Windsor, Ontario, Canada

2016

Engine Vibration of a Compressed Natural Gas Engine as an Effect of Combustion

by

Scott Hunt

APPROVED BY:

_____

Dr. M Mirhassani
Department of Electrical and Computer Engineering

_____

Dr. R Gaspar

Department of Mechanical, Automotive and Materials Engineering

_____

Dr. C Novak, Advisor

Department of Mechanical, Automotive and Materials Engineering

May 20, 2016

DECLARATION OF ORIGINALITY

I hereby certify that I am the sole author of this thesis and that no part of this thesis has been published or submitted for publication.

I certify that, to the best of my knowledge, my thesis does not infringe upon anyone's copyright nor violate any proprietary rights and that any ideas, techniques, quotations, or any other material from the work of other people included in my thesis, published or otherwise, are fully acknowledged in accordance with the standard referencing practices. Furthermore, to the extent that I have included copyrighted material that surpasses the bounds of fair dealing within the meaning of the Canada Copyright Act, I certify that I have obtained a written permission from the copyright owner(s) to include such material(s) in my thesis and have included copies of such copyright clearances to my appendix.

I declare that this is a true copy of my thesis, including any final revisions, as approved by my thesis committee and the Graduate Studies office, and that this thesis has not been submitted for a higher degree to any other University or Institution.

ABSTRACT

In the medium to heavy duty truck market there is an increased interest to convert diesel engines currently in use to operate on compressed natural gas (CNG). For CNG to be a viable fuel for this application, it must also provide similar or improved performance characteristics compared to diesel. One such parameter is the noise and vibration output of the engine. This study investigated the relationship between the combustion pressure of a CNG engine and vibration at the engine mount locations. Multiple analysis methods for quantifying the vibration and combustion pressure were investigated to determine which provided the best data correlation. Although similar correlation trends were found with all of the analysis methods, the overall displacement provided a linear relationship with the average maximum pressure of combustion for conditions where the vibration resulting from combustion exceeded the inherent mechanical vibration. Recommendations for improvements to the test methodology are also provided.

ACKNOWLEDGEMENTS

I would like to thank Dr. Colin Novak for his encouragement and guidance throughout the course of my graduate program. Without his support and understanding this would not have been possible. I would also like to extend gratitude to my committee members, Dr. Robert Gaspar and Dr. Mitra Mirhassani for their time and assistance.

I would also like to thank Pete Peterson of North American Repower as well as Andrew Bosscher, Justin Lair and Dan Archer at McLaren for providing the engine and test facility as well as the time and resources required to support an engine test of this nature. In addition to the provided resources for testing, thanks to the NAR and McLaren for allowing data collected during this project to be released for use in this thesis resulting in completion of my graduate program.

Special thanks to my employer, Brüel & Kjær, for their support of this project. Brüel & Kjær provided the vibration transducers, data acquisition system as well as all of the analysis software. To list the names of each individual at B&K who supported or encouraged this activity would take an entire page, so a simple thank you must suffice.

Many others deserve thanks for their support of this project by answering many of my questions directly and personally. I would like to extend my gratitude to Thomas Reinhart, Dr. In-Soo Suh, Ed Green, Eric Frank and Emerald Simmons for the information and clarification you have all provided.

Finally, I would like to thank my wife, Andrea, for all of the support during the late nights and long weekends as I worked on this thesis. Also for her help proofreading and editing this paper allowing for my thoughts to come out on paper in legible manner.

Again…. Thank you all!

TABLE OF CONTENTS

LIST OF TABLES

LIST OF FIGURES

LIST OF APPENDICES

NOMENCLATURE

NEPA	National Energy Policy Act
NAR	North American Repower
CNG	compressed natural gas
NVH	noise, vibration and harshness
Dyno	dynamometer
TPA	transfer path analysis
SPC	source path contribution
$P_{receiver,acoustic}$	noise at receiver due to acoustic path
$P_{receiver,structure}$	noise at receiver due to structure path
$P_{receiver}$	total noise at receiver
Q	acoustic source strength
F	structural source strength
P/Q	frequency response function between receiver and acoustic source
P/F	frequency response function between receiver and vibration source
FRF	frequency response function
SPL	sound pressure level
Hz	Hertz (1 cycle per second)
TN	total engine noise
MN	engine mechanical noise
CEC	combustion excitation content of total noise
iMN	increase in mechanical noise due to combustion
deg	angular degree
Pmax	maximum peak pressure
MPRR	maximum pressure rise rate
WOT	wide open throttle
rpm	revolutions per minute
TDC	top dead center
BTDC	before top dead center
CNI	combustion Noise Index
dB	decibel
mg	milligram
R	coefficient of correlation for Combustion Noise Index
FFT	fast Fourier transform
a	acceleration
v	velocity
d	displacement
f	frequency
P-V	pressure vs volume
psi	pounds per square inch
µs	microseconds
m/s^2	meters per second squared
OAL	overall level
CPB	constant percentage bandwidth
DFT	discreet Fourier transform

G(f)	frequency spectrum
g(t)	time signal
f	frequency (Hz)
j	$\sqrt{(-1)}$
t	time (sec)
N	total # of points in transform, block size
n	individual transform point
k	frequency index
hp	horsepower
ft-lb	foot pound
Nm	newton meter
EPA	Environmental Protection Agency
ecm	engine control module
RSS	root sum square
x	x axis
y	y axis
z	z axis
S_x	standard deviation of the data set
x	individual test result
$\bar{x}$	mean value of test results
n	Number of sample
CI	confidence interval

- -

CHAPTER 1: INTRODUCTION

Throughout human history, people have needed to trade the goods and services that are readily available where they live for other goods and services available elsewhere. Along with the need for trade comes the need for transportation. We have used, and continue to use, various means of transportation (ship, rail, air, etc.), however for the past 100 years, the internal combustion engine has made truck transportation a very effective and popular means to move products from point A to point B. Typically, diesel engines are used in medium and heavy-duty service truck applications. In the United States, federal regulatory policies resulting from the implementation of the National Energy Policy Act (NEPA) will encourage the adoption and use of alternative fueled vehicles [1]. In an effort to meet this criteria, fleet vehicle operators are moving toward using alternative fuels to power their vehicles as an alternative to diesel. Rather than replacing the vehicle's entire powertrain with an alternative energy source, many opt to convert the existing engine to operate on alternative and less costly fuels.

North American Repower (NAR), based out of San Diego, California, is a clean-tech company that specializes in compressed natural gas (CNG) fuel engine technology. Rather than develop a complete CNG engine from scratch, they specialize in the modification of existing diesel engines to operate on CNG. These retro fit kits give truck fleet owners a cost-effective alternative to purchasing an entirely new CNG engine.

In order to be a suitable replacement for its diesel counterpart, a CNG engine must be able to deliver the same or improved performance in every aspect. This includes not only power-torque output and operating costs, but also noise and vibration performance.

Noise and vibration characteristics are becoming increasingly important as a part of product development and customer perception, as the development and tuning of a vehicle powertrain mounting system is an essential ingredient to vehicle NVH characteristics [2]. Given that an engine configuration can be used in many vehicles, vibration level at the engine mounts is a useful tool for proper engine calibration and engine mount selection for the customer. It is also a reliable indicator for operator comfort, as the engine mount is an integral component of the vibration transfer path from the vibration source (engine) to the receiver (the operator) [3].

NAR has enlisted the support of McLaren Performance Technologies (Livonia, Michigan) to participate in the development of a CNG conversion kit for the International DT-466 engine line. Operating engine tests were performed at the McLaren engine dynamometer test facility including calibration, component evaluation, and durability. Engine vibration and cylinder pressures were also evaluated during the development process. However, due to the nature of the project, there were several situations where either the vibration or the cylinder pressure data could not be acquired.

Previous studies have shown relationships between engine noise or vibration and cylinder pressure at combustion. These previous studies focused more on traditional fuels such as gasoline and diesel rather than compressed natural gas. The ability to better understand the relationship between cylinder pressure at combustion and engine vibration would allow for the calculation of one from the measured results of the other. If combustion pressure could be calculated from engine vibration when cylinder pressure data is not available, the need to instrument pressure transducers in the cylinder head would be reduced or eliminated. Likewise, if engine vibration could be calculated based on the

measured combustion pressure, it would allow for an estimation of mount vibration into the vehicle without actual vibration measurement data. Both possibilities would save valuable time during vehicle design and testing.

This study investigates the relationship between engine mount vibration and cylinder pressure at combustion in a compressed natural gas engine. In addition, the question of which analysis method is best suited for this type of comparison is addressed.

The layout of this thesis is as follows. Chapter 2 is a review of available literature discussing the human perception of engine noise and vibration, as well as an understanding of how the noise and vibration produced by the engine reaches the occupants of the vehicle. This is followed by a discussion of the relationship between combustion pressure to both engine noise and vibration, and finally a look into both cycle-to-cycle and cylinder-to-cylinder variations in cylinder pressure. Chapter 3 reviews the theory regarding the analysis methods that will be used for data analysis. Chapter 4 details the experimental setup and test procedures used in the data acquisition portion of the measurement. Analysis of the data is provided in chapter 5, followed by a discussion of the results in chapter 6. Finally, the conclusions and recommendations are discussed in chapter 7.

CHAPTER 2: LITERATURE STUDY

The internal combustion engine has been around for well over 100 years, and over the course its history a great deal of research has been undertaken to understand and make advancements to their design. Given this, there are a considerable number of papers available for review on all subject maters regarding engines and the vehicles powered by them. This chapter will review some of the literature which is more directly related to the scope of the combustion of the CNG engine and how it may or may not correlate with the vibration of the engine.

There are many aspects to what is important regarding an engine's integration into a vehicle and how it is perceived by the operator. Since the engine that is being studied for this research was originally a diesel engine that has been converted to CNG, there are obvious areas of concern that an integrator might have selecting this engine as the power plant for a vehicle. Will the vehicle occupants find any unpleasant NVH issues with the engine? How does CNG compare with Diesel? What is the correlation between combustion and the NVH of the engine? There are answers to these questions as they relate to diesel and gasoline fueled engines, however there is little information regarding the same for CNG fueled engines. From the literature available that do show relation any between the NVH characteristics and the combustion forces of the engine, these tend to focus on noise rather than vibration. As the primary scope of this study is to investigate engine vibration resulting from combustion using CNG fuel, there is very little information available regarding that subject.

2.1 NVH Perception

Regardless of how well an engine performs regarding its designed intent, if it does not sound or feel right the operator and/or the bystander can have a negative perception of the product. The level of discontentment based on the NVH characteristics of a product could be very mild to severe enough that government imposed regulations are enacted to control the effect on the community. Vehicle manufacturers give much focus to understanding and fulfilling customer's NVH expectations as well as meeting the government regulations that they fall under. Of course noise is always a concern for both the operator and the community as it is airborne and can be detected at significant distance from the machine. Vibration is also a concern as the operator and the occupants of the vehicle can detect it through physical contact with their body.

2.1.1 Noise Annoyance Comparison between Ethanol and Diesel Engines

As previously noted, most heavy duty vehicles are powered by diesel engines. The demands from society are continuing to increase the demand for greater reduction of noise and air pollution from these vehicles. Diesel engine manufacturers are continually striving to improve their products performance in this regard. However, vehicle manufacturers are not opposed to investigating alternatives to the traditional choice of the diesel engine to provide power for their product. A study at Luleå University of Technology by Khan, Johansson and Sundbäck investigated the annoyance of response of engine noise between an ethanol and a diesel engine [4].

The focus of this study was aimed at determining if there is any notable difference in annoyance response between ethanol and diesel engines, as well as identify the parameters that describe the annoyance response. Two 11-liter diesel engines were used, with one of the engines modified to operate using ethanol as its fuel. The engines were operated in a hemi-anechoic dynamometer (dyno) cell under the same operating conditions. Recordings were made using microphones located in front of the engine at a distance of one meter from the center line of the engine and at a one-meter elevation above the floor.

A jury study was organized using 12 subjects, each giving a subjective rating the "annoyance level" of each condition on a scale as the sound recordings of the two engines were played. These subjective values, along with objective sound quality metrics such as loudness, impulsiveness, roughness, sharpness, etc. were used to develop a model for the annoyance response [4]. It was found that the annoyance response increased as engine speed increased. It was also found that annoyance response between the ethanol and diesel engine was not significantly different.

Relating this back to this research, CNG and ethanol fueled engines both use spark induced combustion as compared to the diesel engine which relies on the increased pressure and temperature in the cylinder to ignite the fuel mixture. Since the annoyance response of a diesel engine that was converted to run on ethanol was not significantly different between the two from an acoustic perspective, there is a distinct possibility the same can be true for an engine that operates on CNG.

2.1.2 The Influence of Vibrations on Perception

Diesel engines have historically received a bad perception in regard to NVH performance compared to their gasoline counterparts. Most notably diesels engines have been described as “Rough”, “Loud” and “Clattery”. A study performed by Renault and Ircam [5] investigated the influence of vibrations on the diesel character rating of an engine. For this study, survey participants were asked to rate the “diesel-ness” of 3 different cars on a scale from 0 to 1 based on their own experience of what a diesel engine is like versus what a gasoline engine is like.

The participants were seated in a simulation bench that was equipped with a steering wheel and a car seat. Shakers were attached to the test bench to reproduce the vehicle vibrations in all three axes on the steering wheel and the platform. Headphones were provided for the audio playback. Six different operating conditions of the three different cars were replayed to each of the participants, which were seated in the driving position with both hands on the steering wheel. One set of stimulus was only the acoustic data played back through the headphones, while the other set had both the acoustic sounds and the vibration applied to the platform.

The results of the survey showed that the ranking of diesel-ness increases as vibration is introduced into the experience. The graphs below (Figure 1) show each of the three vehicles for each of the driving conditions. The blue line, labeled A, is the acoustic only ratings, while the pink line, labeled VA, is the ratings with the subject experiencing both the vibration and acoustic inputs at the same time.

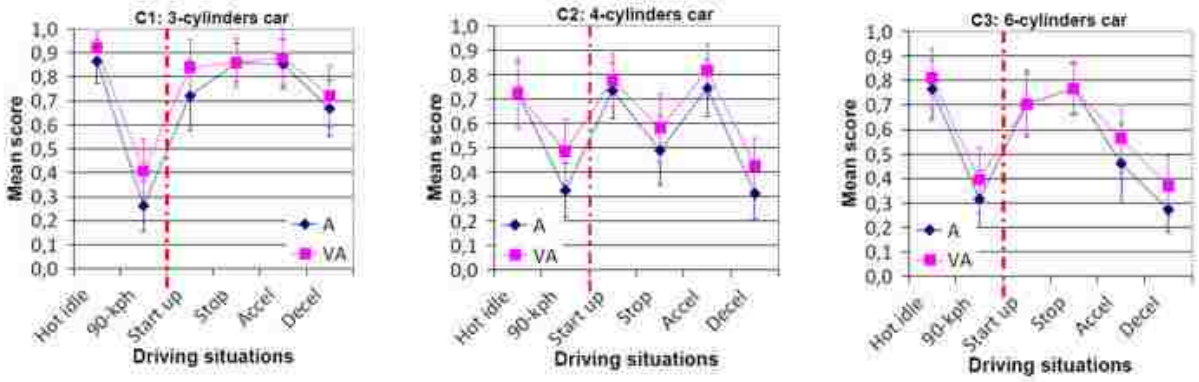

Figure 1 - Dieselness with and without vibration [reprinted – 5]

2.2 Source Path Contribution

Engine sound and mount vibration are significant contributors to the sound and vibration that the occupants of a vehicle experience [3]. The previously study by Renault and Ircam indicated that the overall experience is not defined by just the sound or vibration alone but rather a combination of the two. For the occupant of a vehicle to detect the sound and vibration from an engine, there must be a path that the sound and vibration must travel from the source (Engine) to the receiver (Occupant). The in-depth analysis to understand the interaction between the source and the receiver is called Transfer Path Analysis (TPA) or also called Source Path Contribution (SPC).

The principle concept of source path contribution (SPC) is that there are three interacting components; The Source, the Path and the Receiver. The source is the component that is creating the noise and vibration, in terms of this discussion this would simply be the engine. There must also be a receiver, this is a location that is detecting the noise and vibration from the source. Typically, the receiver in terms of this discussion is

the occupants of the vehicle, both driver and passenger in the cab of the truck. Then there must also be a path for the noise and vibration to get from the source to the receiver. Transfer paths can be either air-borne or structure-borne [3].

An air-borne path is typically associated with acoustical sound waves that are radiated from the source and detected by the receiver. This is simple to visualize in a direct line of sight with no obstructions the sound wave can travel directly from the source to the receiver. This gets much more complicated once obstructions are put in place such as integrating an engine into a full vehicle.

Structure-borne paths require physical contact and transmit the vibration from the source to the receiver. The vibration that is transferred can be picked up as a vibration at the receiver location or can be transformed into sound at the receiver's ear location. The forces transmitted through engine mounts resulting from engine operation are structure-borne sources of interior sound and vibration [3].

The SPC analysis method builds a model of the vehicle by quantifying both the acoustical and the structural excitation and the transfer paths from the source to the receiver. This process can be summarized as:

$$P_{receiver,acoustic} = \sum [(P/Q)*Q)]$$

$$P_{receiver,structure} = \sum [(P/F)*F)]$$

$$P_{receiver} = P_{receiever,acoustic} + P_{receiver,structureborne}$$

Where Q is the source strength of each acoustic source, F is the force put into the structure from each structural source of vibration. (P/Q) is the frequency response function

(FRF) measured with an acoustic noise source (typically white or pink noise) between the source location and the receiver location. (P/F) is the FRF measured with either a shaker or a modal hammer between the source and the receiver location. The total noise at the receiver is due to the contribution from all acoustic and structural sources and paths. The sources are characterized by measurement of their operating levels, while the paths are characterized by FRFs measured under artificial excitation conditions. [6]

In a study of an agricultural crop spraying machine by AGCO [6], the SPC method was used to determine the contributions to the sound as measured at the operator's ear position. They found that the sound pressure level (SPL) at this location was dominated by the structure-borne sources below 250 Hz while the acoustic sources were at frequencies above 375 Hz. The lower frequency (structure-borne), included the 3rd engine order, and was found to be transferred through the front mounts in the vertical direction. The acoustic noise that was found to be above 375 Hz was the engine radiated noise. Figure 2 shows the measured noise spectrum (bold line) with the estimated structure-borne contribution (light gray solid) and airborne contribution (dashed) of this study.

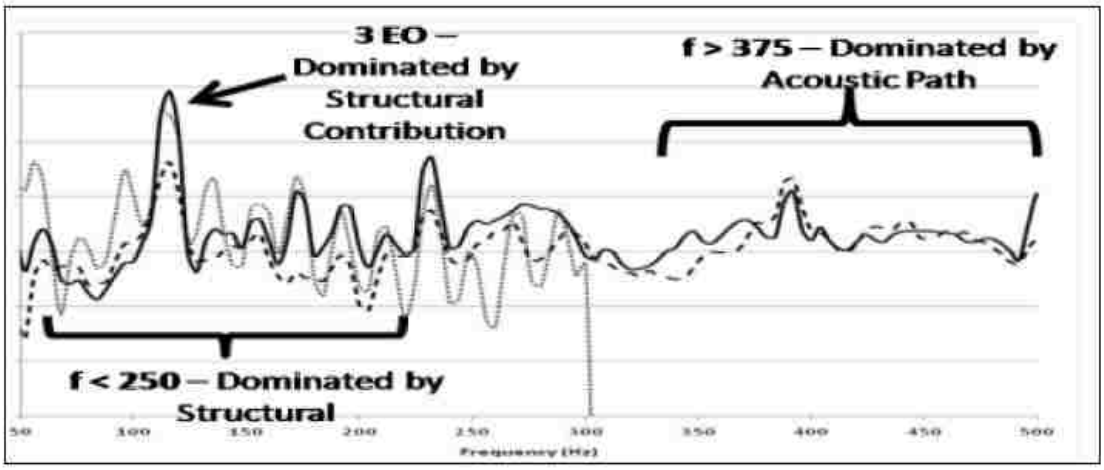

Figure 2 - Estimated structure-borne and airborne contribution of measured cabin noise [reprinted – 6]

2.3 Engine Mounts as a Path for Noise and Vibration

Once the source and the path are determined, design changes can be applied to reduce and control the noise and vibration. Efforts can be applied to reduce the level of excitation of the source or attenuate the noise and vibration along the path to the receiver. Since the engine mounts are a very relevant transfer path relating to engine vibration, different methods can be used to control the vibration energy that gets transferred through the mounts.

On a very basic level engine mounts are not complicated parts. They consist of a vibration isolator sandwiched between two mounting brackets which one side gets bolted to the engine and the other to the vehicle. Over the evolution of vehicle designs, the shape, size and material composition have changed, however the function remains the same. That is to secure the engine in its mounting location while minimizing the vibration transfer into

the vehicle. The forces transmitted through the engine mounts resulting from engine operation are structure-borne sources. The relative displacement across the engine mounts are proportional to the forces transmitted through the mounts from the engine and into the vehicle frame [3].

With vibration isolation and ride comfort becoming one of the major competitive factors, most automakers spend significant effort and budget on improving this vehicle attribute. The development and tuning of a powertrain mounting system is an essential part regarding NVH characteristics [2]. Today's engine mount designs use mixed finite element and multi body dynamic modeling to tune the mount for the application. Operational engine data can be added to the model to improve the results.

Alternatively, active hydraulic engine mounts are also used to attenuate the source vibration from the vehicle frame. These active engine mounts have proven significantly effective for the reduction of the first and second engine firing orders in regard to interior noise of the vehicle cabin [7]. Isuzu Advanced Engineering and Tokyo University have developed a control method for hydraulic engine mounts that modifies the traditional LMS algorithm to extend the frequency range of control beyond just the 1st and 2nd engine firing orders, but rather to a wide frequency band. This has proven effective up to 500 Hz [7].

Although the design and implementation of engine mounts is beyond the scope of this project, it is important to understand that the vibration energy present on the engine side of the mount location can be attenuated and controlled through the mounts reducing its impact to the vehicle.

2.4 The Engine as the Source of Noise and Vibration

The principle of source path contribution indicates that in order for someone to perceive a sound or vibration, there must be a source that initially produces the excitation of a sound and/or vibration. Within the context of this research, the only source that is of focus is the engine itself. The source of noise and vibration from an engine is a combination of many components. The mechanical noise due to the rotation of the internal components and the structural response of the engine structures, combustion noise due to the forces directly from the combustion process plus the coupling of the combustion and mechanical noise due to the additional forces of combustion influencing the noise and vibration characteristics of the mechanical noise of the engine [8].

Mechanical noise of an engine is made up of many subsystems. Every part that moves or supports the movement of fluids on an engine produces its own unique set of noise and vibration properties. The list of components that contribute to the mechanical noise and vibration of an engine includes but is not limited to the crank train, valve train, piston assembly, fuel system, induction system, lubrication system, exhaust system and accessory systems as well as the influence of the structural sensitivities of the engine itself [8, 9, 10]. A basic understanding of the mechanical noise can be obtained by measuring the engine in a "motored" condition. This is typically done by using an external motor coupled with the engine to rotate the crankshaft. During this process there is no fuel delivery to the engine and therefore combustion does not take place. Combustion noise and the influence of the combustion forces on mechanical noise cannot be detected during this

type of operation resulting in a true indication of the mechanical noise and vibration of the engine.

Combustion noise is due to the combustion of the air and the fuel mixture under pressure in the cylinder. This occurs when the spark from the spark plug ignites the compressed mixture in a gasoline or compressed natural gas engine or when the fuel mixture ignites on its own due to the intense pressure and temperature in the cylinder such as for the case for a diesel engine. The force of the explosion is primarily directed to move the piston down the cylinder and transfer the energy of the combustion to the rotating crankshaft. The force of the combustion also creates a side effect, as the additional force of the combustion can affect the noise and vibration characteristics of the rotating mechanical components.

There have been several methodologies developed to separate the mechanical noise from the combustion noise. These methodologies are referenced in a paper written by Virtual Vehicle and AVL List GmbH, "Procedure for Separating Noise Sources of Combustion Engines" [9]. The purpose of their investigation was to develop software to separate the combustion and mechanical noise for use as a tool in engine noise reduction and sound quality optimization work. In this, the authors define the noise contributions resulting from the different excitation mechanisms of the engine as:

TN = MN + CEC +iMN

Where:

TN = Total engine Noise

MN = Engine noise at motoring

CEC = Combustion excitation content of total noise

iMN = Further increase of motoring noise by mechanical excitation due to combustion

This investigation focused strictly on the acoustical noise measured by 4 microphones in a semi-anechoic dynamometer test cell. Both diesel and gasoline engines were tested. The results of this study were reported and compared in 1/3 octaves. It was found that combustion excitation content of the total noise is generally below 1.2 kHz. Above 1.2 kHz the mechanical noise of the engine tends to dominate the total noise content. The increase in mechanical noise due to the combustion excitation was found to be above 4 kHz.

Separating the combustion noise from the mechanical noise as was done in the study with Virtual Vehicle and AVL is beyond the scope of the investigation that is being performed for this thesis. It is important to note that their findings of combustion noise being the dominant noise below 1.2 kHz relates to directly to the comparison of the different calibrations that are to be tested for this thesis. Since all of the calibrations will be tested on the same engine, it is fair to assume that the mechanical noise will be the same for each calibration configuration and therefore negligible when comparing the results as only the differences in combustion excitation content and the increase in mechanical noise due to combustion will be readily seen in the results.

2.5 Combustion Noise

Since combustion noise is a large characteristic of the engine noise signature, a great deal of research has been done to understand and control it. There is no shortage of technical papers written on the subject of combustion noise. The scope of a majority of

these papers focuses on the acoustic aspect of the combustion noise. The investigations generally consist of microphone measurements to compare and report the overall sound pressure level, frequency content as well as some sound quality metrics.

The concern for the acoustic properties of the engine does make sense as the first impression that a person might have with a product is the sound that they hear emitting. This extends beyond just what the operator of the vehicle and machinery hear to what the people who might be "casual observers", such as the passengers in a quiet car next to a noisy diesel truck at a stop light, or home owner located next to a busy road or construction site with noisy trucks and machines operating throughout the day. The perception of how an engine sounds also goes to the consumer who is going to purchase the product. For example, if a fleet manager is going to buy engines for a fleet application, the perception of the sound of the engine may make or break the sale due to the perception of quality [11, 12]. It is easy to see why much effort is put into the understanding and control of combustion noise.

There is little information available on combustion relating to vibration. In the literature reviewed, only one paper investigated the correlation between combustion and mount vibration "Combustion on Radiation Noise and Mount Vibration from a V8 Gasoline Engine" by In-Soo Suh of DiamlerChrysler Corp [8]. Suh's study was able to find some correlation between combustion and mount vibration using similar methods to noise radiation. The methods used will be discussed in a later section.

2.6 Analysis of Combustion Pressure and Acoustic Noise

There are several reason why one may want to analyze and correlate combustion cylinder pressure data and sound pressure level measured by a microphone. In some cases, it is to optimize the combustion process to have the best trade-off for efficient combustion as well as low noise levels. This can be done either through adjustments of the calibration strategy [8, 13] or the selection of physical components on the engine [14]. Correlation is also important for noise prediction early in the design cycle to aid in the CAE prediction regarding the combustion noise [15, 16]. The correlation of combustion pressure to measured noise has been found to be a valuable tool for estimating the combustion noise of an engine when a proper acoustic measurement environment is not available [17].

Various methods for correlating the cylinder pressure level during combustion to the acoustic noise were investigated in each of the papers reviewed. All of the methods agree that a cylinder pressure transducer is required to measure the cylinder pressure and a microphone is required to measure the acoustic noise. Some studies focused on diesel engines, and others on gasoline. Each of the papers have similarities in methodology and results, and in some cases there are some disagreement. Discussions here will be on the similarities, except when noted.

It is very common to look at cylinder pressure traces relative to crank angle. This provides the pressure level inside the cylinder at each of the angle of crank position as the engine rotates. From this data, it is easy to see the "shape" of the combustion as it affects the cylinder pressure throughout the entire duty cycle of the engine (0-720 degrees). From

this data, the maximum peak pressure, Pmax, can easily be extracted (Figure 3(a)) which has been used in several studies to correlate cylinder pressure to acoustic noise [8, 18].

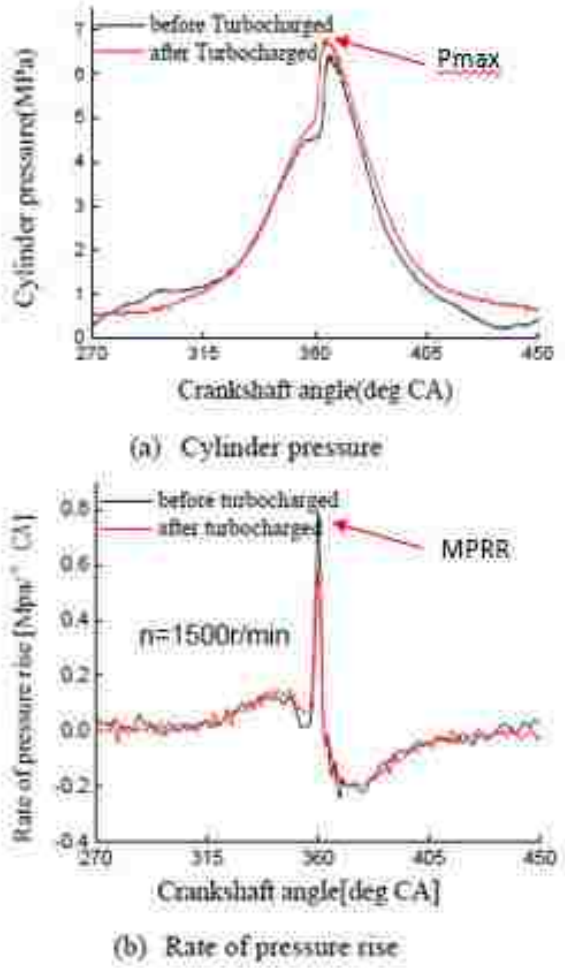

Figure 3 - (a) Cylinder pressure (b) Rate of pressure rise [reprinted – 14]

It is agreed that combustion noise is caused by the pressure rise in the cylinder resulting from the heat release during the combustion process [10]. So by differentiating the cylinder pressure data, the pressure change rate can be evaluated (Figure 3(b)). During combustion, the rate of pressure change increases sharply and the maximum value of the

pressure rise rate (MPRR) is often used as a metric to correlate to sound pressure values [8, 10, 14, 17, 18]

In a study performed on a 5.7 L gasoline engine at DaimlerChrysler [E], Suh found a near linear relationship between both the Pmax and the MPRR during his test (Figure 4). In this test, the engine was operated at wide open throttle (WOT) at speeds from 1200 rpm to 5000 rpm at 400 rpm increments. At each speed increment, the Pmax and the MPRR values were averaged for 500 engine duty cycles to report a single value for that condition. To change the combustion properties at each speed, the spark timing was incremented from 5 degrees before top dead center (BTDC) to 22 deg. BTDC.

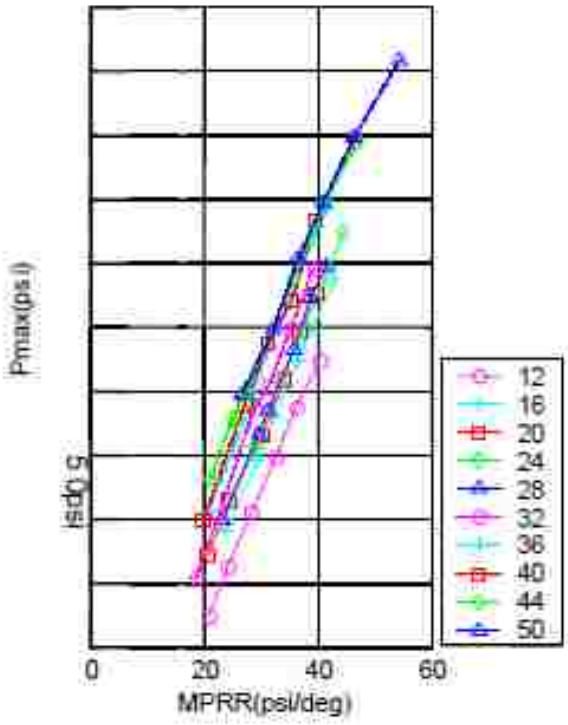

Figure 4 - Relationship between Pmax and MPRR at varied spark timing [reprinted – 8]

The acoustic noise was also measured at the same operating conditions. Microphones where placed at a distance of 1m from the engine, which was located in a hemi-anechoic test cell according to the SAE- J1074 standard [19]. The acoustic noise data was reported as overall sound pressure level and compared to the MPRR at each one of the operating conditions. The results show acoustic noise increasing in a near linear relationship with MPRR (Figure 5).

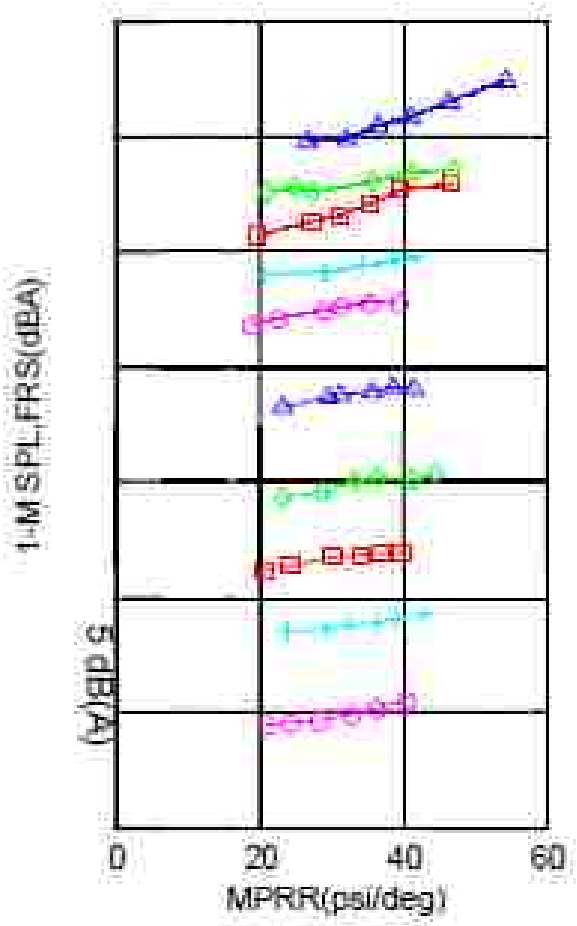

Figure 5 - Engine acoustic noise vs MPRR [reprinted – 8]

Similar results have been seen for diesel engines in an experiment at Tianjin University [14] where combustion noise was compared before and after a turbo charger was added to the engine. It was found that the addition of the turbo charger reduced the MPRR of the engine and also lowered the combustion noise level. This difference between the turbo and non-turbo configurations was more defined at higher load conditions as they found that with turbo charging, the pressure and wall temperature in the cylinder is elevated compared to the non-turbocharged configuration. As such, the rate of the pressure rise is smaller since the turbo charged engine has a higher starting pressure than the non-turbo [14].

Not all studies agree that the MPRR has the best correlation with combustion noise. In a study performed by Hyundai Motor Company and KIA Motors Corp [17] on a 1.7 L diesel engine, it was found that the MPRR had low correlation to combustion noise. The study did agree that the rapid change of the in-cylinder pressure was the root of combustion noise. Their findings showed two samples with the same MPRR resulting in a significant difference in sound pressure level at frequencies above 1 kHz.

To establish a better tool to correlate the cylinder pressure to acoustic noise, they developed a Combustion Noise Index (CNI). Since the initial results of their testing showed a significant difference in sound pressure level between 1 kHz to 3.15 kHz for the two samples. They computed the CNI as the sum of the 1-3.15 kHz range of the 1/3 octave band level as given by the following expression:

$$CNI(dB) = 10*\log(10^{(1kHz\ level/10)}+10^{(1.25kHz\ level/10)}+\ldots+10^{(3.15kHz\ level/10)})$$

To test the newly developed CNI, the focus was between 1250 rpm and 2250 rpm and the fuel quantity from 10 mg to 25 mg. Figure 6 shows all of the data points collected during this study, where sound pressure data was also collected at each data point. The ranges were selected as being the area of interest regarding measuring exhaust emission, and therefore, the area where there must be a trade-off between combustion noise and exhaust emission requirements.

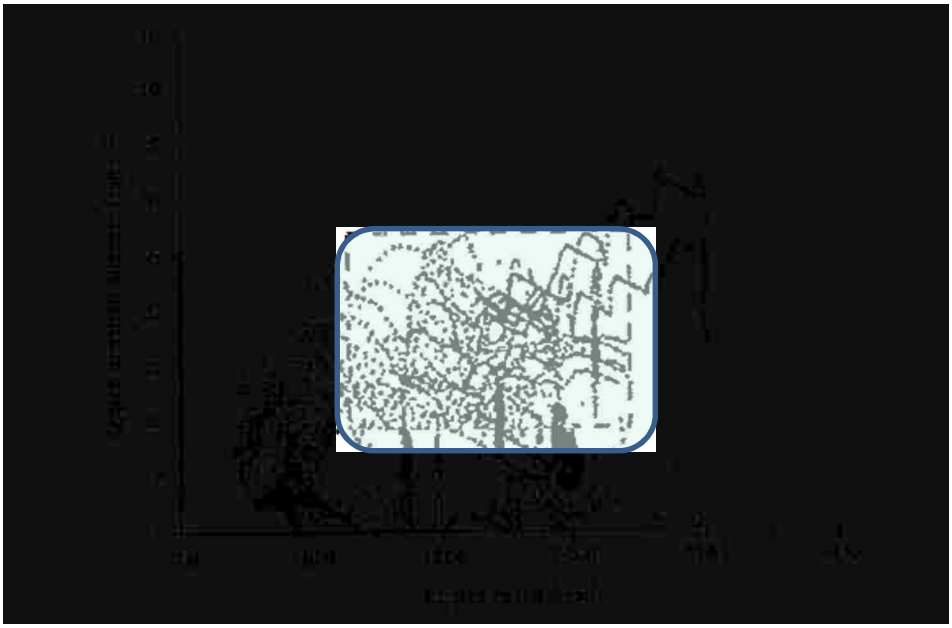

Figure 6 - Engine operating test conditions for CNI [reprinted – 17]

The new CNI performed much like the MPRR as when the CNI value increased, the resulting sound pressure level also increased. Likewise, as the CNI decreased, the measured sound level also decreased. To compare the CNI to the MPRR they found the coefficient of correlation for each of the values as they correlate to the measured sound pressure level. The coefficient of correlation is considered perfectly correlated at an R value equal to 1. The CNI was calculated to have an R value of 0.93 while the MPRR R value was found to be 0.74. Figure 7 shows a sample of the combustion noise at 1500 rpm

and 19.3 mg fuel quantity. The injection parameters such as timing, pressure and pilot injection quantity and separation were adjusted. The measured combustion noise and the calculated CNI can be seen in the four graphs. The trend of the newly developed CNI track was within 1.5 dB with the measured combustion noise. To predict the combustion noise using the CNI the following equation was developed:

$$\text{Combustion Noise Level} = (\text{CNI}-58.66)/1.508$$

Figure 7 - Combustion noise and CNI [reprinted -17]

Although this method of combustion noise prediction using the CNI tends to show reliable results, there are a few conditions that did not correlate well. Figure 8 shows the measured combustion noise compared against the CNI for the same conditions. It was found that when the injection timing was retarded by 2 degrees, the combustion noise

spiked while the calculated CNI could not predict that. However, for the purpose of engine development at Hyundai/KIA, this new method was suitable for the required development of their 1.7L diesel engine, allowing them to tune their engine for both emission and noise targets in a non-acoustically treated test chamber.

Figure 8 - Combustion noise spike not predicted by CNI [reprinted -17]

2.7 Analysis of Combustion Pressure and Vibration

Much like the previous section regarding the analysis and correlation of the in-cylinder combustion pressure and acoustic noise, vibration can also be analyzed and correlated in a similar manner. The number of papers on this subject are significantly less than what was available for the acoustic noise. This could be due to the greater emphasis on acoustic engine noise to both occupants and bystanders to the vehicle or perhaps it is because there is no need for a special acoustic test cell to measure vibration. Without the requirement of an acoustic test cell, vibration measurements can be readily collected using most any dynamometer or in-vehicle environment, and therefore, easier to measure during the development process as the prototype engines are being tested. It has been determined

that the vibration at the engine mount locations is critical to the characterization of the structure-borne noise inside the vehicle. Understanding the correlation of combustion pressure and engine vibration will help to develop an NVH-optimized engine early in the development process as well as help the later stage of NVH development during the powertrain adaptation and engine calibration development [8].

In the same experiment with the 5.7 L gasoline V8 engine as mentioned in the last section, Suh from DiamlerChrysler also measured vibration at the engine mount locations in addition to the acoustic data previously discussed. The vibration data was simultaneously collected with the microphone and cylinder pressure data using several tri-axial accelerometers. The acceleration signal was double integrated to get displacement in order to best describe the excitation forces [from the engine] of which the mount rubber delivers to the vehicle body side path. The dynamic displacement should be used as the descriptive parameter for mount excitation when using overall levels to quantify the vibration, as overall levels are obtained by summing over the frequency range of interest [25]. A high pass filter having a cut off frequency of about 30 Hz was applied to remove the lower frequency contents that were erroneously generated by the double integration process [8].

In order to derive a correlation between the combustion and the mount vibration, the MPRR was used as an indicator of the combustion. The MPRR did show some correlation with the engine mounts, Figure 9, however, it did not show as clear of a linear relationship as was shown with the acoustic data. This could be due to the lower frequency range of the vibration below 500 Hz which is more accentuated due to the nature of analyzing displacement rather than acceleration [8] (to be discussed in the next chapter).

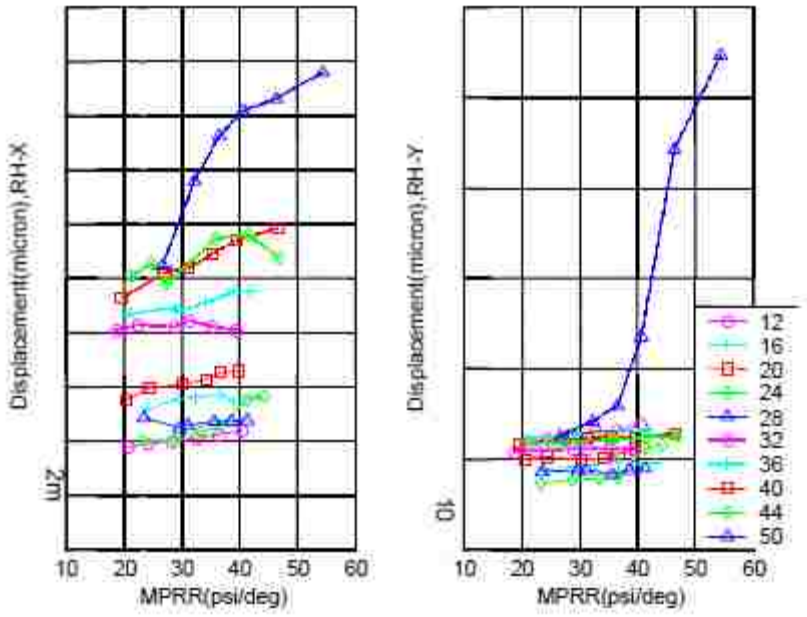

Figure 9 - Right mount X & Y direction vs. MPRR at various spark timing increments [reprinted – 8]

It was found that the lower frequency of the engine vibration has more influence from the overall nature of combustion rather than each cylinder's pressure rise rate. This means that other variables, such as cycle-to-cycle and cylinder-to-cylinder variation might have better correlation to the engine mounts, rather than MPRR as investigated in this study [8]. Suh also admits that the measuring techniques need to be more refined with respect to the lower engine orders, such as the 1st order of rotation [8].

Another study, performed jointly by the University of Lecce and the University of Catania [13], was to investigate the effects of fuel injection parameters on the combustion noise of a diesel engine, also analyzed the engine vibration. Only one engine cylinder was instrumented for the in cylinder pressure data collection. Two accelerometers were mounted to the exterior surface of the engine with one of the accelerometers mounted

perpendicular to the axis of the instrumented cylinder on the engine block and the other mounted parallel to the axis of the instrumented cylinder on the top of a head mounting bolt. For this test setup there was no consideration given to the engine mount locations. The engine was operated at 1400 rpm (46.67 Hz) and the data was analyzed using both FFT and third octave analysis, Figure 10.

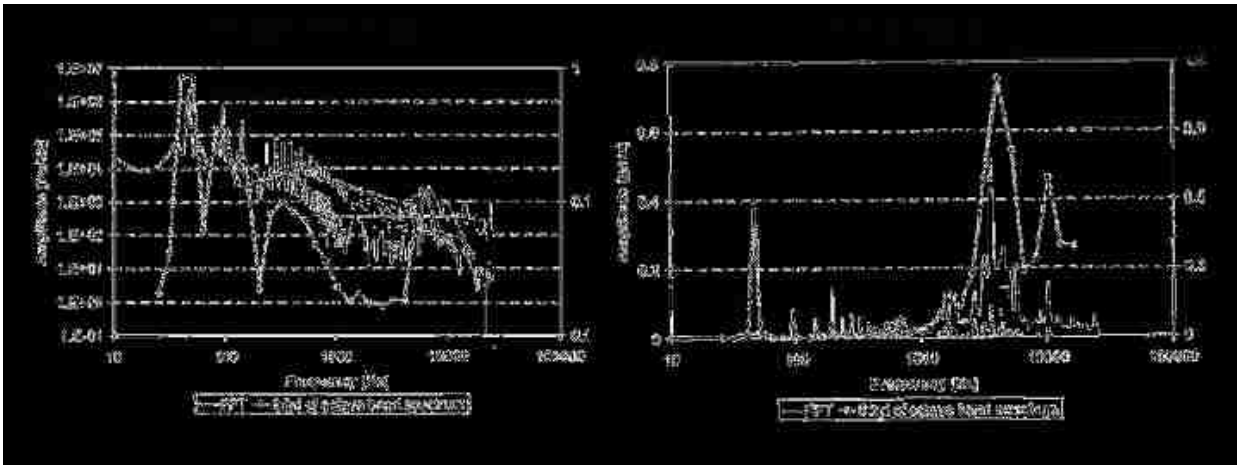

Figure 10 - Cylinder pressure and acceleration [reprinted – 13]

They found that the low frequency components of the acceleration spectrum matched closely with the pressure spectrum. These components where believed to be related to the peak pressure and can be seen at 46, 93 and 140 Hz. The higher frequency harmonics are related to the resonant oscillations of the charge inside the combustion chamber. These can be easily seen above 300 Hz in the cylinder pressure plot of figure 10. The coherence at high frequencies between the in-cylinder pressure and accelerometer signals were determined not to be achievable with the same confidence for lower frequencies. [13]

The elevated levels shown in the acceleration plot of figure 10 between 2-8 kHz could also be due to the natural attenuation of the block. Although performed on a different

engine in a different study by Polytechnic University of Valencia [H], they found that the attenuation of vibration of the engine block is lower between the frequencies of 1-5 kHz. This is due to the influence of the engine block structure itself. Figure 11 shows the attenuation curve of the engine as measured by Polytechnic University of Valencia. The frequencies and attenuation level represented in this curve could have shifted due to the unique structure for each engine block design, potentially explaining the high frequency content evident in figure 10.

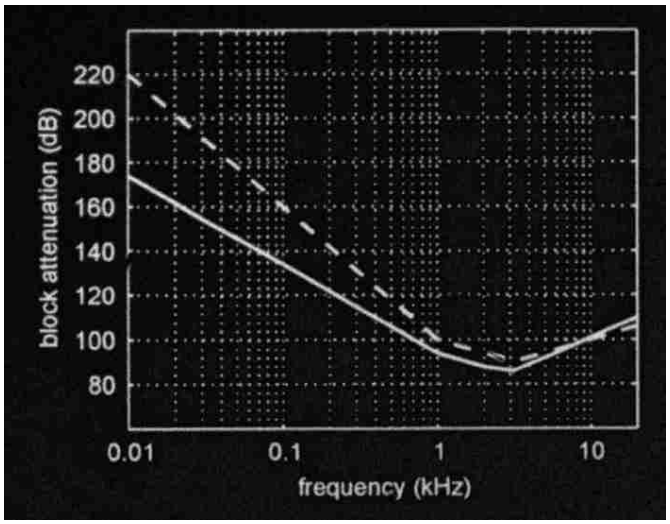

Figure 11 - Block attenuation curve [reprinted – 13]

2.8 Cylinder to Cylinder Variation

For multi-cylinder engines, it is ideal that all of the cylinders have the exact same pressure trace for any specific duty cycle of the engine. Unfortunately, this is not always possible, and a typical overlay of the pressure traces of a multi-cylinder engine may be seen in figure 12 where the blue line represents each individual cylinder pressure trace for a single cycle. It can be seen from this single cycle that the peak cylinder pressure varies

from cylinder to cylinder. The red line is the averaged results over several hundreds of cycles, which still indicates a variation between each individual cylinder. [8]

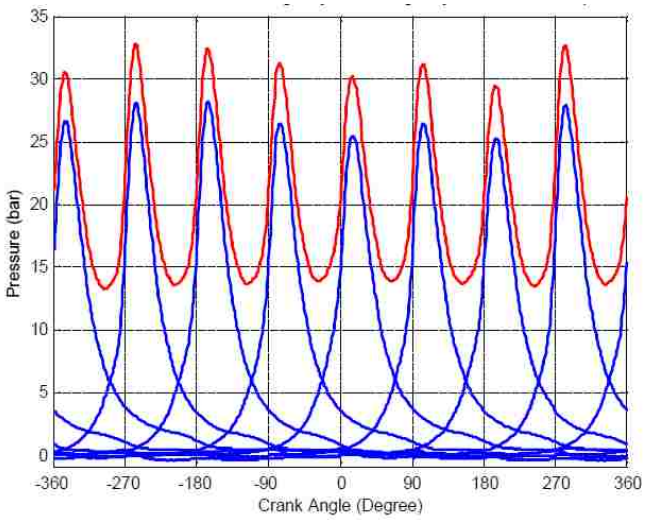

Figure 12 - Cylinder-to-cylinder variation in a V8 engine [reprinted – 8]

There are many variables that may affect each cylinder differently to induce variability between the cylinders. Some are due to the design and manufacturing variation. This could be due to the compression ratio, port geometry and compression leakage through the piston assembly gap. Some variation could also be due to variation in operation due to uneven flow distribution through the intake manifold and port to each cylinder, transient flow characteristics, spark or fuel deliver timing or anything else that could affect the flame propagation for each cylinder [8].

2.9 Cycle to cycle variation

As the previous section described the cylinder-to-cylinder variation of single cycle, cycle-to-cycle variation is similar in concept. However, cycle-to-cycle variation indicates

the repeatability of an individual cylinder's pressure trace relative to its complete duty cycle. Ideally there would be no variability between each of the cycles and each pressure trace would overlay the previous line on line. However, in reality that is not possible and the cycle-to-cycle variability can lead to power loss [20] as well as affect engine noise and vibration [8]. Figure 13 shows a sample of typical cycle-to-cycle variation as measured captured for 500 cycles [20]. It can be seen there is nearly a 30 bar difference between the maximum and minimum pressures at a single, steady operating condition.

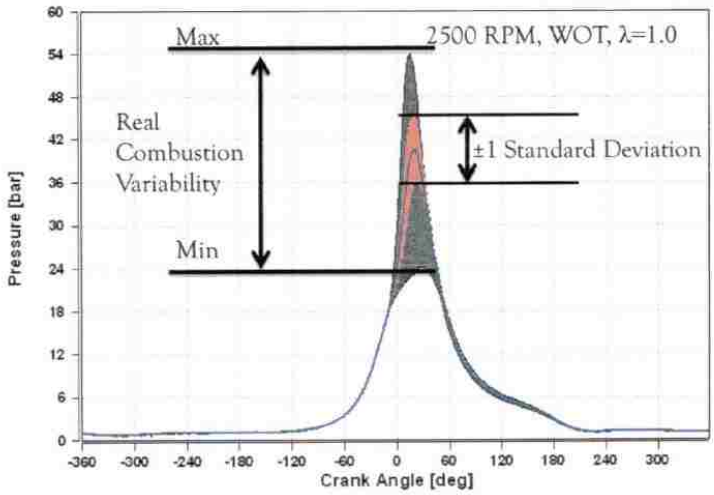

Figure 13 - Cycle-to-cycle variation of a single cylinder [reprinted – 20]

The sources contributing to the variation in each cylinder's cycle are often difficult to identify. It is often assumed that the main contributors are the mixing and flow of the air and fuel [20]. This could be due to fluctuations caused by the preceding cycle such as residual unburned gas in the combustion chamber, poor flame propagation or a misfire. Fluctuation in the same cycle such as variations in cylinder flow and turbulence, variations

in injection or spark delivery as well as the influence of torsional vibrations on the system [18,21].

A study performed by M. Gazon and J. Blaisot investigated cycle-to-cycle fluctuations of combustion noise in a diesel engine [18]. In this study, they acquired 50 cycles of running engine data at five different operating conditions. In-cylinder pressure data and acoustic noise measurements were acquired. The radiated acoustic noise was quantified as a single overall sound pressure level for each cycle as seen in figure 14.

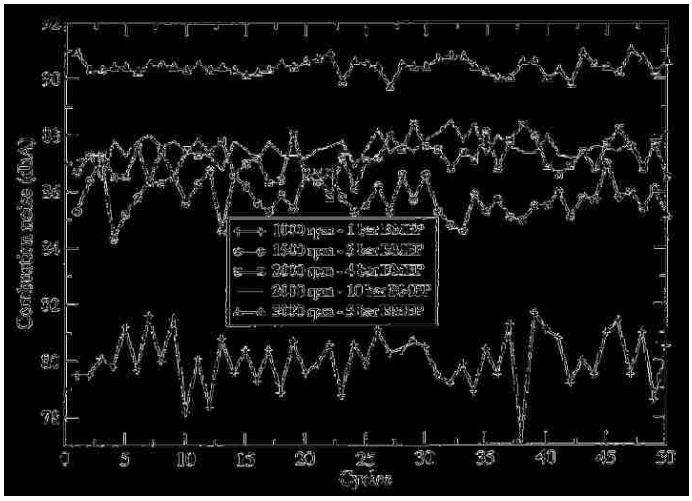

Figure 14 - Acoustic cycle-to-cycle variation for a 50 cycle sample [reprinted – 18]

The results of the Gazon, Blaisot experiment indicated that cyclic fluctuations are always larger for low engine speed and low brake mean effective pressure conditions. The fluctuations of cylinder pressure are only due to the combustion process; the compression stroke does not induce significant fluctuations. On an individual cylinder, correlations exist between the maximum rate of pressure rise, the maximum rate of heat release and the combustion noise. [18]

Although investigating the cycle-to-cycle as well as cylinder-to-cylinder variations is beyond the scope of this project. It is important to understand what can contribute to these variations as they will be seen in the data analyzed in the outcome from this research. Due to the inherent cyclic variations that will be presented in the data of the current study, all of the reported values will be averaged for comparison purposes.

2.10 Literature Review Conclusion

It is evident that a great deal of time and effort have gone into understanding all aspects of engine noise and vibration by the number of papers that have been written in the subject. Consumer perception, driver comfort and environmental noise concerns must be addressed by vehicle manufacturers in order to remain competitive in their market. In many cases the engine is the main source of these unwanted sounds.

The found paper typically considered engines that use the more traditional fuels of diesel or gasoline. There was no mention of compressed natural gas as a fuel for any of the papers reviewed. As alternative fuels for internal combustion engines becomes more mainstream, their effects on the combustion and the noise and vibration characteristics of combustion must be more fully understood.

It was also evident by the literature reviewed, that there is no defined standard for correlating in-cylinder pressure to radiated sound or engine vibration. It was generally agreed that peak pressure and maximum pressure rise rate (MPRR) tend to correlate to radiated acoustic combustion noise overall sound pressure level. In some cases, FFT or

third octave analysis was used, however there is no definitive answer as to what the best analysis tool is for understanding effect of combustion on noise and vibration.

There was only one paper found that investigated a correlation to mount vibration and found that the MPRR had some correlation. Further investigation regarding correlation of in-cylinder pressure and mount vibration is still much needed.

CHAPTER 3: THEORY

In order to quantify the engine vibration as well as the cylinder pressure pulsations for the purpose of analysis and comparison, decisions must be made on how the data should be analyzed. Machinery vibration can be measured using acceleration, velocity or displacement transducers. The raw signals can then be analyzed using a variety of signal analysis techniques. The most common methods of analysis are overall level, octave analysis, Fast Fourier Transform (FFT) and Order. Although each one of these methods provides information about the measured data, the level of detail and relevance varies between them. It is important to understand the differences between these analysis methods when using them to quantify any differences in the test variables. This section will provide details on the different analysis methods that can be used for this type of testing.

3.1 Vibration

This study investigates the vibration of the engine at the engine mount locations. Vibration is the movement of an object in an oscillating motion around a fixed reference position. The number of times a complete oscillation cycle occurs in a second is called frequency and is measured in Hertz (Hz) [21]. This oscillation can result from a wide variety of sources. It is not uncommon for an internal combustion engine to have many sources acting on it. The forces related to the motion of the pistons, rotating shaft imbalance, and valve-train movement, as well the explosive force of combustion, all

contribute to the vibration characteristics of the engine. This magnitude of this oscillation can be quantified a displacement, velocity, or acceleration.

3.1.1 Measuring Vibration

There are a variety of devices available for measuring vibration. Typically for engine vibration testing an accelerometer is used. Although some designs may vary, an accelerometer is a piezoelectric device that gives an output voltage that is relative to the level of measured acceleration. The resulting output can later be integrated using an integrating signal conditioner or post-processing software to give velocity or displacement. Accelerometers come in a variety of shapes, sizes, sensitivities, temperature ratings, and mounting options. They tend to be robust and can handle the harsh environment associated with engine testing including high temperatures, high vibration, and contact with a variety of chemicals. Since they require to be physically mounted to the component surface, it is important to consider the mass of the transducer. If the ratio of the transducer's mas to the mass of the test specimen is too high, the vibration properties of the test specimen could be affected by the additional weight of the transducer. It is recommended that the mass of the accelerometer be at least 1/10 that of the test specimen on which it is mounted [22]. A simple method to test if an accelerometer is mass-loading a structure is to attach a second accelerometer to the accelerometer already mounted to the surface of the structure. This will double the mass of the accelerometer. If there is a frequency shift in the results with a doubling of the accelerometer mass, then it is possible that the original accelerometer is mass-loading the structure [23].

The Laser vibrometer is a non-contact method of measuring vibrations. The output of the laser vibrometer can be in displacement, velocity, or acceleration, and much like the accelerometer, it is easy to change the units via integration in post-processing software. These devices are typically used in non-contact situations where the effects of mass loading make accelerometers an unacceptable choice. Special care is also required when preparing the test specimen to properly reflect the laser signal. The presence of dirt and oil can interfere with the specimen's ability to reflect the signal, which means that laser vibrometers are not often used for engine vibration testing.

3.1.2 Displacement, Velocity or Acceleration

There is not one universally accepted standard when it comes to measuring engine vibration with respect to the unit of measure in which the results should be reported. In industry, it is typical to see different unit preferences even within a single company based upon what component or vibration phenomenon is being measured. The results reported in the papers reviewed in the previous chapter were not consistent with one another regarding the measurement units used: one used units of acceleration [13] and another used units of displacement [8] when referencing vibration. The relationship between acceleration, velocity, and displacement is already well known and can easily be calculated in both the time and frequency domains.

Acceleration is easily measured using an accelerometer and is represented in the time domain as:

a = measured acceleration

Integrating the acceleration with respect to time provides the velocity

$$v = \int a \, dt$$

Integrating the velocity with respect to time provides the displacement.

Once the signal has been processed into the frequency domain, it is still possible to convert between acceleration, velocity and displacement at each discrete frequency.

Where:

A = Amplitude of Acceleration

At

f = Frequency (Hz)

Therefore:

For Acceleration

$$a = A$$

For Velocity

$$v = \frac{A}{2\pi f}$$

For Displacement

$$d = \frac{A}{4\pi^2 f^2}$$

Each unit chosen to quantify vibration has advantages and disadvantages. Acceleration is usually the first choice as it is directly measured by the accelerometer, so it does not require any additional integration or calculation to convert it to velocity or

displacement. One consideration when selecting the vibration unit is the frequency range of interest. Acceleration tends not to attenuate any high frequency components, so it is typically used when the frequency range of interest consists of high frequency. Velocity tends to give the best indication of a vibration's severity in the frequency range of 10 to 1000 Hz. Also, the far-field acoustic pressure that is radiated from a vibrating surface tends to relate proportionally to velocity under certain circumstances [24]. Displacement is generally used for investigating lower frequencies in the range where vibration in tight clearances can cause significant damage to a machine. Displacement is often used as an indicator of unbalance as relatively large displacements usually occur at the shaft rotational frequency [21]. The relationship between acceleration, velocity and displacement can be seen in Figure 15.

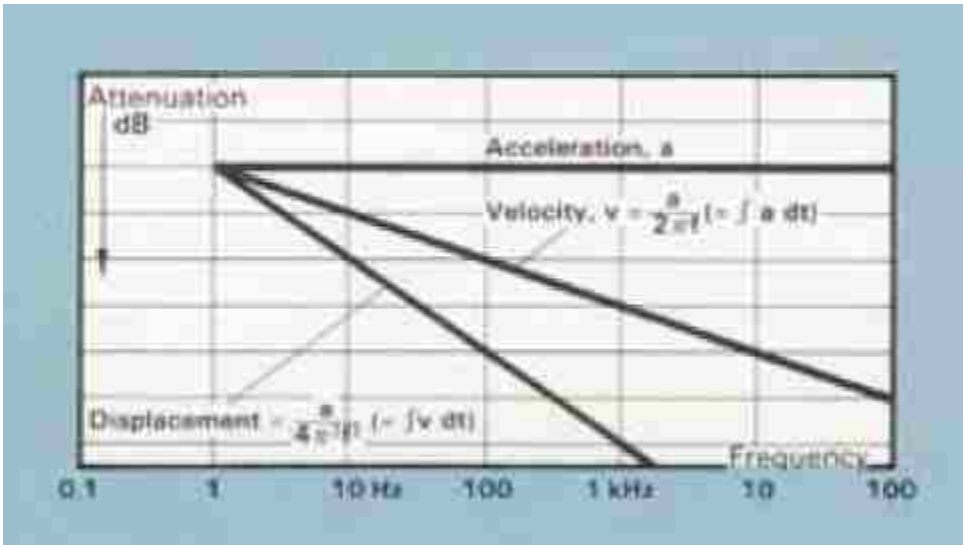

Figure 15 - Relationship between acceleration, velocity and displacement relative to amplitude attenuation [reprinted - 22]

The decision regarding the use of displacement when quantifying the input excitation to engine mounts is because engine mounts are typically rubber compounds. The

input excitation for a rubber engine mount is best described using dynamic displacement rather than acceleration as the excitation forces delivered by the mount rubber to the vehicle body side of the structure borne path can be accurately described with the input dynamic displacement. If a single-frequency component of acceleration is considered, such as the combustion order of an engine rotation, mount vibration can be described as either displacement or acceleration as long as the implication of frequency of both parameters is understood. When overall levels are used, the dynamic displacement should be used as a descriptive parameter of the mount excitation from the powertrain side when trying to quantify the structure borne noise to the vehicle cabin. This is because the overall levels are typically summed over the frequency range of interest [25].

3.2 Cylinder Pressure

An internal combustion engine produces power using the energy released by a controlled explosion. This explosion is the result of a metered mixture of air and a combustible fuel (such as gasoline, ethylene, methane or natural gas) combined with the increasing pressure of a reciprocating cylinder and a well-timed spark to ignite the flame. For most typical engines, the entire combustion process is contained within the reciprocating piston and cylinder assembly, known as the engine block. The number of cylinders in an internal combustion engine may vary depending on the engine size and output power requirements, but the process that the converts the air and fuel mixture to mechanical energy is the same.

The process begins with the piston moving down the cylinder, increasing the volume inside the cylinder and creating a vacuum. A valve opens on the top side of the

cylinder and allows the fuel mixture to enter the cylinder. This is called the intake stroke. When the piston gets to the bottom of its stroke and reverses its direction to start decreasing the volume inside the cylinder, the valve closes, allowing the cylinder pressure to build during the compression stroke. When the piston is near the top of the cylinder, the fuel mixture is at a high pressure and is very volatile. This compressed mixture is ignited with a spark from the spark plug, and increased pressure from the resulting explosion propels the piston back down the cylinder. As the piston moves down the cylinder, the inside volume of the cylinder is increases, the cylinder pressure is decreases, and the force of the combustion is transferred into mechanical energy as the piston rotates the crankshaft. This part of the process is known as the power stroke of the engine. The final step is for the piston to return to the top of the cylinder, forcing the spent residuals from the combustion through an open valve at the top of the cylinder as the volume in the cylinder is decreased. This is the last portion of the process is called the exhaust stroke. Once the piston reaches the top of the cylinder the exhaust valve is closed and the intake valve is opened allowing the process to start all over again with the intake stroke. This can be seen in Figure 3.2.

Due to the relatively high pressure and temperature internal to the cylinder during the combustion process, the transducer choices for measuring the combustion process are limited. Typically, a pressure transducer designed to withstand the high temperatures and pressures is used to acquire the cylinder pressure throughout the cycle. A variety of pressure transducers are available for internal combustion engine applications and the specifics related to the transducers used in this experiment will be discussed in more detail in chapter 4.

If the cylinder volume is known during the engine rotation, the pressure versus volume can be displayed in what is known as a P-V Diagram (Figure 16). This is typically used in the thermodynamic analysis of an engine [26], and is beyond the scope of this study; however, it does provide a very clear picture of how the four-stroke process of the entire cycle works in relation to cylinder volume as described earlier in this section.

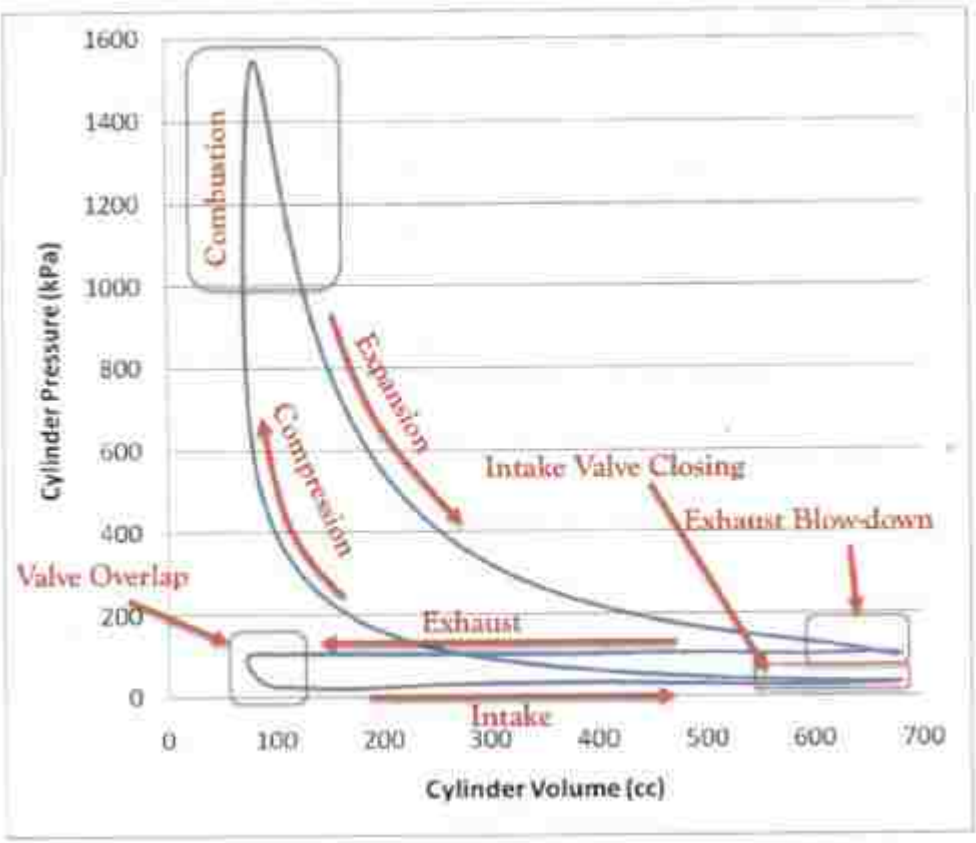

Figure 16 - Typical P-V diagram of a 4 stroke engine [reprinted – 20]

Cylinder pressure can also be viewed relative to crank angle. The nature of this display allows for greater emphasis on the compression and combustion stroke, as that is when the cylinder pressures are at elevated values. This shape provides insight on the combustion of each cylinder regarding the position of the crankshaft in its rotation [20].

More detail regarding acquisition and processing of data in the angle domain is provided in section 3.3.2.

3.3 Signal Processing

A transducer, whether used for measuring vibration or pressure, is in the simplest terms a device that converts a physical property to an electrical signal. The electrical signal is generally scaled relative to the magnitude of the physical property it was designed to measure. A signal analyzer is required to interpret the raw signal from the transducer and perform computations to transform the original signal into something that gives the user greater insight as to the behavior of the test specimen.

There are several ways to interpret this signal, each of which can produce useful results that can be used to make comparisons of and decisions about the data. Some methods provide more insight into the various components of the signal, such as time, frequency, order, or angular position of a component within its rotation. This section will discuss these methods.

3.3.1 Time Domain

Regardless of professional background, most people understand the concept of tracking data relative to time. For example, the evening news can give a viewer insight to how the stock market has trending over the past day, month, year or decade. These trends can be displayed and analyzed as they have been recorded over a fixed time sample rate. In the case of the stock market the reported rate may be the end of day closing price, allowing the data to be displayed as stock price in dollars on the y-axis versus time in days

on the x-axis. For NVH applications, the concept of time domain is very similar; however, samples are generally acquired in microseconds (μs) rather than days. Time domain data from the NVH perspective is the acquired signal from the transducer recorded and/or displayed versus a fixed time interval. Figure 17 shows signals displayed in the time domain over a single engine cycle. The top trace is the recorded cylinder pressure in psi and the lower trace is acceleration in m/s^2, both displayed on the same time scale.

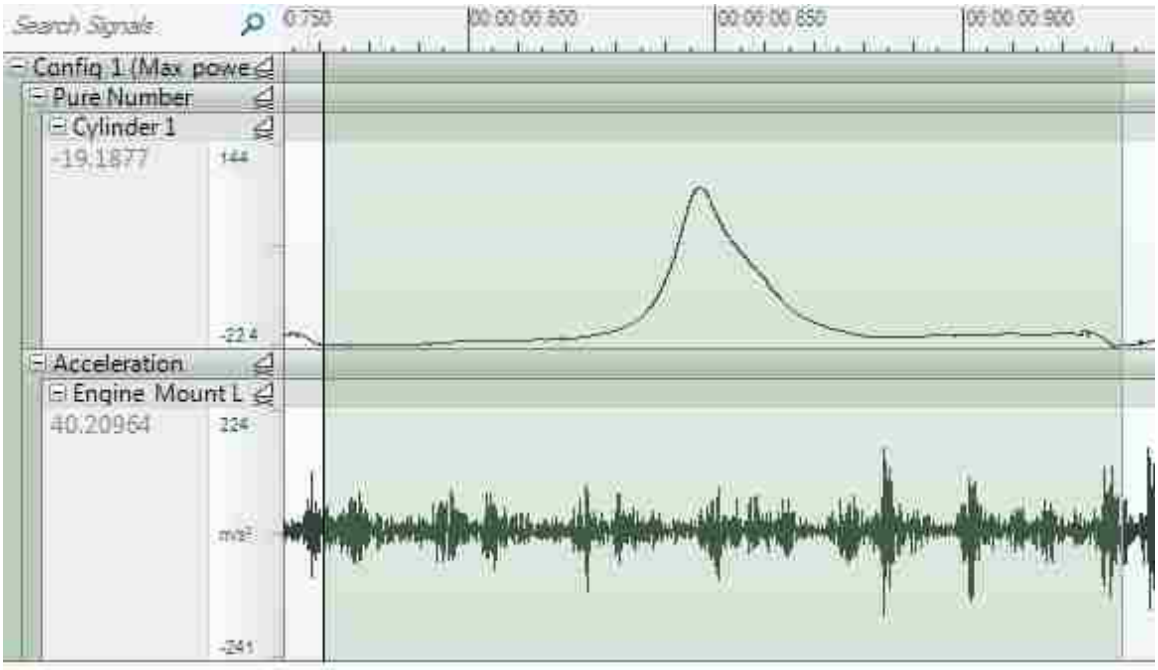

Figure 17- Typical time domain trace of a single cycle

The data displayed on the two traces shown in Figure 17 is the real measured values directly recorded from the transducers. This manner of data comparison makes it easy to see when events happen relative to one another with very good time resolution. However, time domain data does not provide any indication of where the events occur relative to position, or any information about frequency content of the signal. Therefore, it must be transferred and further analyzed in the angle domain or frequency domain.

3.3.2 Angle Domain

As time domain aligns the measured signal relative to time, angle domain aligns the data relative to the measured angular position of a rotating component. This information can be useful in determining exactly at what angular position an event occurred. It is typically used to investigate combustion throughout the entire duty cycle (0-720 deg.) of an engine, as shown in Figure 18.

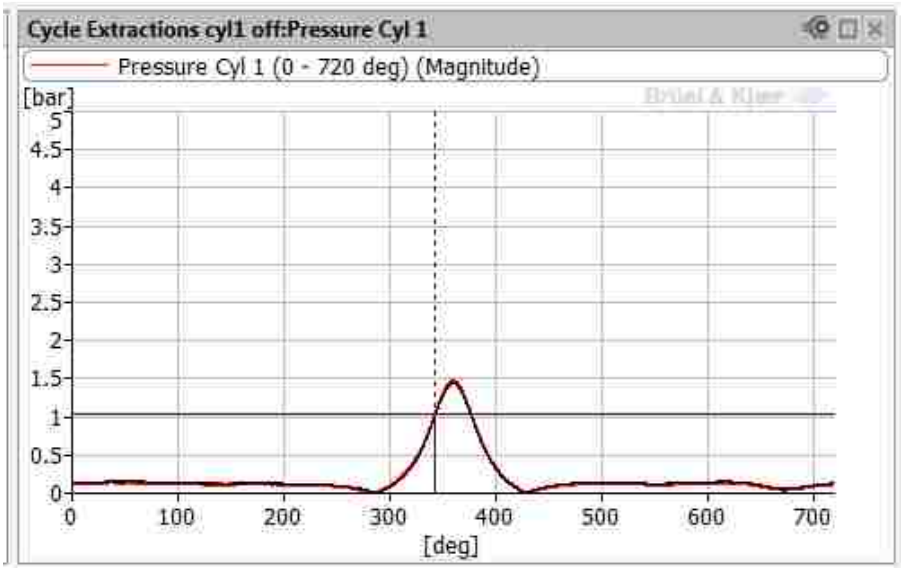

Figure 18 - Typical angle domain trace of a single cycle

Three signals are required to synchronize the dynamic data (vibration and pressure) to angular position (see Figure 19).

1. High resolution angle encoder signal – This transducer provides the angular position of the rotating component throughout its entire rotation.
2. Single point per revolution signal – This signal is generally used as the 0 degree start point.

3. Cycle timing indicator signal – This signal is required to tell at which revolution in the cycle the 0 degree start point is located.

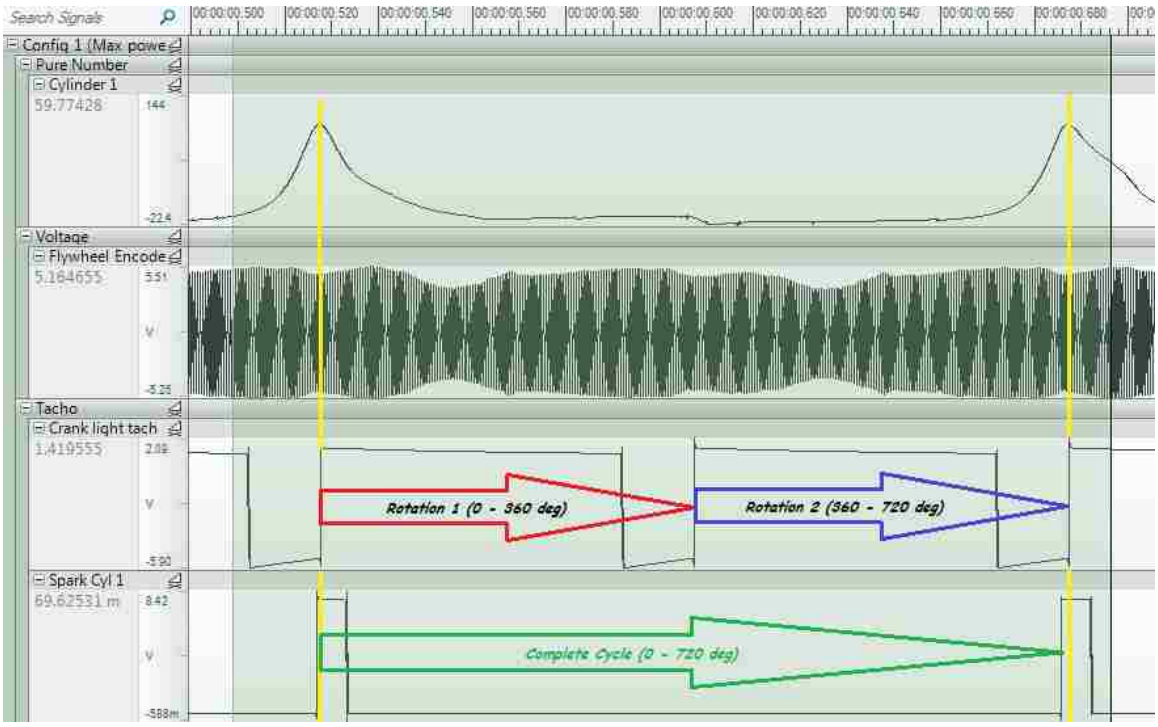

Figure 19 - Requirements for conversion from time domain to angle domain

There are several data acquisition and software packages available that will transform time data into angle domain using the signals discussed above. Brüel & Kjær's commercial Reflex Angle Domain software was used for the analysis in this study.

To convert data from the time domain into the angle domain, an encoder is used to get the angular position as the shaft rotates. This requires another signal to indicate exactly where the 0-degree position is. Typically, a single pulse per revolution tachometer signal is set to trigger on the 0-degree mark. Once the trigger signal has been detected, the angular position will increment based on the signal sent from the high resolution encoder. Once the encoder has made a complete revolution and all of the pulses have been determined,

the angular position returns to 0 deg. and the process repeats. This all that is required for a typical 0-360 duty cycle of a rotating piece of machinery.

For four-stroke internal combustion engines, an additional signal is needed to properly synchronize the high resolution encoder to the proper angle in the engine duty cycle. As previously discussed, an internal combustion engine must go through two complete crank shaft revolutions for the entire combustion process to complete. An additional 1 pulse per cycle signal is required to ensure that the 0 degree start point of the 0-720-degree complete engine cycle is synchronized properly. The timing and angular position of this signal does not have to be exact, but rather act as an indicator as to which revolution of the cycle the event takes place in.

3.3.3 Frequency Domain

Jean Baptiste Fourier determined that any waveform can be generated by combining sine waves [27]. Therefore, it is possible to dissect a complex waveform mathematically from the time domain and determine its amplitude and phase relationship at discrete frequencies. It can be shown that this combination of sine waves is unique. As such, any real world signal can be represented by one combination of sine waves [27].

The time domain graph represents the complex signal as measured by the transducer relative to time, and the angle domain reports the complex signal relative to angle, but the frequency information of these signals is not readily available. The signal reported shows the sum of all of the individual sine waves and is influenced more heavily by the sine waves of greater magnitude. This tends to mask the lower magnitude sine waves that do not make a large contribution to the complex signal. Although these masked

sine waves are of lower magnitude, they may reveal important information about the vibration present in the component being measured.

An example of a common rotating machine is the household washing machine for cleaning clothes. When in operation, a washing machine has various components contributing to the overall characteristics of the vibration of the machine. When the tub is spinning there are contributions from the water moving, motor running, clothes shifting position, and tub imbalance, as well as the rotation of the bearing that allows the tub to spin while securely holding it in position. It may be that the tub imbalance has the highest magnitude of vibration and is the largest contributor to the overall vibration characteristics of the machine. While components such as the bearing are also contributing to the vibration characteristics of the machine, the magnitude of their vibration might not be as noticeable in the time domain trace, because it has been masked by the high magnitude of the vibration from the imbalance. The vibration characteristic of the bearing might be a desirable key indicator as to the condition of the machine and is required for system diagnosis. To further define each component of the complex vibration characteristics of the washing machine, the signals must be further analyzed in the frequency domain.

The frequency domain provides the user with the ability to further investigate a signal's waveform and break it down to a frequency and magnitude. There are several ways these frequencies can be grouped and analyzed, each with advantages of their own regarding the comparison of data. For the scope of this project, overall level, constant percentage bandwidth analysis, fast Fourier transform (FFT) and order analysis will be discussed.

3.3.3.1 Overall Level (OAL)

Although the overall level analyzer does not give frequency information as discussed in the previous example, its setup is frequency dependent and therefore will be categorized with the other frequency domain analyzers.

In the simplest terms the overall level analyzer reports a single numerical value representing the total energy within a set frequency span of the signal being analyzed. Typically, the time signal is passed through a frequency filter before the energy level is detected, averaged and reported. Depending on the type and age of the analyzer the frequency filter can be either analog or a digital filter. The frequency range of the filter can be adjusted and represents the frequency range that is being reported from the overall level analyzer.

Typically, the overall level analyzer is used in applications in which frequency information is not required, but rather a single value to quantify the measurement. An example is shown in Figure 20.

Figure 20 - Typical overall level results

3.3.3.2 Constant Percentage Bandwidth (CPB)

For most noise and vibration analysis, more frequency information is required than what is available using the OAL analyzer. The constant percentage bandwidth (CPB)

analyzer is commonly used to provide the additional frequency information using a processing method similar to the previously mentioned OAL analyzer.

Rather than using a single filter and detector to analyze a signal, the CPB analyzer uses multiple filters that run in parallel. Each filter allows a certain frequency range to pass through. As the signal passes through each of the filters simultaneously, the level is detected and reported based on the center frequency of that particular filter band. The center frequencies for both 1/1 and 1/3 octave intervals are internationally standardized with the IEC Recommendation 225 [28]. Due to its relation to the octave scale, it is commonly referred to as an octave band analyzer.

The frequency bandwidths of the filters are calculated based on a constant percentage applied to the center frequency as specified by the IEC 225, based on a center frequency of 1000 Hz. This results in a 70.7% bandwidth for 1/1 octave and a 23.1% bandwidth for 1/3 octave. A table showing the frequency limits of each frequency band is in Appendix A.

Although 1/1 and 1/3 octave filters are most commonly used, it is possible to use 1/6, 1/12 or even 1/24 octave filters to gain increased frequency resolution, but at a higher cost. Figure 21 shows a sample of the same measurement analyzed using 1/1, 1/3 and 1/24 octave to demonstrate the variation in frequency resolutions.

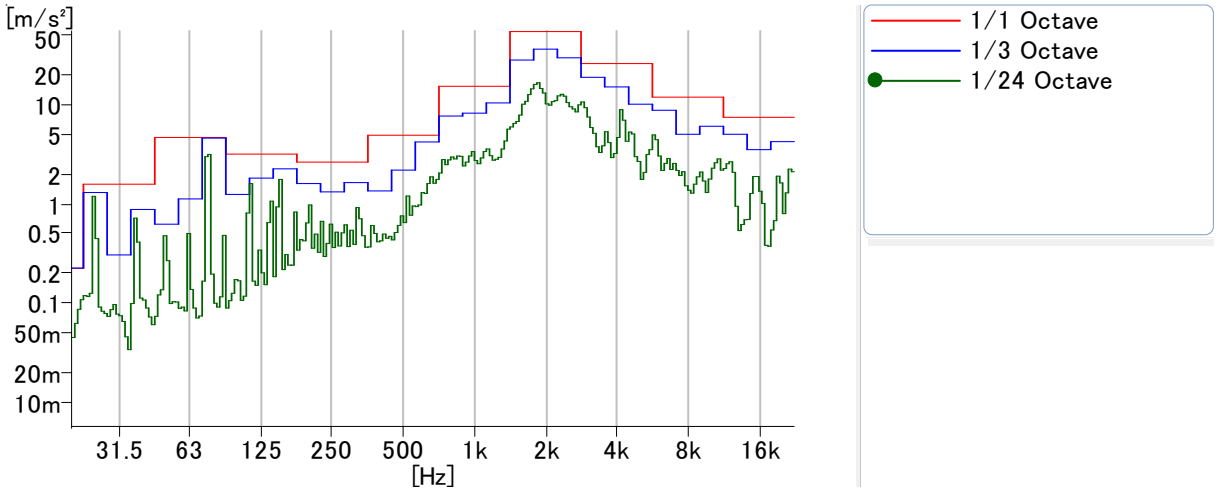

Figure 21 - 1/n octave result comparison of 3 frequency resolutions

The previously mentioned constant percentage bandwidth analyzers do a very good job of providing frequency information of a signal. However, the frequency resolution is limited to the smallest filter size available. Since the size (width) of the filter is a constant percentage of the center frequency, the frequency bandwidth of the filters increases as the center frequency of the 1/n octave band increases. This results in a much larger band frequency bandwidth (less frequency resolution) at high frequencies. Figure 22 shows the same data displayed in Figure 21, but on a linear rather than logarithmic scale in order to show the effect of constant percentage bandwidth filters at the higher frequencies. As the scope of this investigation is focused on frequencies below 800 Hz, this effect is not a significant issue.

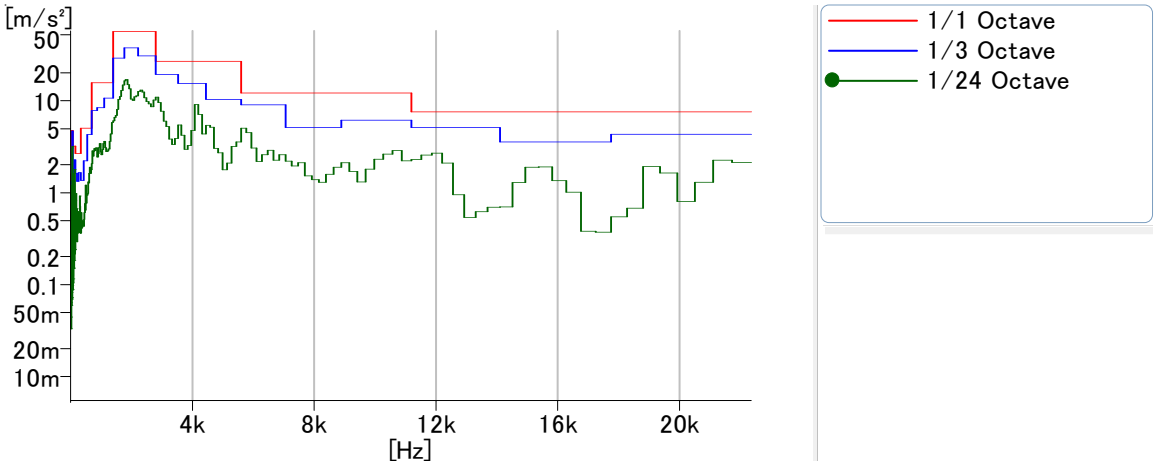

Figure 22 - 1/n octave results on a linear scale

3.3.3.3 Fast Fourier Transform (FFT)

Unlike the prior two methods, there is another approach to calculating the frequency content of a signal does not use filters. Rather than using a filter bandwidth based on a constant percentage of a known center frequency, the fast Fourier transform (FFT) performs a mathematical calculation with the results shown with a constant frequency bandwidth for each data point. The principle behind this was developed by Jean Baptiste Fourier and thus is named the Fourier transform.

The Fourier transform allows for an infinite time signal to be transformed to the frequency domain, and also allows for the frequency spectrum to be transformed back into the time domain again as follows:

Due to the fact that the integral is infinite, this is a theoretical concept rather than a practical way to perform a frequency analysis on real world applications. The time signal must be limited before the analysis is made. The time signal is segmented into small sections called time blocks. A time block consists of voltage values spaced at regular time intervals for a specific duration of time. The Fourier transform can then be calculated for each time block; however, since it is no longer an infinite time signal it is referred to as the Discrete Fourier Transform.

$$G(f_k) = \frac{1}{N}\sum_{n=0}^{N-1} g(t_n) e^{-j\frac{2\pi nk}{N}}$$

The Fast Fourier Transform (FFT) is a type of Discrete Fourier Transform (DFT), with an important distinction: the FFT limits the transform size (N) to a power of 2 resulting in in quicker, more efficient calculations [24].

This type of analysis is referred to as "Block Analysis" because it is performed on time blocks (defined above). The size of these time blocks is directly related to the desired frequency resolution of the result. For a high frequency resolution spectrum, a long time block is required. Conversely, if a short time block is used, the resulting frequency spectrum will have much less resolution. When performing this analysis with a signal analyzer, the length of the time block is determined by the frequency span and resolution, which is generally entered by the operator.

One issue with the DFT or FFT is the assumption that the time block is representative of the entire signal and is repetitive, meaning that the end value of the time block matches the beginning value of the time block. This generally is not true, as the true signal is rarely perfectly sized to match the block length. Therefore, when the time block is created there is a transient mismatch at the ends which is called leakage. The effect of leakage is a broadening of the peaks in the frequency spectrum. To reduce leakage, a windowing function is applied to bring the values at the ends of the time block to zero before the FFT calculation is made. Figure 23 shows some examples of time blocks with no weighting ("Rectangular"), compared to time blocks with a windowing function applied ("Hanning") in order to bring the end values to zero.

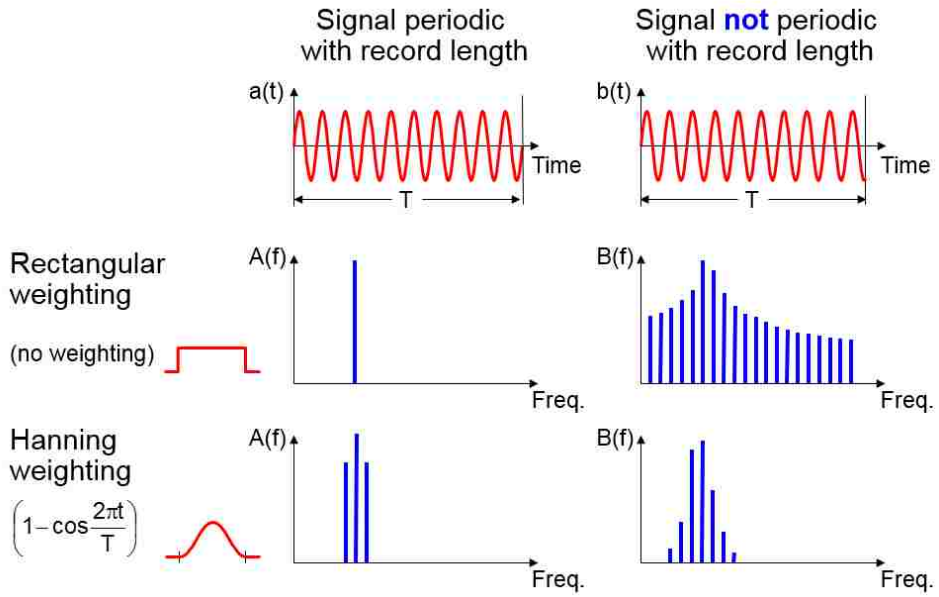

Figure 23 - Time weighting on FFT time blocks [reprinted – 22]

Regardless of the size of the time block or available frequency resolution, the function of the FFT analyzer remains the same: that is, to transform time data, with a fixed time spacing, into a frequency spectrum. Signals that are periodic relative to the time

domain appear as peaks in the resulting frequency spectrum. Figure 24 shows a frequency spectrum as calculated by an FFT analyzer for a 6-cylinder engine operating at a constant speed.

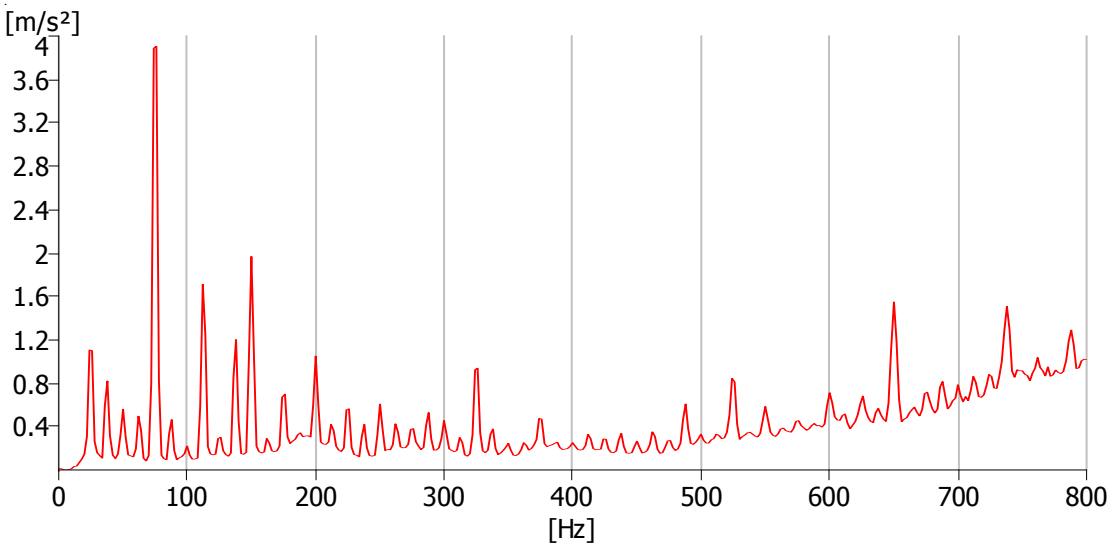

Figure 24 - Typical FFT spectrum

3.3.3.4 Order

Another type of "Block" analysis is the order analyzer. The calculation used in the order analyzer is the same as that of the FFT. However, rather than taking a sample block relative to a fixed time, the order analyzer takes a sample block relative to the number of revolutions of a rotating component. This is primarily used for rotating machinery measurements where the focus of the study is on harmonics relative to shaft speed. Since this type of analysis is sampled based on shaft speed, the results are always consistent relative to the shaft speed.

In order to have synchronous sampling with the speed of a drive shaft, shaft speed must be measured. This is typically done using a tachometer. A tachometer, commonly

referred to as a tach, can be a single pulse per revolution or multiple pulses per revolution. The resulting output of a tach signal is typically a square wave or "pulse" signal. This signal will provide the order analyzer with the required angular position, angular speed, and acceleration information that is needed to synchronize the time sample to shaft rotation.

Like the FFT, the number of lines of resolution determines the block length required. Unlike the FFT, which has a fixed time length for its block size, the order analyzer has a fixed number of revolutions. This means that if higher order resolution is desired, more revolutions are needed to complete one data block. This gives the order analyzer an advantage over the FFT analyzer for use with rotating machinery. Since the number of revolutions for a data block is fixed, the results are consistent throughout the entire operating speed range regardless of the rate of acceleration of shaft speed. The FFT analyzer uses a constant time block size which does not account for any changes in speed. Therefore, at higher shaft speeds or in the cases of rapid acceleration, the FFT analyzer might not produce consistent results, as the shaft speed may change significantly within the constraints of a single time block.

The order spectrum represents the order, or the number of times the signal is periodic during one complete revolution, on the X-axis. The first order is related to any event that happens once per revolution. An out of balance shaft will have a high amplitude first order value. The second order is related to events that happen twice during one revolution of the shaft. A two-blade aircraft propeller is a good example of second order, as a blade pass event occurs twice per single revolution at any stationary point relative to the shaft centerline.

In the context of the 4-stroke internal combustion engines, it takes two complete revolutions for a single cylinder in an engine to make a complete combustion cycle. Since combustion is the primary force of noise and vibration of an engine, and it happens every other revolution, it can be described as 0.5-order for a single cylinder engine. In a multi-cylinder engine, the order for the combustion can be seen as 0.5 x the number of cylinders. Since engines are usually designed to have equally spaced combustion timing, a 6-cylinder engine will have three cylinders on the compression/power stroke while the other three cylinders are on the exhaust/intake stroke. This can be described as 3rd order as the combustion event happens three times per crankshaft revolution. Figure 25 shows an order spectrum of a 6-cylinder engine.

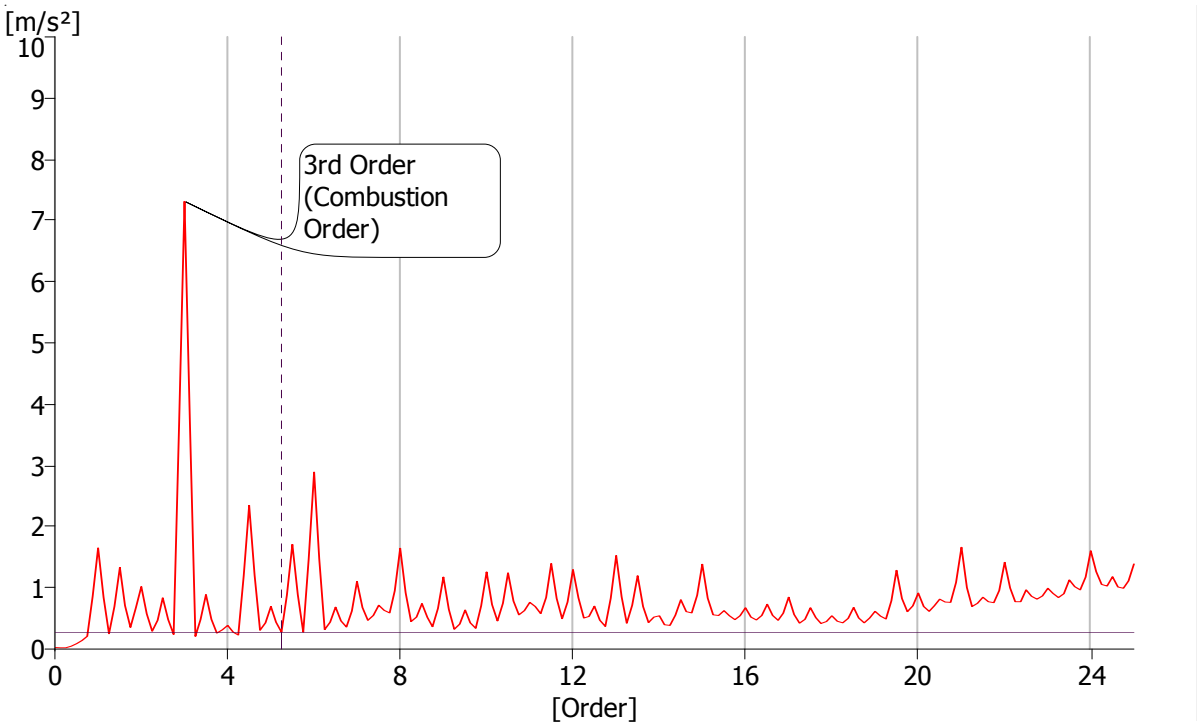

Figure 25 - Typical order spectrum

CHAPTER 4: EXPERIMENT DETAILS

There are two options to perform operational measurements on an internal combustion engine. These being in-situ or with an engine dynamometer (dyno). There are both advantages and disadvantages with both options.

In-situ measurements provide real world conditions, allowing the engine to be operated in the vehicle and on the road as it would be in daily service. This type of setup is not always the most efficient for engine development programs as there are variables that cannot be controlled such as weather, traffic, and track conditions, which can lead to delays in testing. It is also difficult to get full access to the parts on the engine depending on the packaging of the engine in the vehicle engine compartment. This leads to difficulties in instrumentation as well as part changes, both of which can result in longer down time between tests.

Engine Dynamometer testing does not always provide exactly the same results as operating the engine in vehicle, as the full effects of variables such as the driveline and road input conditions are not available. However, the lack of these variables is often very desirable as it allows the focus to be placed on the performance characteristics of the engine. Engine dynamometer controllers can be programmed to run simulated real world conditions as well as conditions beyond the capability of a test vehicle, in an environment not affected by uncontrollable climate conditions.

For the development of the engine used in this study, North American Repower chose to use the dyno testing facilities at McLaren. McLaren has a dedicated test cell configured for CNG engines. This test cell is a single engine, single dyno test cell capable of performing a wide number of conditions. Brüel & Kjær provided the noise and vibration measurement equipment that was used to acquire and analyze the data used in this experiment. Data was acquired using four different engine calibrations. Each calibration was configured for a certain horsepower and torque rating for specific end user applications. Both steady state (constant rpm) and speed sweeps (increasing rpm) we used at various load conditions. The following provides full details on the test setup and conditions measured during the experiments.

4.1 Experimental Engine and Dynamometer Setup

All of the engine and dyno test cell configurations were designed and set up by North American Repower and McLaren. This section will describe the details related to the engine and dyno side of the experiment.

4.1.1 Engine

North American Repower provided the engine which was an International DT466 6-cylinder diesel engine that has been converted to operate on methane and compressed natural gas. In order for the engine to operate using CNG as a fuel, the following modifications were made with a complete rebuild:

- Throttle Body Injection / Injector Housing
- Modified Cylinder head for Spark Plug ports
- New ECU and ignition system plus Wiring Harness
- Recirculation/Blow off Valve
- New Fuel Delivery System
- Modified Intake Manifold
- New Valves, Valve Guides and seats
- NAR spec Pistons and Rings
- NAR spec Intake and Valve cover gasket

The general specifications of the engine after conversion are as listed:

- Engine: International DT466 308, Dedicated Lean Burn Natural Gas Conversion
- Type: Turbocharged, 6-cylinder
- Engine Displacement: 7.6L
- Compression Ratio 12:1
- Max Power: 250HP (2200 RPM)
- Max Torque: 660 ft-lb (1500 RPM)
- Emission: EPA
- Injection System: Single Point Electronic Fuel Injection

4.1.2 Engine Test Stand

Most engine dyno test cells use an engine test cart to mount the engine test fixture to prior to being placed in the test cell (Figure 26). This allows for easy access to the engine and test stand for fabrication work and also allows the engine dyno to operate one engine while the next is being prepared.

Figure 26 - Engine on test cart

In an effort to keep the dyno test engine as close to the vehicle condition as possible, a large section of the truck frame was modified to fit on the dyno test cart. This allowed the engine to be mounted using the factory engine mounts, and also insured that the correct orientation regarding pitch, yaw, and roll relative to the in-vehicle application would be properly met. The standard engine bell housing and clutch were used with an adapter to couple the clutch with the dyno input shaft. This can be seen with the engine and test stand located in the dyno test cell (Figure 27).

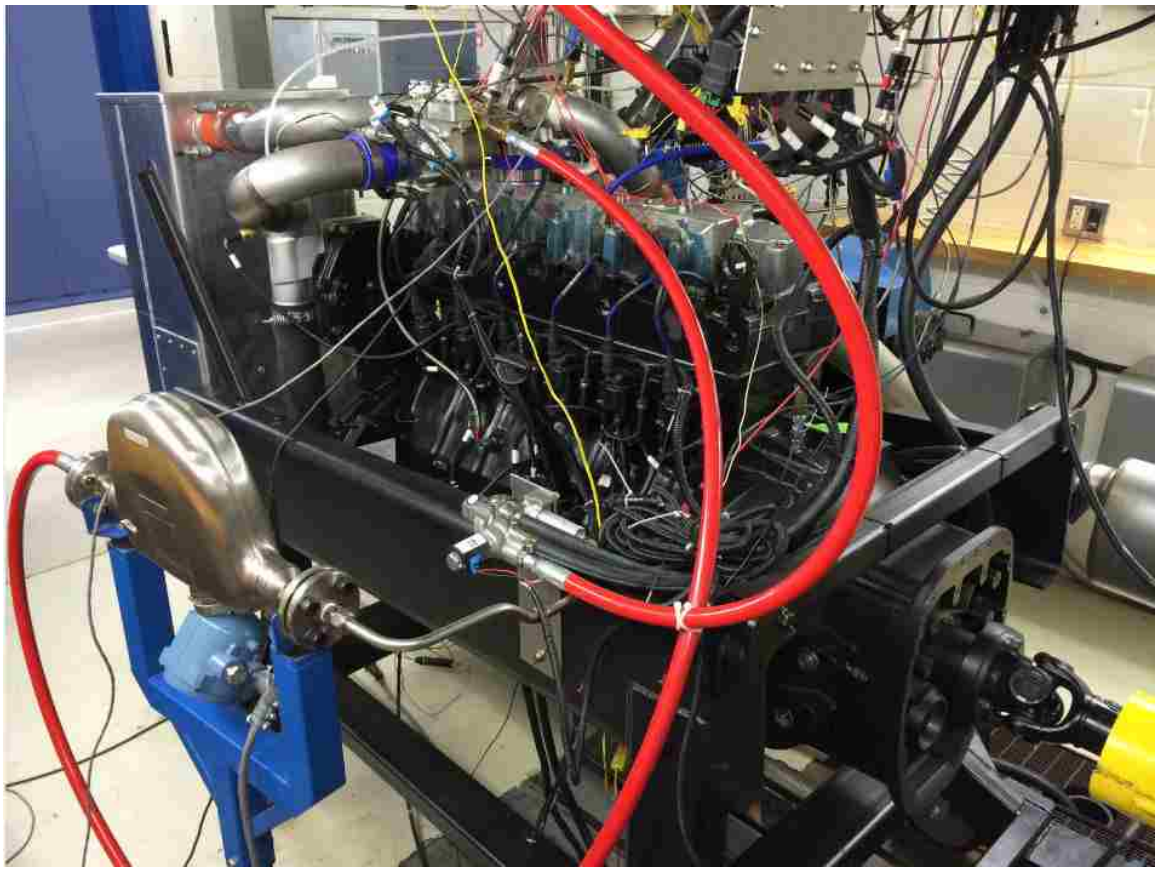

Figure 27 - Engine in test cell

4.1.3 Dynamometer and Controls

The engine was coupled to a Froude AG 250 eddy current dynamometer. The AG 250 dyno can only apply resistance to the engine up to 335 hp and 1200 Nm up to a maximum speed of 6,000 rpm. A Dynlok controller was used in conjunction with WinDyno as the data acquisition and control software.

4.2 Instrumentation and Data Acquisition

To measure the cylinder pressure and engine mount vibration, pressure transducers were mounted into the cylinders' heads and accelerometers were mounted to the engine side of the engine mount. This data was collected using a Brüel & Kjær LAN-XI data acquisition front end and Brüel & Kjær PULSE software. The data was recorded into a time file at a sample rate of 65.5 kHz. Along with the vibration and pressure channels, additional channels were required to understand the timing of events within the engine. A bolt-on angle encoder was placed on the crank pulley on the front of the engine, and a magnetic pickup was used on the ring gear of the flywheel to provide the angular position of the crankshaft during its revolution. Single pulse-per-revolution laser tachometers where used to determine the 0-degree position, and a clip-on inductive pickup was used on the spark plug wire to indicate when spark current was sent to cylinder 1.

4.2.1 Engine Mount Vibration

To measure the engine mount vibration levels, Brüel & Kjær Type 4527 tri-axial accelerometers were mounted on the engine side of the engine mount. The Type 4527 accelerometer was chosen for this application due to its sensitivity of 1 mV/ms^{-2} and high temperature range of up to +180 degree Celsius. The accelerometers were fixed to the engine using dental cement due to its ability to withstand high temperatures and provide electrical isolation between the accelerometer and the engine block (Figure 28).

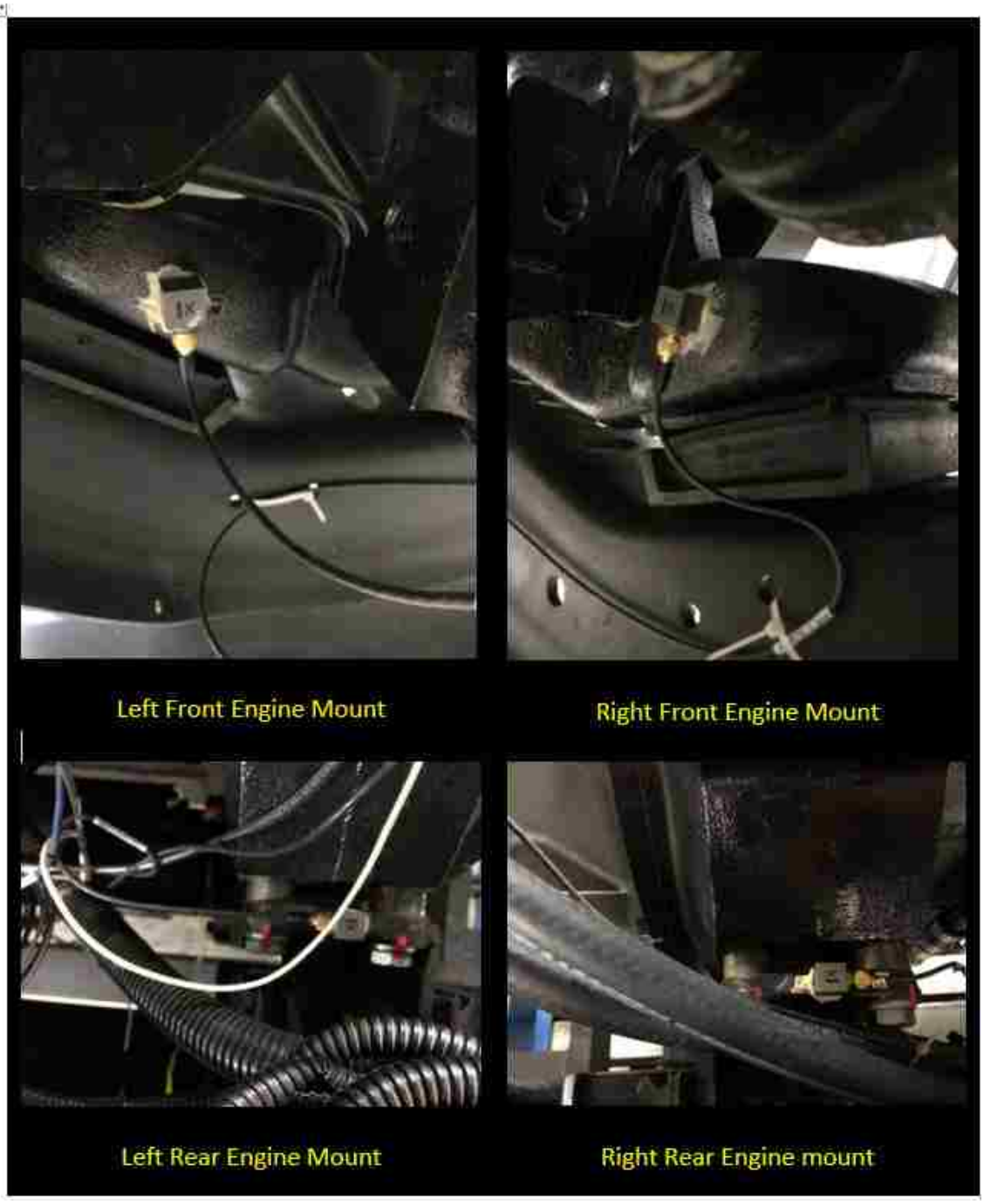

Figure 28 - Accelerometer mounting locations

4.2.2 Cylinder Pressure Transducers

There are two options available for cylinder pressure transducers for internal combustion engines. Spark plug pressure transducers are the simplest choice as they can be threaded easily into the spark plug hole on the cylinder head to provide a good pressure measurement. The drawback to a spark plug pressure transducer is that it replaces the proper plug for the engine, so it does not record the true cylinder pressure when different types of spark plugs are used. The alternative to the spark plug sensor is to mount a pressure transducer in a modified cylinder head.

The cylinder head was modified to support one Kistler 6053 pressure transducer. With the pressure transducer integrated into the head, the proper spark plug which was specified by NAR could be used for the test.

4.2.3 Engine Crankshaft Angular Position and Timing Indicators

Part of this experiment required investigation of the combustion pressure as measured by the cylinder pressure transducer. In order to properly see the effect of combustion on the cylinder pressure, it is generally viewed in the angle domain, as the pressure trace can be seen relative to crank shaft angular position rather than just a fixed time interval. For that to be possible, the angle information must be recorded.

To capture high resolution angle data, an AVL 365 angle encoder was mounted to the crank pulley. This is an optical transducer that reads a disc with 360 equally spaced

slots. This disc is fixed to the crank pulley and rotates with the engine, and the signal is read as the slots in the encoder disc break the light from the optical sensor.

An alternative to using a high resolution bolt-on encoder is to use the starter ring gear on the flywheel. With this method, a magnetic pickup can be used to pick up the flywheel's teeth passing during the engine operation. Resolution is limited to the number of teeth that are on the flywheel. This data was acquired as a backup during this study.

To capture the top dead center position of cylinder 1, a Brüel & Kjær Type 2981 laser tachometer was used. Reflective tape was placed on the crank pulley at the top dead center reference point. This was used to determine the 0-degree reference for the crank position.

A clip-on inductive pickup was placed on the spark plug wire for cylinder 1. This was later used to determine where in the cycle the 0-degree top dead center point was.

4.2.4 Data Acquisition and Sample Rate

All data taken during this experiment was digitally recorded using Brüel & Kjær PULSE LabShop software and a Brüel & Kjær LAN-XI front end for the purpose of processing at a later time. Special considerations were made when setting up the system to make the recording with regard to the fixed sample rate. Typically, digital data recorders are set up with a fixed sample rate of 2.56 x the highest frequency that is required during analysis. This factor of 2.56 is referred to as the Nyquist criteria [27].

For this experiment, the frequency range of interest for the vibration measurements was below 800 Hz, as those are the frequencies that can be classified as structure borne and

potentially contribute to the operator's comfort level. For 800 Hz, the minimum sample rate for the recording should be 2,048 kHz. If the goal of the test was just to measure vibration, then a 2,048 kHz sample rate would be used. However, some other factors were considered in determining the proper sample rate for the recording.

In order to examine the cylinder pressure traces with respect to the crankshaft's angular position, the tooth pass frequency of the encoders must be taken into account. In consideration of this, the maximum rotational speed of the engine is 2200 rpm. The high resolution encoder has 360 equally spaced pulses per revolution. This results in a tooth pass frequency of 13.2 kHz for the high resolution encoder. The settings in Pulse Labshop for the LAN-XI configuration that was used in this experiment allowed for the highest sample rate setting to be 65.5 kHz. This sample rate was good for recording data up to 25.6 kHz, which exceeded the requirements of this measurement. The second highest sample rate available was 32.8 kHz, which was only good up to an analyzed frequency of 12.8 kHz and therefore could not be used.

Part of the hardware setup configuration was a Brüel & Kjær Type 3056 LAN-XI module that has been developed for recording high resolution angular encoders such as what was used in this test. The 3056 has two dedicated channel pairs, with the first channel in the pair set up to sample the high resolution encoder at 1 MHz, and the second channel as a 0-degree reference. When the two are used together, the second channel will act as a trigger to start measuring angle at 0 degree with the first channel and continue for the full 360 degree of rotation when the high resolution encoder and the 0-degree mark line up again. This results in angle vs. time data collected at the point of entry during the data acquisition. This method is beneficial because it eliminates the need to post-process the 0-

360-degree angle information and adds the ability to use a lower sample rate based on the needed frequency range of the vibration and pressure channels. The reduction of the fixed sample rates across all of the channels allows for smaller file sizes and reduced processing times in the post-processing software.

For this experiment the 3056 module was used to acquire angle information at the point of entry. However, the data was still recorded at 65.5 kHz based on the needs of the angle encoder. This was done as a backup to ensure that the angle data was properly acquired.

4.3 Test Conditions

There are a number of test conditions that can be used to test internal combustion engines on an engine dynamometer. Generally, most tests are divided into two groups: steady state, during which the engine is held at a steady operating RPM while the measurement is taken; or speed sweeps, during which the engine is operated through a set range of engine speeds.

4.3.1 Steady State Conditions

Steady state test conditions offer some advantages as the test duration at a constant known speed and load can be held for a longer duration. Data acquisition for a particular condition can be started after the engine temperatures and pressures have had time to stabilize at that condition. Once the data acquisition is started, it can be allowed to continue averaging samples for any length of time, providing a stabilized result. In industry, this often leads to a single measurement being taken at a single condition. The disadvantage of

doing a steady state measurement is that it can be time-consuming if the measurement time is too long or if the engine requires a long time to stabilize between conditions.

For the case of this experiment, four 30-second steady state conditions were recorded and analyzed, as follows:

- 750 RPM, idle condition
- 1500 RPM, 15% throttle
- 1500 RPM, 50% throttle
- 1500 RPM, 100% throttle

The 750 RPM, idle condition was selected as it is the engine idle condition that is the normal "at rest" condition of the engine. This condition is seen in the vehicle's daily service when it sits at rest, not undergoing any motion. The 1500 RPM conditions were selected as they represent the operating speed of peak torque at 100% throttle, as well as the normal engine operating speed of the engine as it cruises on the highway for long durations. The throttle position was varied (15%, 50% and 100%) to determine the effect of loading on the vibration and cylinder pressures.

4.3.2 Speed Sweep Conditions

Speed sweep measurements are a method of collecting operating engine data through a set engine speed range while the data acquisition equipment plots the results relative to engine speed. For a speed sweep run-up measurement, the engine operates at a stable operating condition, and the dyno allows the speed of the engine to increase at a fixed rate until the maximum engine speed was obtained. For a run-down condition, the

operation is reversed: the start speed is at maximum engine speed while the stop speed is at the minimum speed. Typically, the throttle position is set throughout the entire speed range.

For this experiment a wide open throttle (WOT) sweep up and sweep down was performed. In WOT condition, the throttle position is at 100% open. This allows for maximum horsepower and torque to be obtained throughout the speed range. This data was used to confirm that the engine was operating properly from an engine performance standpoint as the horsepower and torque curves could be compared.

4.4 Test Variables

North American Repower provided four different engine calibration configurations to be used as the variables for the tests. Each calibration used different parameter settings, such as fuel quantity, injection and spark timing to control the power output of the engine. Three of the configurations are the planned calibrations for different applications of the production level engines to be made available to consumers and are denoted by the maximum horsepower and output torque capable of that calibration. The calibration configuration known as “Max Power” is not intended to be made available for production, rather to be used for development and for their durability qualification tests. Throughout this study, the different calibrations will be referred to as follows.

Configuration 1 – Max Power

Configuration 2 – 230 HP / 660 ft-lb

Configuration 3 – 210 HP / 520 ft-lb

Configuration 4 – 190 HP / 420 ft-lb

4.5 Test Sequence

The engine control module (ECM) allows for only one calibration to be used at a time. As such, the process used to acquire all of the data consisted of repeating the following steps for each configuration.

1. Flash calibration configuration into ECM
2. Start engine and warm up to proper operating temperature (180 degrees F)
3. Return to idle
4. Acquire data for WOT sweep
5. Acquire Idle condition steady state- 30 sec
6. Acquire 1500 rpm 15% throttle steady state – 30 sec
7. Acquire 1500 rpm 50% throttle steady state – 30 sec
8. Acquire 1500 rpm 100% throttle (WOT) steady state – 30 sec
9. Return to idle for cool down
10. Shut down

This sequence was repeated 5 times for Configuration 1 (Max Power) to confirm repeatability and to understand the variability within a single calibration configuration. A single set of data was acquired for each of the remaining configurations due to the results of the repeatability study, which will be discussed in the following chapter.

CHAPTER 5: DATA ANALYSIS

5.1 General Analysis

Upon completion of the data acquisition in the dyno test cell, as mentioned in the previous chapter, analysis of the data was carried out. The vibration, pressure and angle encoder channels that were acquired using Brüel & Kjær PULSE Labshop software were post-processed using Brüel & Kjær PULSE Reflex software. Microsoft Excel was used for further calculations and plot comparisons as needed.

In an effort to understand the overall vibration at each mount location, a root sum square (RSS) or "Vector Summation" calculation was made. This calculation combines the individual signals of each axis of an accelerometer to produce a single value representative of the magnitude of the vibration. This calculation is performed during the processing as:

$$\text{RSS Result} = \sqrt{(x^2 + y^2 + z^2)}$$

The data plots and graphs shown in this chapter will be a sample of typical results or an important comparison. In general, unless otherwise noted, the 1500 rpm 100% throttle comparisons will be shown in the main body of this chapter as they tend to show the greatest differences between the various calibration configurations. All data is made available in the Appendices

5.2 Engine Performance Confirmation

At the time of testing, the engine calibration configurations were still in development. In order to confirm the actual performance of each calibration configuration, output power and torque curves were acquired in a WOT sweep from 1000 to 2200 rpm (Figures 29 and 30 respectively).

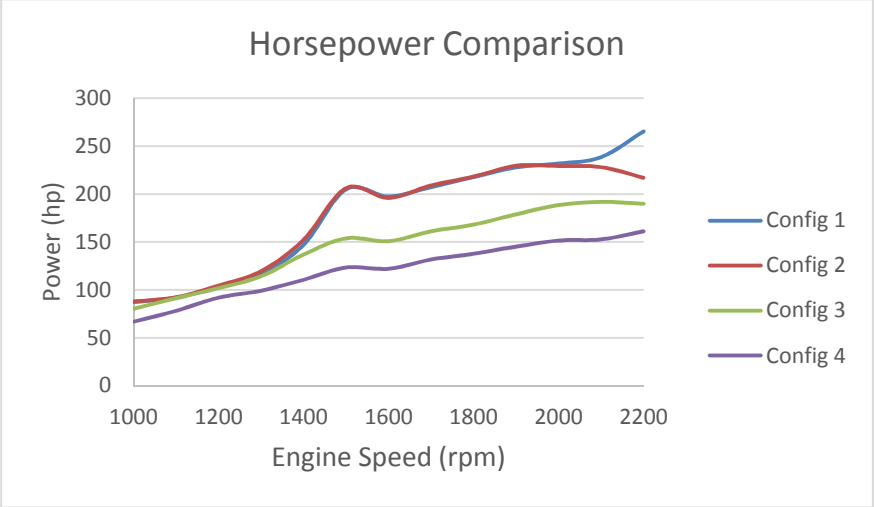

Figure 29 - Calibration configuration power comparison

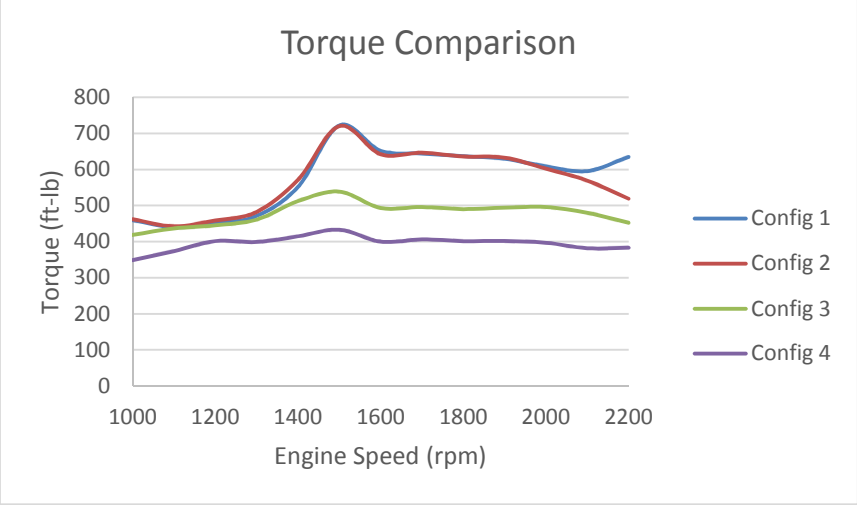

Figure 30 - Calibration configuration torque comparison

It is noted that the actual output from the engine differs slightly from the target output for the calibrations. In general, the peak torque output was higher than the target set for all three of the proposed production calibrations, while peak horsepower was lower than the target for the calibration configurations 3 and 4. At the time of the measurements, it was understood that further development was needed to tune the calibrations to the expected levels.

The actual horsepower and torque values of the steady state test conditions are listed in Table 1.

Calibration Configuration	750 RPM Idle (hp / ft-lb)	1500 RPM 15% Throttle (hp / ft-lb)	1500 RPM 50% Throttle (hp / ft-lb)	1500 RPM 100% Throttle (hp / ft-lb)
1 (Max Power)	0.5 / 3.5	22 / 77	135 / 471	205 / 721
2 (230-660)	0.4 / 3	20 / 71	106 / 373	202 / 705
3 (210-520)	0.5 / 3.4	16 / 56	79 / 276	150 / 526
4 (190-420)	0.5 / 3.7	15 / 51	64 / 226	124 / 432

Table 1 - Horsepower and torque as tested

5.3 Data Repeatability and Variability

As typical in industry, engine vibration measurements are commonly acquired and processed using computer-based signal analysis systems. For steady state measurements, it is common to take 20- to 60-second averaging times, resulting in a stable measurement. It is uncommon for multiple steady-state recordings to be made for a single steady-state condition [29].

There is a need to confirm the repeatability and variability of the measured vibration results at each of the steady-state operating conditions. This will allow for the determination if the differences seen in the measured results are due to variability inherent in the operation of the engine, or if they are actual differences between the engine calibration configurations. A single calibration configuration was used to acquire the vibration at the four operating conditions.

To determine the variability of the measurements at steady-state conditions, the maximum power calibration configuration of the engine was run until normal operating temperatures and pressures were obtained. The engine was brought down to the first condition of 750 rpm idle and a 30-second recording was made. Upon completion of condition 1, the engine was brought to the second condition of 1500 rpm and 15% throttle, and a 30-second recording was made. The engine condition was then changed to 1500 rpm and 50% throttle, and a 30-second recording was made. Upon completion of condition 3 the engine was adjusted to 1500 rpm and 100% throttle for another 30-second recording. Upon completion of the fourth condition, the engine was returned to idle condition and the test sequence was repeated four more times until a total of five measurements for each operating condition was recorded.

The test sequence was as follows:

	Measurement Sequence				
750 rpm Idle	1	5	9	13	17
1500 rpm 15% Throttle	2	6	10	14	18
1500 rpm 50% Throttle	3	7	11	15	19
1500 rpm 100% Throttle	4	8	12	16	20

Table 2 - Repeatability validation test sequence

Upon completion of the test sequence, the data was processed using PULSE Reflex software for both 1/3 octave analysis as well as order domain analysis. The results were exported to Excel and the standard deviation and confidence interval of each condition were calculated.

The standard deviation of the five runs at each engine mount location for each of the operating conditions was calculated using the formula

$$S_x = \sqrt{\frac{\sum(x - \bar{x})^2}{(n-1)}}$$

Where:

S_x = Standard deviation of the data set

x = Individual test result

$\bar{x}$ = Mean value of test results

n = Number of samples

The standard deviation of the five runs was plotted along with the five-run average for all of the conditions. Figure 31 shows a typical comparison of the third-octave data and Figure 32 shows a typical comparison of the order domain data. The data for all of the conditions is located in Appendix B.

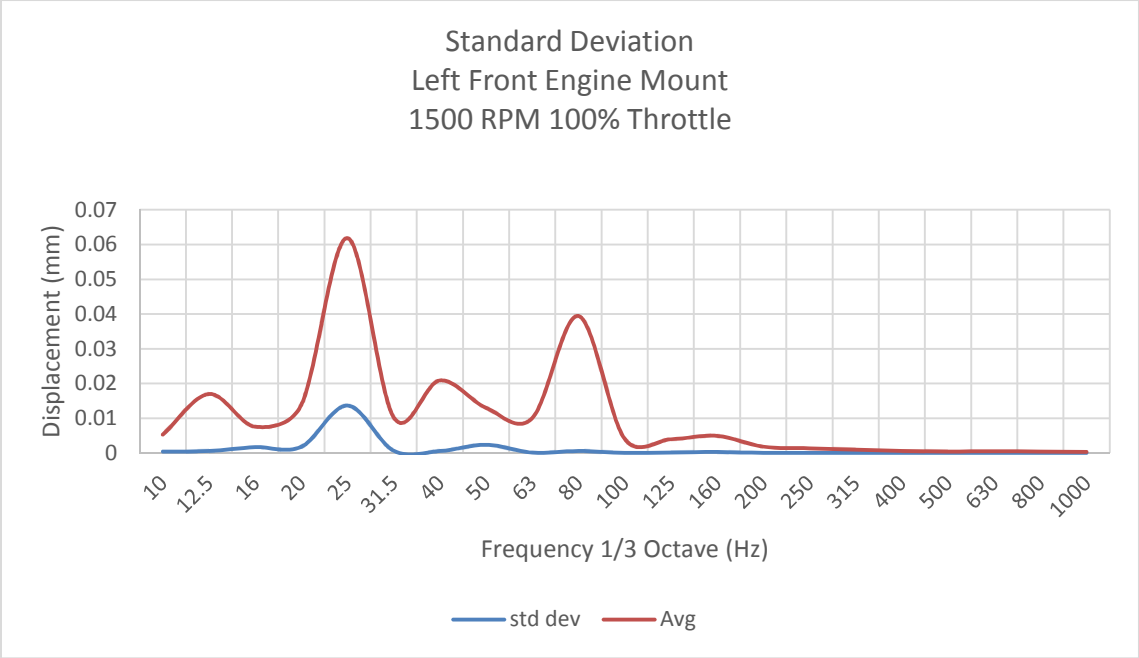

Figure 31 - Typical standard deviation compared against the five-run average in 1/3 octave

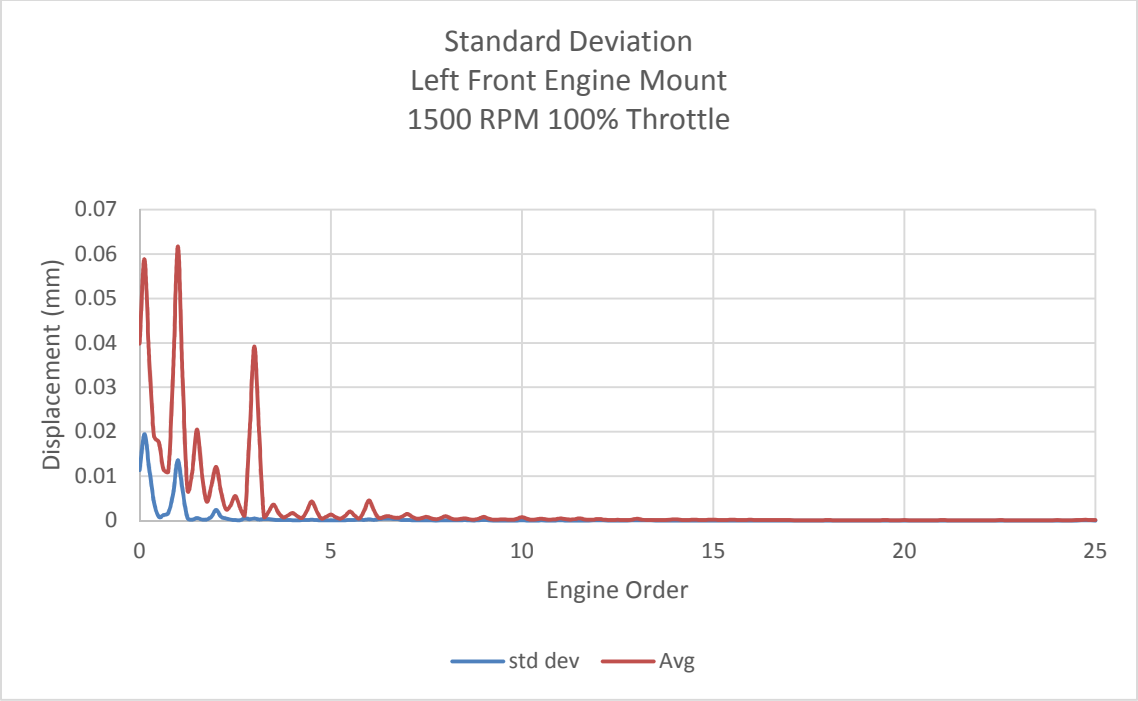

Figure 32 - Typical standard deviation compared against the five-run average in order domain

A confidence interval for each mount location was calculated to determine the range of possible true mean values for each test condition. The confidence interval calculation was based on an assumption of 99% confidence. This was chosen as it results in a wider confidence interval which encompasses a larger margin of error that the sample size of five samples might have missed. The confidence interval was calculated using the formula:

$$CI = \bar{x} \mp 2.58 \left(\frac{S_x}{n^2}\right)$$

Where

CI = Confidence interval

$\bar{x}$ = Mean value of test results

Sx = Standard deviation of the data set

n = Sample size

The upper and lower limits as calculated by the confidence interval were plotted for both the third-octave (Figure 33) data as well as the order domain data (Figure 34). The area between the upper limit (orange line) and the lower limit (blue line) indicates the range of possible true mean values using 99% confidence based on the sample data measured. In other words, if thousands of data samples were taken and averaged, it could be stated with 99% confidence that this true mean vibration value would fall within the confidence interval calculated using the available five data samples. The wider the spread between the upper and lower limit of the confidence interval, the less repeatability from one sample to another. The complete data set is given in Appendix C.

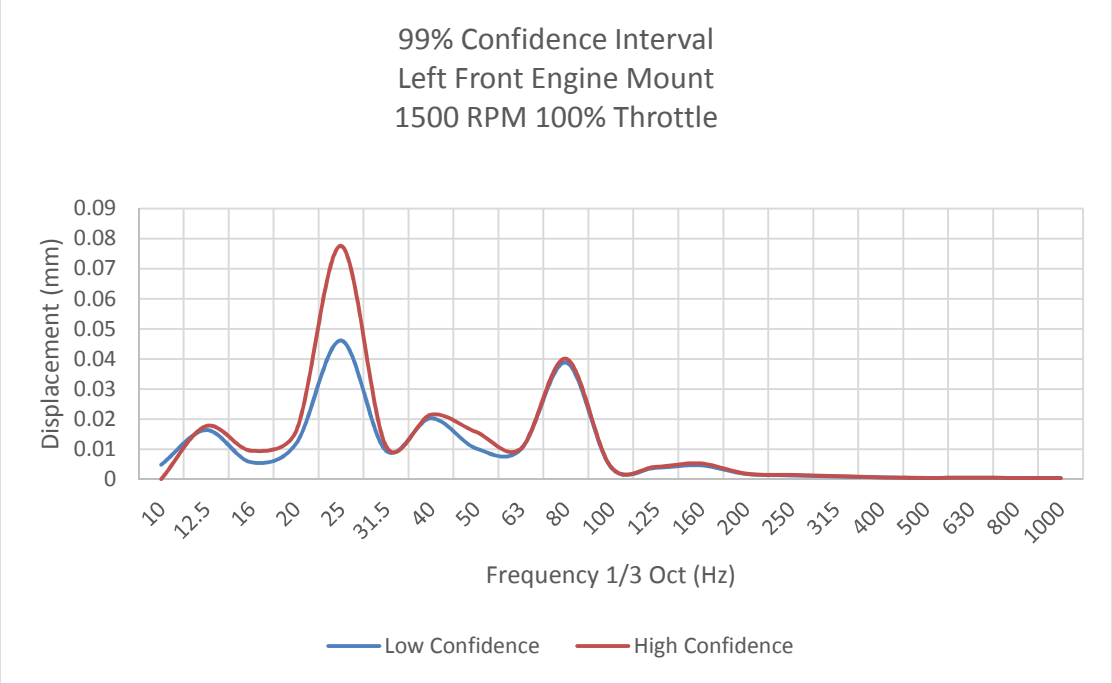

Figure 33 - Typical 99% confidence level for 1/3 octave

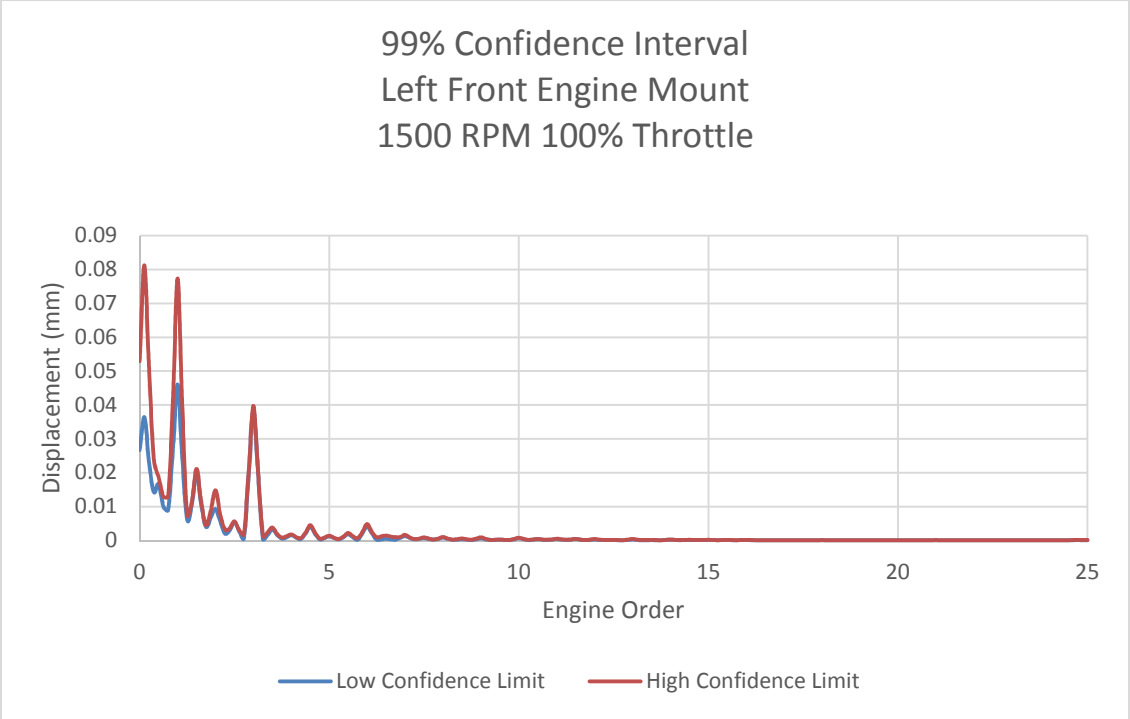

Figure 34 - Typical 99% confidence level for order domain

5.4 Cylinder Pressure

Cylinder pressure data was acquired in each of the 6 cylinders at all of the operating conditions. This data was analyzed using PULSE Reflex Angle Domain software to convert the complete 30-second time history into angle domain. Transforming the data from time domain to angle domain allows the cylinder pressure to be compared relative to the angular position of the crank shaft. This also allows for the data to be sectioned into individual engine duty cycles, therefore separating the time data into 0-720 degree increments. This allows for accurate event timing relative to the crank position and therefore is unaffected by the rotational speed fluctuation inherent to internal combustion engines.

5.4.1 Cycle to Cycle Fluctuation

Chapter 3 discussed the issue of cycle-to-cycle fluctuations in internal combustion engines. The cylinder pressure traces for all cycles of all of the cylinders at a single test condition can be seen in Figure 35 revealing the inherent cycle-to-cycle fluctuation. Although the investigation of this fluctuation is beyond the scope of this investigation, the variation between cycles confirms the need to calculate the average of each cylinder's pressure trace for all of the cycles in measurement for reporting and comparison purposes. Appendix D reports all of the cycle-to-cycle variation data.

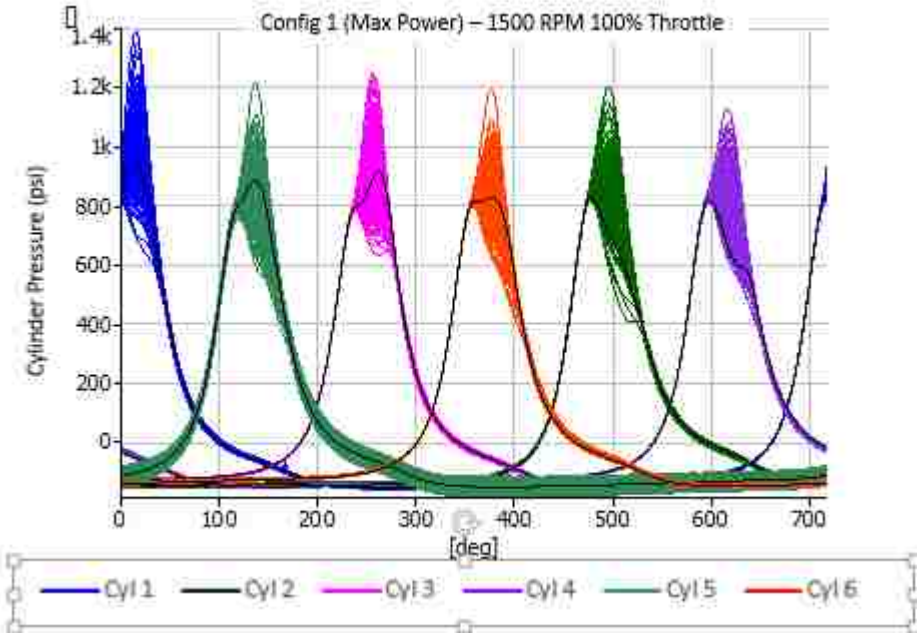

Figure 35 - Typical cycle-to-cycle fluctuation

5.4.2 Maximum Pressure, Pmax

Once the cylinder pressure data was converted to angle domain, all of the cycles of each individual cylinder were averaged together for the duration of the recording. A typical

example of the averaged cylinder pressure data can be seen in Figure 36. The complete data for each of the operating conditions is in Appendix E.

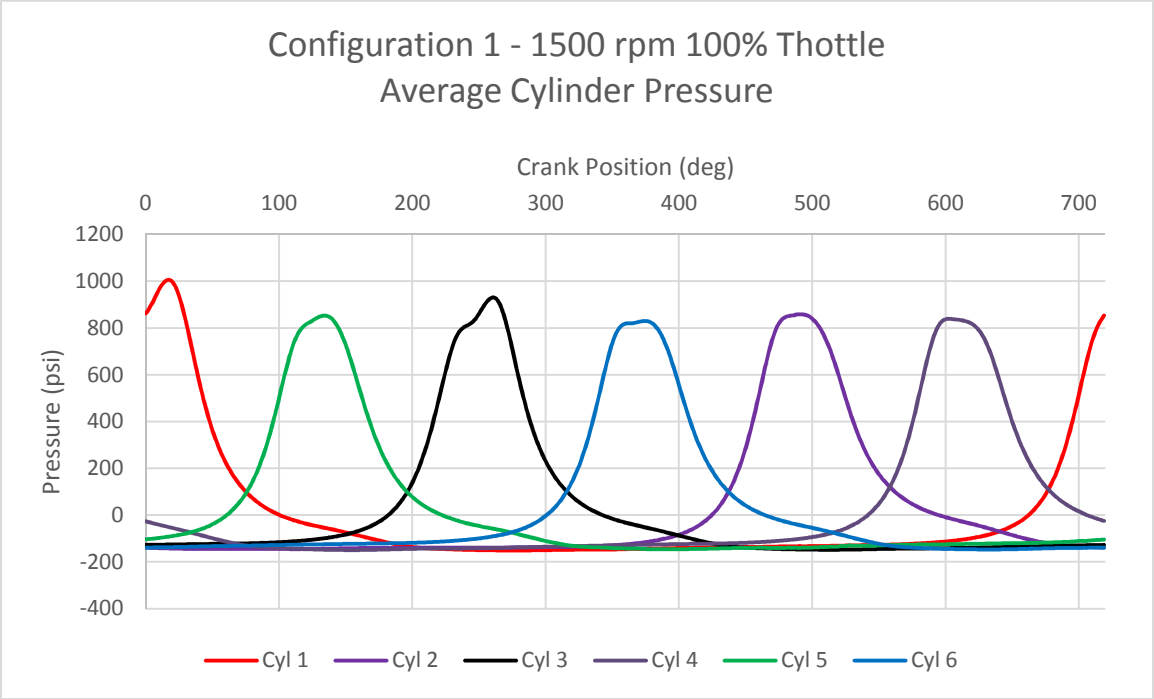

Figure 36 - Average cylinder pressure relative to crank angle

For each test condition, the maximum cylinder pressure of all 6 cylinders was averaged together to provide a single maximum pressure (Pmax) value representative of that condition. The results for all of the conditions are listed in Table 3.

	Pmax (psi)			
Configuration	750 RPM Idle	1500 RPM 15% Throttle	1500 RPM 50% Throttle	1500 RPM 100% Throttle
1 (Max Power)	107.28	197.59	597.64	886.20
2 (230-660)	110.22	187.40	498.19	874.45
3 (210-520)	111.96	177.90	387.19	676.14
4 (190-420)	112.84	172.69	337.60	565.51

Table 3 - Average maximum pressure (Pmax) for all conditions

5.4.3 Maximum Pressure Rise Rate, MPRR

The rate of cylinder pressure change relative to crank angle was calculated for each condition in Excel from the averaged cylinder pressure data discussed in the previous section. Figure 37 shows a typical example of the average maximum pressure rise rate. Complete results are shown in Appendix F.

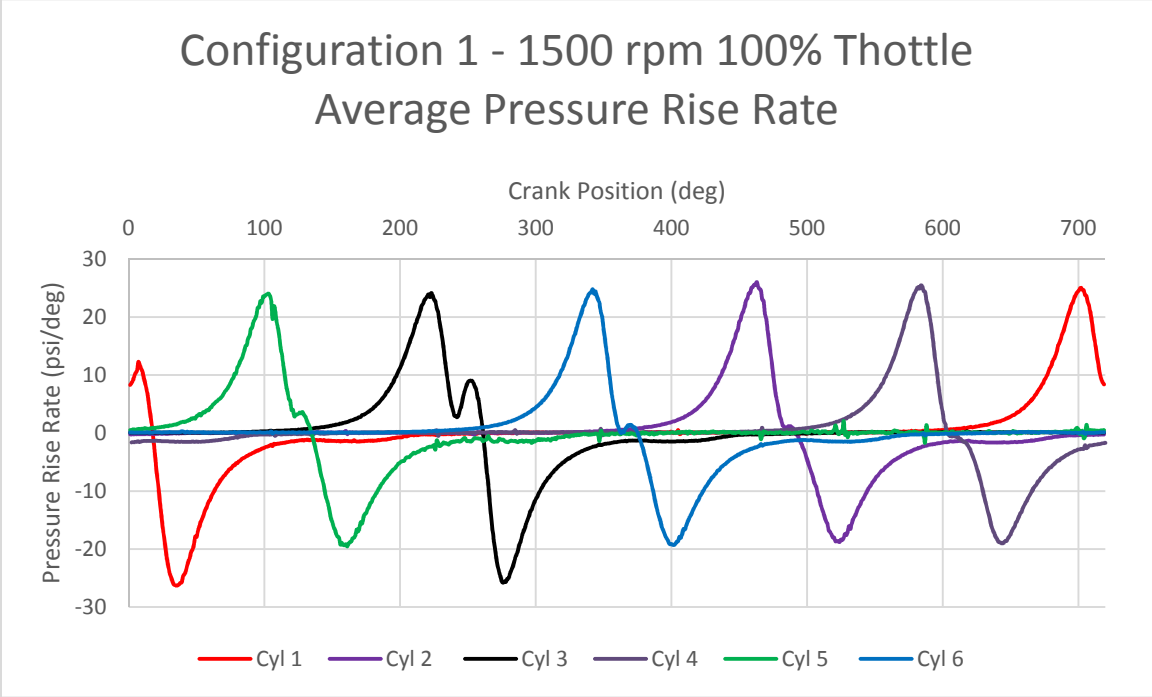

Figure 37 - Typical average maximum pressure rise rate

For each test condition, the maximum pressure rise rate of all 6 cylinders was averaged together to provide a single maximum pressure rise rate (MPRR) value representative of that condition. The results for all of the conditions are listed in Table 4.

	MPRR (psi/deg.)			
Configuration	750 RPM Idle	1500 RPM 15% Throttle	1500 RPM 50% Throttle	1500 RPM 100% Throttle
1 (Max Power)	3.21	5.73	16.91	24.91
2 (230-660)	3.29	5.34	13.72	24.23
3 (210-520)	3.33	5.08	11.31	18.93
4 (190-420)	3.36	4.90	9.98	15.82

Table 4 - Average maximum pressure rise rate (MPRR)

5.5 Vibration Analysis

The vibration channels were processed a using a variety of analysis methods as discussed in chapter 3. Overall level, 1/3 octave, order analysis and fast Fourier transform (FFT) were used to process the data.

Several decisions were made regarding the parameters used in the data processing based on the information covered in Chapters 2 and 3. These parameter settings will be used throughout the entire analysis unless otherwise noted. Since the focus of the study is based on the structure-borne noise and vibration transferring through the engine mounts, the vibration data is represented in terms of displacement. The upper limit of the frequency range is 800 Hz. Some considerations were made regarding the lower frequency limits as recommended by the study by Suh [8]. A high-pass filter was applied to the data to remove the first-order content typically associated with the vibration present due to imbalance within the rotating assembly. For the 750 rpm condition a high-pass filter of 20 Hz was used, while a filter of 40 Hz used for the 1500 rpm condition.

5.5.1 Overall Level Analysis

The vibration data was analyzed using the overall level analyzer as described in chapter 3. The result of this type of analysis is a single value quantifying the sum of the vibration within the frequency range of interest.

The overall level results for the idle and 15% throttle conditions, Figures 38 and 39, do not show any distinct trends relative to the calibration configuration that is represented. The results show some difference between the levels represented at each mount location. At the 750 RPM Idle condition the left side mounts exhibit higher vibration levels than the right side mounts, as shown in Figure 38. The 15% throttle condition shows higher vibration levels on the front mounts as compared to the rear mounts, show in Figure 39.

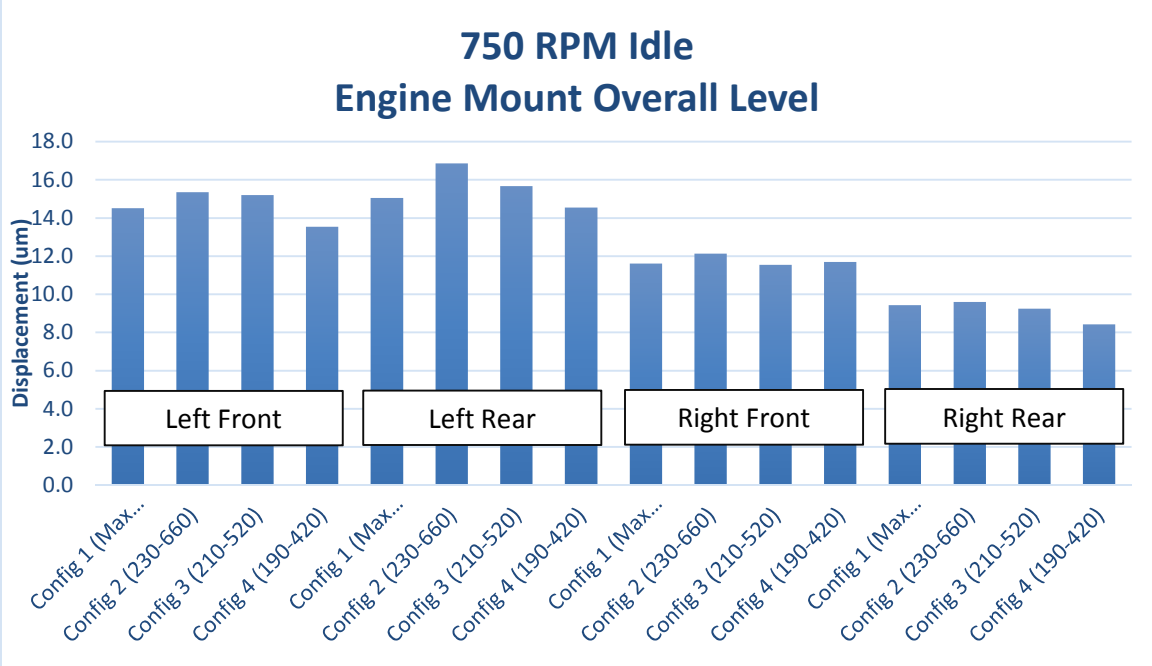

Figure 38 - Overall Level, 750 RPM Idle

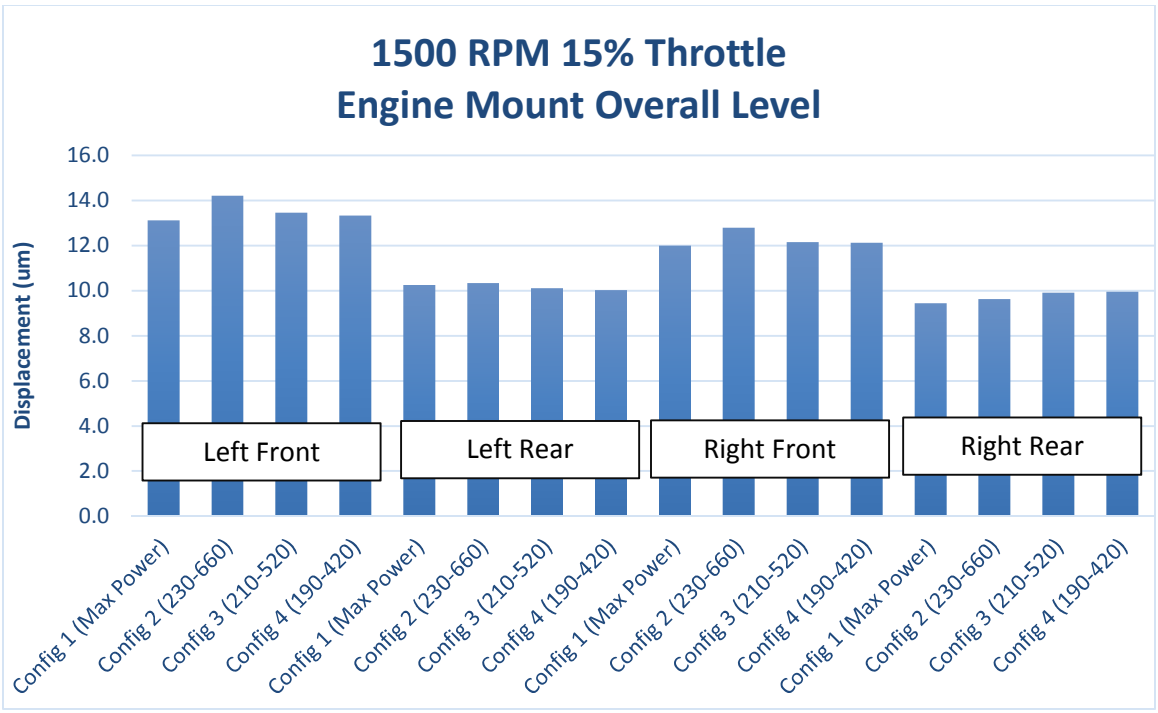

Figure 39 - Overall Level, 1500 RPM, 15% Throttle

The overall vibration levels for the 50% and 100% throttle conditions at 1500 RPM, Figures 40 and 41, show two distinct trends. The overall vibration levels tend to decrease as the rated power level of the calibration configuration is reduced. It can also be seen that the front mounts experience higher vibration levels than the rear mounts.

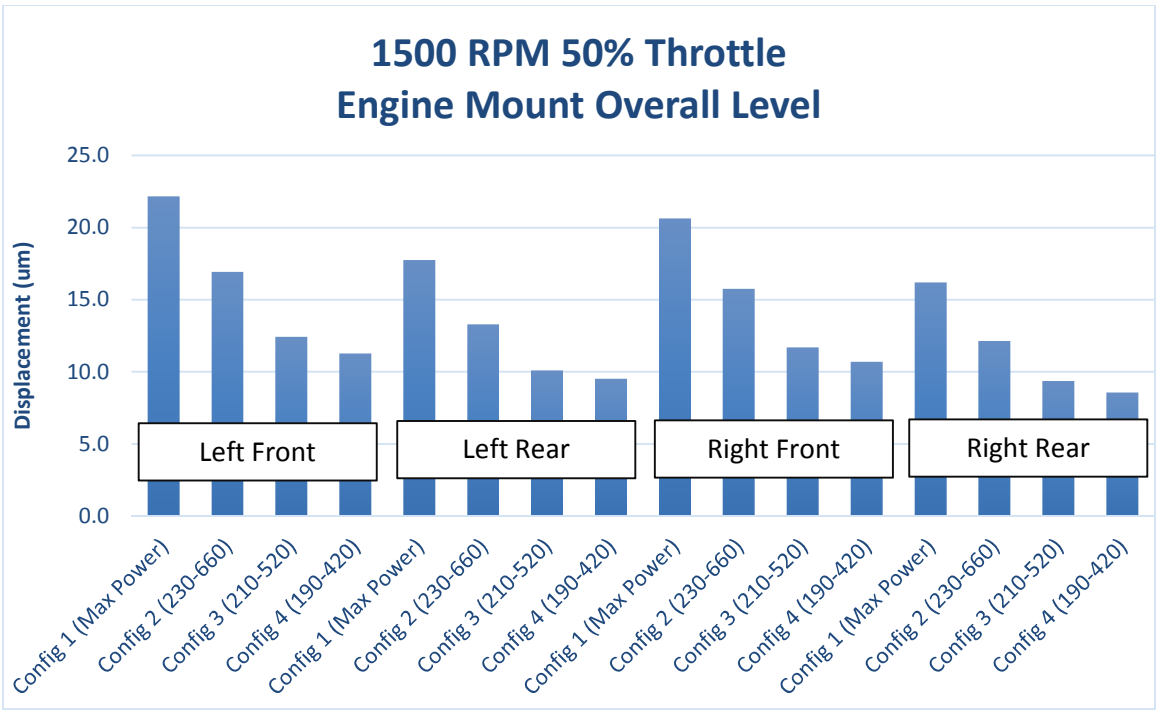

Figure 40 - Overall Level, 1500 RPM 50% Throttle

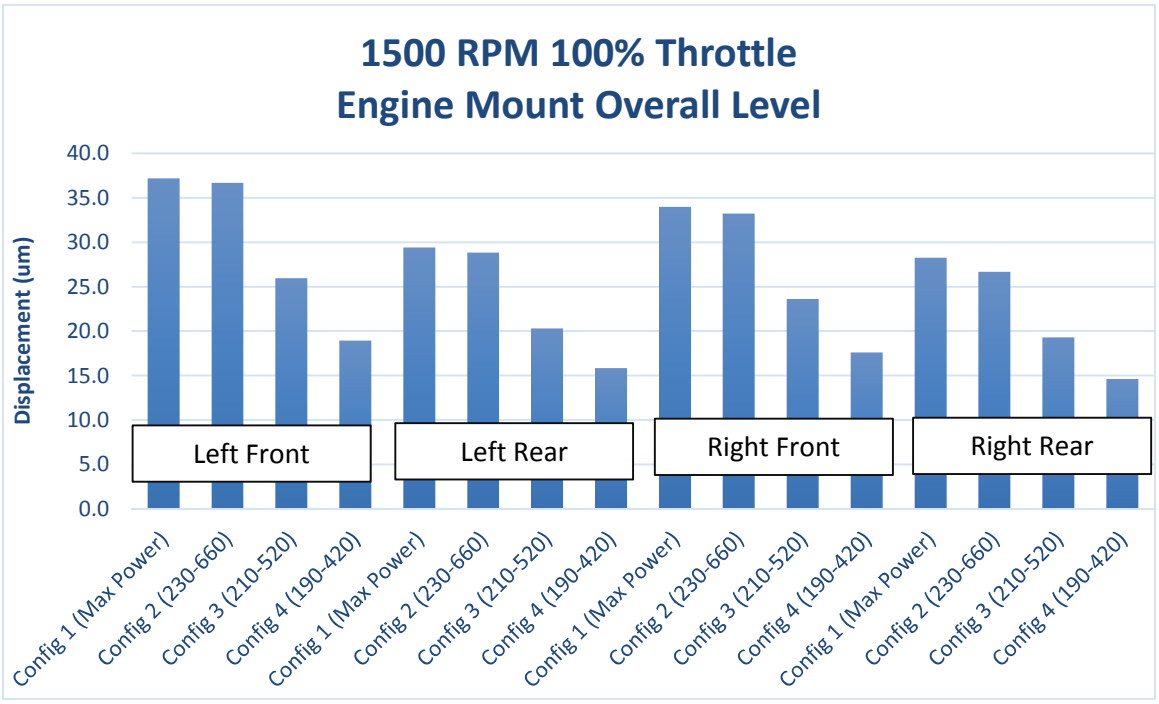

Figure 41 - Overall Level, 1500 RPM 100% Throttle

5.5.2 Constant Percentage Bandwidth: 1/3 Octave Analysis

For the vibration analysis using the constant percentage bandwidth analysis, 1/3 octave frequency resolution was selected. It understood that a 1/12 or 1/24 octave frequency would provide higher resolution, however, to be consistent with the papers reviewed in chapter 3 [13, 17], 1/3 octave analysis was used. Some of the notable results will be reported in this section. The complete data set is available in Appendix G.

Figure 42 shows the 1/3 octave analysis of each operating condition compared at each mount location for a single calibration configuration. Each mount location shows similar displacement at each respective operating condition.

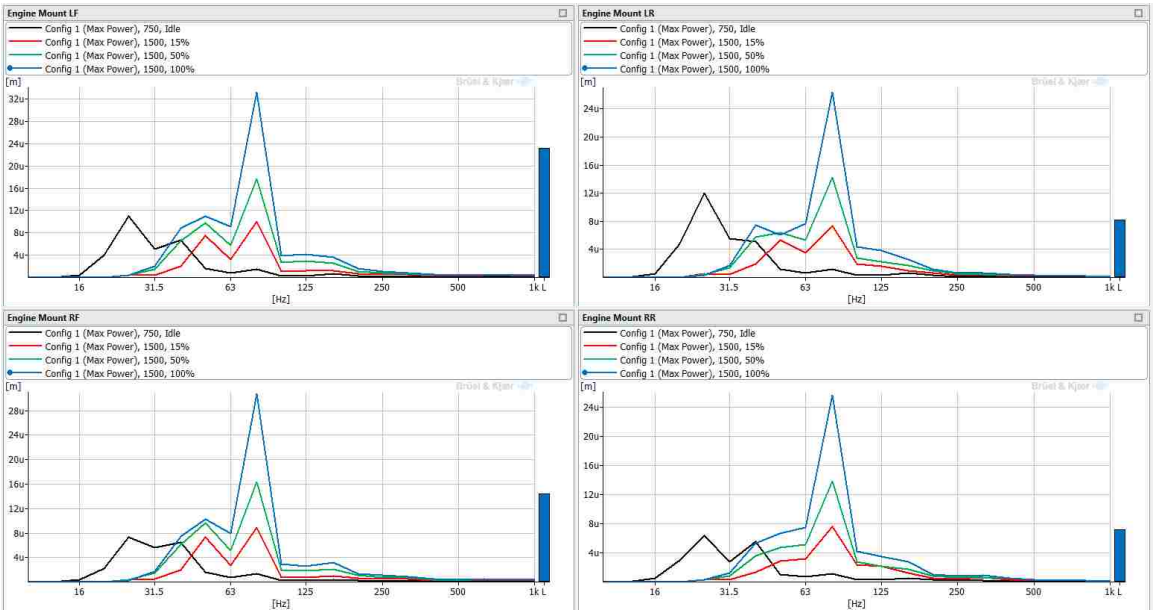

Figure 42 - 1/3 Octave analysis of a single calibration configuration at all operating conditions at each mount

A comparison of a single mount location for all configurations at a single operating condition shows each trace on the graph to have two distinct peaks, shown in Figure 43. The frequency at each peak is directly related to the operating speed of the engine. At 750 RPM the fundamental rotational frequency is 12.5 Hz. The first significant peak for the 750 RPM operating condition is 25 Hz which is twice the rotational frequency, or second harmonic. The second significant peak of the 750 RPM condition is 40 Hz which is approximately 3x the rotational frequency, or third harmonic.

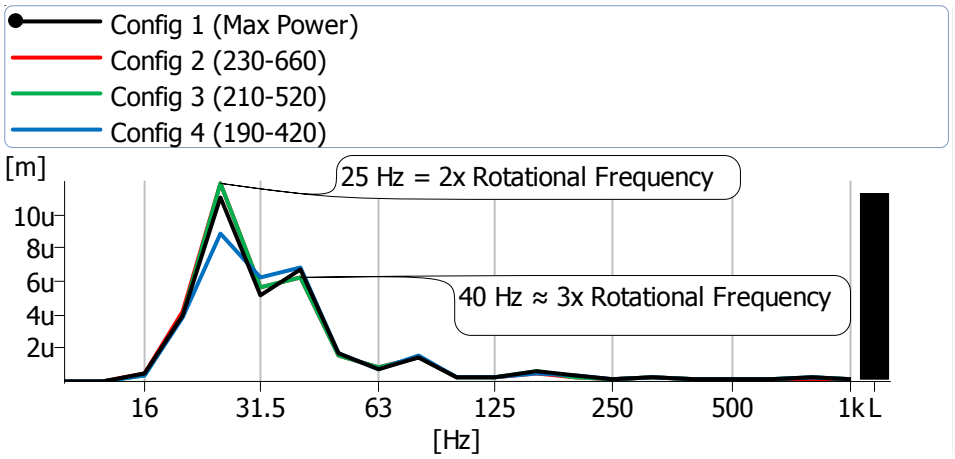

Figure 43 - Calibration comparison, left front engine mount, 750 rpm, idle

Figure 44 shows a comparison of all of the calibration configurations at a single 1500 RPM operating condition. This comparison is typical of all of the 1500 RPM operating conditions as the first peak is 50 Hz, which is exactly twice the fundamental rotational frequency of 25 Hz. The second peak is 80 Hz which is approximately three times the rotational frequency.

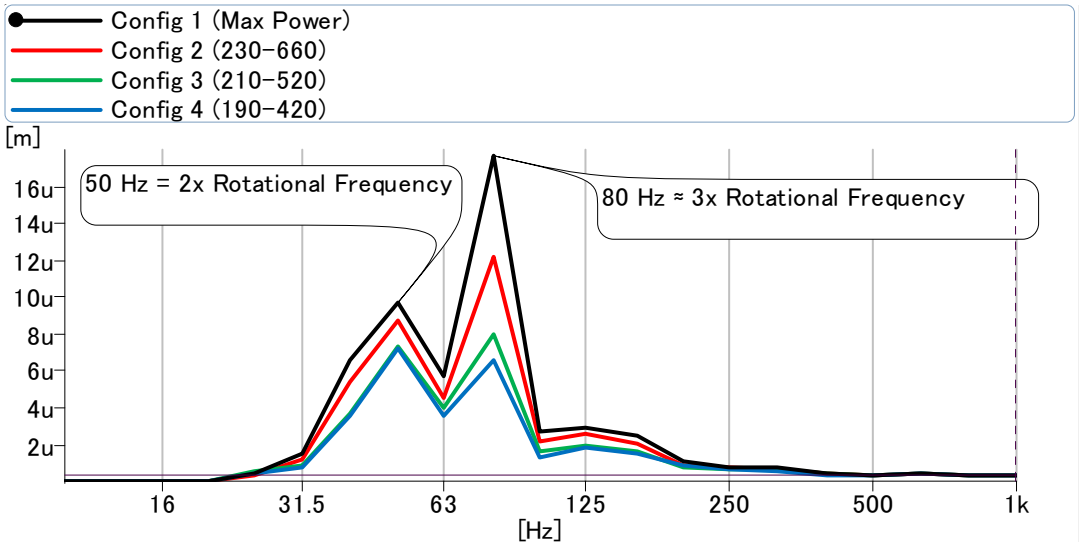

Figure 44 - Calibration comparison, left front engine mount, 1500 rpm, 50% throttle

The low load conditions, idle and 15% throttle, do not show significant differences between the different calibration configurations. The 50% and 100% throttle conditions show greater separation between the different calibration configurations at the 80 Hz 1/3 octave band, which is representative of the three times rotational frequency. In general, the order ranking of the configurations shows Config 1 (Max Power) as the highest magnitude followed by Config 2, Config 3 then Config 4 respectively. The ranking, by order of magnitude, of the configurations at 80 Hz tends to follow the measured horsepower and torque values listed in Table 1. This indicates that the higher the horsepower, or torque value, the higher the magnitude of the 80 Hz 1/3 octave band. This is represented in Figure 45 for the left front engine mount, but is similar for the other engine mounts as well.

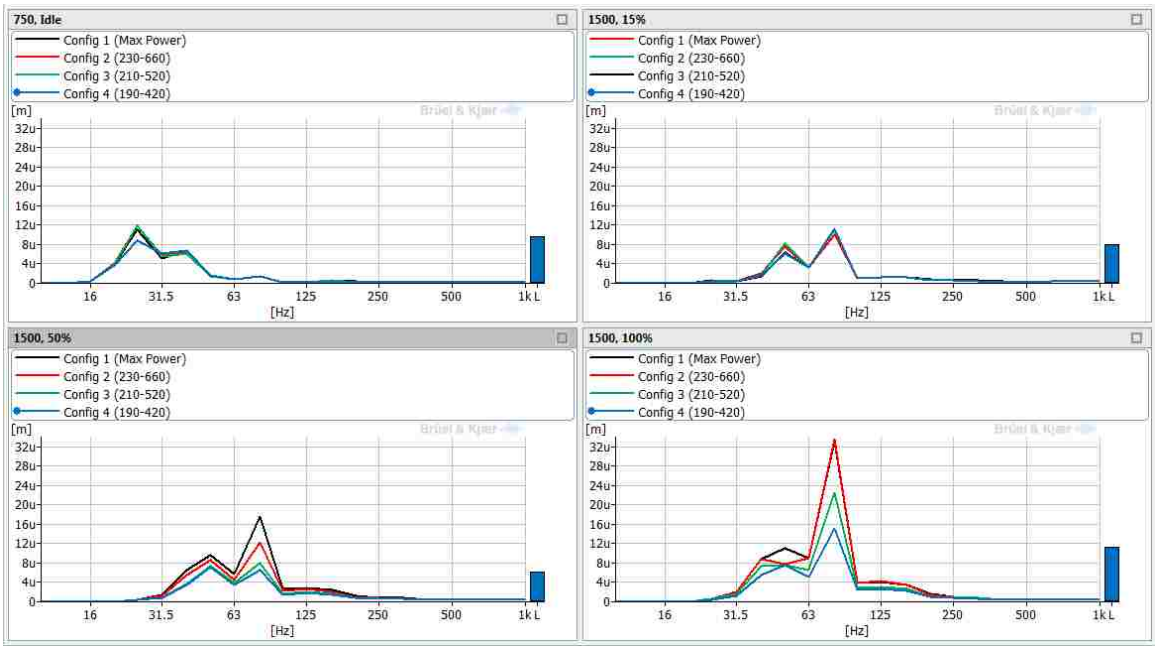

Figure 45 - 1/3 Octave, all calibrations, all operating conditions for left front engine mount

5.5.3 Order Analysis

The vibration signals were analyzed up to 25th order using the order analyzer with 0.125 resolution. Upon initial review of the data, vibration displacement levels above 7th order were very low and negligible as compared to the vibration levels between 1.5 and 5 order. Therefore, the data is reported and displayed only up to 12th order to allow for better visual representation of the area of interest. Some of the notable results will be reported in this section; however, the complete data set is given in Appendix H.

A comparison of a single calibration configuration at each operating condition for each mount location can be seen in Figure 46. The order content at each mount location is very similar. It can also be seen that the 3rd order displays the most significant difference in displacement levels between the different operating conditions.

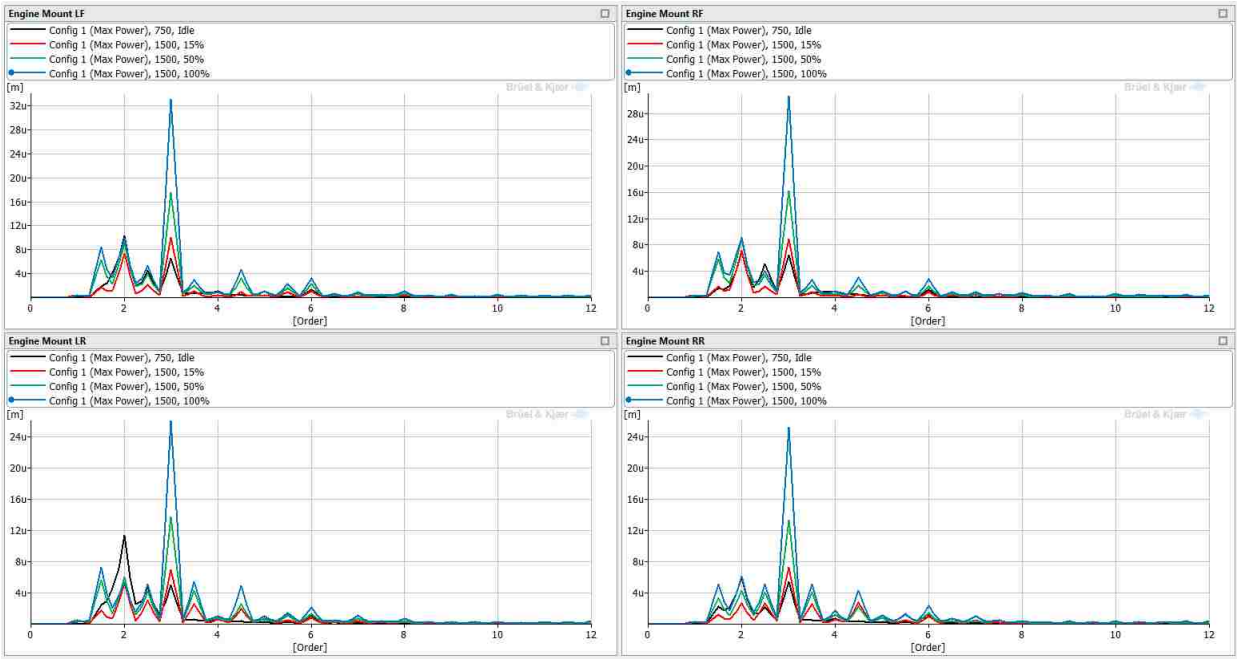

Figure 46 - Order analysis, configuration 1, all mounts, and all conditions

At low load conditions, 750 rpm idle and 1500 rpm 15% throttle, there is very little difference between the various calibration configurations. However, at the higher load conditions, 1500 rpm 50% and 100% throttle, there is a more significant difference in the 3rd order between the different calibration conditions. Figure 47 shows these differences as measured at the left front engine mount for all calibration configurations at all operating conditions.

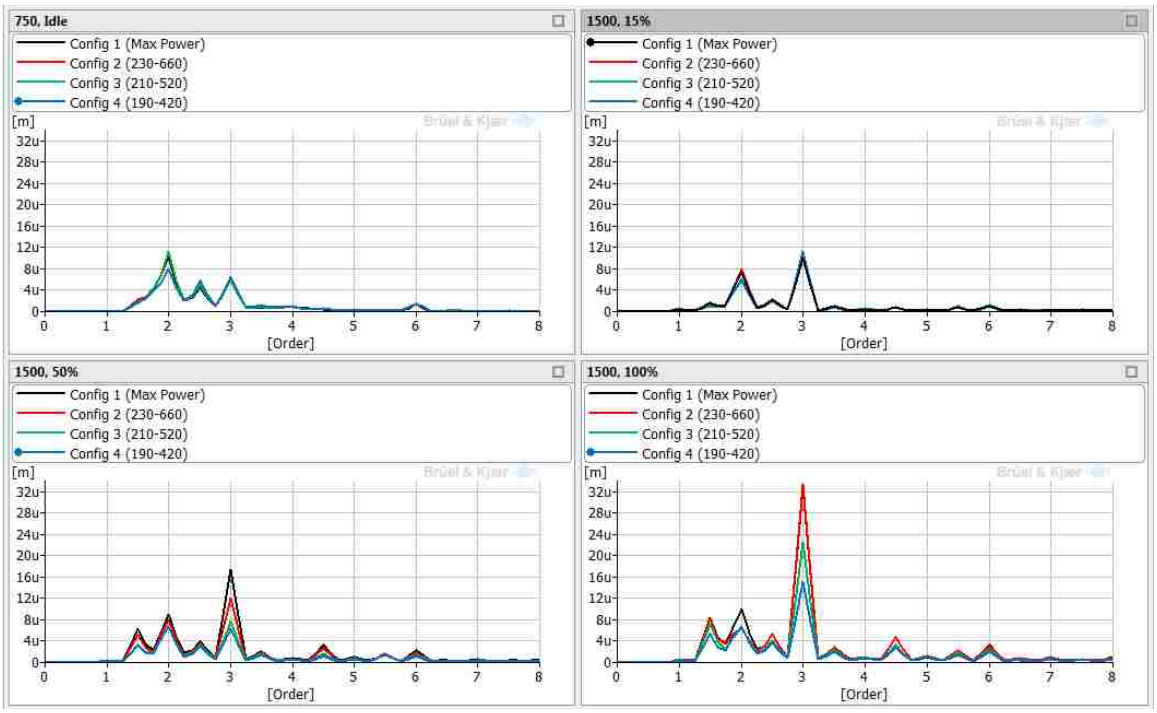

Figure 47 - Order comparison, all calibrations, all operating conditions for left front engine mount

It can also be seen in Figure 47 that the 2nd order is the dominant order of the 750 rpm idle condition for all of the calibrations. The magnitude of displacement for 2nd order stays fairly consistent for each engine mount at each operating condition and each calibration. This indicates that the 2nd order vibration is not significantly influenced by changes in the engine calibration or operating condition.

5.5.4 FFT Analysis

The vibration signals were analyzed up to 800 Hz using the FFT analyzer with a frequency resolution of 1 Hz. Upon initial review of the data, vibration displacement levels above 200 Hz were very low and negligible as compared to the vibration levels below 200 Hz. Therefore, the data is reported and displayed only up to 200 Hz to allow for better

visual representation of the area of interest. Some of the notable results will be reported in this section; however, the complete data set is available in Appendix I.

A comparison of a single calibration configuration at each operating condition for each mount location can be seen in Figure 48. It can be seen from these plots that the 750 rpm vibration, indicated by the black trace, extends below 40 Hz as compared to the 1500 rpm conditions. This is due to the lower operating speed of the engine resulting in a fundamental rotational frequency of 12.5 Hz at 750 rpm, while the fundamental rotational frequency of the 1500 rpm condition is 25 Hz. It is critical to account for the difference in the operating speeds of the data presented in this plot in order to make accurate comparisons of the data, meaning a vibration peak at 25 Hz for the 750 rpm condition should be compared to the vibration at 50 Hz for the 1500 rpm condition.

Figure 48 also shows that all of the 1500 rpm operating conditions have a peak in the vibration spectrum at 75 Hz. This is three times the rotational frequency at that speed, which is related to the combustion timing of the engine. The magnitude of displacement at 75 Hz for the 1500 rpm condition varies according to the load on the engine, therefore 100% throttle has the highest vibration and 15% throttle has the lowest.

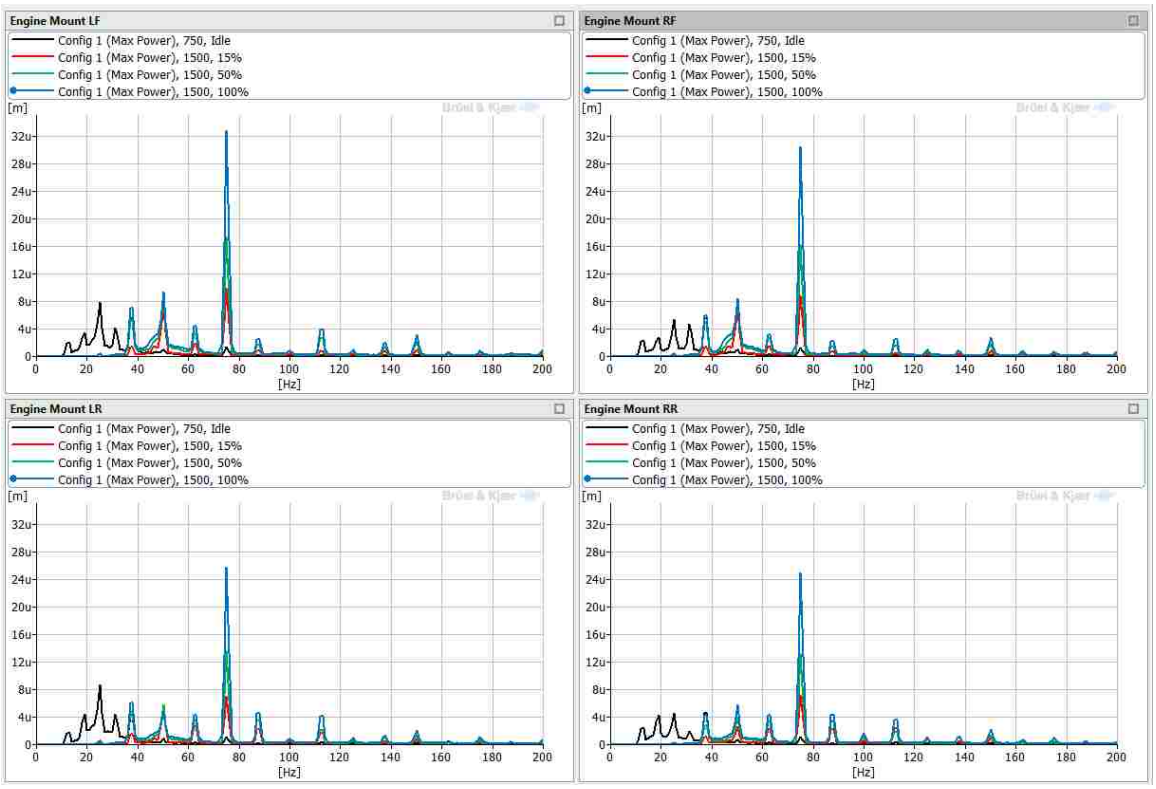

Figure 48 - FFT analysis, configuration 1, all mounts, all conditions

All of the calibration configurations are shown in Figure 49 for the left front engine mount at each operating condition. Much like the results mentioned in the previous sections, there is not a significant difference in the vibration characteristics of the idle and 15% throttle condition. The 50% and 100% throttle conditions show more significant differences between the calibration configurations. This can be seen at 37 Hz, 50 Hz and most notably at 75 Hz.

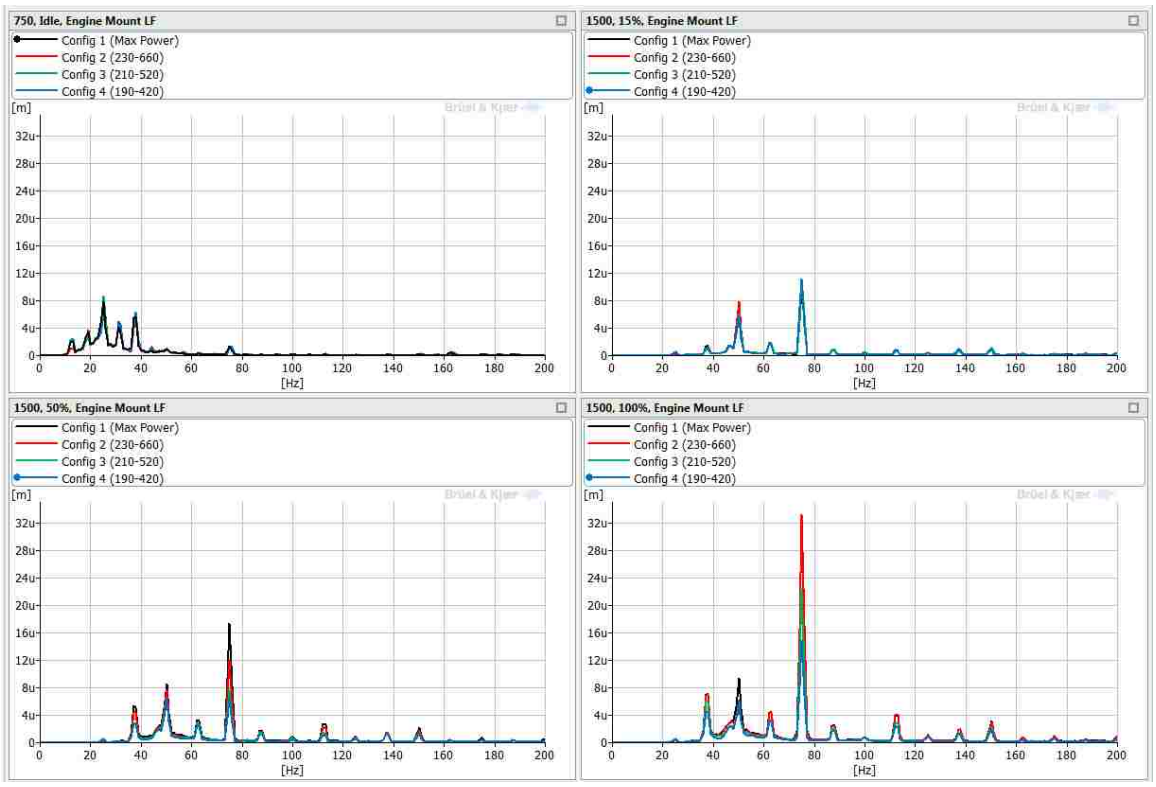

Figure 49 - FFT comparison, all calibrations, all operating conditions for left front engine mount

5.6 Vibration Results Relative to Cylinder Pressure.

The previous section discussed each of the vibration analysis results individually: each of the analysis methods (overall level, 1/3 octave, FFT and order) were compared within their own domain using the test parameters such as engine calibration and operating condition as the variable. In an effort to understand which analysis method best correlates with the cylinder pressure data, all of the results from the previous section must be compiled into a common metric so that they can be displayed against one another using the cylinder pressure as the common axis.

The results of the previous section showed that the overall vibration level, as well as the magnitude of the frequency corresponding to three times the engine's rotational

speed, displayed significant differences between each engine calibration configuration. These two metrics will be used to find a relationship between the engine mount vibration and the cylinder pressure during combustion. Both the maximum pressure and the maximum pressure rise rate will be used for this comparison.

The left front engine mount data will be used for comparison purposes for this section, as the results from the other three mounts are also very similar. The complete data set can be seen in Appendix J.

5.6.1 Overall Level

The result of an overall level analysis is a single value quantifying the entire total vibration energy within a set frequency range. For the scope of this project a frequency range of 20-800 Hz was used for the low speed idle operating condition, while a 40-800 Hz frequency range was used for the high speed 1500 rpm operating conditions. A high-pass filter was applied to the time files to remove vibration energy below the lowest frequencies desired in the analysis. The upper limit of each analyzer was set to 800 Hz. The total vibration energy between these two limits can then be calculated and reported as an overall level.

The overall level analyzer automatically reports the single value of the total energy within a set frequency span. The other analyzers used required the extra step of calculating the total level from the results in either the frequency domain or the order domain. This step was done in the PULSE Reflex software and is plotted in Appendix J.

Figures 50 and 51 show the overall left front engine mount vibration relative to the maximum cylinder pressure (Pmax) and the maximum pressure rise rate (MPRR) calculated in section 5.4. The shape of the resulting curve is typical for all of the engine mount locations for both the Pmax and the MPRR.

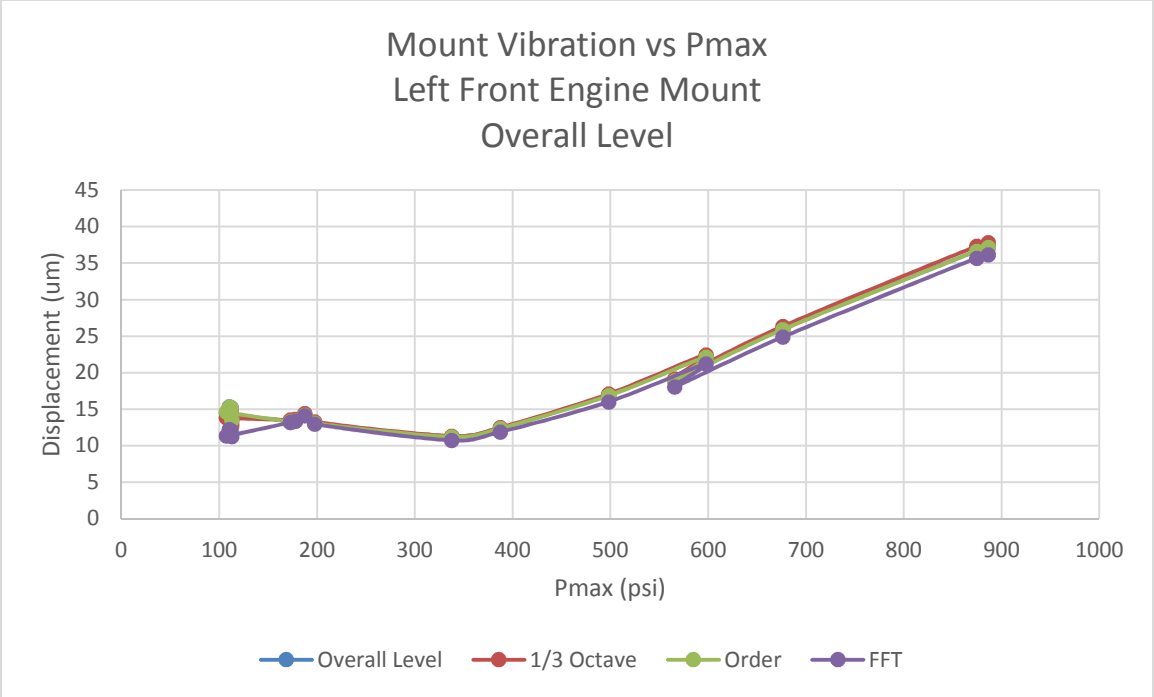

Figure 50 - Overall vibration vs Pmax

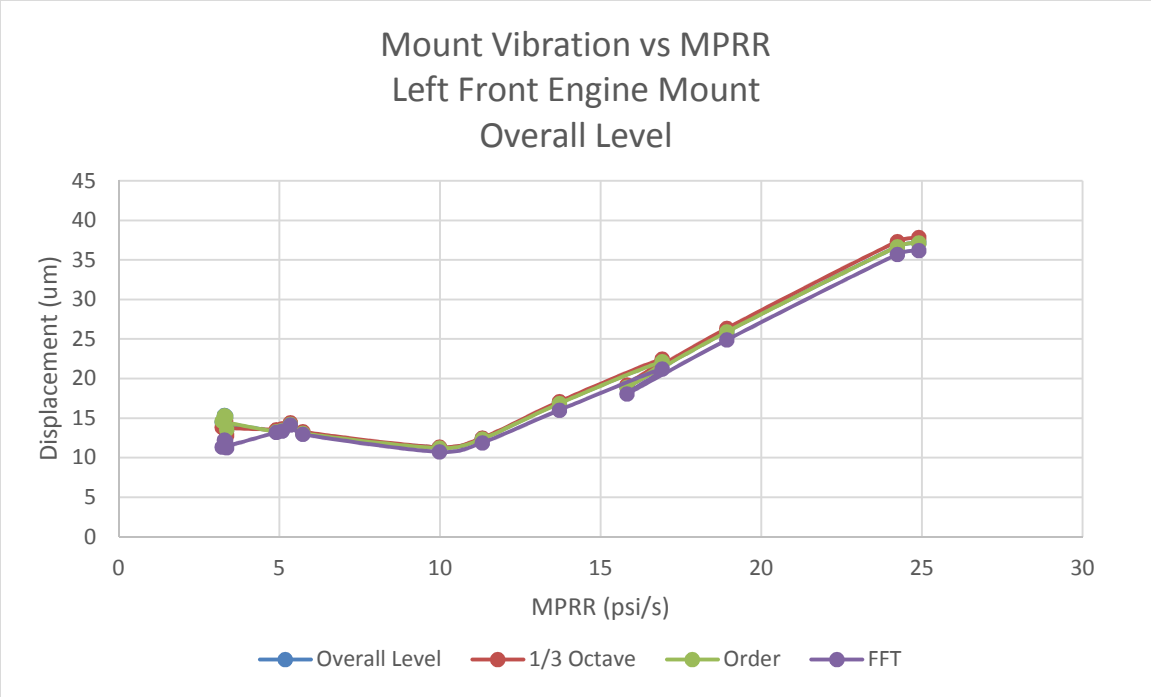

Figure 51 - Overall mount vibration vs MPRR

It can be seen in both Figures 50 and 51 that the overall level calculation produces similar results regardless of which analysis method is used.

5.6.2 Combustion Frequency (3rd Order)

The results in section 5.5 showed high vibration with regard to frequency of combustion. In a 6-cylinder, 4-stroke engine, the combustion frequency is 37.5 Hz at 750 rpm and 75 Hz at 1500 rpm. In order to make a fair comparison between all of the analysis methods, the vibration energy at the combustion frequency needs to be extracted.

It is not possible to get any frequency information from the overall level analysis, as the nature of the overall analyzer is to report a single numerical value for the total energy

within a known frequency span. Therefore, the overall level results will be represented as simply the overall level in the combustion frequency comparison.

The 1/3 octave results have a limited frequency, as this type of analysis sums the total energy that is within a certain percentage of a known center frequency into a single value and reported as a 1/3 octave band. For this comparison the 40 Hz value was used for the 750 rpm idle condition and the 80 Hz value was used for the 1500 rpm conditions. The 40 Hz center frequency value was representative of the total energy between 35.5 Hz and 44.7 Hz. The 80 Hz center frequency value was representative of the total energy between 70.8 Hz and 89.1 Hz. The values used for this comparison were extracted from the data available in Appendix G.

The FFT analysis allows for a much higher frequency resolution analysis compared to the overall level and 1/3 octave analyses. Therefore, the vibration values for the combustion frequency were easily selected at 37.5 Hz and 75 Hz from the FFT results in Appendix I.

It was not possible to select the combustion frequency vibration with respect to frequency during the order analysis, as the order analyzer reports vibration frequency in terms of order, or multiples of shaft revolution. A 6-cylinder, 4-stroke internal combustion engine has a combustion frequency of 3rd order or three times the crankshaft speed. The 3rd order magnitudes used for this comparison were taken from the results in Appendix H.

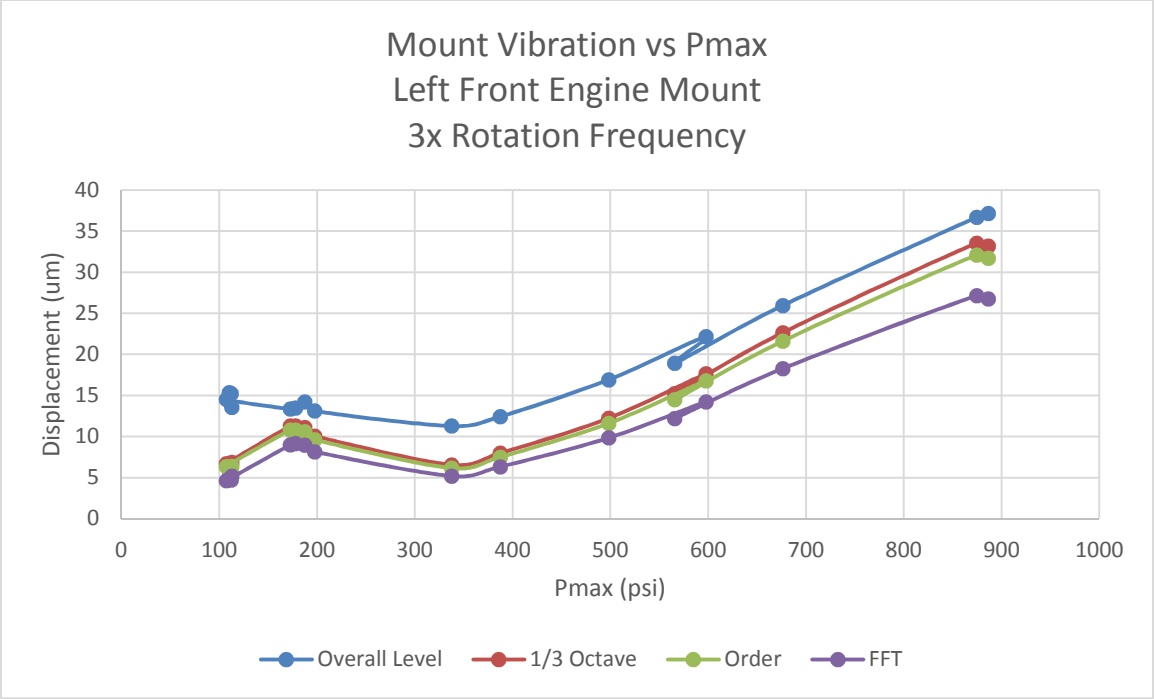

Figure 52 - Engine mount vibration (3x rotational frequency) vs Pmax

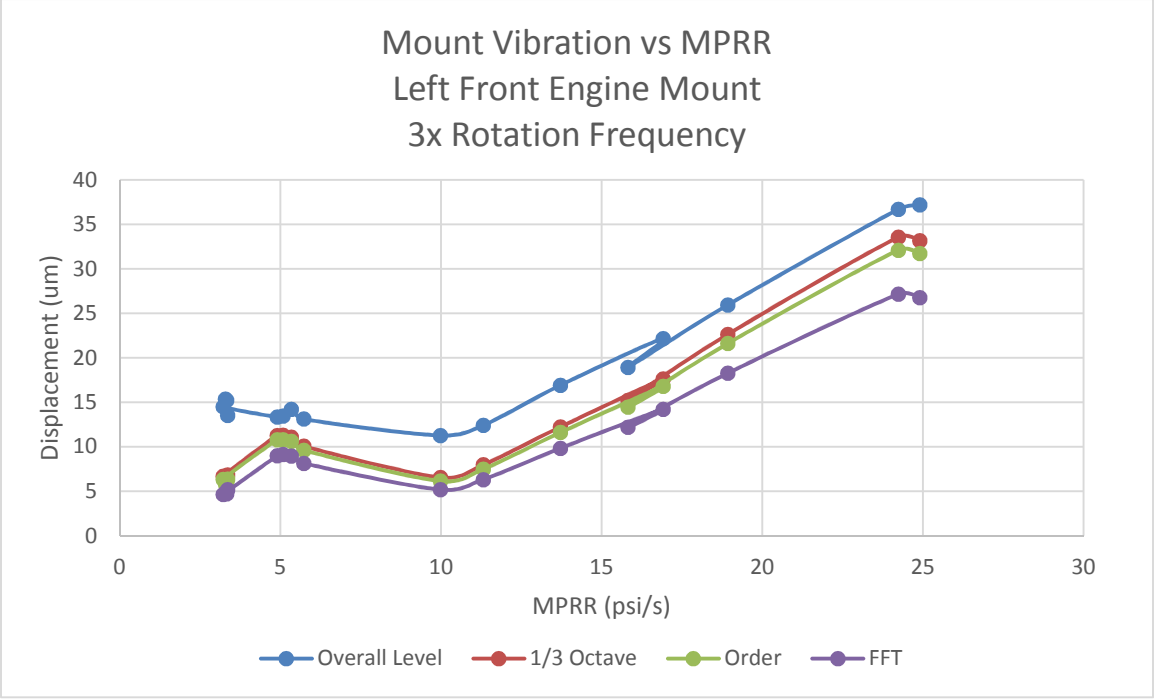

Figure 53 - Engine mount vibration (3x rotational frequency) vs MPRR

Figures 52 and 53 show the left front engine mount vibration level at the combustion frequency for both Pmax and MPPR Respectively. It can be seen from these graphs that focusing on the frequency of interest reduces the vibration displacement level from the overall level results. This is due to the elimination of the vibration energy outside of the area of interest.

It is also clearly shown that the 1/3 octave results show a higher displacement level than the FFT results. This is due to the vibration energy contained in the wider frequency span of a 1/3 octave band as compared to the narrower frequency resolution of the FFT calculation. When the frequency resolution is reduced, each data point spans a wider frequency band (e.g., 8 Hz as opposed to 2 Hz). A wider frequency band will naturally contain more vibration energy than a narrower band, simply by merit of being wider. Conversely, when the frequency resolution is decreased, the frequency band will contain less vibration energy. This concept also holds true with the order analysis: as the order resolution increases, the reported vibration level will be reduced as there is less vibration energy in the smaller increments between reported orders.

5.6.3 Effect of Throttle Position

Regardless of the vibration analysis or the cylinder pressure metric, there are two distinct trends in the data results. Figure 54 shows the overall level vs. Pmax results for the left front engine mount. The shape of the vibration results as plotted against cylinder pressure are typical for all engine mount locations and the complete data set is in Appendix J.

The data previously discussed shows that the lower throttle conditions have insignificant differences between the different calibration configurations regarding both vibration and cylinder pressure as compared to the levels recorded at the higher throttle conditions.

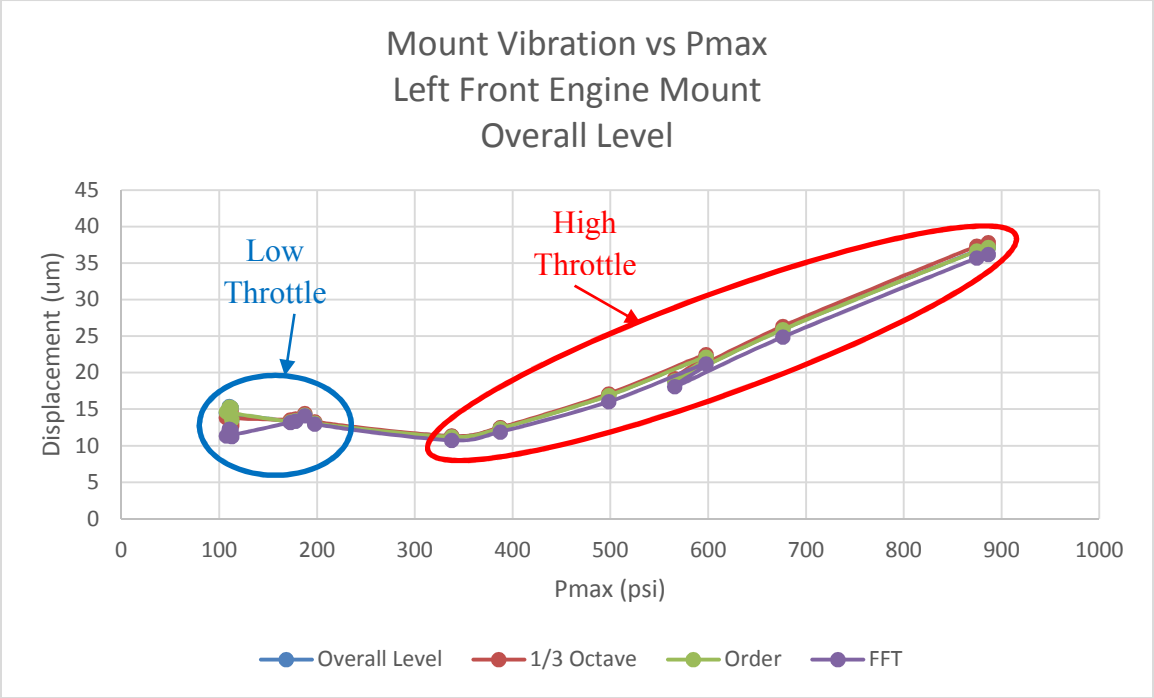

Figure 54 - Trends in the vibration vs cylinder pressure results

5.6.3.1 Low Throttle Positions

At low throttle position conditions 750 rpm Idle and 1500 rpm 15% Throttle, there is not a significant difference between any of the calibrations configurations with respect to mount vibration or cylinder pressures. Data throughout this chapter indicates that at these low throttle conditions, there is a significant contribution at 2x the engines rotational frequency. It can be seen in Figure 47 that the 2nd order is greater than the 3rd order for

the 750 rpm idle condition and approximately 75% of the magnitude for the 3rd order at 1500 rpm 15% throttle condition.

5.6.3.2 High Throttle Positions

At the higher throttle positions, such as 1500 rpm 50% and 100% throttle, cylinder pressures range between 300-900 psi. Data throughout this chapter support that the dominant characteristic of the measured vibration at the mounts was related to the vibration at three times the engine's rotational speed. This vibration is directly related to the frequency of the engine's combustion cycle. Using either the overall level (Figures 50-51) or the 3rd order (Figures 52-53) a linear relationship can be seen between the vibration level at the engine mounts and the cylinder pressure metrics (Pmax and MPRR).

5.6.4 Linear Relationship between Vibration and Cylinder Pressure

A linear relationship can be found between the engine mount vibration and the cylinder pressure when the 3rd order is the dominant order, as in the higher throttle conditions. Since the overall vibration level plot shows that this relationship is constant among all of the different analyzer types (figures 50-51), it will be used for the correlation equation. The overall vibration at each engine mount location relative to maximum cylinder pressure at combustion can be seen in Figure 55.

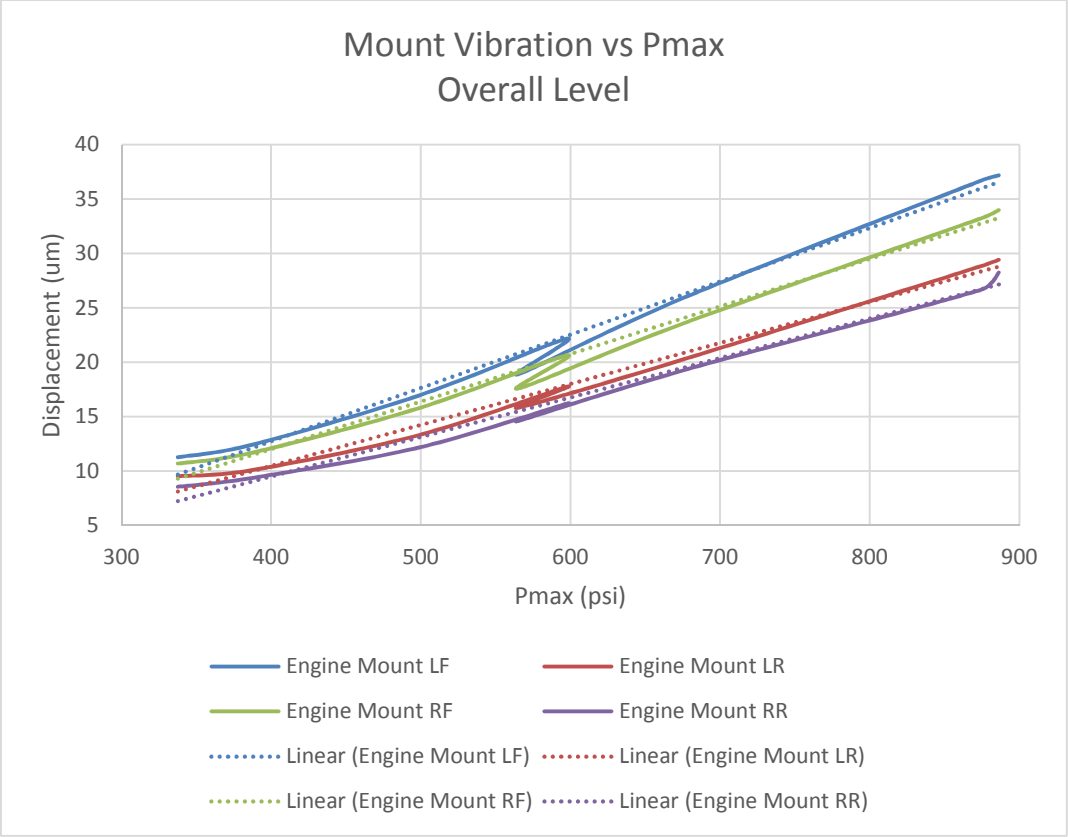

Figure 55 - Mount vibration vs Pmax, overall level for each engine mount

The linear relationship between Pmax and overall level is defined for each engine mount in Table 5. There is also a linear relationship between the engine mount vibration and the MPRR as seen in Figure 56, with the equations shown in Table 6.

Left Front Engine Mount (um)	Right Front Engine Mount (um)
OAL = 0.0489(Pmax)-6.8207	OAL = 0.0437(Pmax)-5.4219
Left Rear Engine Mount (um)	Right Rear Engine Mount (um)
OAL = 0.0377(Pmax)-4.5729	OAL = 0.0362(Pmax)-4.9615

Table 5 - Mount vibration overall level correlation equations with Pmax

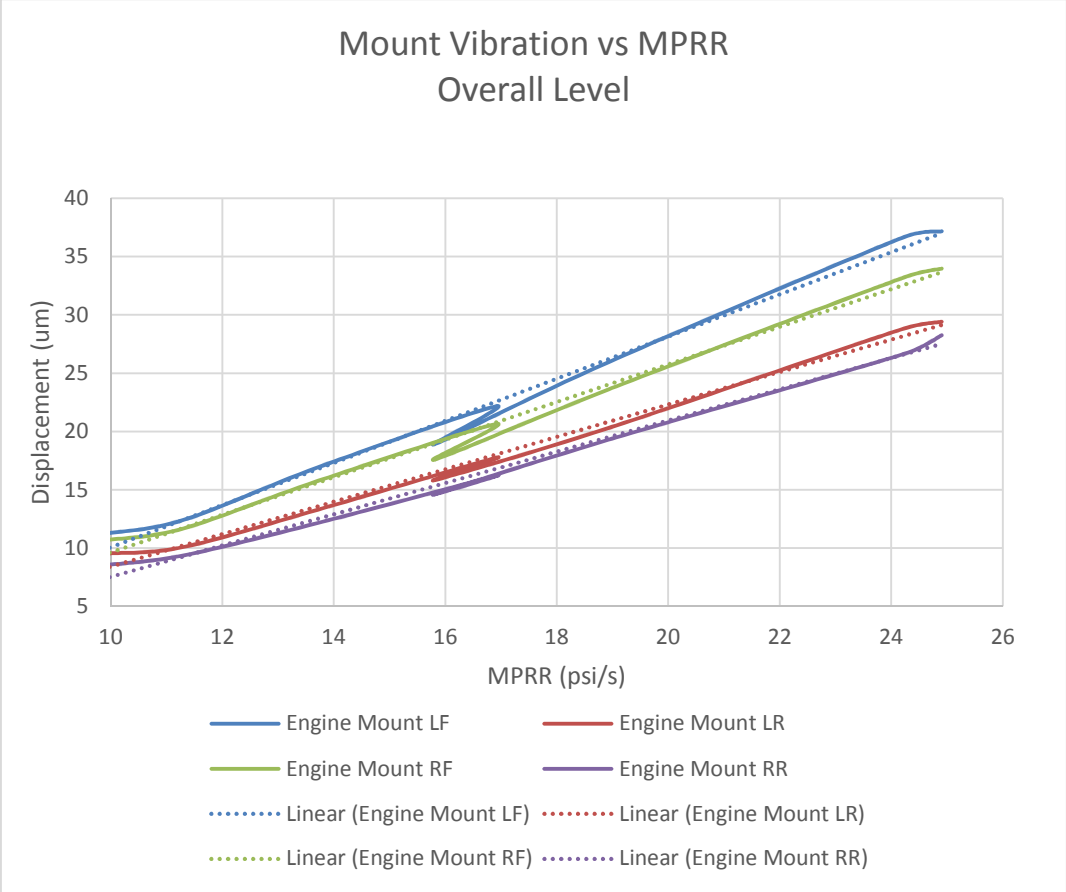

Figure 56 - Mount vibration vs MPRR, overall level for each engine mount

Left Front Engine Mount (um)	Right Front Engine Mount (um)
OAL = 1.8078(MPRR)-8.0027	OAL = 1.6127(MPRR)-6.4805
Left Rear Engine Mount (um)	Right Rear Engine Mount (um)
OAL = 1.3914(MPRR)-5.4939	OAL = 1.304(MPRR)-5.8652

Table 6 - Mount vibration overall level correlation equations with MPRR

CHAPTER 6: DISCUSSION

6.1 Data Validity

The run-to-run consistency of the data was confirmed by using a single calibration configuration. In an effort to keep the data comparison concise, only the 1/3 octave and the order analyzers were used. The 1/3 octave analyzer served to show the data consistency in the frequency domain, which could indicate any frequencies where the data had a large deviation from run to run. The order analyzer was used to check if the any run-to-run deviation was related to multiples of crank shaft rotation. The overall level analyzer was not used as it would not give any indication of frequencies or orders of interest. The FFT analyzer was also not used in this analysis, as any deviation in the frequency content would easily be displayed using the 1/3 octave results and any deviation related to engine speed would be evident in the order analysis.

The first order, actual crankshaft rotation speed, showed the highest displacement as well as the highest standard deviation at each condition. Since 1st order is generally associated with unbalance or eccentricity [30], it is a mechanical characteristic and would be affected less by combustion forces than by rotational speed. It is also important to note that any 1st order contribution would have been filtered out by the high pass filter as demonstrated by the study by Suh [8].

Although not as high in displacement as the 1st order, the 2nd order showed some inconsistency between like runs, especially at lower engine speed and throttle position. However, the standard deviation is only 0.001 mm at idle condition, and once the speed is increased to 1500 rpm the standard deviation falls to 0.0004 mm which is only 6%. Typically, 2nd order is associated with misalignment [30] and therefore with a mechanical vibration characteristic inherent in the system. At higher speeds the magnitude of the vibration at 2nd order is reduced a bit and stabilizes, providing further evidence that this is a mechanical characteristic of the test setup rather than a characteristic of vibration due to combustion.

The vibration data, for 3rd order and above, were very consistent with little variation between similar runs. Third order and its associated frequency band increased with respect to the throttle position, and therefore, engine power output level. This was expected as the 3rd order is the combustion frequency of a 6-cylinder engine. This confirmed that the engine could produce consistent results at each test condition and that a single 30-second average would suffice for testing each calibration configuration at each test condition.

6.2 Cycle to Cycle Fluctuation

Inherent to all internal combustion engines is the cycle-to-cycle fluctuation due to the combustion within the cylinder. There are a number of reasons that this variability occurs: differences in air/fuel mixture, residual gases left in the cylinder from the prior cycle, and spark timing, for example. In an ideal scenario, there would be no fluctuation between the cycles and all of the cylinder pressure traces would be identical. Great improvements have been made in the past 25 years regarding improvements in cycle-to-

cycle stability. Direct injection, improved build tolerances and computer controlled engine strategies have all helped to improve the stability of the combustion shape.

The test engine used in this study was an International DT466 which began production in 1984. Even though the engine used in this study had been modified to the specifications set by North American Repower to operate on compressed natural gas, the basic design of the engine is 30 years old. Therefore, there are components inherent to the design of the engine that provide challenges regarding the cycle-to-cycle stability such as the intake manifold, single point fuel injection, and head design. At the time of the measurements, the engine control calibrations were still not optimized to the level required for consumer use. Data collected during this investigation helped provide a baseline to the engine calibrators in support of their strategy changes during their continued work on improving the engine control strategy.

In an effort to get a fair representation of the cylinder pressure results for the comparisons used in this study, a 30-second average was taken which resulted in more stable results.

6.3 Correlation between Mount Vibration and Combustion Pressure

The results of this study found a distinct correlation between mount vibration displacement and combustion pressure. Data points were obtained at four distinct operating conditions:

- 750 rpm idle, 1500 rpm
- 15% throttle, 1500 rpm

- 50% throttle and 1500 rpm
- 100% throttle

The mount vibration displacement was plotted against the maximum pressure (Pmax) and the maximum pressure rise rate (MPRR) for each of the calibration configurations and each operating condition. The data associated with the higher load conditions (50% and 100% throttle) showed a linear correlation between the mount vibration and the cylinder pressure. The lower load conditions (Idle and 15% Throttle), however, did not show the same linearity as the higher load conditions.

6.3.1 Linear Correlation at High Load Conditions

At the 50% and 100% throttle positions, the mount vibration displacement displayed a linear relationship with the cylinder pressure values at combustion. This mostly agrees with the results given by Suh [8] for a gasoline V8 engine. In his study, the engine was only operated at 100% throttle position, and the spark timing was adjusted to vary the combustion properties. He found that the acoustic noise level had a linear relationship to the MPRR value, and that the mount vibration was more influenced from the overall nature of the combustion. It can be seen in Figure 2.9, from the Suh study that the results had a linear relationship between vibration and MPRR for all of the conditions except for the 50-degree spark advance.

In the current study, each calibration configuration had a unique strategy for spark timing and fuel quantity, providing four data points for each operating condition. The 50% and 100% throttle results consisted of eight individual data points, which, when plotted relative to either Pmax or MPRR, resulted in a linear correlation.

While Dr. Suh's study used only 100% throttle operating condition, the current study showed a strong correlation between mount vibration and combustion pressure for both 50% and 100% throttle operating conditions. It could be concluded from these results that there is a linear relationship between mount vibration and cylinder pressure at all throttle positions above 50% throttle; however, further testing is required to confirm that claim.

6.3.2 No Correlation at Low Load Conditions

At the low load conditions (Idle and 15% throttle), there is no distinct trend correlating the mount vibration to combustion pressure. The results show that the individual mount vibration levels have very minimal differences in displacement levels between any of the calibration configurations at a given operating condition. Likewise, at either of the low load operating conditions, the combustion pressure does not show a large enough difference between the different calibration configurations to constitute a trend. At the idle operating condition, the cylinder pressure results show a difference of only 4 %, which falls into the range of cycle-to-cycle variability.

The vibration results of the low load conditions also show high displacement levels at frequencies associated with the 2nd order. This can be seen in the frequency analysis in sections 5.5.2 and 5.5.4 as well as the order analysis in section 5.5.3. In the case of the idle condition, the 2nd order vibration is greater than the 3rd order vibration, and therefore the dominant characteristic of the measured vibration at that operating condition.

With very little difference in the 3rd order displacement levels, which are typically associated with the combustion frequency of a 6-cylinder engine (such as the subject of

this test), and a high 2nd order contributing to the overall vibration level, the correlation between combustion pressure and mount vibration cannot be proven.

6.3.3 The influence of 2nd order.

The results from both the frequency and order analyses performed in Chapter 5 all show evidence that in the higher load conditions, 50% and 100% throttle, the 3rd order is the dominant order for the mount vibration. The low load conditions, idle and 15% throttle, did not have dominant 3rd order influence in the vibration data. It can also be seen from the data that higher load conditions displayed a more significant difference in both vibration and cylinder pressure as compared to the lower load conditions.

The 2nd order vibration was present in all operating conditions, with its highest displacement at the idle condition. At the 1500 rpm condition the magnitude of the 2nd order displacement was fairly consistent at each operating condition relative to each individual mount location. This indicates that combustion pressure did not have a significant effect on the vibration displacement at 2nd order. Since there was little effect on 2nd order with significant changes to the cylinder pressure, the root cause of the 2nd order vibration is potentially mechanical and related to the rotating assembly itself. It is very possible that this is due to a misalignment [30] in the test fixture setup.

Additional measurements would be required to further investigate the root cause of the 2nd order vibration. The mechanical vibration must be isolated from the total vibration that includes the influence of the combustion. To isolate the mechanical vibration, the engine must be rotated with something other than the combustion forces. This can be performed by using the dyno to rotate the engine at the operating speeds performed in the

current experiment. The measurement of the vibration of the engine without the influence of combustion would then allow for isolation and analysis of the mechanical vibration. The dynamometer setup used on this particular engine at McLaren does not have the capabilities to perform this test.

6.4 Vibration Analysis Methods

From the literature review, there was not a definitive agreement as to which analysis method should be used. Most of the studies focused on the correlation of noise and combustion pressure. There was agreement regarding correlation between engine noise and combustion pressure, but there was not a complete agreement on how the analysis should be done, as some studies used the overall level while others used 1/3 octave and still others used FFT. Only Dr. Suh's study [8] investigated the correlation between engine mount vibration and the cylinder pressure at combustion.

6.4.1 Common Analysis settings

It is important to keep in mind that in the context of vehicle operator comfort and perception, the engine acts as a noise and vibration source which transmits vibration through the engine mounts into the vehicle body, where it may be detected by occupants inside the cabin of the vehicle. Based on some of the findings in the literature review as well as a correspondence with Dr. Suh, decisions were made regarding the analysis parameters that would apply to all of the measurements regardless of the analysis method used. These common settings were determined to be frequency range, displacement and high pass filtering.

The study by AGCO and Brüel & Kjær [6], reported that the structure-borne noise contribution of an engine to the cabin of an agricultural crop spraying machine was below 275 Hz. Another study performed by Isuzu Advanced Engineering and Tokyo University [7] reported the capability of hydraulic engine mounts to control transmitted vibration effectively up to 500 Hz. PULSE Reflex post-processing software allows for selection of a variety of upper frequency limits for each of the analyzers used. Although 500 Hz was available as an upper frequency limit, 800 Hz was selected for this investigation in an effort to investigate if there was any significant mount vibration above the ranges specified in the previously mentioned studies in the literature review. The results showed that there was not.

It is typical for vibration to be reported in acceleration units. However, in Dr. Suh's study [8], vibration results were reported as displacement. This was selected because dynamic displacement is the best way to describe the input forces applied to the rubber engine mount, since it is displacement energy that is transferred through the engine mount to the vehicle frame. For this reason, the vibration data measured in the current experiment were double integrated to displacement using the PULSE Reflex software prior to any vibration analysis.

Also in accordance with Dr. Suh's suggestions, a high-pass filter was applied to all of the vibration data to remove the lower frequency content that was erroneously generated by the double integration process as well. The high-pass filter was also used to remove the first order content, as that is typically associated with mechanical vibration known not to be related to engine combustion forces. For the 750 rpm operating condition, the high pass filter was set to 20 Hz, while 40 Hz was used for the 1500 rpm operating conditions.

6.4.2 Overall level Correlation between Analyzers

Regardless of which analyzer is used, an overall level value to quantify the vibration energy below 800 Hz could be easily calculated. The overall analyzer reports only the overall level and additional calculation was not required. For the other analyzers, the total overall vibration level was calculated from 0 to 800 Hz using the PULSE Reflex software during the analysis. The results from this calculation were plotted against cylinder pressure for comparison and are available in Appendix J.

Independent of the analyzer used, the overall level calculations from 0-800 Hz all overlay upon each other almost line on line. This is not surprising as the total vibration energy should be the same within this frequency range regardless of the analyzer used. Therefore, the mount vibration to cylinder pressure correlation formula derived in the previous chapter (Tables 5.4 and 5.5) is valid using any of the four vibration analysis methods.

6.4.3 Combustion Frequency Correlation between Analyzers

As discussed in this chapter and previous chapters, the vibration at the combustion frequency (three times rotational speed) is directly related to the combustion forces transmitted to the engine block. Quantification of the vibration level at this frequency is performed differently depending on which analyzer is used. The complete data set comparing data from all of the analyzers can be seen in Appendix J. It can be seen that the results from each analyzer report a broader discrepancy of values as compared to the overall level values reported from all of the analyzers.

The overall level analyzer does not have the capability to report any frequency information, as it can only provide the total vibration energy within a specified range. Therefore, the overall level analyzer is not a valid tool for determining that the reported vibration level is actually due to the combustion frequency or some other frequency with a higher displacement.

The other analyzers (1/3 octave, FFT and Order) all show a similar trend as they compare with the cylinder pressure data. The displacement magnitudes vary between the analyses methods used.

The results show that the 1/3 octave results have the highest displacement levels. This is due to the wider bandwidth used for quantifying the vibration level at 3x rotation speed. Due to the nature of the 1/3 octave analyzer, the bandwidth at each frequency band is fixed as discussed previously in section 3.3.3.2. Therefore, at 750 rpm, the value reported for the vibration at three times the rotational speed is represented as 40 Hz which is actually the total energy between 35.5 Hz and 44.7 Hz. Likewise, at 1500 rpm, 80 Hz represents the three times rotational speed frequency. The 80 Hz frequency band actually consists of the total vibration energy between 70.8 Hz and 89.1 Hz.

The FFT analyzer and the order analyzer show lower displacement levels than the 1/3 octave results. This is due to the resolution available with these types of analyzers. Since the frequency and order resolution can be adjusted with these types of analyzers, the reported values are a product of the vibration energy that is within the boundaries of the resolution used. Therefore, if the resolution is increased, the reported value at a certain frequency will be reduced as it represents the energy of a smaller frequency span.

Conversely, if the resolution is decreased the reported value will increase as the value it represents is the energy over a larger frequency span. This was detailed previously in section 3.3.3.3

Although the displacement values reported by the FFT and the order analyzers differ, with different resolution settings they could be brought closer together. If the frequency resolution was decreased on the FFT analyzer, the reported displacement values would increase and more closely match the values of the order analyzer. Likewise, if the order resolution is increased on the order analyzer, the reported displacement values would be reduced to levels more comparable to the FFT analyzer.

6.5 Combustion Pressure Analysis Methods

In order to correlate the engine mount vibration to the cylinder pressure, an objective data metric was required. The literature available commonly suggested using the maximum pressure at combustion (Pmax) or maximum pressure rise rate during combustion (MPPR) for correlation with engine noise. Some of the available papers reported better correlation with Pmax, while others reported better correlation with MPRR; there was not universal agreement as to which parameter correlated better with engine noise. Dr. Suh's study showed that engine mount vibration does have correlation to the MPRR; however, not as significant as the engine noise. For the current study both Pmax and MPRR were investigated to determine which one might be best suited for correlation to the engine mount vibration.

As previously discussed in this chapter, engine mount vibration shows a linear correlation to combustion pressure in the high load conditions. This is where the 3rd order

vibration levels are dominant in the engine mount vibration. The Pmax and the MPRR both showed a linear correlation at these data points, and would be valid tools to use for determining mount vibration from cylinder pressure data. At the low load conditions, there was no correlation between engine mount vibration levels and cylinder pressure for either Pmax or MPRR.

CHAPTER 7: CONCLUSIONS AND RECOMMENDATIONS

The results of this study do support the claim that the engine mount vibration on a CNG engine correlates to the cylinder pressure. With that being said, there are some caveats that should be clarified in more detail, as well as some areas that would benefit from additional research.

7.1 Correlation of Engine Mount Vibration with Combustion Pressure.

There is correlation between the engine mount vibration and the combustion pressure at the high load conditions (50% and 100% throttle). At these conditions the combustion frequency is the dominant frequency of the engine mount vibration. This correlation can be seen with the using any of the analyzers relative to both the Pmax and the MPRR values at the high load conditions.

At the low load conditions (idle and 15% throttle position) there is not enough evidence to support the claim of any correlation between the mount vibration and the combustion pressure. At these operating conditions, there was not a significant enough difference between the vibration levels of each calibration configuration to show any change due to calibration. These operating conditions also show a significant contribution to the vibration level from the 2^{nd} order, which is typically associated with mechanical vibration.

Further investigation is required to determine the root cause of the 2^{nd} order vibration. In addition, efforts to reduce the mechanical vibration that is dominating the

mount vibration at the lower load operating condition would assist in a root cause analysis. One solution would be to motor the engine using the dynamometer to provide the rotational power. This would provide data showing only the mechanical vibration characteristics, as no combustion would be taking place during that test. This data could then be used to determine if mechanical vibration is present. Appropriate countermeasures could then be applied to reduce the mechanical vibration.

Another approach would be to use source path contribution software to investigate contribution of the combustion process with the motored mechanical vibration removed. This could more effectively reveal any existing correlation between mount vibration and combustion at the lower throttle condition.

In order to properly isolate the mechanical vibration of this engine, it would need to be motored by a dynamometer or something similar. The test cell that this project utilizes does not have motoring capabilities.

7.2 Max Pressure or Maximum Pressure Rise Rate

The results of this study did show a correlation between the mount vibration and the combustion pressure. While previous other studies have come to different conclusions as to whether Pmax or MPRR produced better results, the results from this study show that either can be used.

In a practical application, it might be more advantageous to use the Pmax value, as this value can be easily measured a variety of ways on a wide variety of equipment. The MPRR value, however, requires the calculation of a derivative of the pressure trace.

Although this is possible to do using many different types of software, it is an additional step that can be eliminated by simply using the Pmax. Pmax also lends itself well to field applications where the user does not have access to equipment capable of performing the MPRR calculation.

7.3 Overall Level or Combustion Frequency

It has been established that there is a linear correlation between the mount vibration and the combustion pressure at the high load conditions. The results show that the engine mount overall vibration level and the vibration level at the engine combustion frequency both correlate well.

The overall vibration level tends to lend itself well to obtaining the desired correlation results. This is because it does not matter which analyzer is used to perform the overall level calculation; the calculation of the total vibration energy is the same. Therefore, any of the analyzers used in this study will provide the same results.

The combustion frequency, 3^{rd} order for this 6-cylinder engine, is also a very effective way to obtain the vibration directly related to combustion. However, it is important to note that the reported vibration levels may vary depending on the settings in each analyzer, thus resulting in a different correlation equation for each method. Since the results from an overall level analysis and the 3^{rd} order vibration both point to a linear relationship between the mount vibration and the combustion pressure, it is best to use the overall level as it can be calculated regardless of the analyzer used.

7.4 Correlation Equation, Overall Vibration Level and Pmax

As previously discussed, the overall mount vibration level can easily be reported from a variety of analyzers and correlates with the maximum cylinder pressure of this 6 cylinder CNG engine as a linear relationship. However, this only holds true at the higher load operating conditions where the 3rd order vibration is the dominant characteristic in the mount vibration. The following equations have been developed as a tool to allow calculation of engine mount vibration from Pmax.

Left Front Engine Mount (μm) OAL = 0.0489(Pmax)-6.8207

Left Rear Engine Mount (μm) OAL = 0.0377(Pmax)-4.5729

Right Front Engine Mount (μm) OAL = 0.0437(Pmax)-5.4219

Right Rear Engine Mount (μm) OAL = 0.0362(Pmax)-4.9615

The correlation equation between overall mount vibration and Pmax allows for easy conversion from one to the other. This will be valuable in testing environments that have the ability to measure vibration or cylinder pressure but not both. This is a common scenario in field applications, as it is not always possible to instrument an engine for cylinder pressure transducers. Therefore, the use of vibration transducers on the engine mount to get an estimation of the cylinder pressure is a valuable tool. Likewise, vibration equipment may not always be available, resulting in the need to estimate the vibration from the cylinder pressure data.

7.5 Potential Improvements and Recommendations

The results from this test did provide valuable information to North American Repower and McLaren regarding the relationship between combustion pressure and the vibration displacement at the mounts. There were also some valuable lessons learned that could improve or help understand the results in more detail. Therefore, the following recommendations should be considered.

More operating points should be measured. The current study only used four, consisting of 750 rpm idle, 1500 rpm 15%, 50% and 100% throttle steady state conditions. The results of this activity showed a strong linear correlation at 50% and 100% and little to no correlation at idle and 15% throttle. Additional operating points should be measured between 50% and 100% throttle. This would confirm that the area above 50% shows linear correlation as discussed in this experiment. It would also be beneficial to measure additional operating conditions between the 15% and 50% throttle positions. This would help to determine the lowest throttle percentage at which a linear relationship exists between the combustion and vibration.

The mechanical vibration of the motored engine needs to be evaluated. This would require the engine test stand to consist of a dyno that has the capability to spin the engine without combustion taking place. If the mechanical vibration inherent to the rotating engine assembly were understood, the influence of the combustion forces on the vibration would be easier to understand.

7.6 Current Status and Future Work

At the time of writing of this thesis, the testing on the DT466 engine used in this study was concluded. The equations derived in this study were used to estimate the cylinder pressures in situations where pressure ports were not available in the head to allow for direct measurement. It was found that the intake systems design, which worked well for the diesel application, lead to problems when used with CNG. This was due to the uneven distribution of the fuel and air mixture to the cylinders. Cylinder-to-cylinder and cycle-to-cycle fluctuation were both found to be higher than the acceptable for this engine design.

There are plans to move forward using the generation II, 4 valve head design. This redesigned head and intake system will provide more even distribution of the air-fuel mixture to the cylinders and should improve the stability of the engine regarding cylinder-to-cylinder and cycle-to-cycle fluctuation. During this process, head modifications and changes may not allow for direct measurement of cylinder pressure with a pressure transducer. Therefore, the estimation method derived in this study will be used for determining the cylinder pressure based off of the mount vibration. Of course, an initial test would need to be made measuring both the cylinder pressures and the engine vibration to obtain the new correlation equation. Once this equation has been determined and confirmed, it will useful tool for cylinder pressure estimation.

Although North American Repower and McLaren are currently only working on an International engine conversion, there are plans to expand this technology to other existing

diesel engines such as Detroit Diesel, Cummins and Caterpillar. In each case, a unique cylinder pressure to vibration correlation equation can be used to estimate cylinder pressure from the mount vibration or vice-versa.

REFERENCES/BIBLIOGRAPHY

[1] Ahouissoussi, N.B.C, and Wetzstein, M.E., "A Comparative Cost Analysis of Biodiesel, Compressed Natural Gas, Methanol, and Diesel for Transit Bus Systems" *Resource and Energy Economics*, Vol. 20, No. 1, March 1998, pp 1-15

[2] Keshavarz, A., Khaknejad, M.B., and Azadi, S., "Improving Vehicle NVH Behavior via Tuning the Engine Mount Stiffness Using DOE Method" Society of Automotive Engineers Technical Paper 2011-01-1510, 2011

[3] Samardzic, N., and Novak, C., "Transfer Path Analysis Using Engine Radiated Sound and Mount Vibration" *Canadian Acoustics – Acoustique Canadienne*, Vol. 37, No. 3, p198-199, September 2009

[4] Khan, Md, Johansson, O., and Sundback, U., "A comparison of annoyance response between ethanol and diesel engines noise." *INTER-NOISE and NOISE-CON Congress and Conference Proceedings.* Vol. 1995. No. 4. Institute of Noise Control Engineering, 1995.

[5] Frère, A, Weber, R., Peteul-Brouillet, C., Guyader, G., Misdariis, N. and Susini, P. "What is the influence of vibrations on the diesel character rating of a vehicle?" *INTER-NOISE and NOISE-CON Congress and Conference Proceedings. Vol*. 2010. No. 8. Institute of Noise Control Engineering, 2010.

[6] Cerrato, G., Pietila, G., Tadlock, B., Pell, M., Entriken, S., Kascht, B., Heitkamp, M. and Connelly, T. "Noise and Sound Quality Optimization of Agricultural Machine Cab." No. 2010-01-1988. Society of Automotive Engineers Technical Paper, 2010.

[7] Togashi, C., Nakano, M., and Nagai, M., "A Study on Active Hydraulic Engine Mount to Reduce Interior Car Noise and Vibration over Wide Frequency Band," No. 2011-01-1636. Society of Automotive Engineers Technical Paper, 2011

[8] Suh, I. "Combustion on Radiation Noise and Mount Vibration from a V8 Gasoline Engine." No. 2003-01-1730. Society of Automotive Engineers Technical Paper, 2003.

[9] Arndt, R., Priebsch, H., Brandle, F. and Veit, J. "Procedure for Separating Noise Sources of Combustion Engines." No. 2009-26-0054. Society of Automotive Engineers Technical Paper, 2009.

[10] Chiatti, G., and Chiavola, O. "Combustion Induced Noise in Single Cylinder Diesel Engines." No. 2004-32-0071. Society of Automotive Engineers Technical Paper, 2004.

[11] Alt, Norbert W., Wiehagen, N., Steffens, C. and Heuer, S. “Comprehensive combustion noise optimization”. No. 2001-01-1510. Society of Automotive Engineers Technical Paper, 2001.

[12] Cerrato, G. “Automotive Sound Quality - Powertrain, Road and Wind Noise” *Sound and Vibration Magazine*, May 2009

[13] Carlucci, P., Ficarella, A., Chiara, F., Giuffrida, A and Lanzafame, R. “Preliminary studies on the effects of injection rate modulation on the combustion noise of a common rail diesel engine.” No. 2004-01-1848. Society of Automotive Engineers Technical Paper, 2004.

[14] Li, Z., Shu, G. and Wei, H. "Study of combustion noise under turbocharged condition in DI-Diesel engine." *INTER-NOISE and NOISE-CON Congress and Conference Proceedings*. Vol. 2008. No. 7. Institute of Noise Control Engineering, 2008.

[15] Siano, D., and Bozza, F. “Combustion noise prediction in a small diesel engine finalized to the optimization of the fuel injection strategy”. No. 2009-01-2077. Society of Automotive Engineers Technical Paper, 2009.

[16] Desantes, J M., Torregrosa, A.J and Broatch, A. “Wavelet transform applied to combustion noise analysis in high-speed DI diesel engines.” No. 2001-01-1545. Society of Automotive Engineers Technical Paper, 2001.

[17] Jung, I., Jin, J., So, H., Ham, C and Won, K. “An advanced method for developing combustion noise through the analysis of diesel combustion.” No. 2013-01-1901. Society of Automotive Engineers Technical Paper, 2013.

[18] Gazon, M. and Blaisot, J. “Cycle-to-cycle fluctuations of combustion noise in a diesel engine at low speed.” No. 2006-01-3410. Society of Automotive Engineers Technical Paper, 2006.

[19] SAE Recommended Practice J1074, “Engine Sound Level Measurement Procedure,” Society of Automotive Engineers, Troy MI, February 1987

[20] Prucka, R., Anderson, D., Callies, J. and Xiao, B., "Firing on All Cylinders," *Race Engine Technology*, High Power Media, England, Vol. 9 No. 1, pp 48-55, 2011.

[21] Brüel & Kjær. *Measuring Vibration*. Naerum, Denmark: Brüel & Kjær Publication, 1982

[22] Kunio, J. “Principles of Vibration,” Course handout from Brüel & Kjær training on principles of vibration, Sept 2014.

[23] Ashory, M. R. "Assessment of the mass-loading effects of accelerometers in modal testing." *SPIE Proceedings Series*. Society of Photo-Optical Instrumentation Engineers, 2002.

[24] Cooley, J. W. and Tukey, J. W. "An algorithm for the machine calculation of complex Fourier series". Math. Comput. Vol. 19: pp 297–301. 1965.

[25] Suh, I. Personal communication via email 2/24/2015

[26] Pulkrabek, Willard W. “Engineering fundamentals of the internal combustion engine”. Vol. 478. Upper Saddle River, NJ: Prentice Hall, 1997.

[27] Agilent Technologies. “Fundamentals of signal analysis (Application note 243)” Agilent Technologies, Santa Clara, CA, 2000

[28] Randall, R. B. *Frequency Analysis*. Naerum, Denmark: Brüel & Kjær,p 83, 1987

[29] Reinhart, T. E., Sampath, A., Bagga, K. S., and Leistensnider, G. W. “NVH Variations in Diesel Engine Populations,” No. 2003-01-1723. Society of Automotive Engineers Technical Paper. 2003.

[30] Wowk, V. *Machinery vibration: measurement and analysis*. New York, NY: McGraw Hill Professional, 1991. pp 274-275

APPENDICES

Appendix A: Octave Table.

Frequency *(Hz)*					
Octave Bands			1/3 Octave Bands		
Lower Band Limit *(Hz)*	Center Frequency *(Hz)*	Upper Band Limit *(Hz)*	Lower Band Limit *(Hz)*	Center Frequency *(Hz)*	Upper Band Limit *(Hz)*
11	16	22	14.1	16	17.8
			17.8	20	22.4
			22.4	25	28.2
22	31.5	44	28.2	31.5	35.5
			35.5	40	44.7
			44.7	50	56.2
44	63	88	56.2	63	70.8
			70.8	80	89.1
			89.1	100	112
88	125	177	112	125	141
			141	160	178
			178	200	224
177	250	355	224	250	282
			282	315	355
			355	400	447
355	500	710	447	500	562
			562	630	708
			708	800	891
710	1000	1420	891	1000	1122
			1122	1250	1413
			1413	1600	1778
1420	2000	2840	1778	2000	2239
			2239	2500	2818
			2818	3150	3548
2840	4000	5680	3548	4000	4467
			4467	5000	5623
			5623	6300	7079
5680	8000	11360	7079	8000	8913
			8913	10000	11220
			11220	12500	14130
11360	16000	22720	14130	16000	17780
			17780	20000	22390

From : http://www.engineeringtoolbox.com/octave-bands-frequency-limits-d_1602.html

Appendix B: Standard Deviation, 1/3 Octave & Order

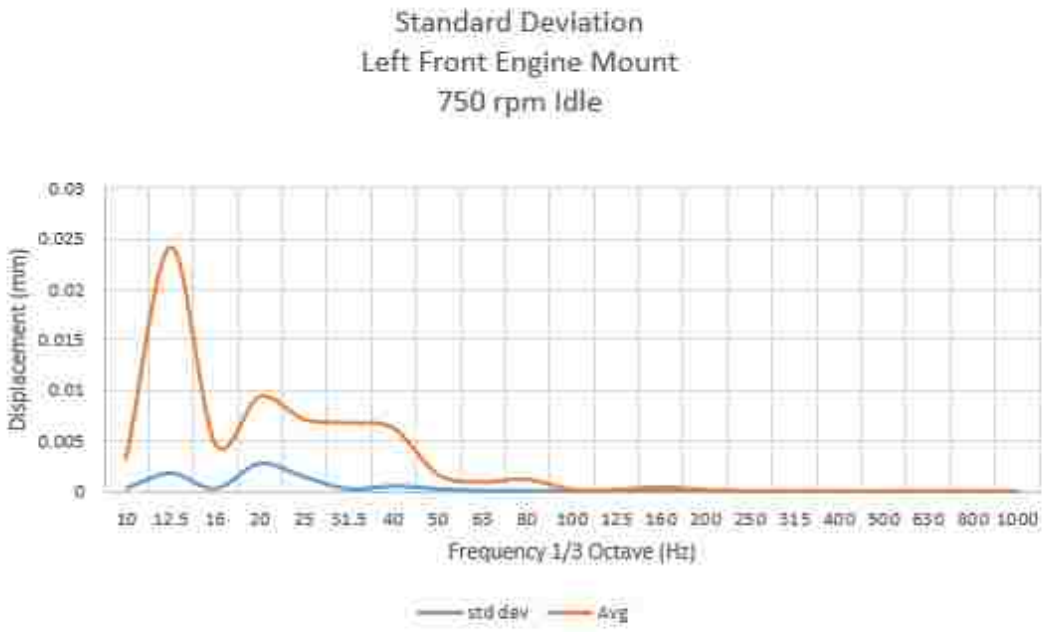

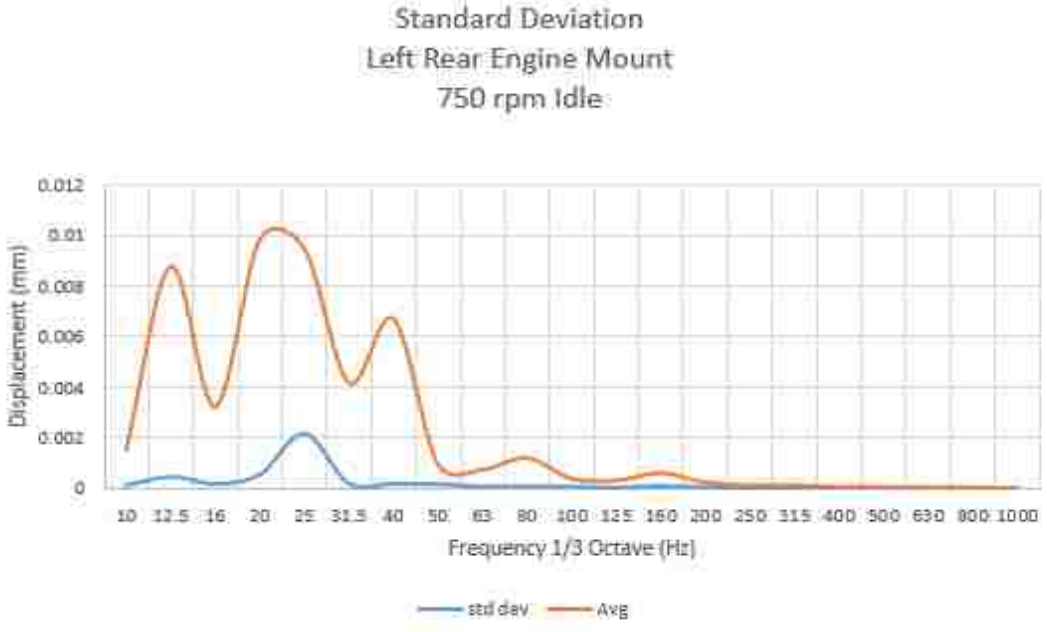

Standard Deviation
Right Front Engine Mount
750 rpm Idle

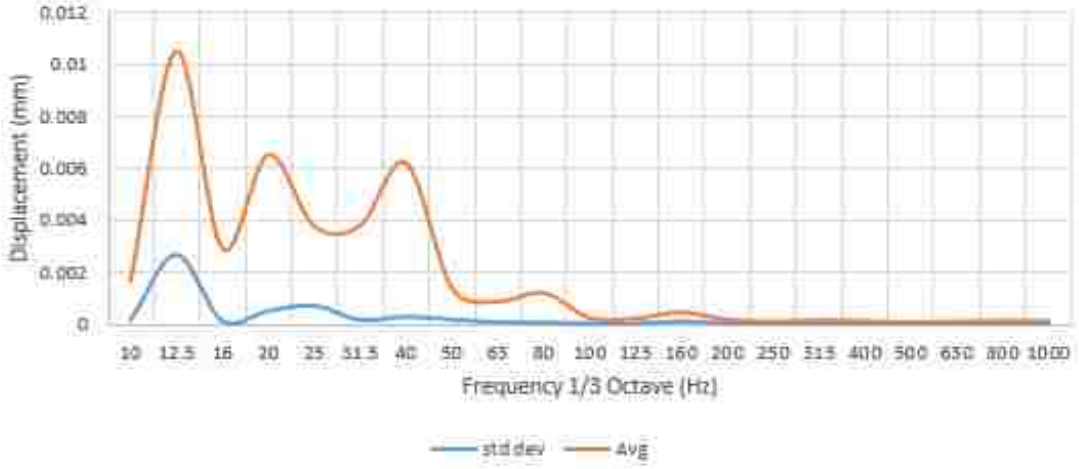

Standard Deviation
Right Rear Engine Mount
750 rpm Idle

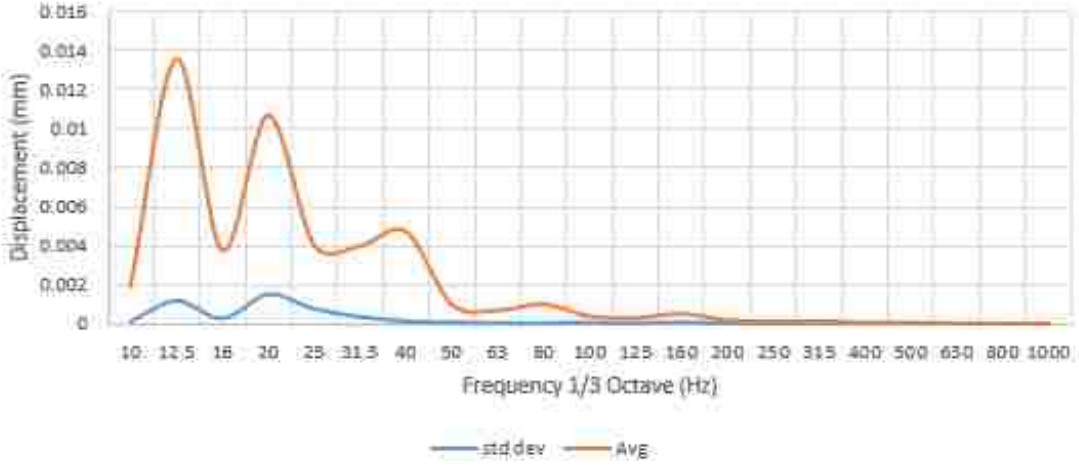

Standard Deviation
Left Front Engine Mount
1500 RPM 15% Throttle

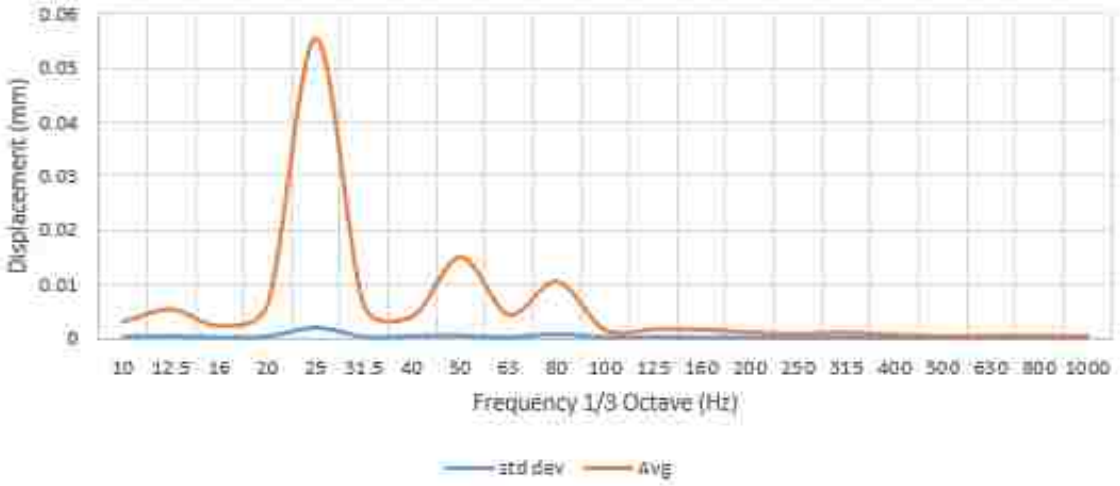

Standard Deviation
Left Rear Engine Mount
1500 RPM 15% Throttle

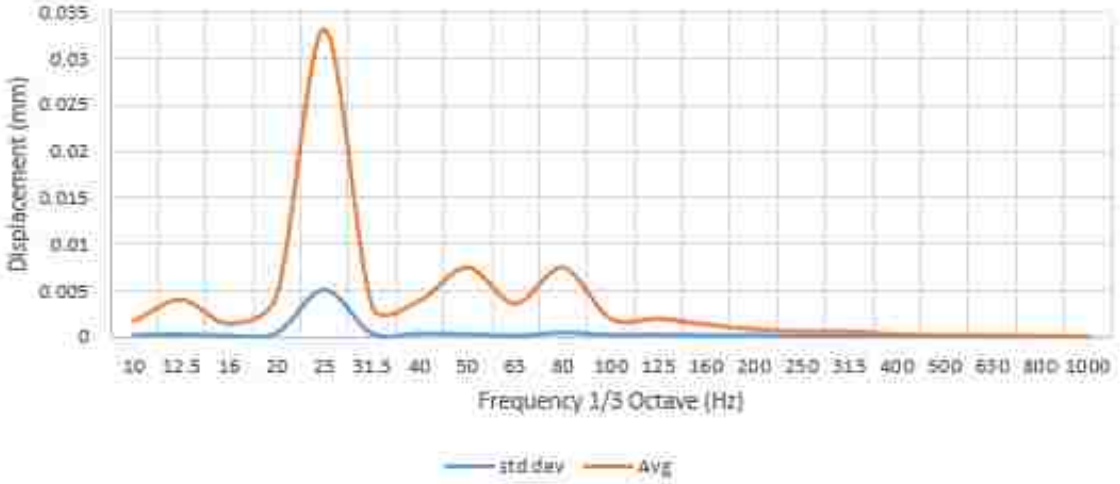

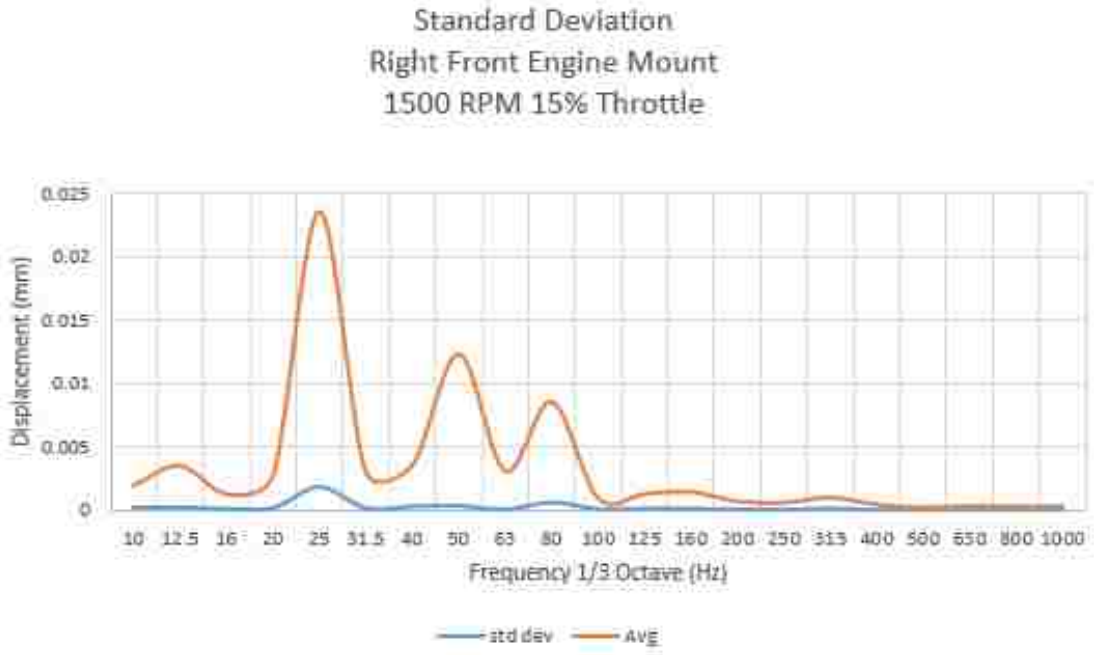
Standard Deviation
Right Front Engine Mount
1500 RPM 15% Throttle
Displacement (mm)
0.025
0.02
0.015
0.01
0.005
0
10 12.5 16 20 25 31.5 40 50 63 80 100 125 160 200 250 315 400 500 630 800 1000
Frequency 1/3 Octave (Hz)
std dev
avg

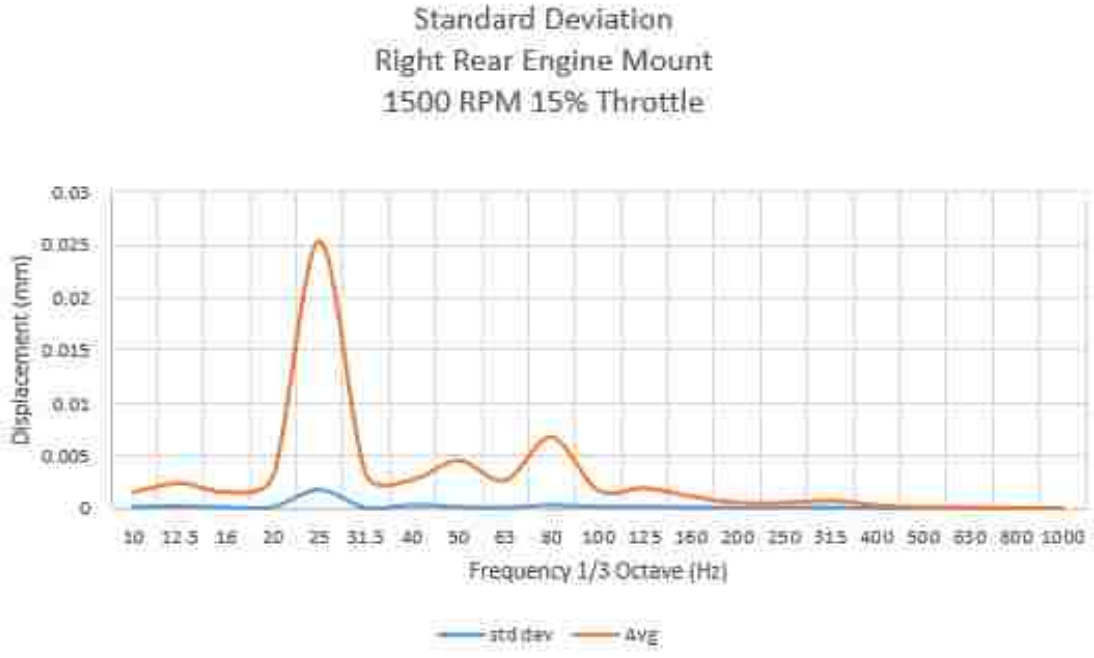
Standard Deviation
Right Rear Engine Mount
1500 RPM 15% Throttle
Displacement (mm)
0.03
0.025
0.02
0.015
0.01
0.005
0
10 12.5 16 20 25 31.5 40 50 63 80 100 125 160 200 250 315 400 500 630 800 1000
Frequency 1/3 Octave (Hz)
std dev
avg

Standard Deviation
Left Front Engine Mount
1500 RPM 50% Throttle

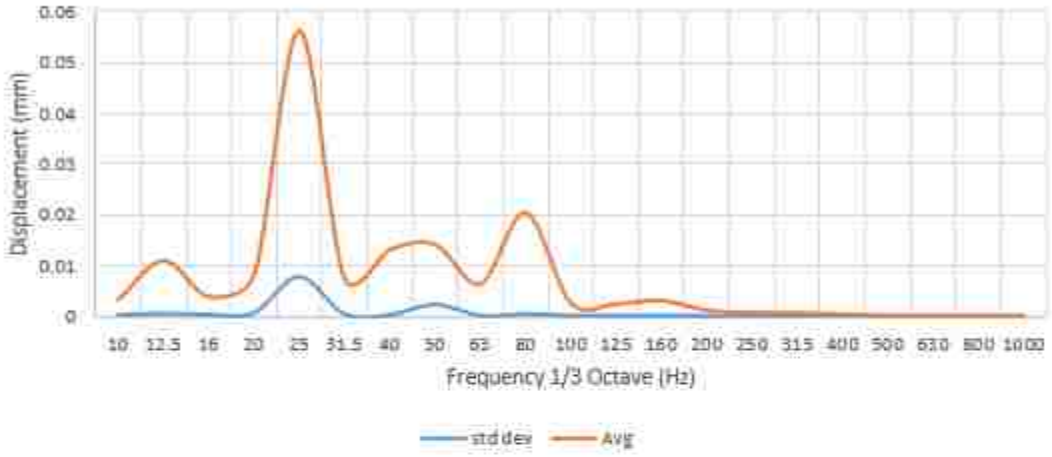

Standard Deviation
Left Rear Engine Mount
1500 RPM 50% Throttle

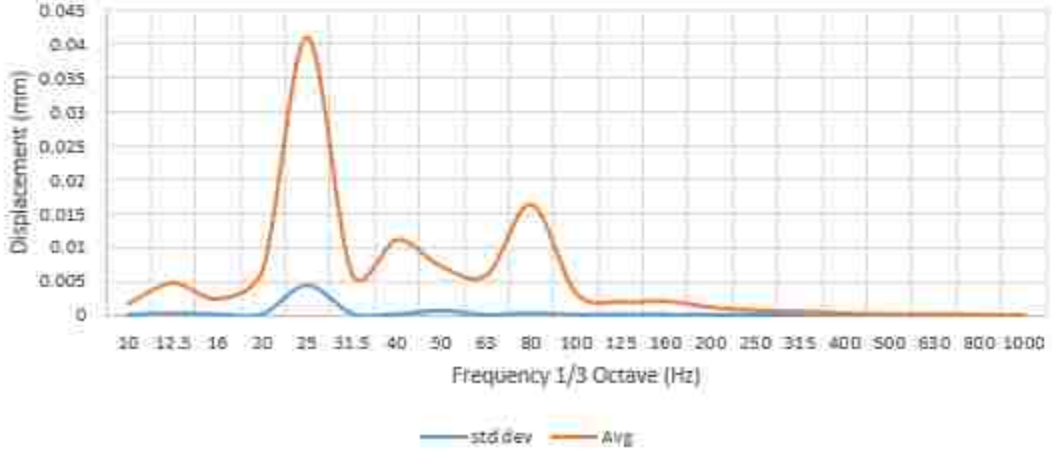

Standard Deviation
Right Front Engine Mount
1500 RPM 50% Throttle

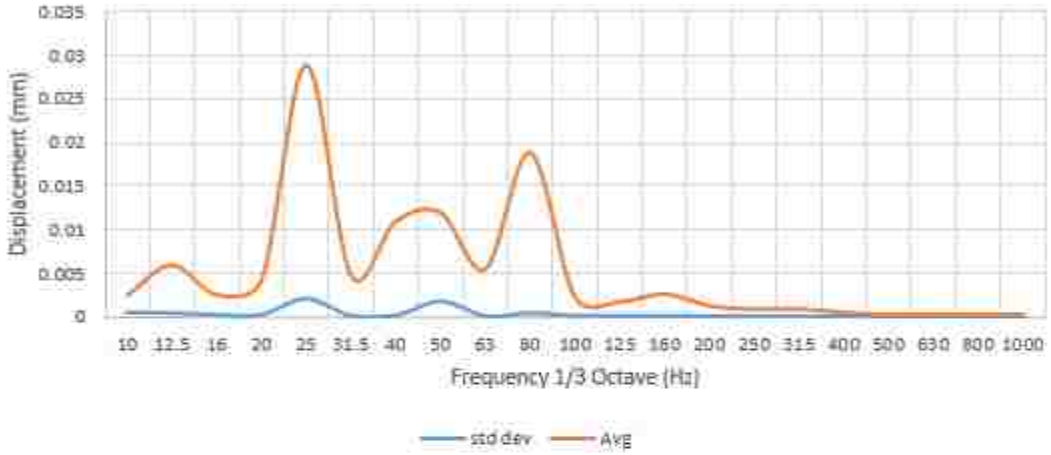

Standard Deviation
Right Rear Engine Mount
1500 RPM 50% Throttle

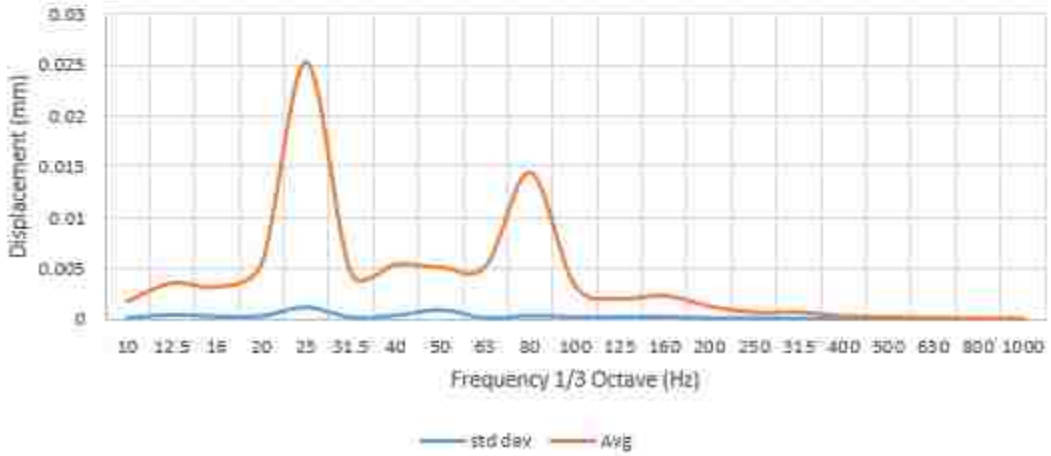

Standard Deviation
Left Front Engine Mount
1500 RPM 100% Throttle

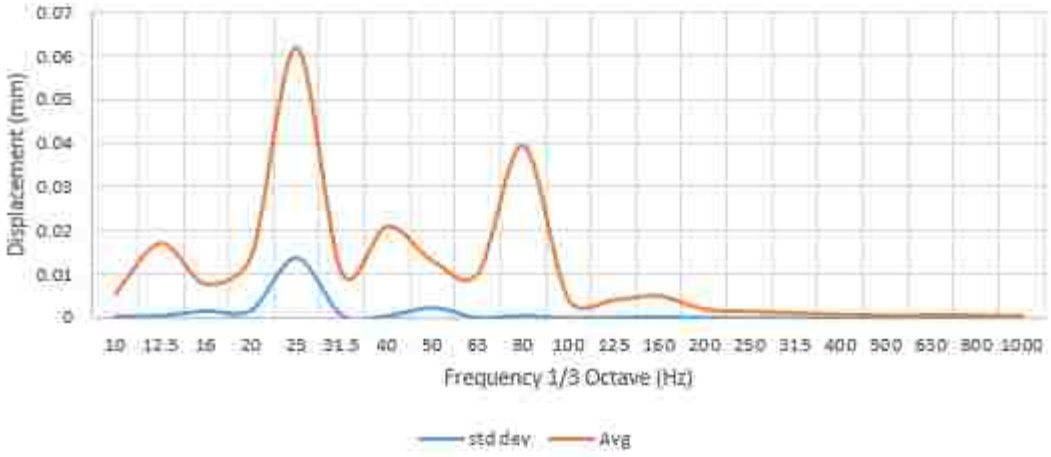

Standard Deviation
Left Rear Engine Mount
1500 RPM 100% Throttle

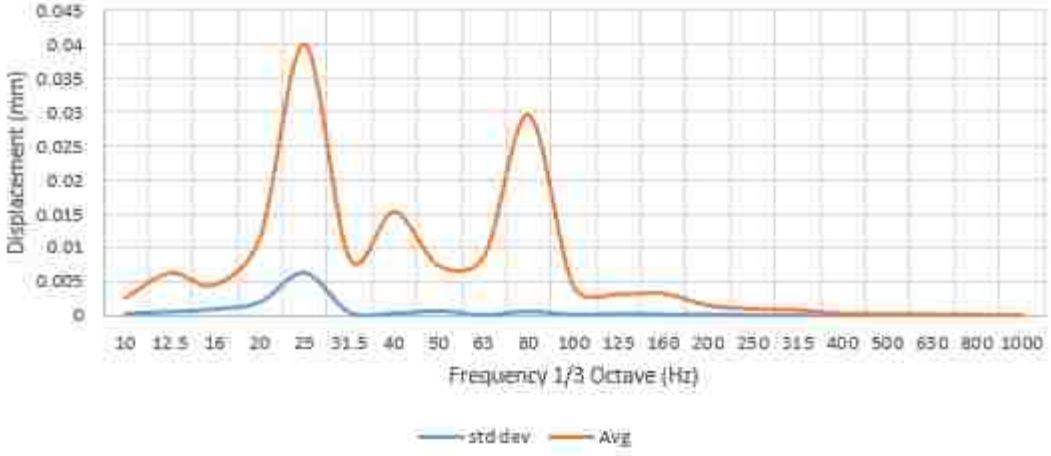

Standard Deviation
Right Front Engine Mount
1500 RPM 100% Throttle

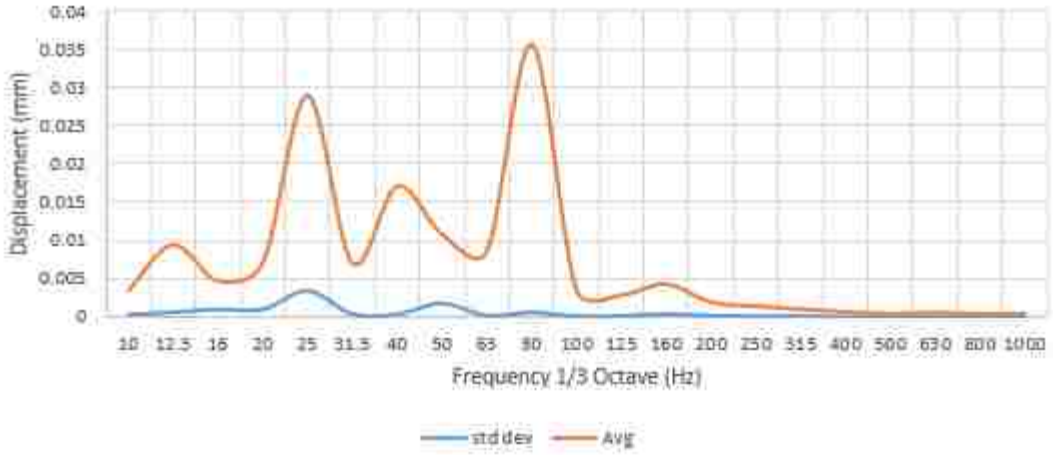

Standard Deviation
Right Rear Engine Mount
1500 RPM 100% Throttle

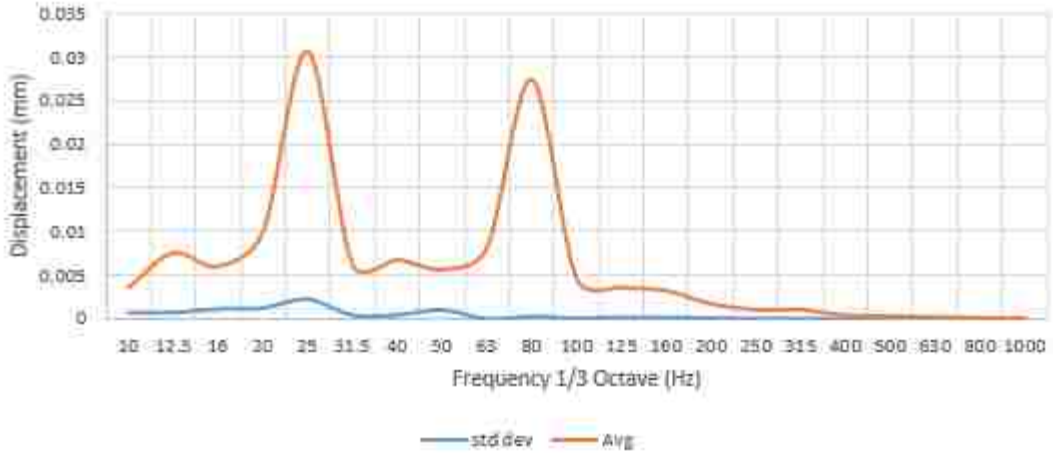

Standard Deviation
Left Front Engine Mount
750 RPM Idle

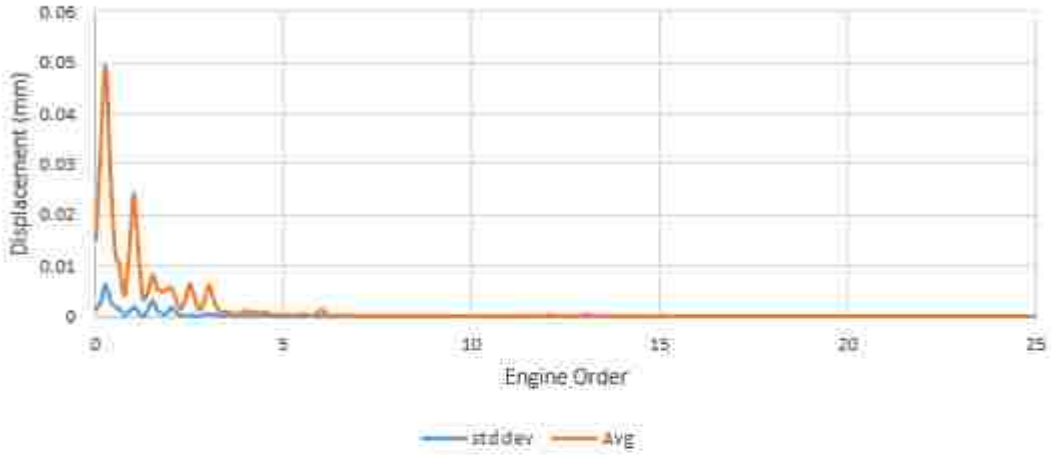

Standard Deviation
Left Rear Engine Mount
750 RPM Idle

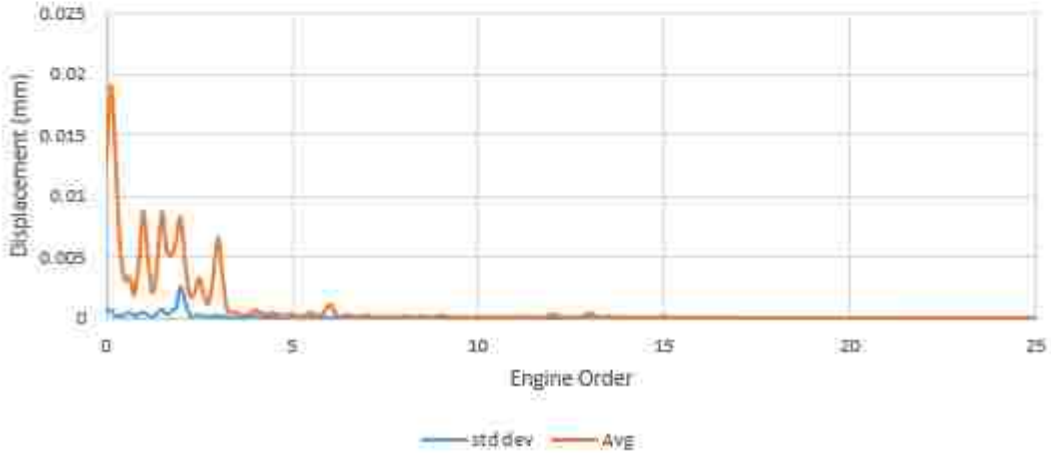

Standard Deviation
Left Front Engine Mount
750 RPM Idle

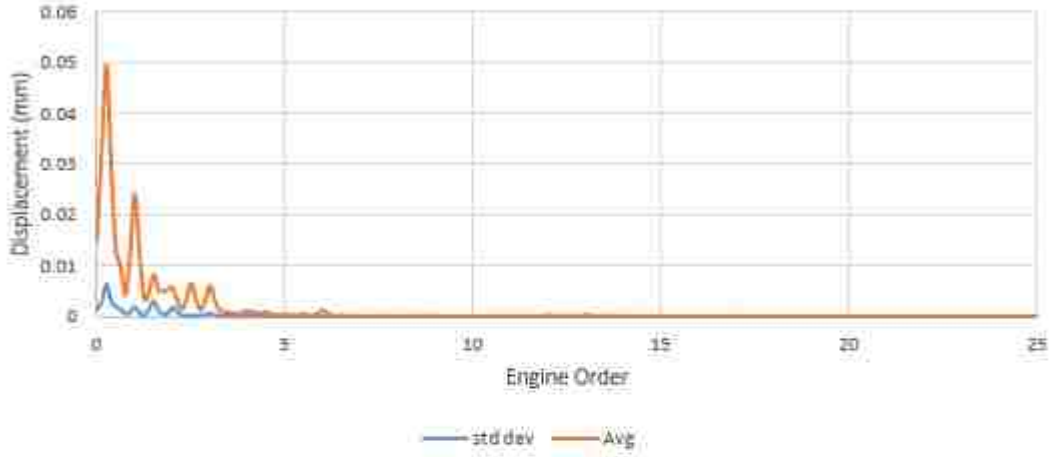

Standard Deviation
Left Rear Engine Mount
750 RPM Idle

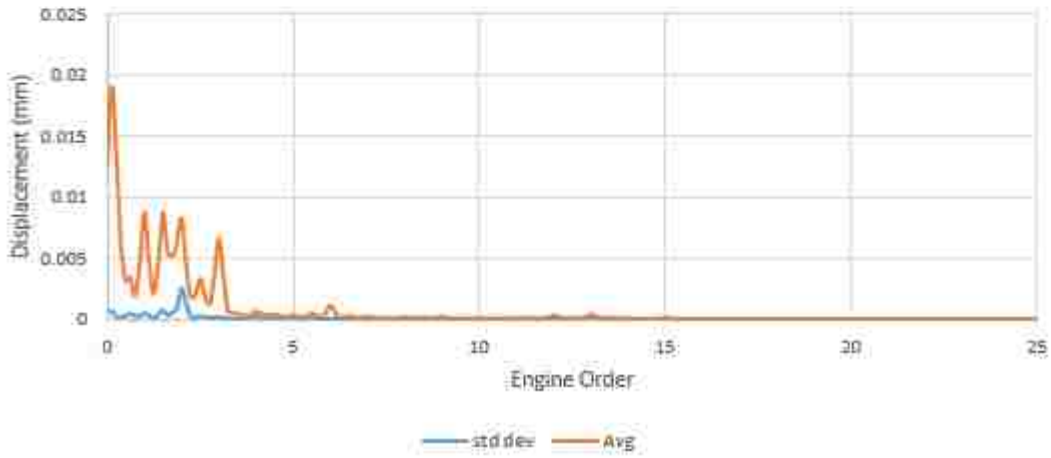

Standard Deviation
Front Right Engine Mount
750 RPM Idle

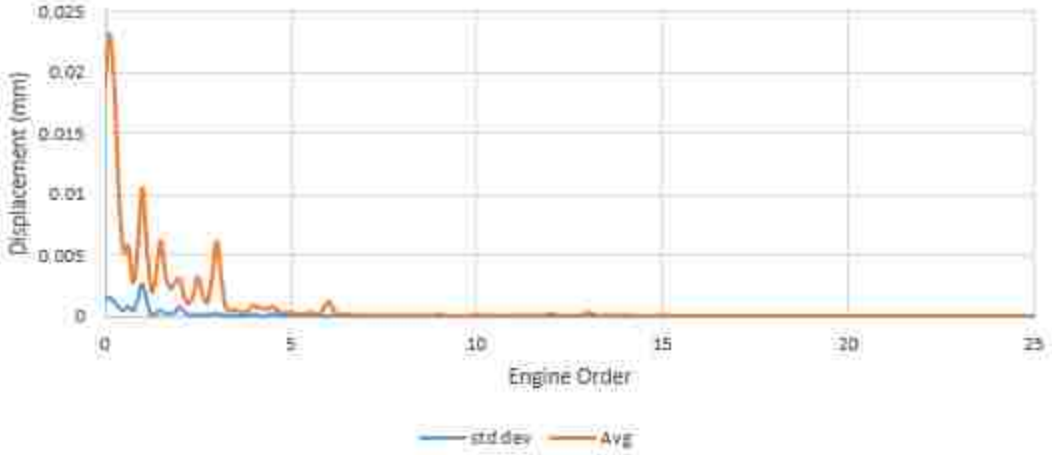

Standard Deviation
Right Rear Engine Mount
750 RPM Idle

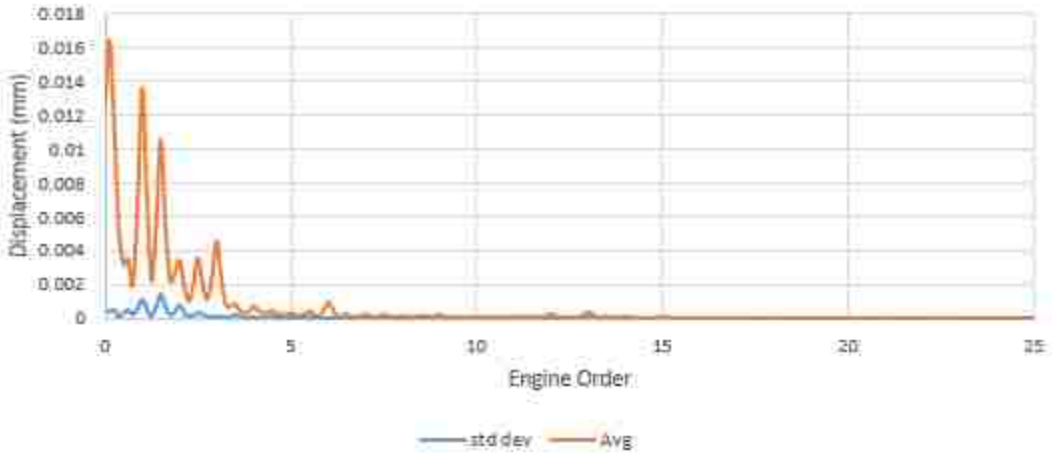

Standard Deviation
Left Front Engine Mount
1500 RPM 15% Throttle

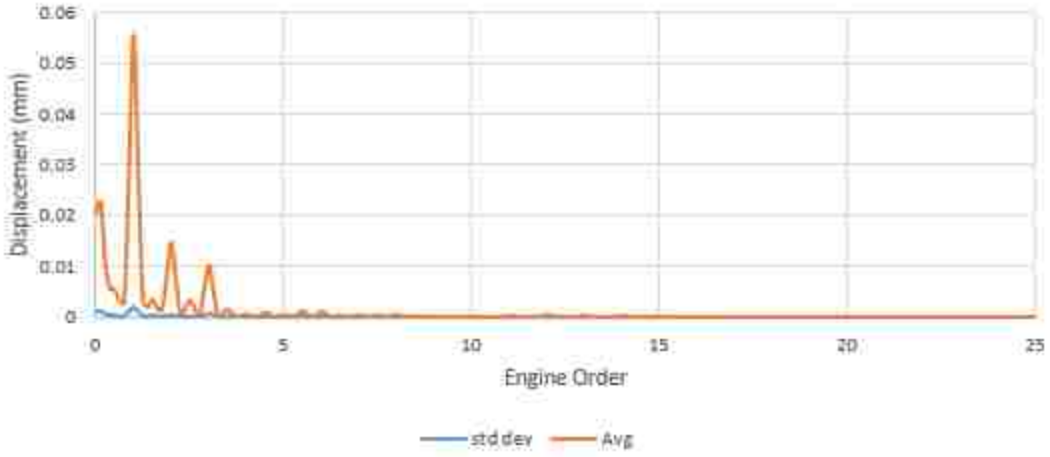

Standard Deviation
Left Rear Engine Mount
1500 RPM 15% Throttle

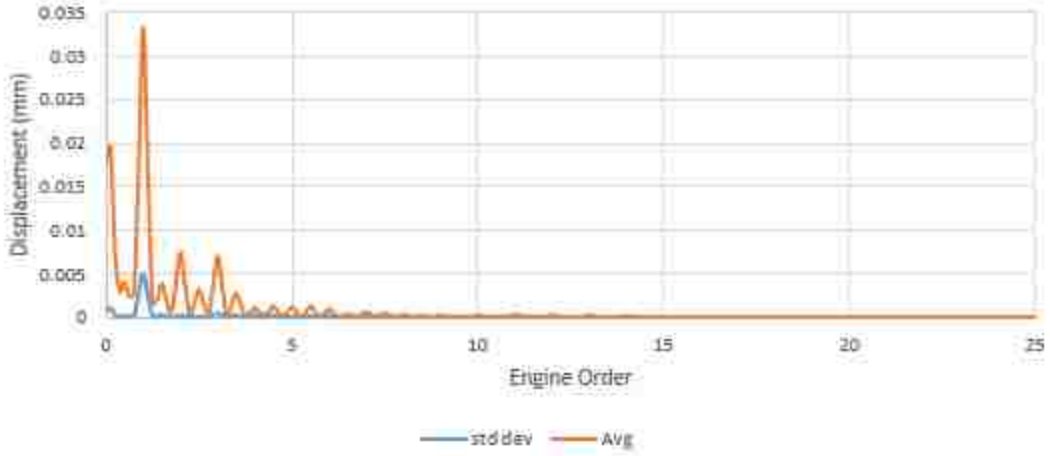

Standard Deviation
Front Right Engine Mount
1500 RPM 15% Throttle

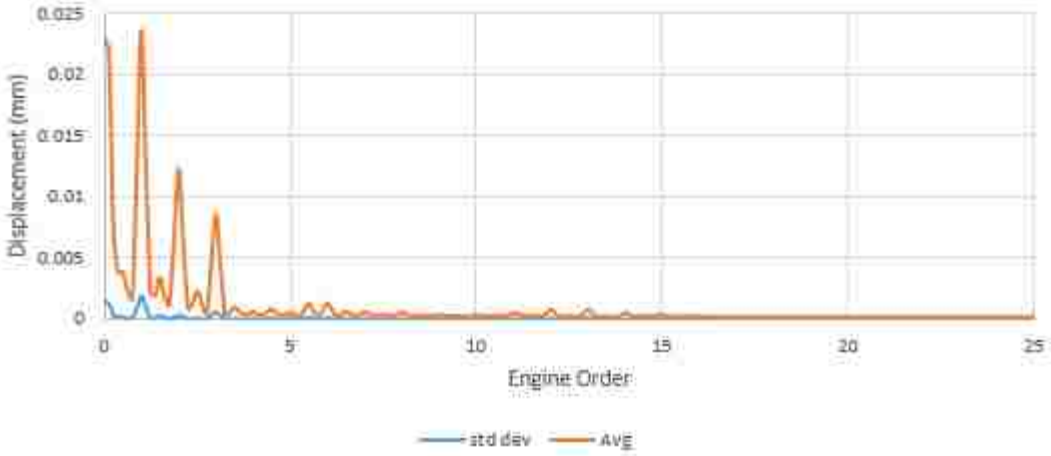

Standard Deviation
Right Rear Engine Mount
1500 RPM 15% Throttle

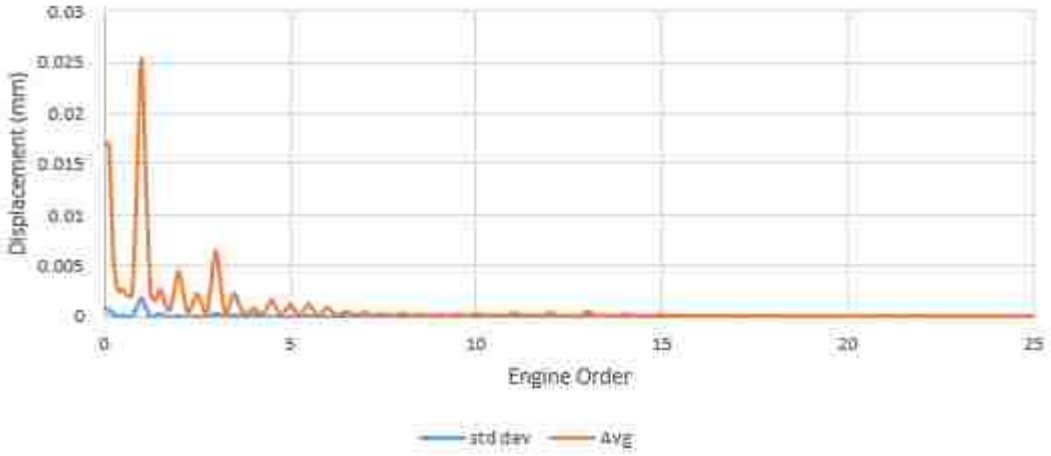

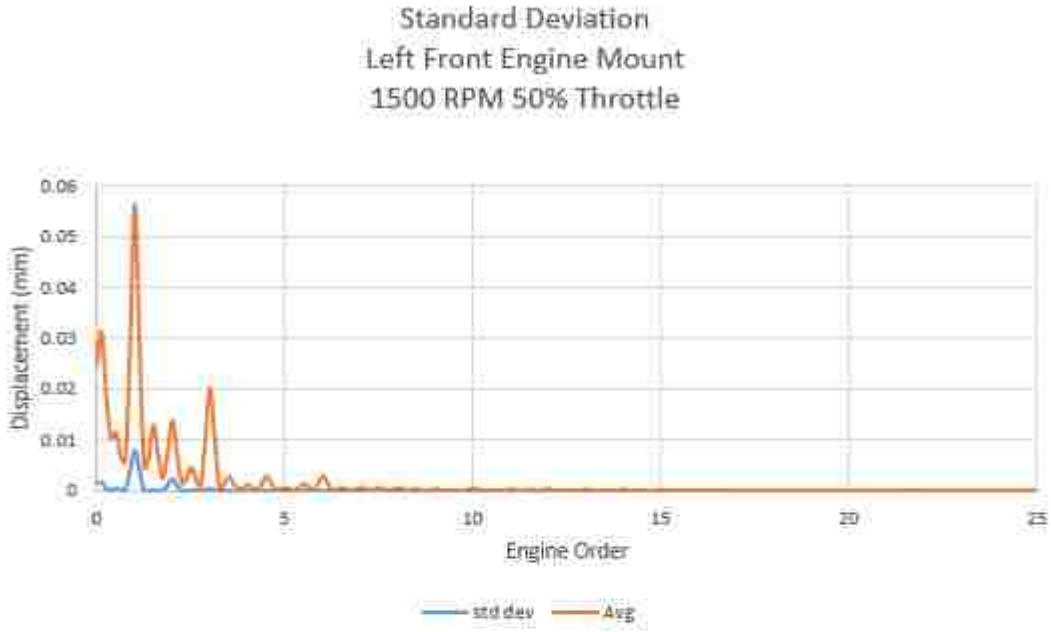
Standard Deviation
Left Front Engine Mount
1500 RPM 50% Throttle
Displacement (mm)
0.06
0.05
0.04
0.03
0.02
0.01
0
0
5
10
15
20
25
Engine Order
std dev
Avg

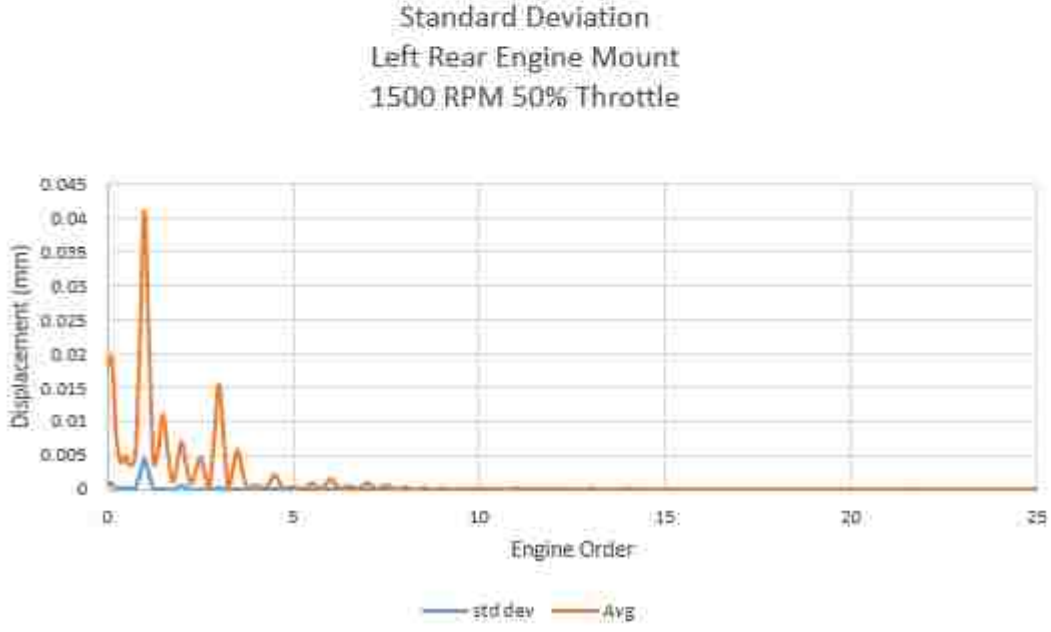
Standard Deviation
Left Rear Engine Mount
1500 RPM 50% Throttle
Displacement (mm)
0.045
0.04
0.035
0.03
0.025
0.02
0.015
0.01
0.005
0
0
5
10
15
20
25
Engine Order
std dev
Avg

Standard Deviation
Front Right Engine Mount
1500 RPM 50% Throttle

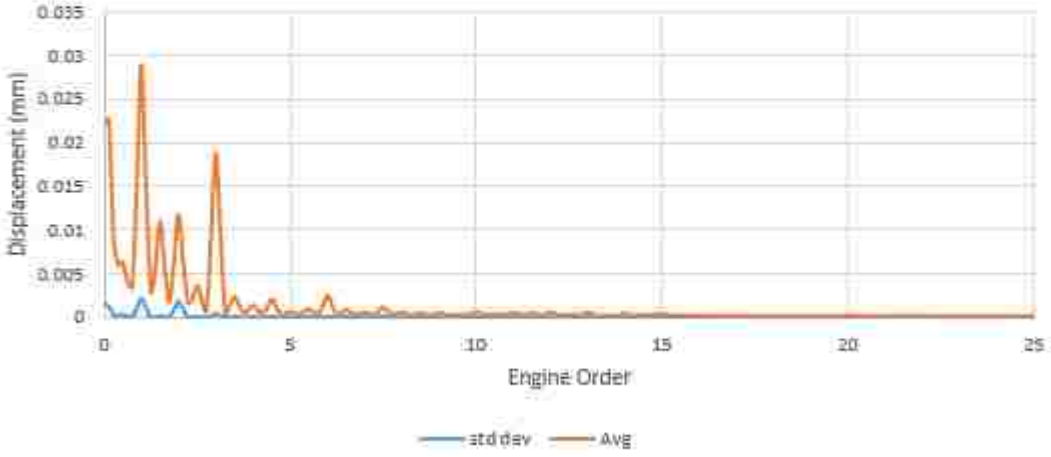

Standard Deviation
Right Rear Engine Mount
1500 RPM 50% Throttle

Standard Deviation
Left Front Engine Mount
1500 RPM 100% Throttle

Standard Deviation
Left Rear Engine Mount
1500 RPM 100% Throttle

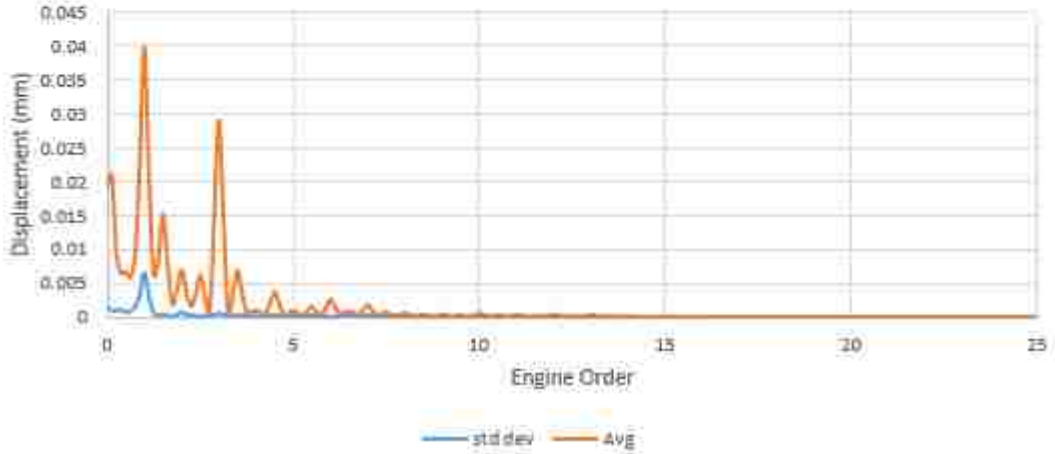

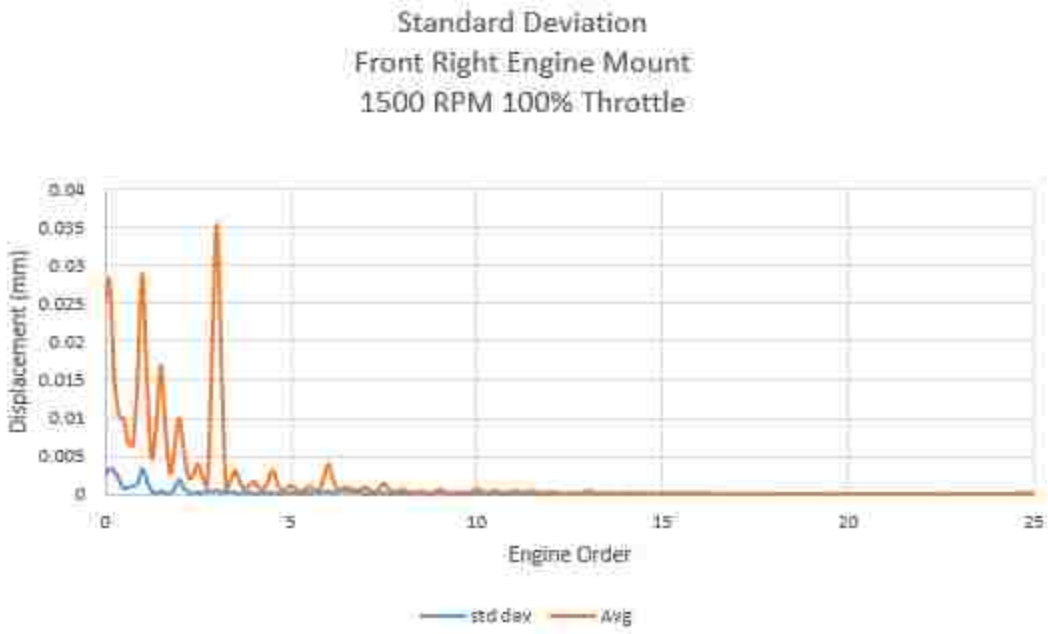
Standard Deviation
Front Right Engine Mount
1500 RPM 100% Throttle
Displacement (mm)
0.04
0.035
0.03
0.025
0.02
0.015
0.01
0.005
0
0
5
10
15
20
25
Engine Order
std dev
Avg

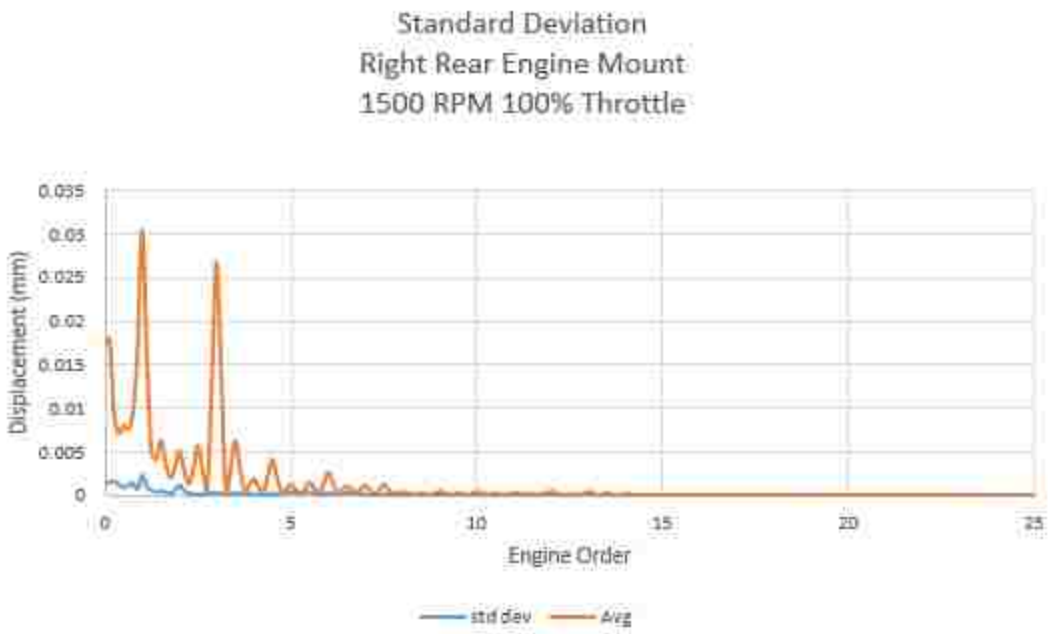
Standard Deviation
Right Rear Engine Mount
1500 RPM 100% Throttle
Displacement (mm)
0.035
0.03
0.025
0.02
0.015
0.01
0.005
0
0
5
10
15
20
25
Engine Order
std dev
Avg

Appendix C: Confidence Interval, 1/3 Octave & Order

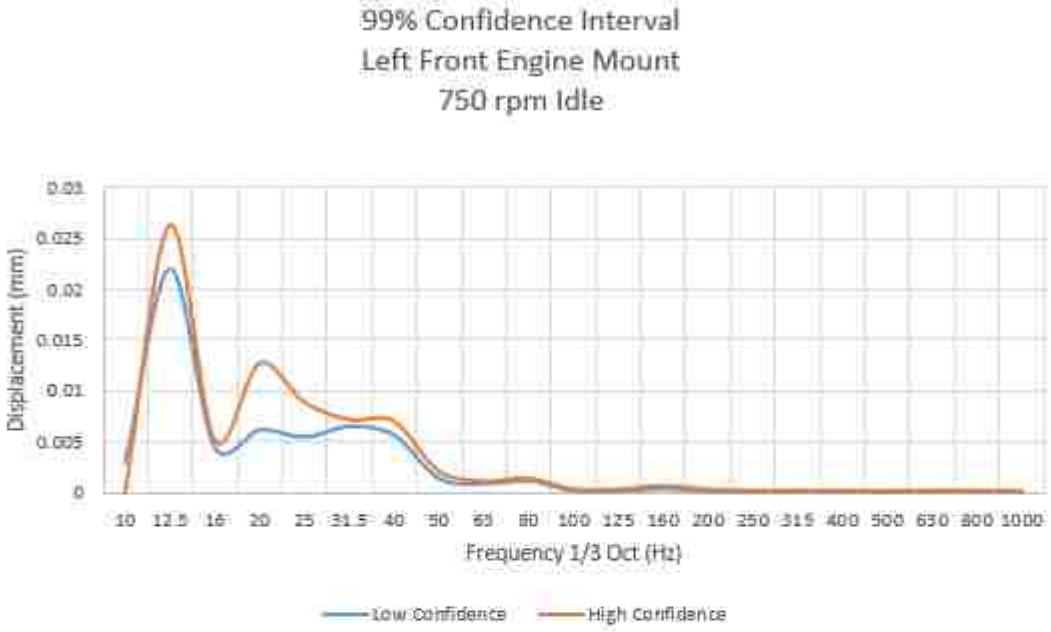

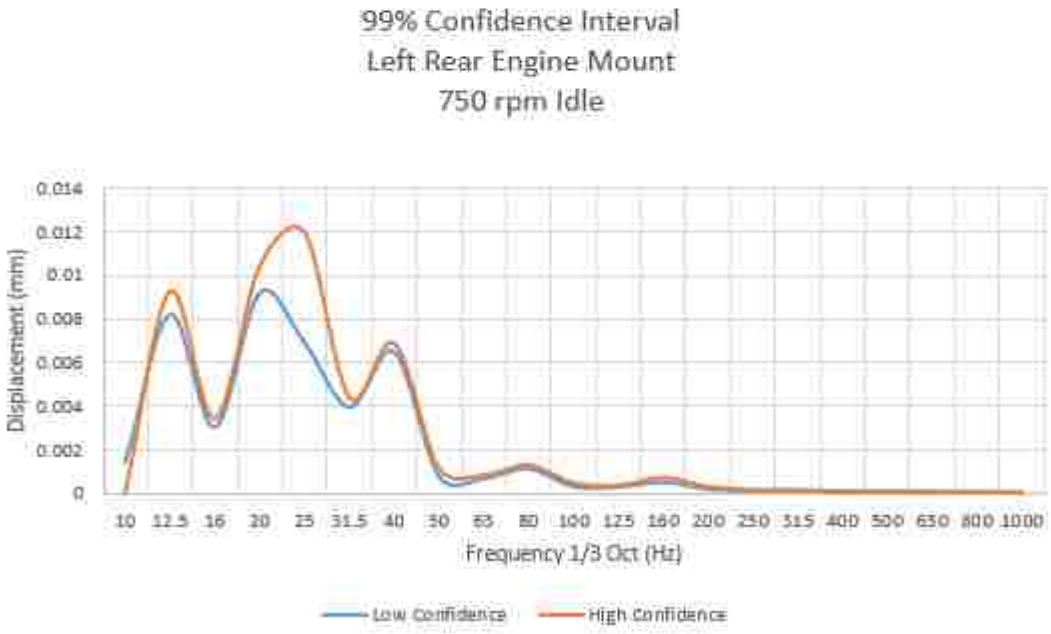

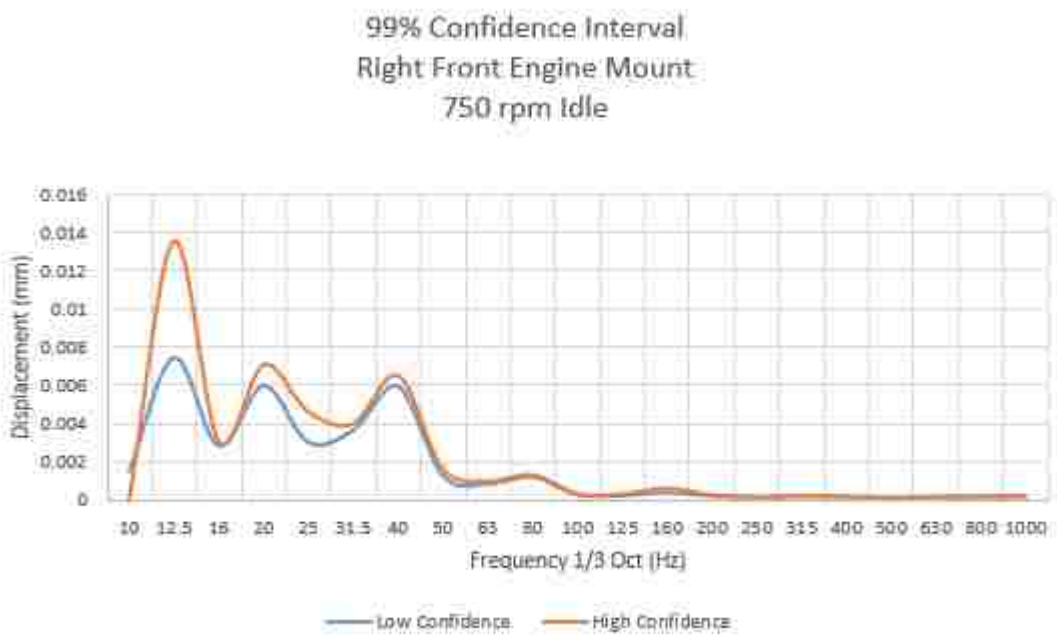
99% Confidence Interval
Right Front Engine Mount
750 rpm Idle
Displacement (mm)
0.016
0.014
0.012
0.01
0.008
0.006
0.004
0.002
0
10 12.5 16 20 25 31.5 40 50 63 80 100 125 160 200 250 315 400 500 630 800 1000
Frequency 1/3 Oct (Hz)
Low Confidence
High Confidence

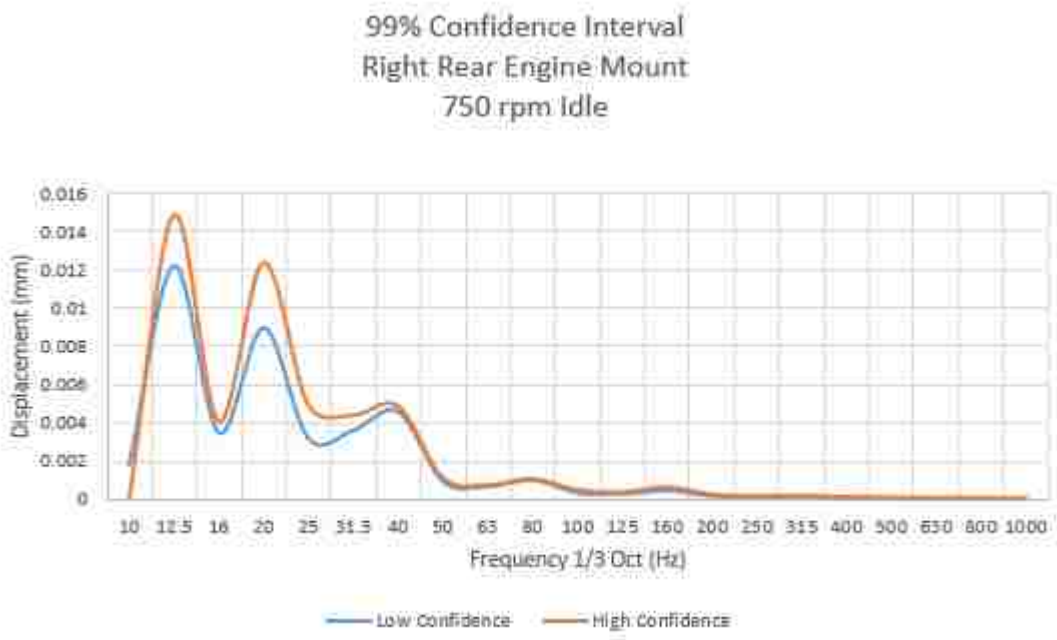
99% Confidence Interval
Right Rear Engine Mount
750 rpm Idle
Displacement (mm)
0.016
0.014
0.012
0.01
0.008
0.006
0.004
0.002
0
10 12.5 16 20 25 31.5 40 50 63 80 100 125 160 200 250 315 400 500 630 800 1000
Frequency 1/3 Oct (Hz)
Low Confidence
High Confidence

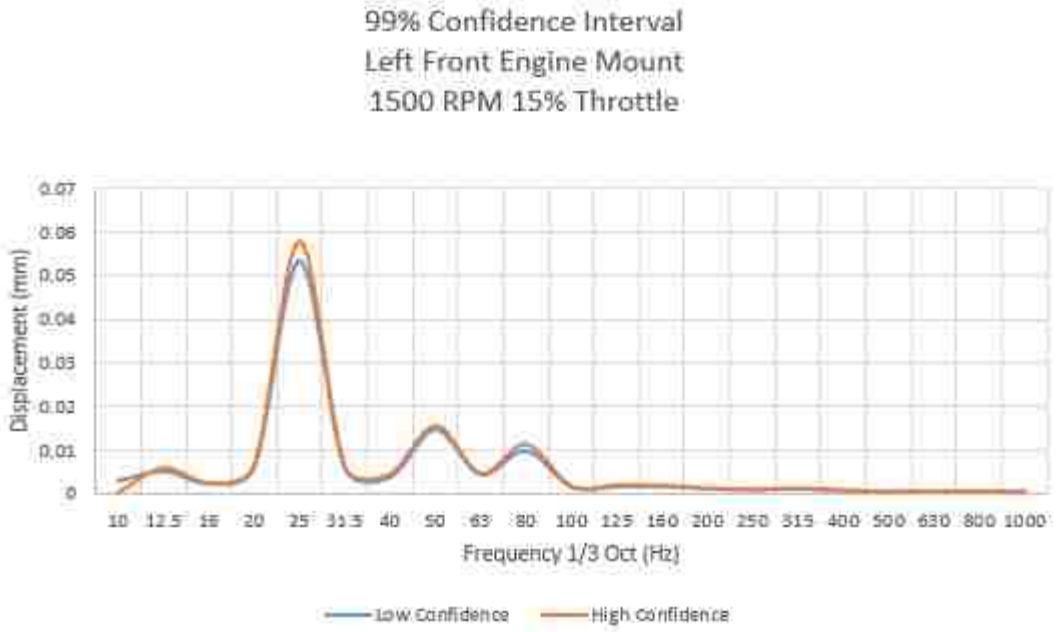
99% Confidence Interval
Left Front Engine Mount
1500 RPM 15% Throttle
Displacement (mm)
0.07
0.06
0.05
0.04
0.03
0.02
0.01
0
10 12.5 16 20 25 31.5 40 50 63 80 100 125 160 200 250 315 400 500 630 800 1000
Frequency 1/3 Oct (Hz)
Low Confidence
High Confidence

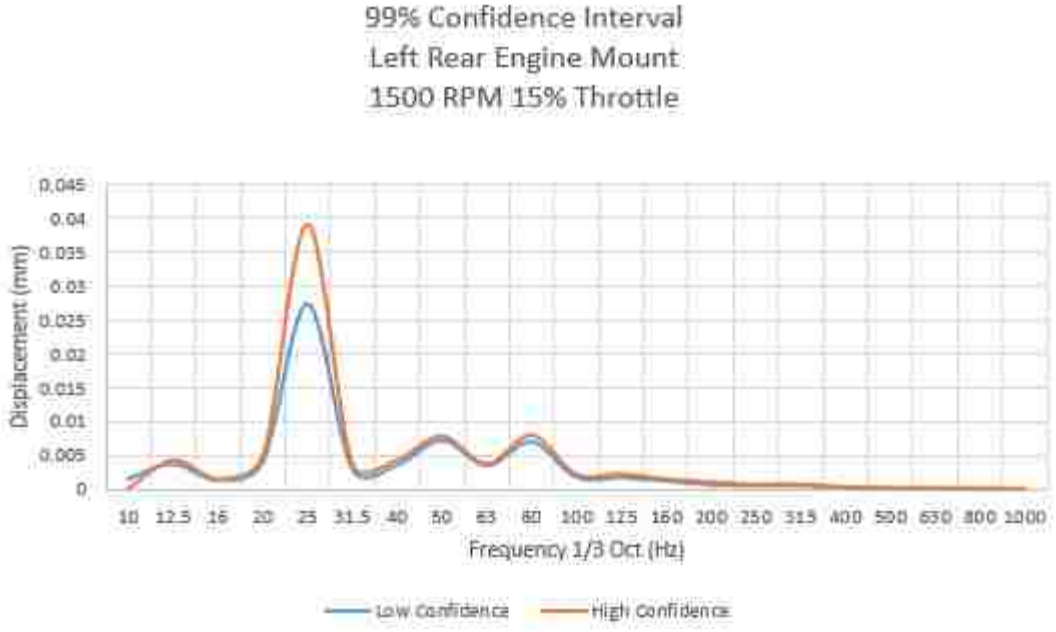
99% Confidence Interval
Left Rear Engine Mount
1500 RPM 15% Throttle
Displacement (mm)
0.045
0.04
0.035
0.03
0.025
0.02
0.015
0.01
0.005
0
10 12.5 16 20 25 31.5 40 50 63 80 100 125 160 200 250 315 400 500 630 800 1000
Frequency 1/3 Oct (Hz)
Low Confidence
High Confidence

99% Confidence Interval
Right Front Engine Mount
1500 RPM 15% Throttle

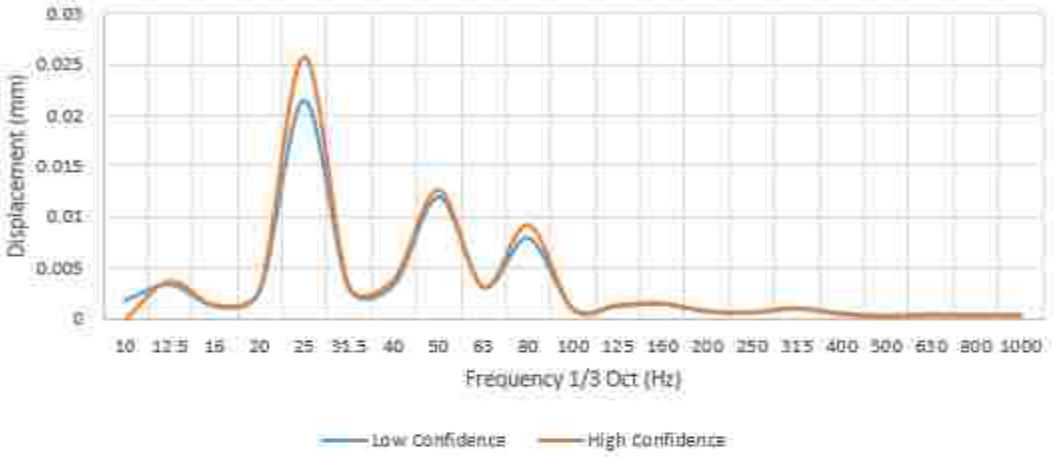

99% Confidence Interval
Right Rear Engine Mount
1500 RPM 15% Throttle

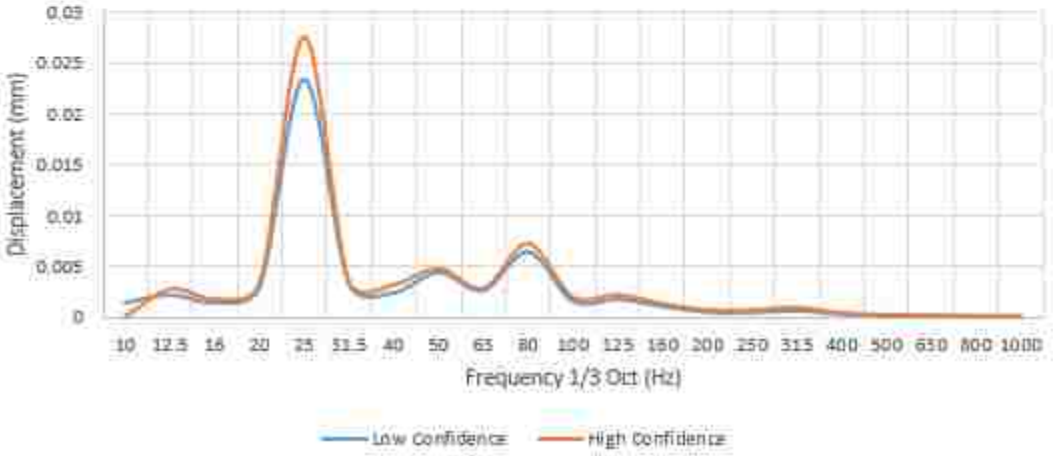

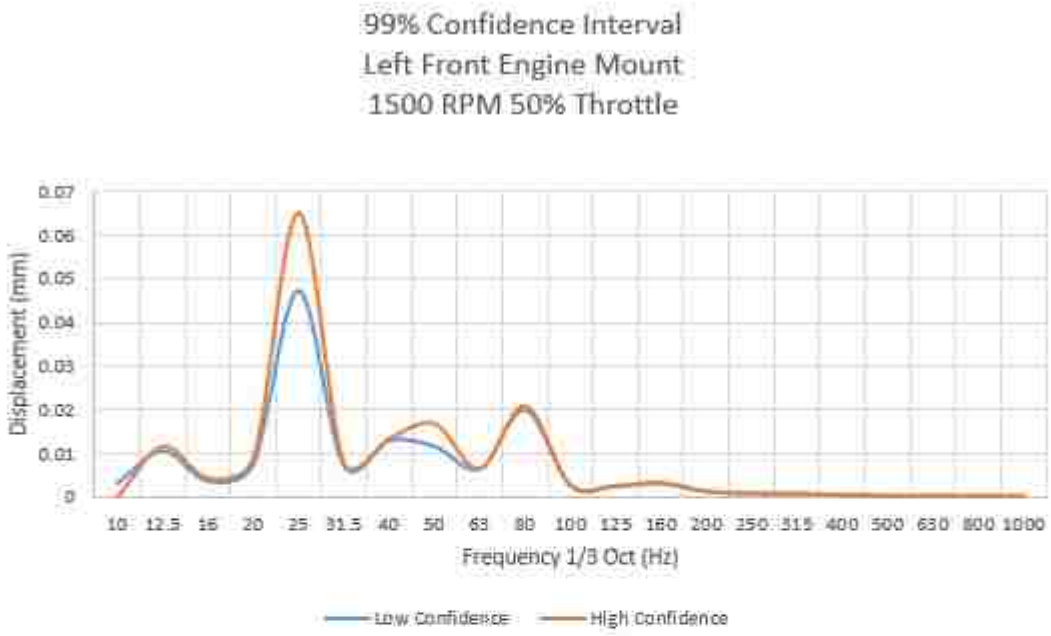
99% Confidence Interval
Left Front Engine Mount
1500 RPM 50% Throttle
Displacement (mm)
0.07
0.06
0.05
0.04
0.03
0.02
0.01
0
10 12.5 16 20 25 31.5 40 50 63 80 100 125 160 200 250 315 400 500 630 800 1000
Frequency 1/3 Oct (Hz)
Low Confidence
High Confidence

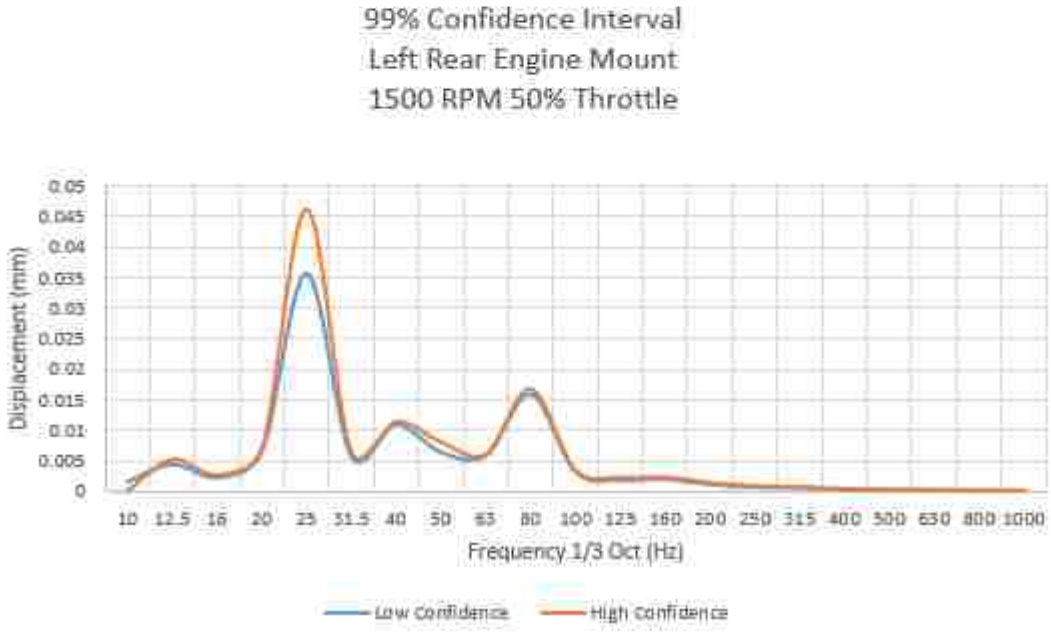
99% Confidence Interval
Left Rear Engine Mount
1500 RPM 50% Throttle
Displacement (mm)
0.05
0.045
0.04
0.035
0.03
0.025
0.02
0.015
0.01
0.005
0
10 12.5 16 20 25 31.5 40 50 63 80 100 125 160 200 250 315 400 500 630 800 1000
Frequency 1/3 Oct (Hz)
Low Confidence
High Confidence

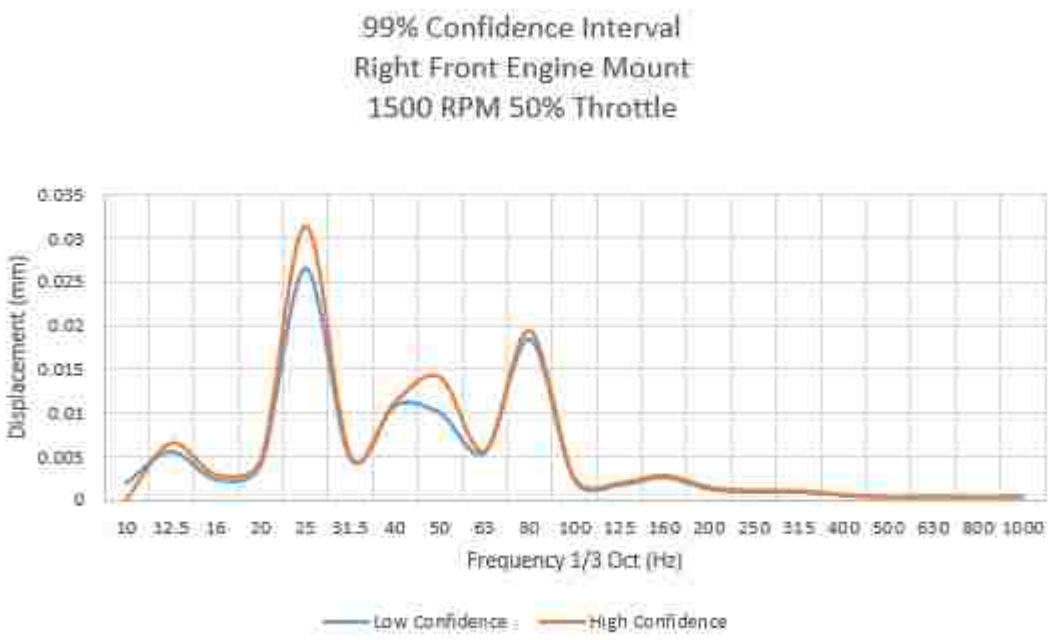
99% Confidence Interval
Right Front Engine Mount
1500 RPM 50% Throttle
Displacement (mm)
0.035
0.03
0.025
0.02
0.015
0.01
0.005
0
10 12.5 16 20 25 31.5 40 50 63 80 100 125 160 200 250 315 400 500 630 800 1000
Frequency 1/3 Oct (Hz)
Low Confidence
High Confidence

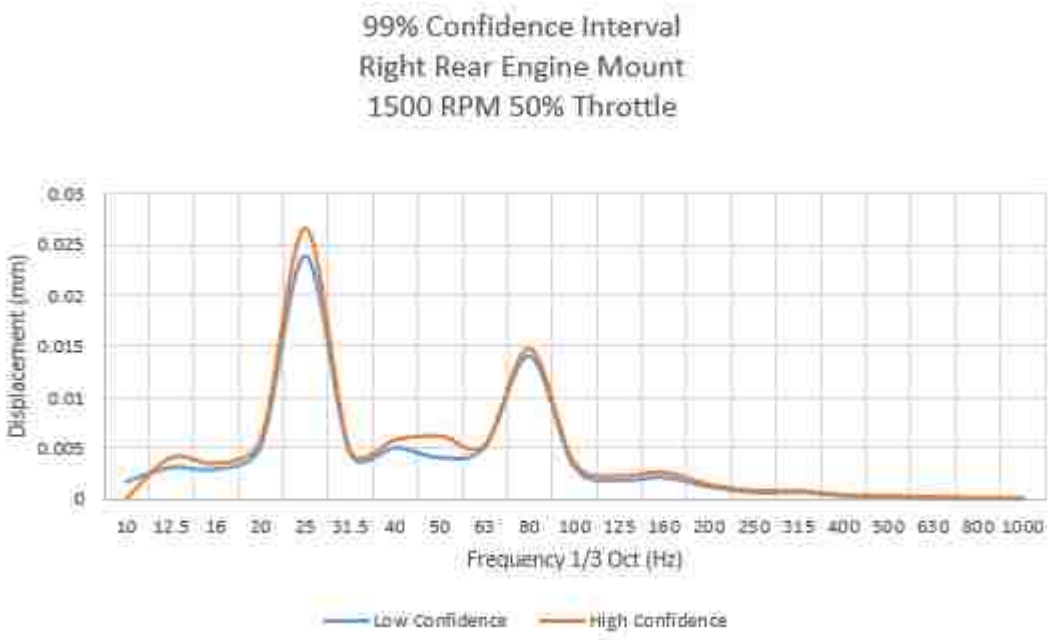
99% Confidence Interval
Right Rear Engine Mount
1500 RPM 50% Throttle
Displacement (mm)
0.03
0.025
0.02
0.015
0.01
0.005
0
10 12.5 16 20 25 31.5 40 50 63 80 100 125 160 200 250 315 400 500 630 800 1000
Frequency 1/3 Oct (Hz)
Low Confidence
High Confidence

99% Confidence Interval
Left Front Engine Mount
1500 RPM 100% Throttle

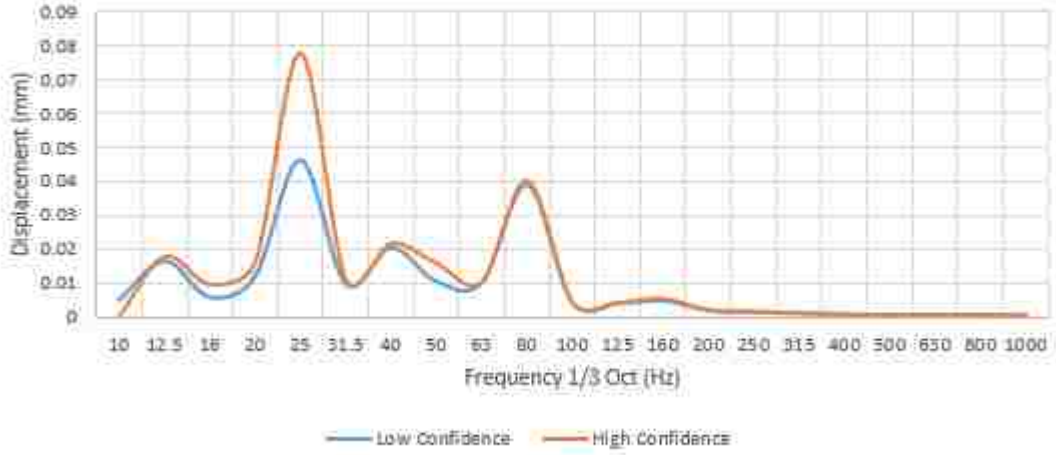

99% Confidence Interval
Left Rear Engine Mount
1500 RPM 100% Throttle

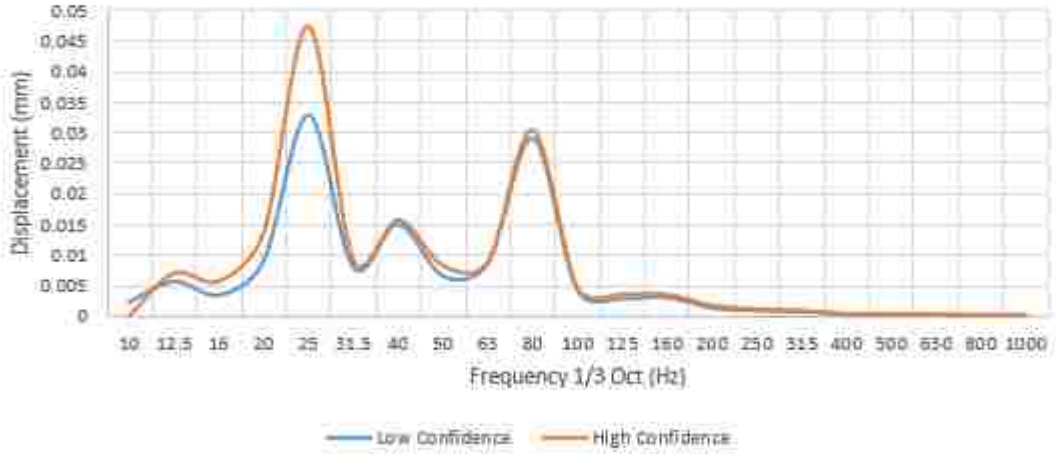

99% Confidence Interval
Left Front Engine Mount
1500 RPM 100% Throttle

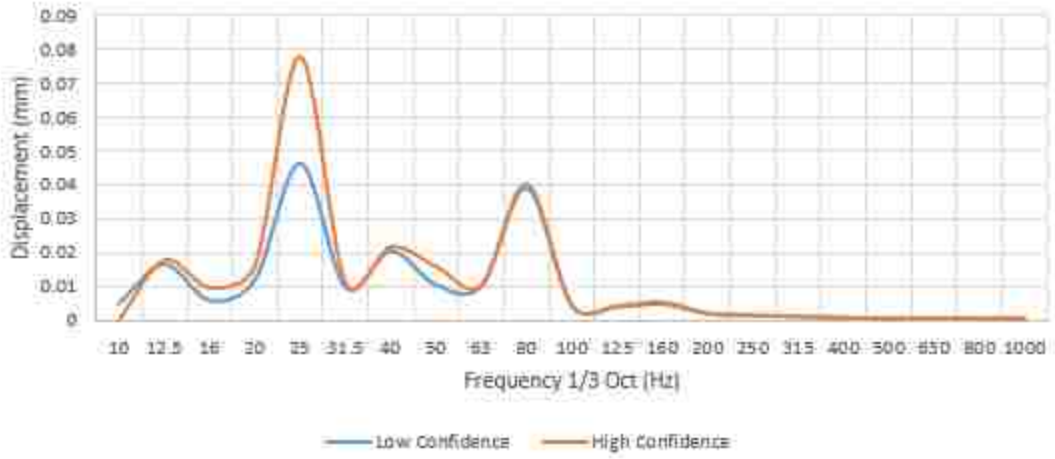

99% Confidence Interval
Left Rear Engine Mount
1500 RPM 100% Throttle

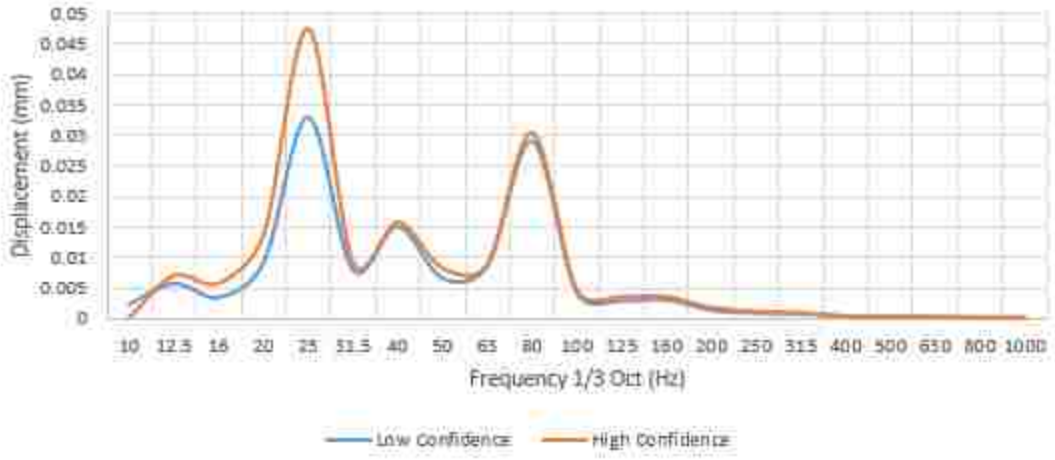

99% Confidence Interval
Right Front Engine Mount
1500 RPM 100% Throttle

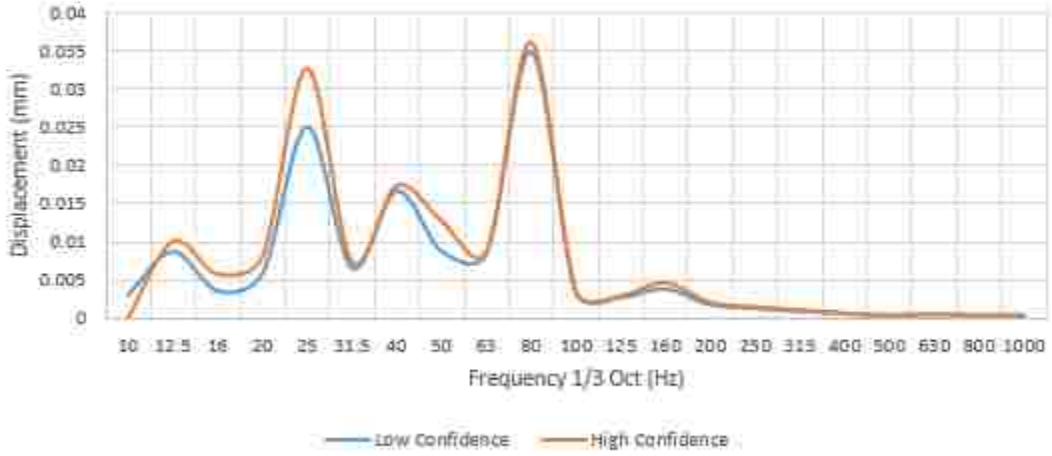

99% Confidence Interval
Right Rear Engine Mount
1500 RPM 100% Throttle

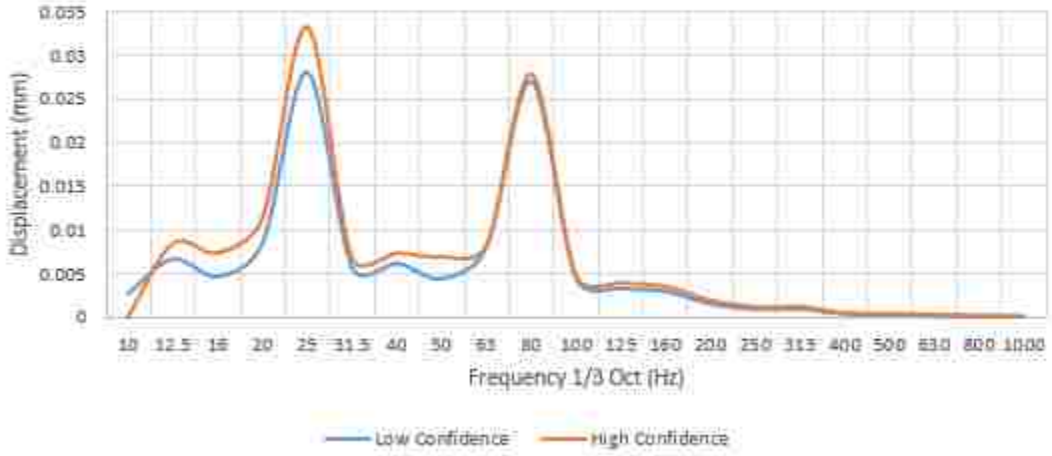

99% Confidence Interval
Left Front Engine Mount
750 RPM Idle

99% Confidence Interval
Left Rear Engine Mount
750 RPM Idle

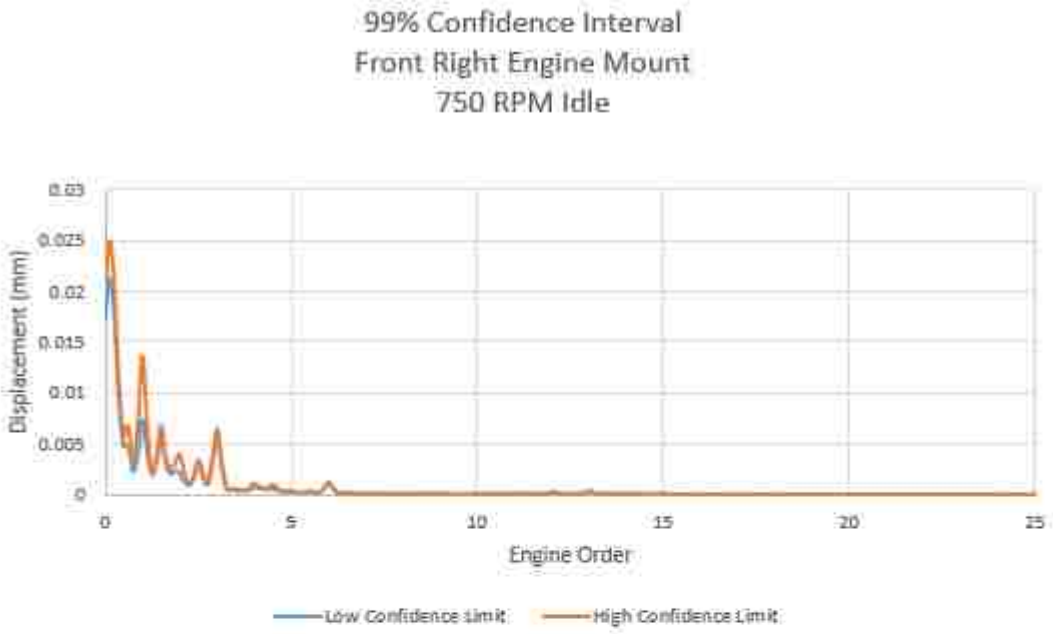
99% Confidence Interval
Front Right Engine Mount
750 RPM Idle
Displacement (mm)
0.03
0.025
0.02
0.015
0.01
0.005
0
0
5
10
15
20
25
Engine Order
Low Confidence Limit
High Confidence Limit

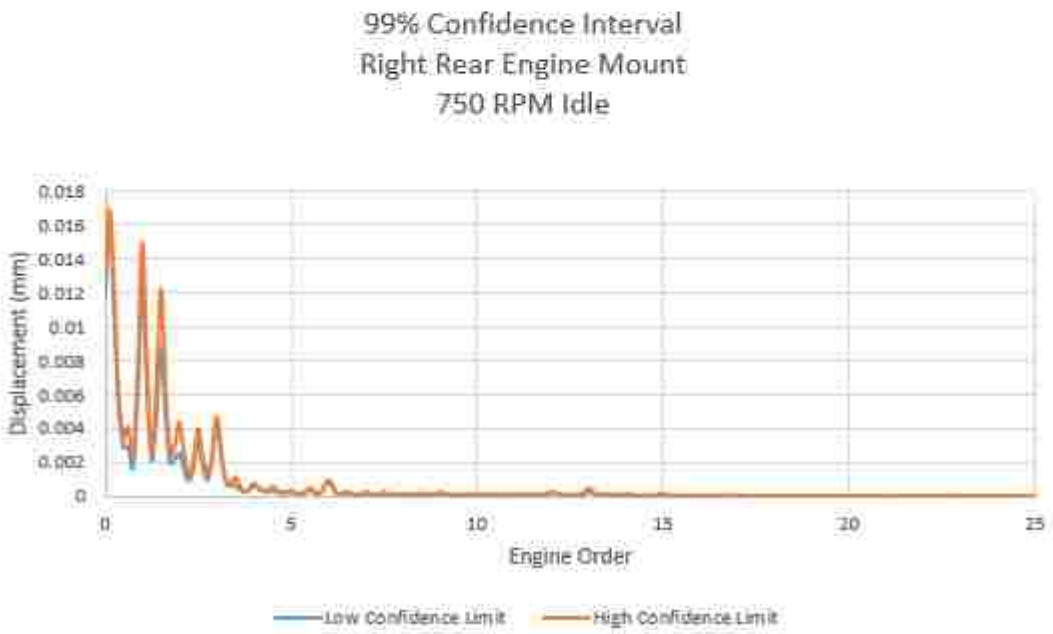
99% Confidence Interval
Right Rear Engine Mount
750 RPM Idle
Displacement (mm)
0.018
0.016
0.014
0.012
0.01
0.008
0.006
0.004
0.002
0
0
5
10
15
20
25
Engine Order
Low Confidence Limit
High Confidence Limit

99% Confidence Interval
Left Front Engine Mount
1500 RPM 15% Throttle

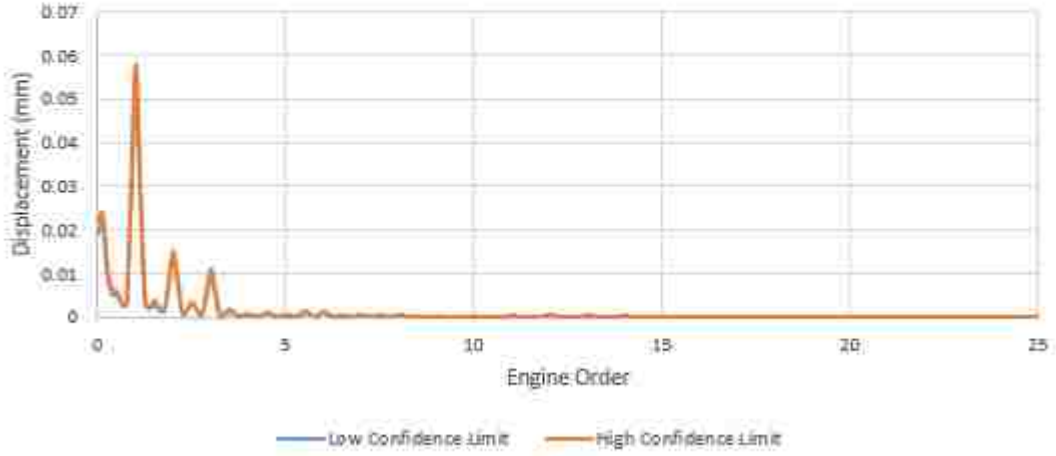

99% Confidence Interval
Left Rear Engine Mount
1500 RPM 15% Throttle

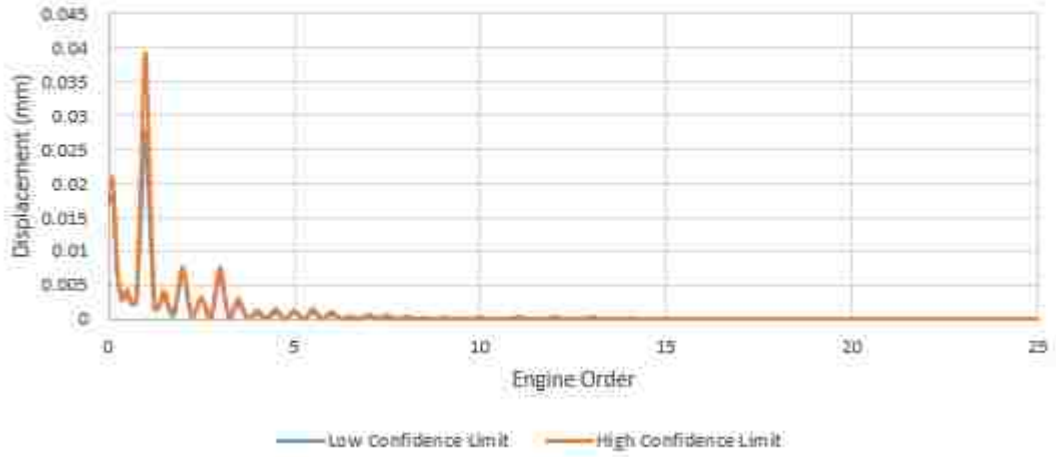

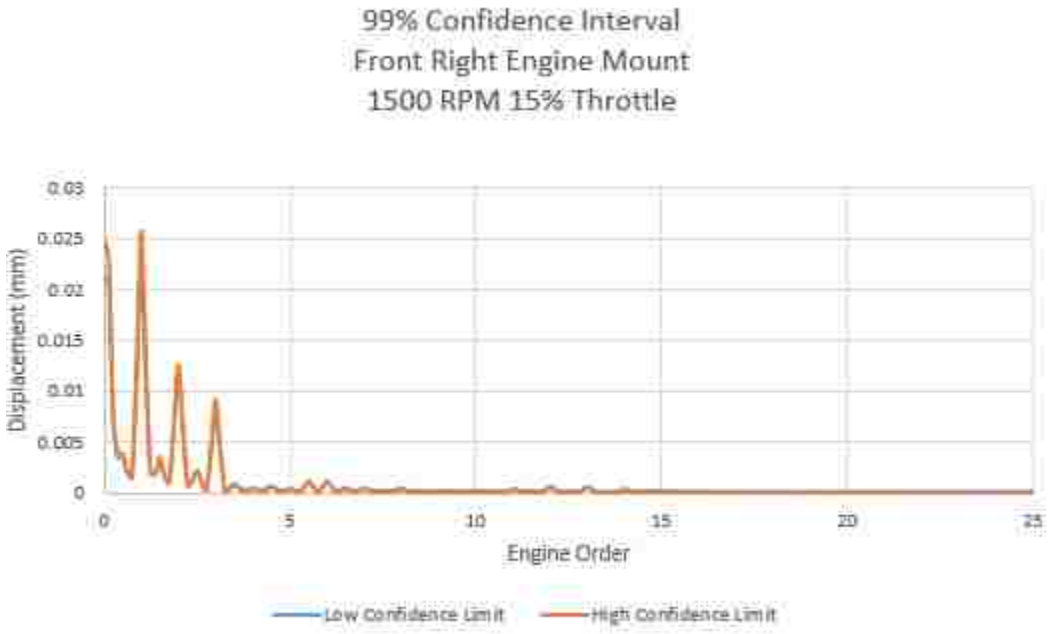
99% Confidence Interval
Front Right Engine Mount
1500 RPM 15% Throttle
Displacement (mm)
0.03
0.025
0.02
0.015
0.01
0.005
0
0
5
10
15
20
25
Engine Order
Low Confidence Limit
High Confidence Limit

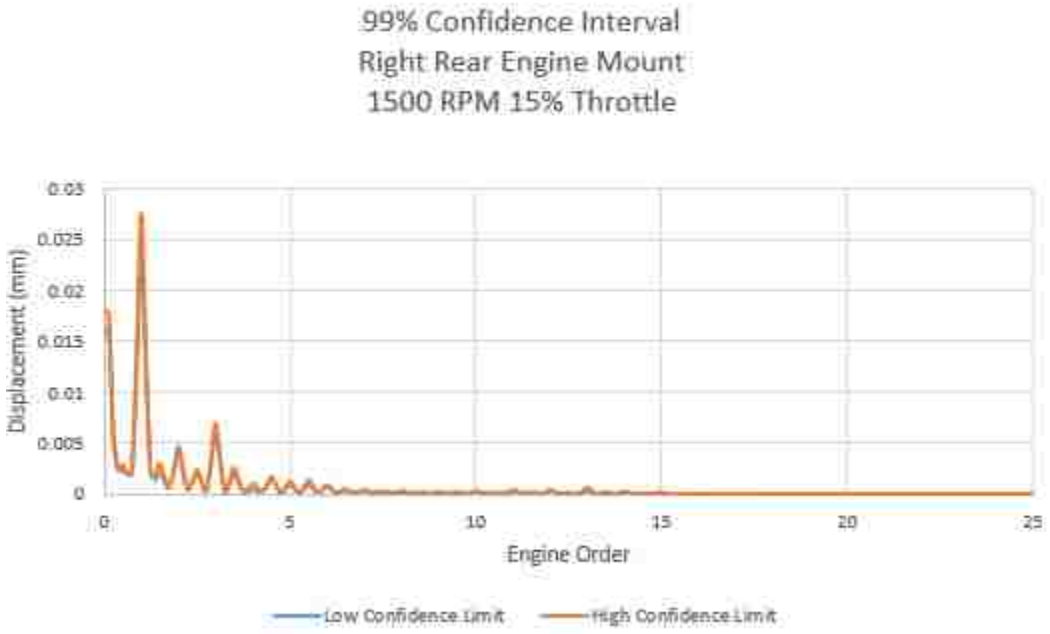
99% Confidence Interval
Right Rear Engine Mount
1500 RPM 15% Throttle
Displacement (mm)
0.03
0.025
0.02
0.015
0.01
0.005
0
0
5
10
15
20
25
Engine Order
Low Confidence Limit
High Confidence Limit

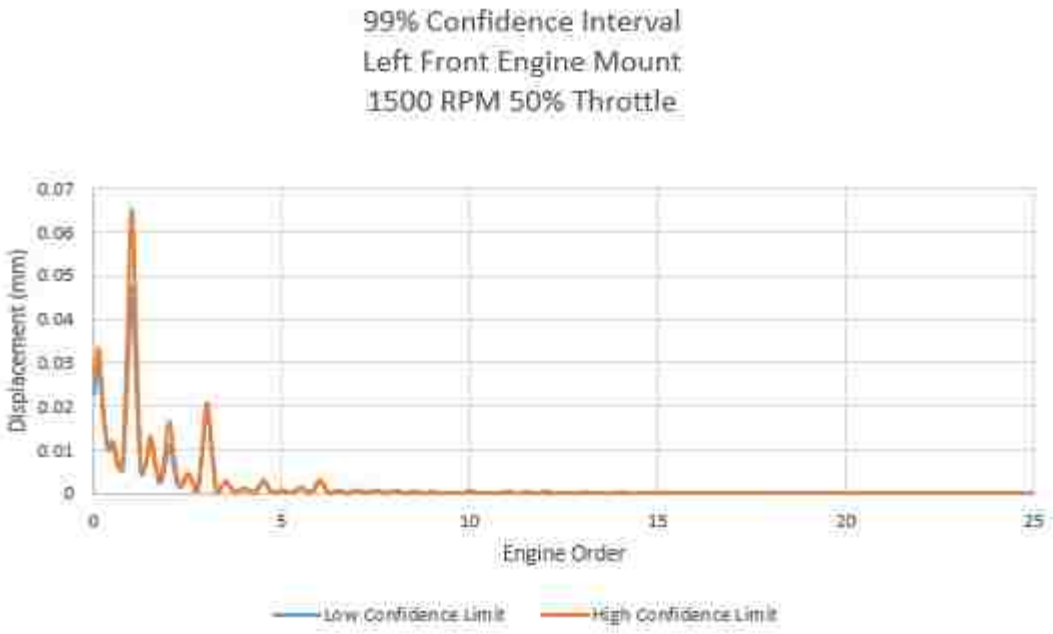
99% Confidence Interval
Left Front Engine Mount
1500 RPM 50% Throttle
Displacement (mm)
0.07
0.06
0.05
0.04
0.03
0.02
0.01
0
0
5
10
15
20
25
Engine Order
Low Confidence Limit
High Confidence Limit

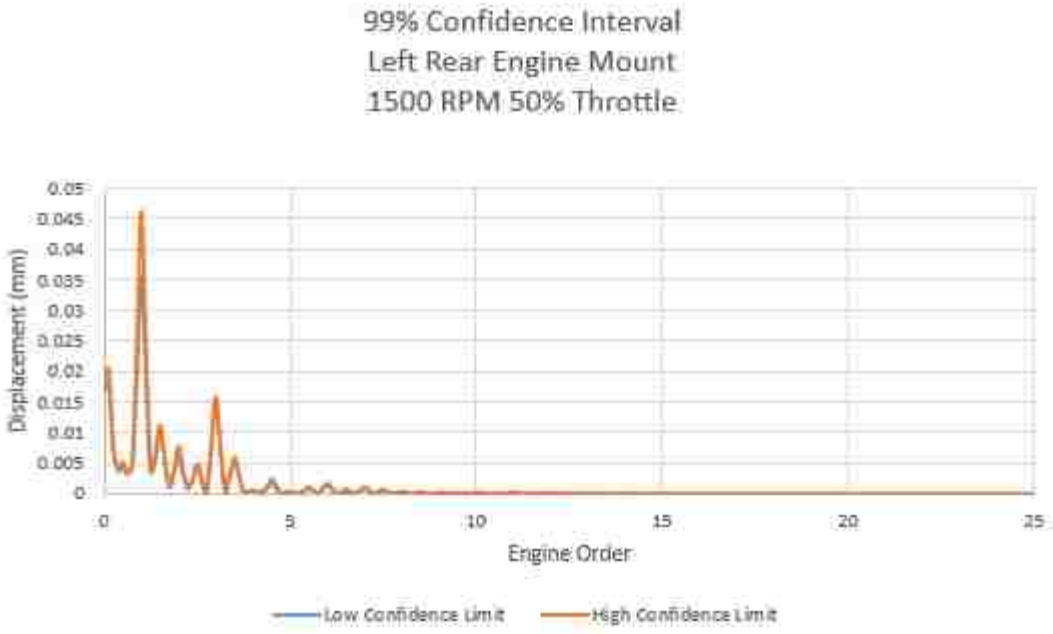
99% Confidence Interval
Left Rear Engine Mount
1500 RPM 50% Throttle
Displacement (mm)
0.05
0.045
0.04
0.035
0.03
0.025
0.02
0.015
0.01
0.005
0
0
5
10
15
20
25
Engine Order
Low Confidence Limit
High Confidence Limit

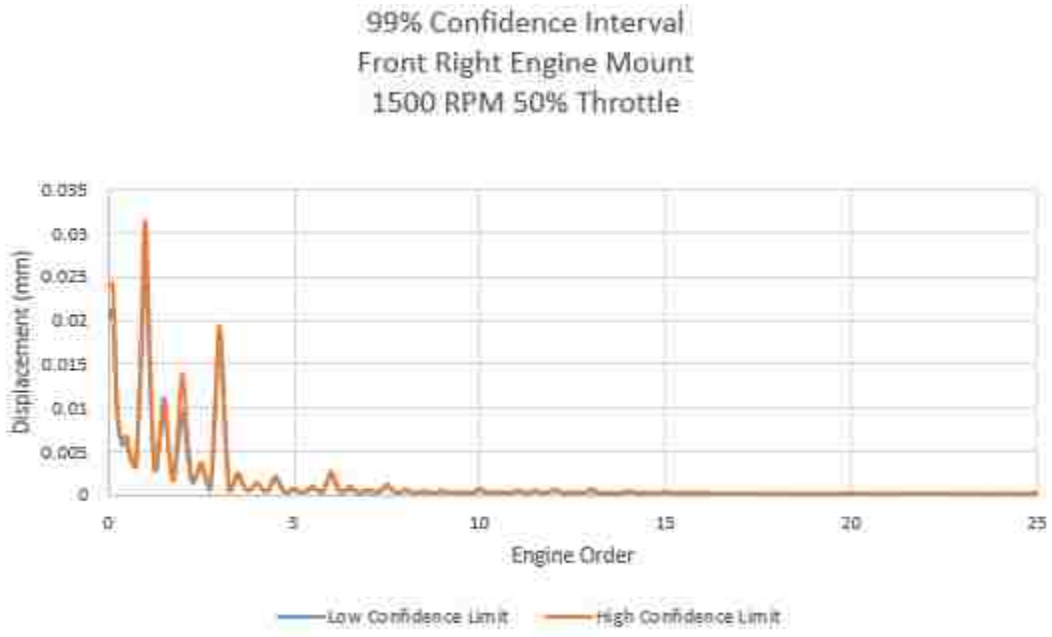
99% Confidence Interval
Front Right Engine Mount
1500 RPM 50% Throttle
Displacement (mm)
0.035
0.03
0.025
0.02
0.015
0.01
0.005
0
0
5
10
15
20
25
Engine Order
Low Confidence Limit
High Confidence Limit

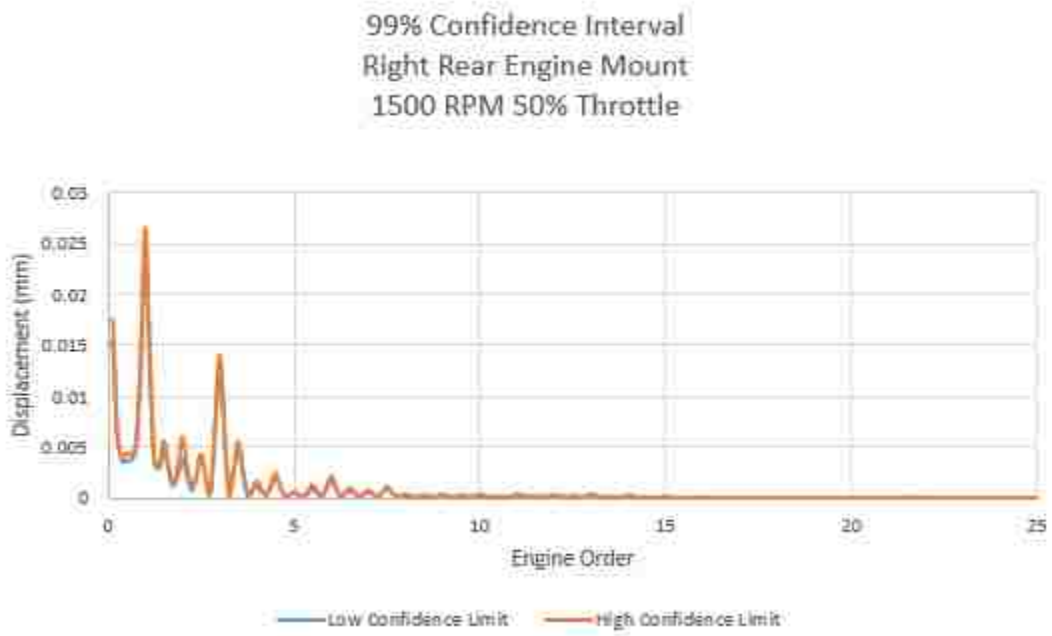
99% Confidence Interval
Right Rear Engine Mount
1500 RPM 50% Throttle
Displacement (mm)
0.03
0.025
0.02
0.015
0.01
0.005
0
0
5
10
15
20
25
Engine Order
Low Confidence Limit
High Confidence Limit

99% Confidence Interval
Left Front Engine Mount
1500 RPM 100% Throttle

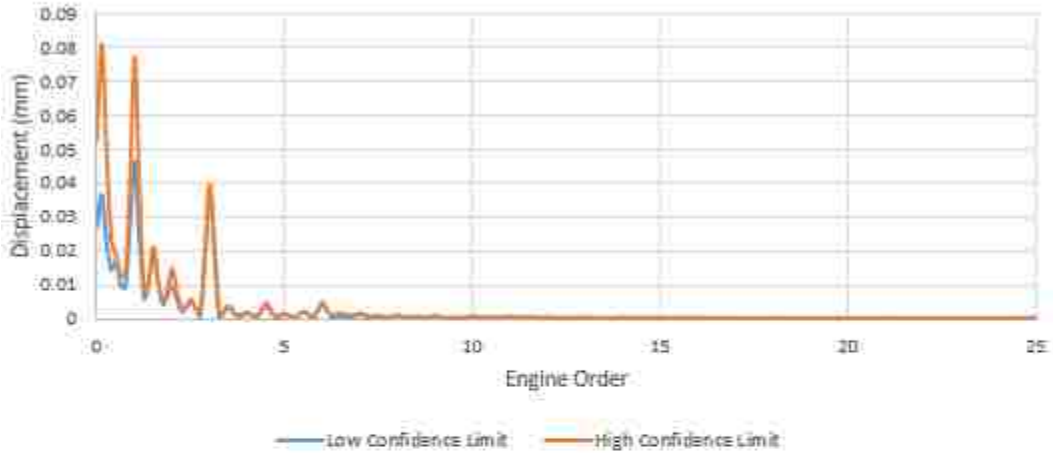

99% Confidence Interval
Left Rear Engine Mount
1500 RPM 100% Throttle

99% Confidence Interval
Front Right Engine Mount
1500 RPM 100% Throttle

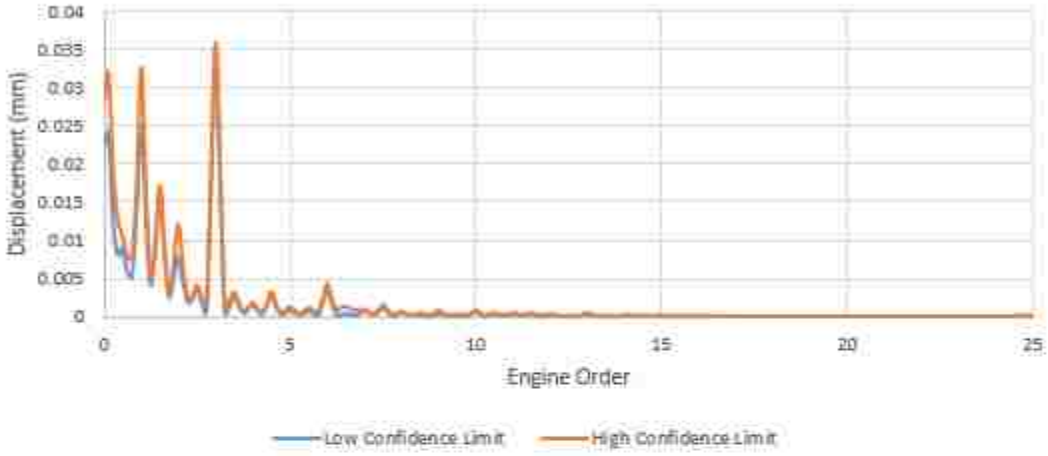

99% Confidence Interval
Right Rear Engine Mount
1500 RPM 100% Throttle

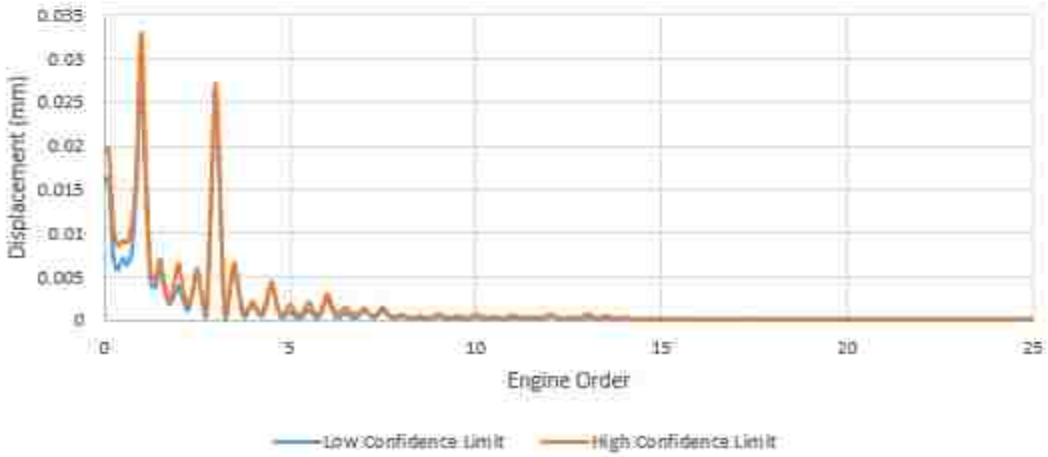

Appendix D: Cycle to Cycle Variation, Cylinder Pressure

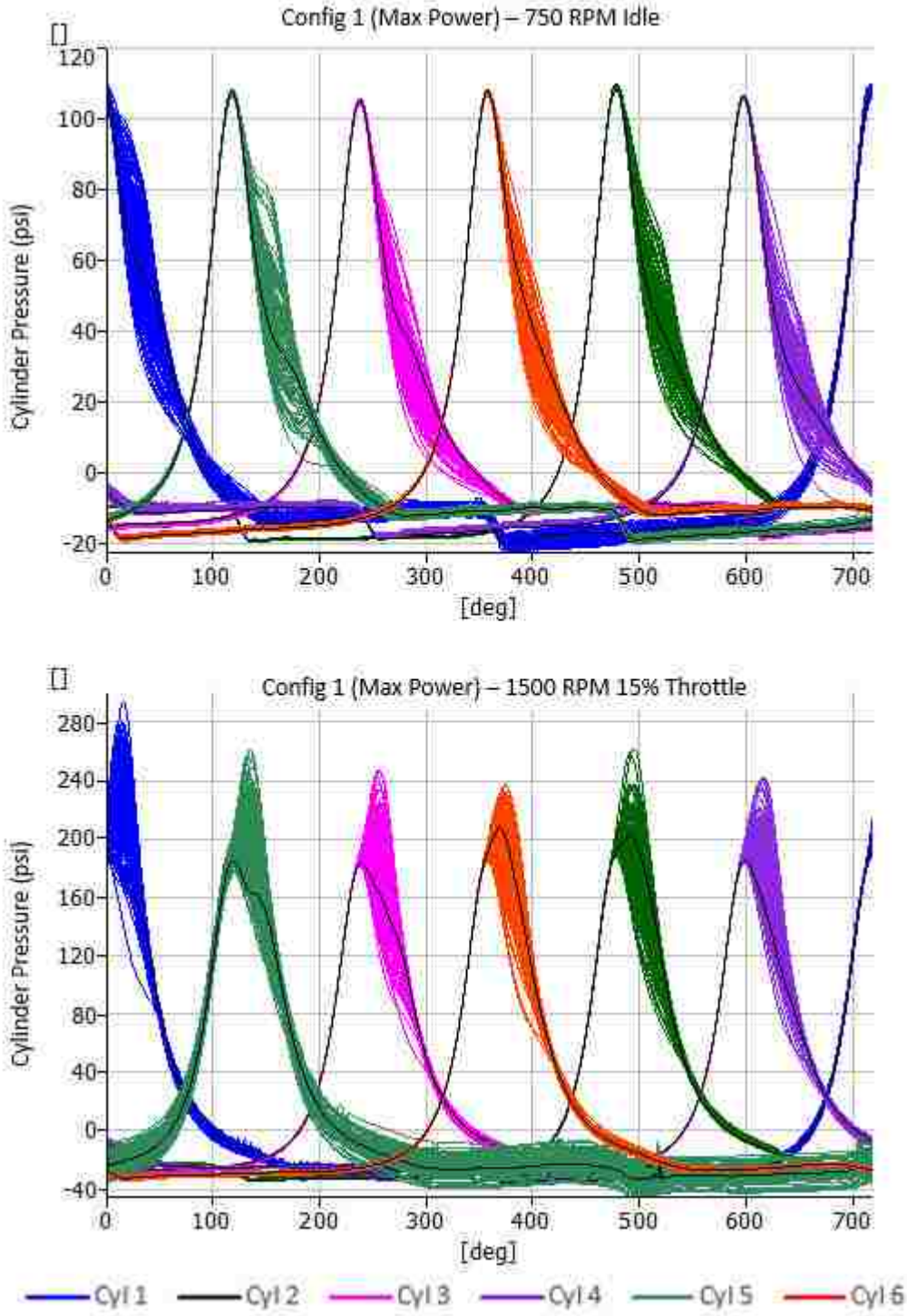

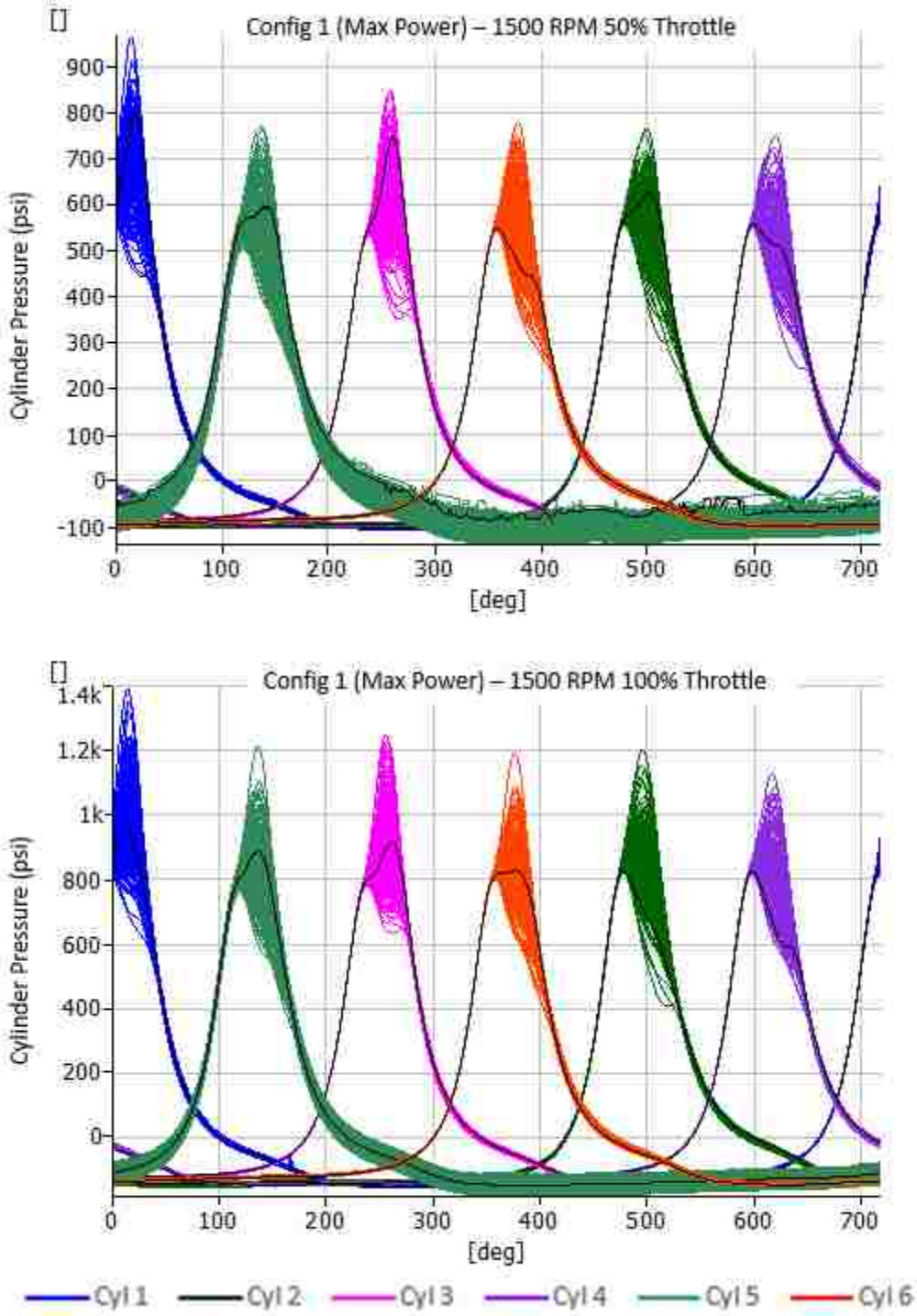
[]
Config 1 (Max Power) – 1500 RPM 50% Throttle
Cylinder Pressure (psi)
900
800
700
600
500
400
300
200
100
0
-100
0
100
200
300
400
500
600
700
[deg]
[]
Config 1 (Max Power) – 1500 RPM 100% Throttle
Cylinder Pressure (psi)
1.4k
1.2k
1k
800
600
400
200
0
0
100
200
300
400
500
600
700
[deg]
Cyl 1
Cyl 2
Cyl 3
Cyl 4
Cyl 5
Cyl 6

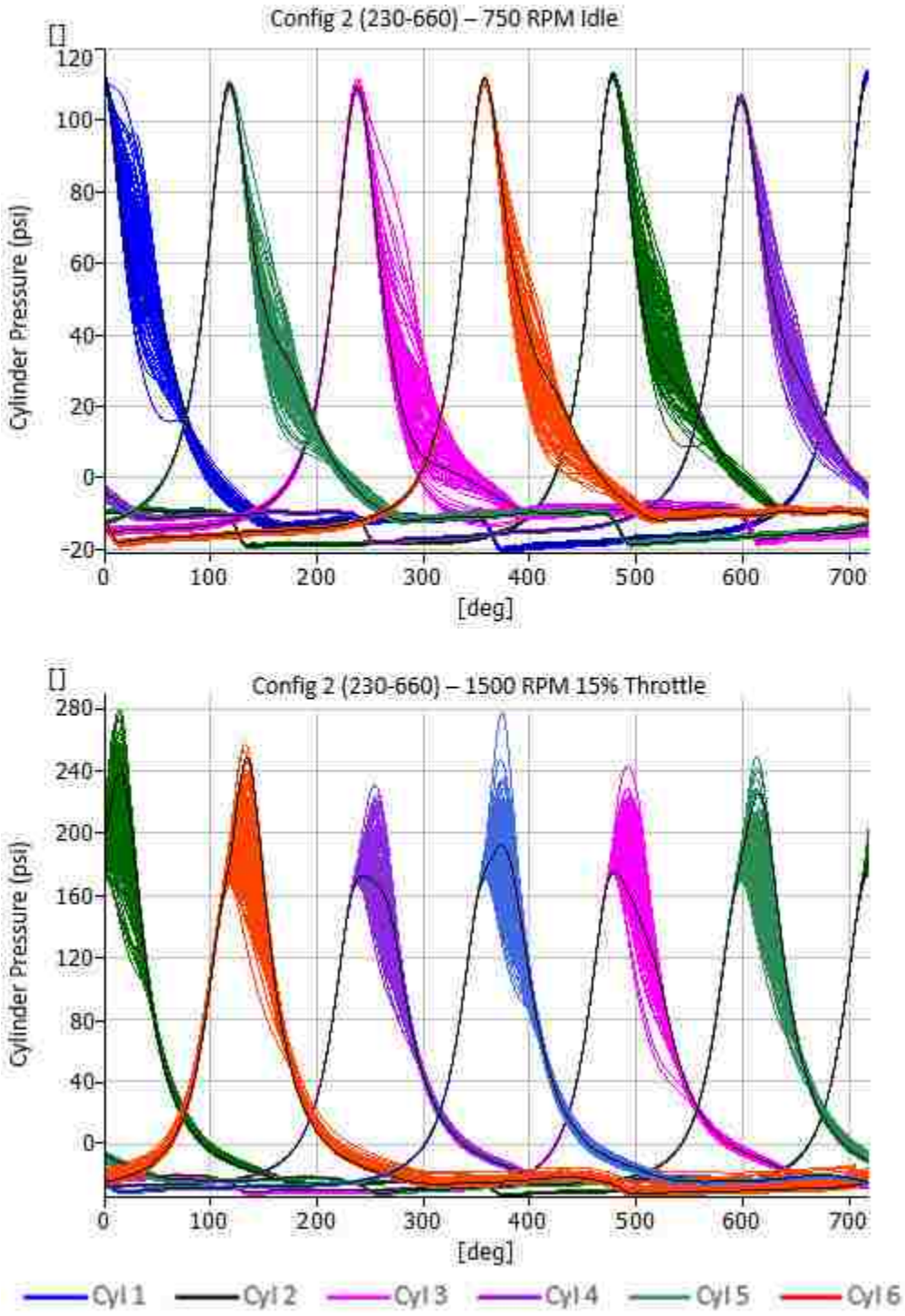
Config 2 (230-660) – 750 RPM Idle
[]
Cylinder Pressure (psi)
120
100
80
60
40
20
0
-20
0
100
200
300
400
500
600
700
[deg]
Config 2 (230-660) – 1500 RPM 15% Throttle
[]
Cylinder Pressure (psi)
280
240
200
160
120
80
40
0
0
100
200
300
400
500
600
700
[deg]
Cyl 1
Cyl 2
Cyl 3
Cyl 4
Cyl 5
Cyl 6

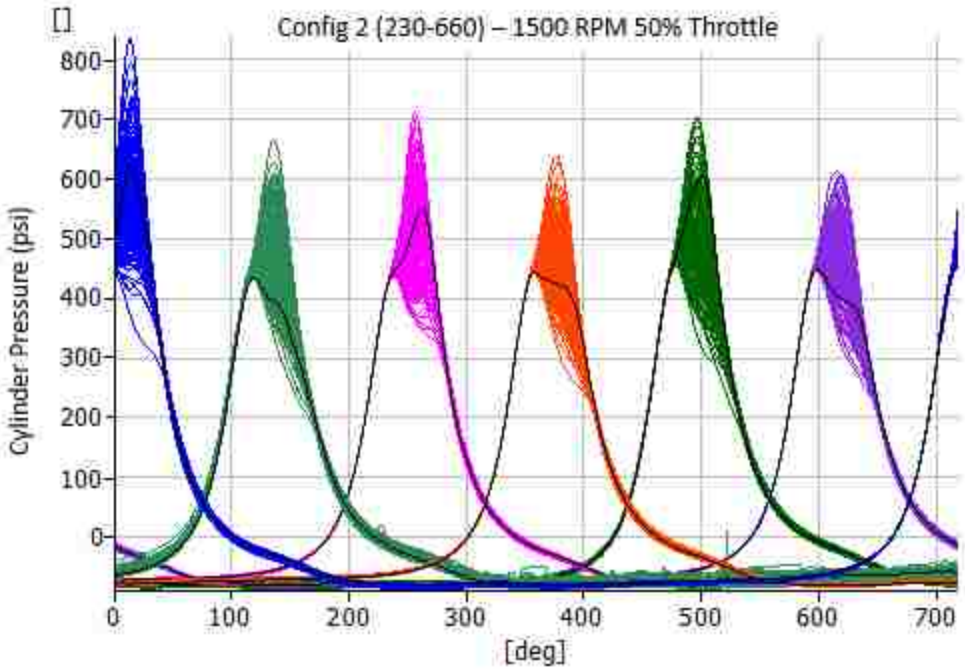
[]
Config 2 (230-660) – 1500 RPM 50% Throttle
Cylinder Pressure (psi)
800
700
600
500
400
300
200
100
0
0
100
200
300
400
500
600
700
[deg]

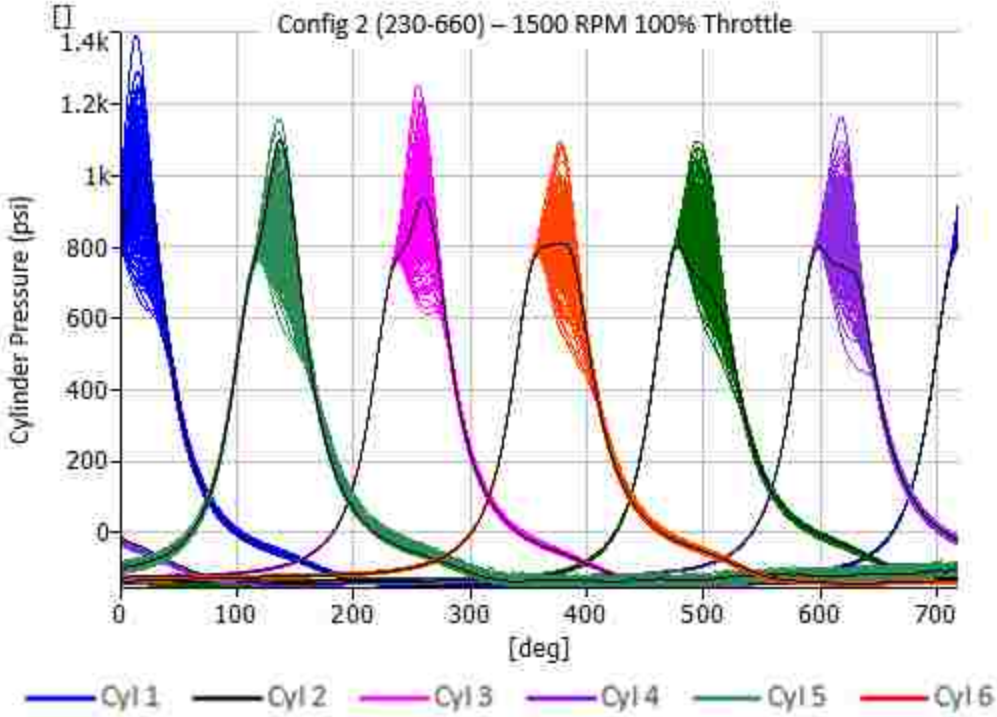
[]
Config 2 (230-660) – 1500 RPM 100% Throttle
Cylinder Pressure (psi)
1.4k
1.2k
1k
800
600
400
200
0
0
100
200
300
400
500
600
700
[deg]
Cyl 1
Cyl 2
Cyl 3
Cyl 4
Cyl 5
Cyl 6

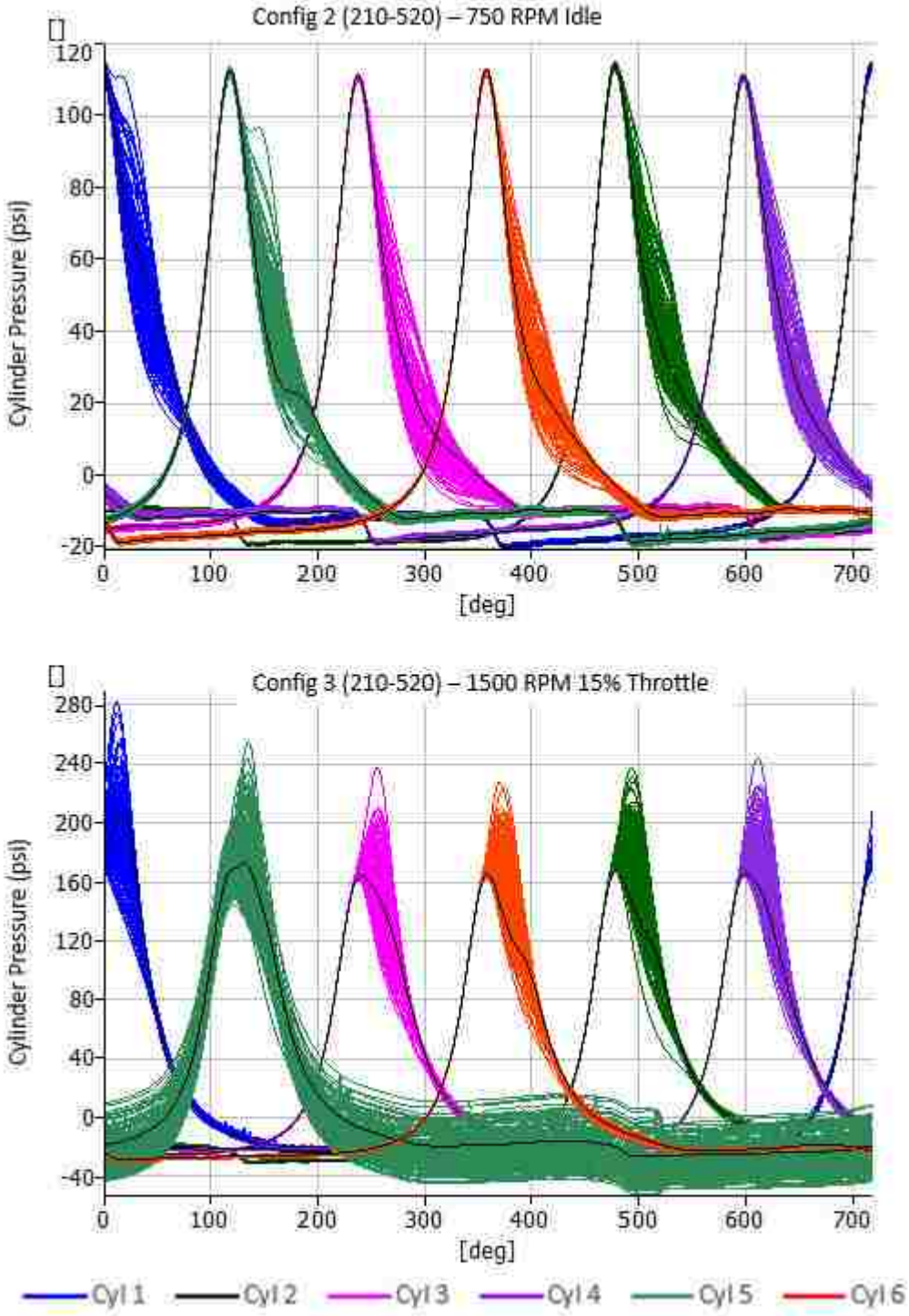
Config 2 (210-520) – 750 RPM Idle
Cylinder Pressure (psi)
120
100
80
60
40
20
0
-20
0
100
200
300
400
500
600
700
[deg]
Config 3 (210-520) – 1500 RPM 15% Throttle
Cylinder Pressure (psi)
280
240
200
160
120
80
40
0
-40
0
100
200
300
400
500
600
700
[deg]
Cyl 1
Cyl 2
Cyl 3
Cyl 4
Cyl 5
Cyl 6

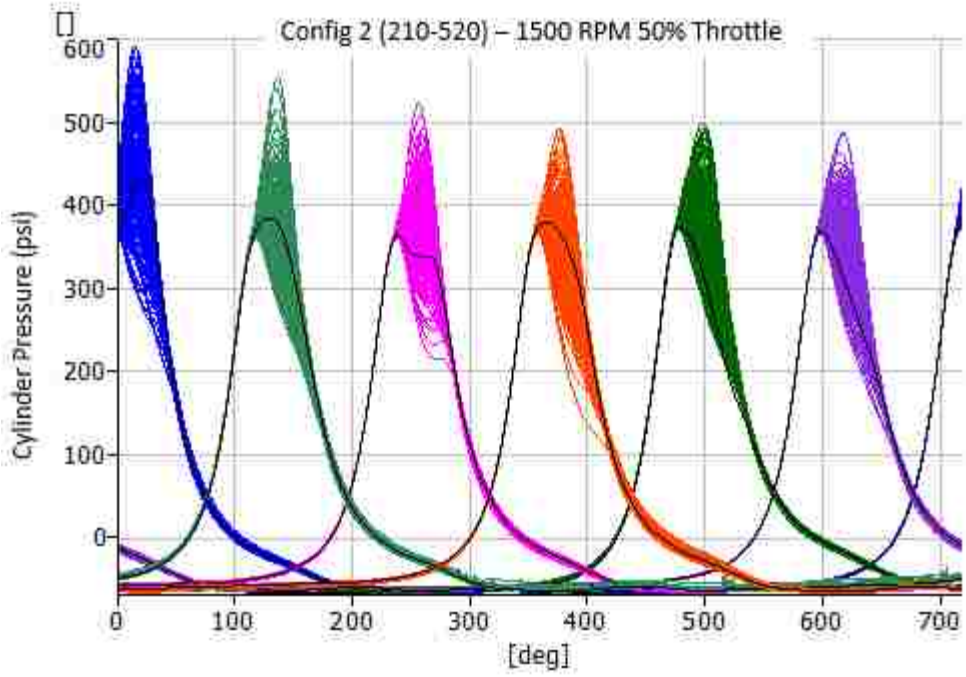
Config 2 (210-520) – 1500 RPM 50% Throttle
Cylinder Pressure (psi)
600
500
400
300
200
100
0
0
100
200
300
400
500
600
700
[deg]

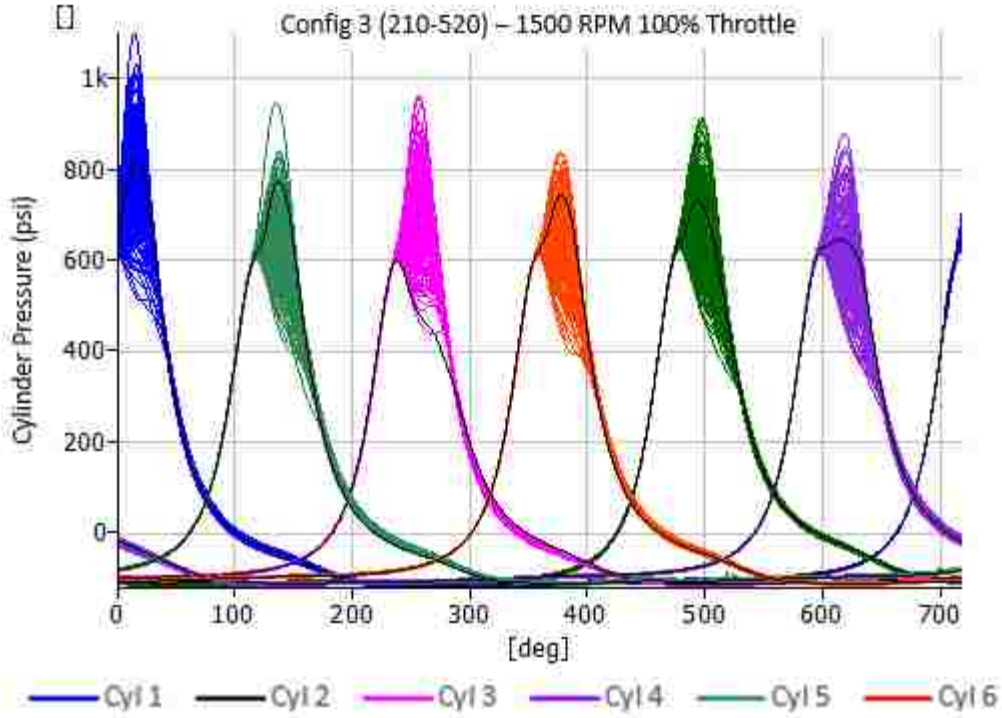
Config 3 (210-520) – 1500 RPM 100% Throttle
Cylinder Pressure (psi)
1k
800
600
400
200
0
0
100
200
300
400
500
600
700
[deg]
Cyl 1
Cyl 2
Cyl 3
Cyl 4
Cyl 5
Cyl 6

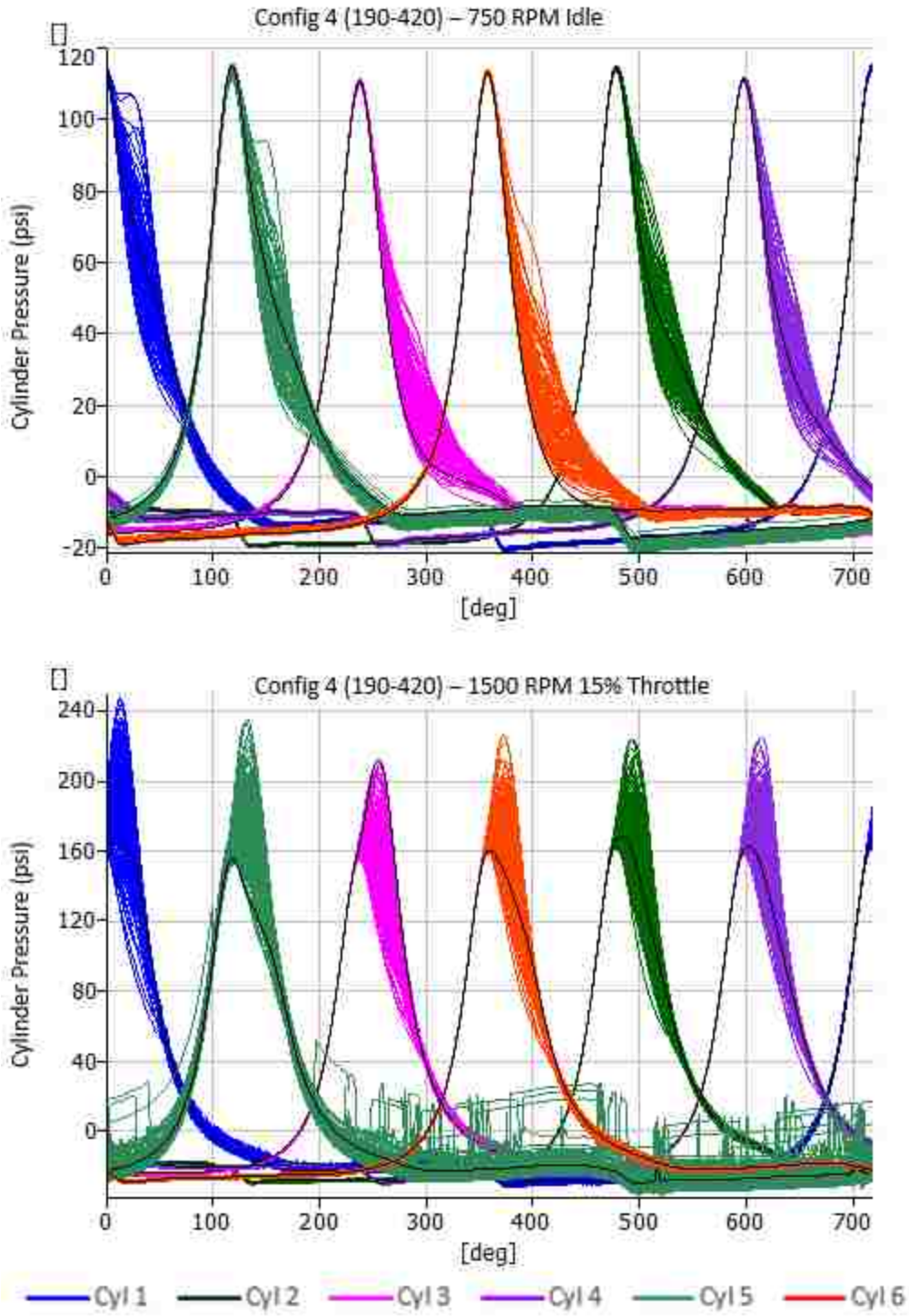
Config 4 (190-420) – 750 RPM Idle
Cylinder Pressure (psi)
120
100
80
60
40
20
0
-20
0
100
200
300
400
500
600
700
[deg]
Config 4 (190-420) – 1500 RPM 15% Throttle
Cylinder Pressure (psi)
240
200
160
120
80
40
0
0
100
200
300
400
500
600
700
[deg]
Cyl 1
Cyl 2
Cyl 3
Cyl 4
Cyl 5
Cyl 6

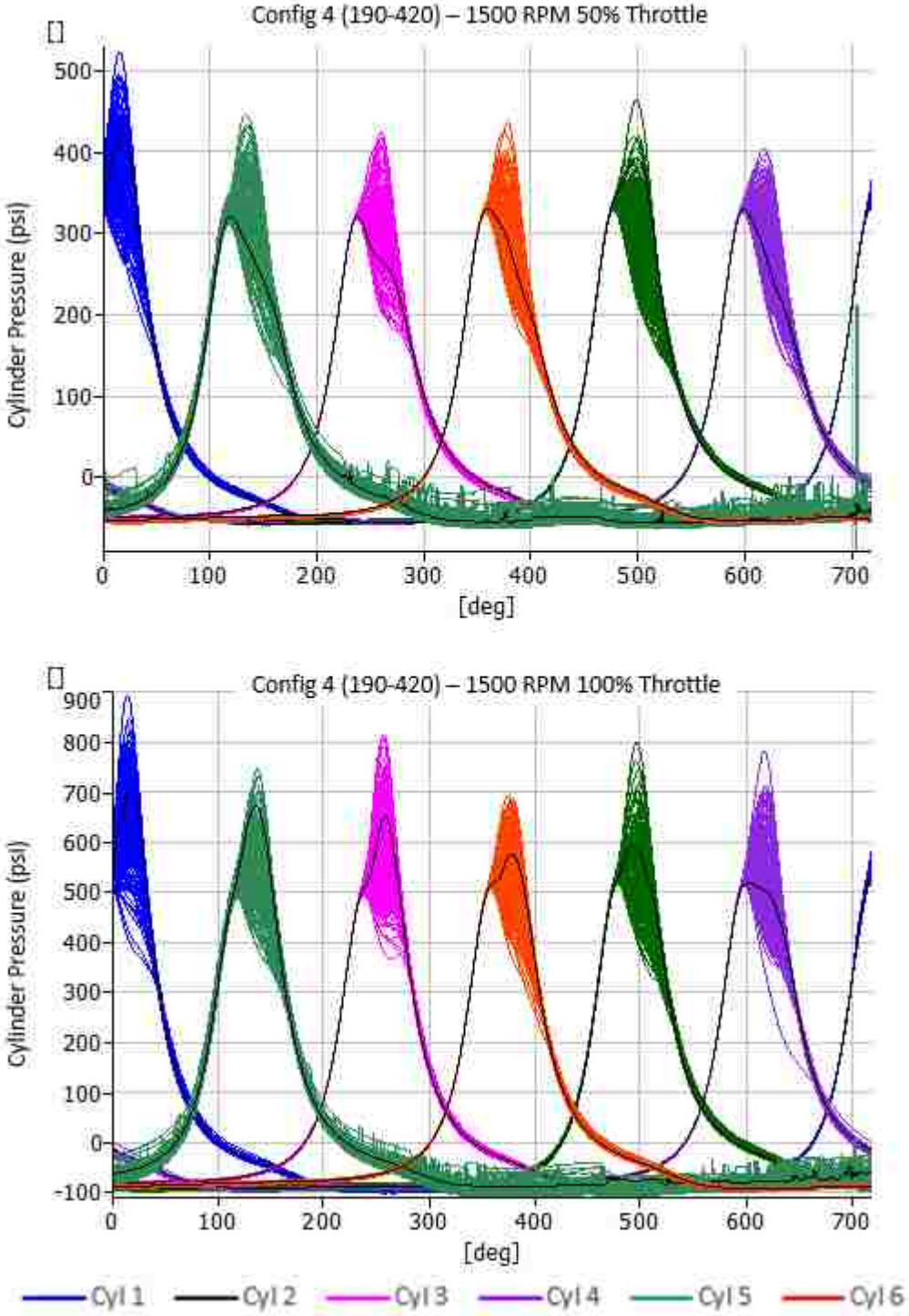
Config 4 (190-420) – 1500 RPM 50% Throttle
[]
Cylinder Pressure (psi)
500
400
300
200
100
0
0
100
200
300
400
500
600
700
[deg]
Config 4 (190-420) – 1500 RPM 100% Throttle
[]
Cylinder Pressure (psi)
900
800
700
600
500
400
300
200
100
0
-100
0
100
200
300
400
500
600
700
[deg]
Cyl 1
Cyl 2
Cyl 3
Cyl 4
Cyl 5
Cyl 6

Appendix E: Multi-cycle Average, Cylinder Pressure

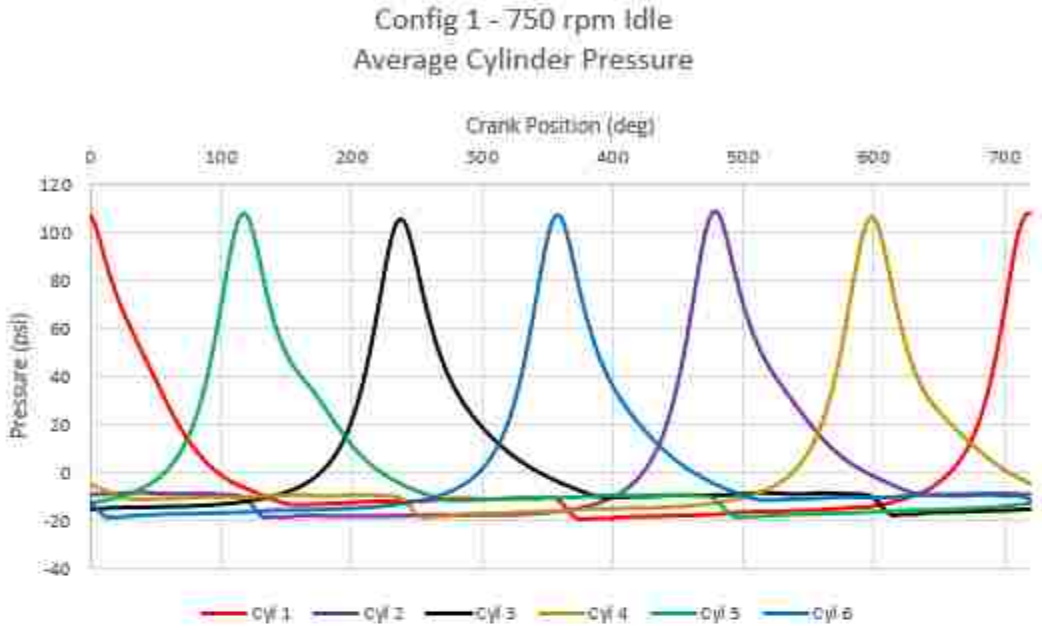

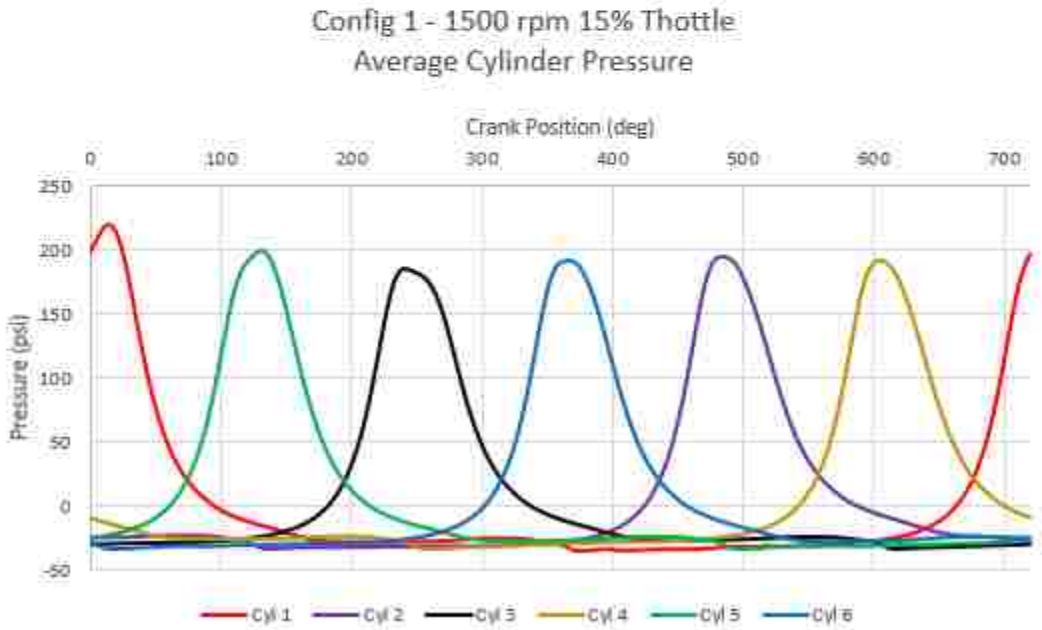

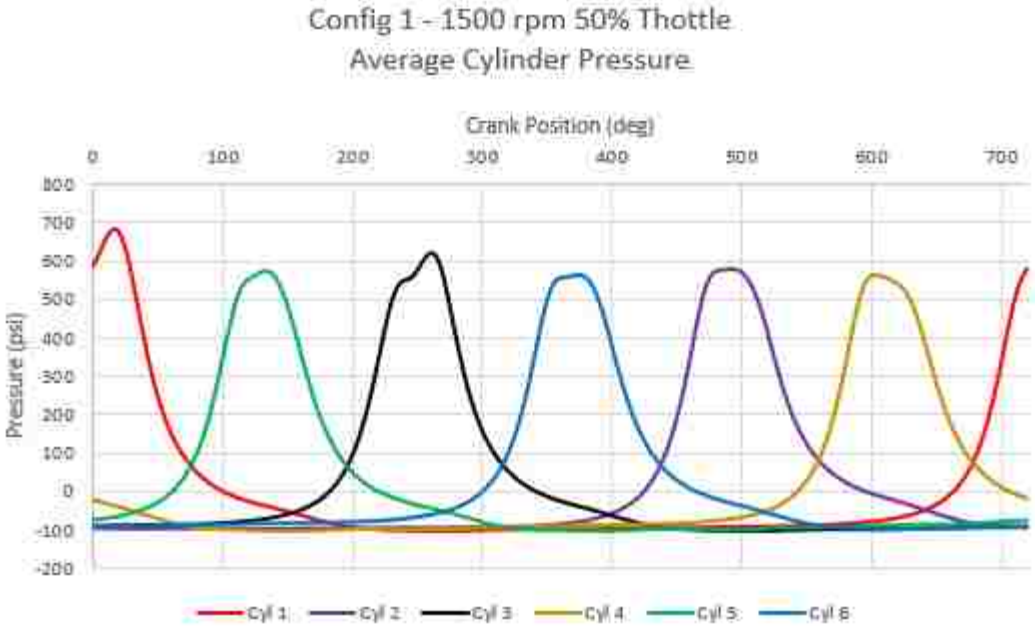
Config 1 - 1500 rpm 50% Thottle
Average Cylinder Pressure
Crank Position (deg)
0
100
200
300
400
500
600
700
800
700
600
500
400
300
200
100
0
-100
-200
Pressure (psi)
Cyl 1
Cyl 2
Cyl 3
Cyl 4
Cyl 5
Cyl 6

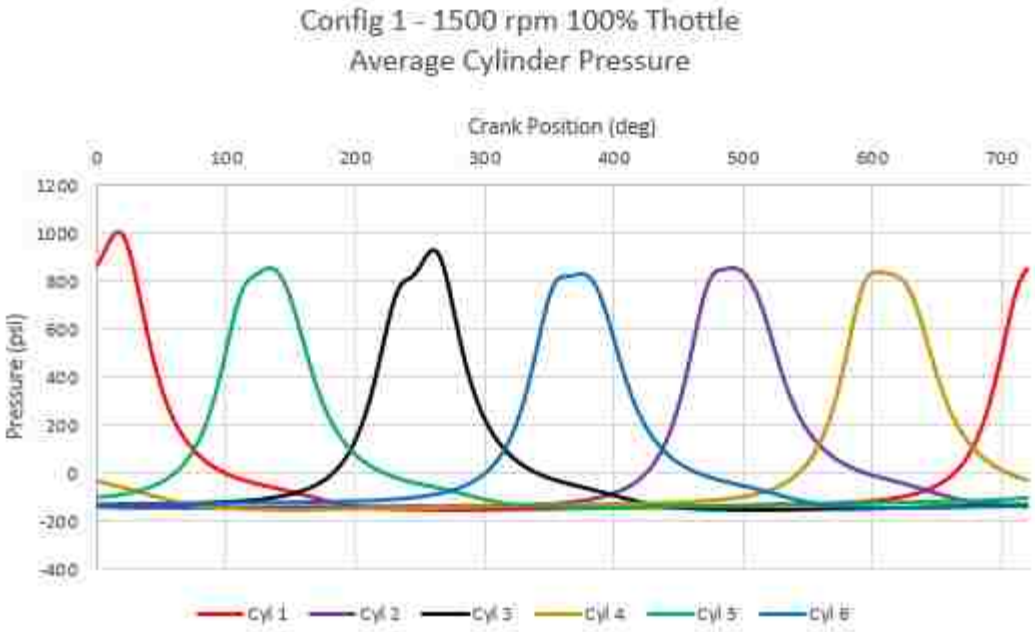
Config 1 - 1500 rpm 100% Thottle
Average Cylinder Pressure
Crank Position (deg)
0
100
200
300
400
500
600
700
1200
1000
800
600
400
200
0
-200
-400
Pressure (psi)
Cyl 1
Cyl 2
Cyl 3
Cyl 4
Cyl 5
Cyl 6

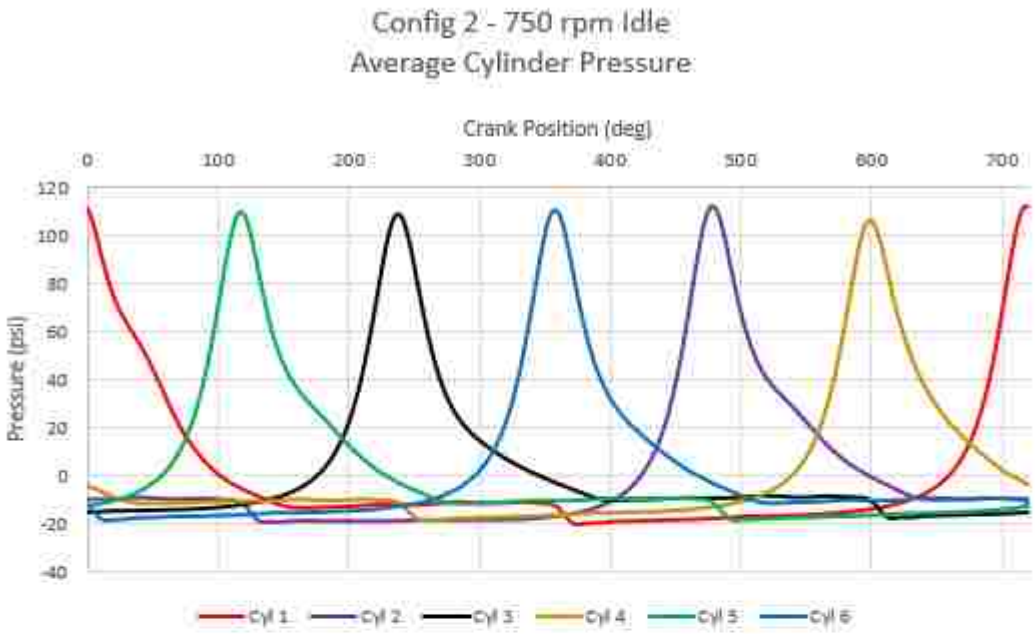
Config 2 - 750 rpm Idle
Average Cylinder Pressure
Crank Position (deg)
0
100
200
300
400
500
600
700
120
100
80
60
40
20
0
-20
-40
Pressure (psi)
Cyl 1
Cyl 2
Cyl 3
Cyl 4
Cyl 5
Cyl 6

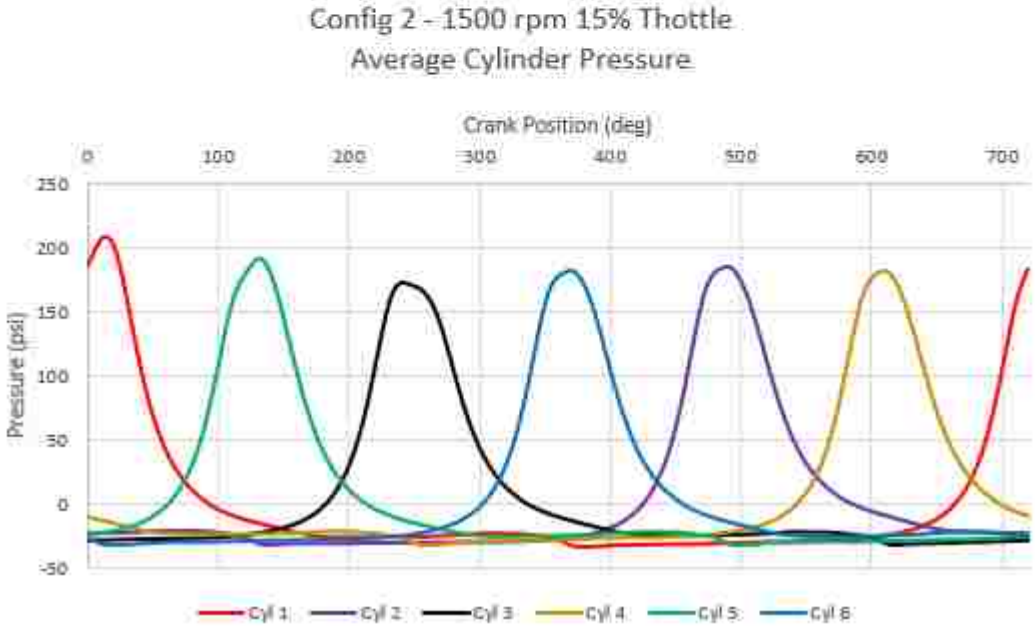
Config 2 - 1500 rpm 15% Thottle
Average Cylinder Pressure
Crank Position (deg)
0
100
200
300
400
500
600
700
250
200
150
100
50
0
-50
Pressure (psi)
Cyl 1
Cyl 2
Cyl 3
Cyl 4
Cyl 5
Cyl 6

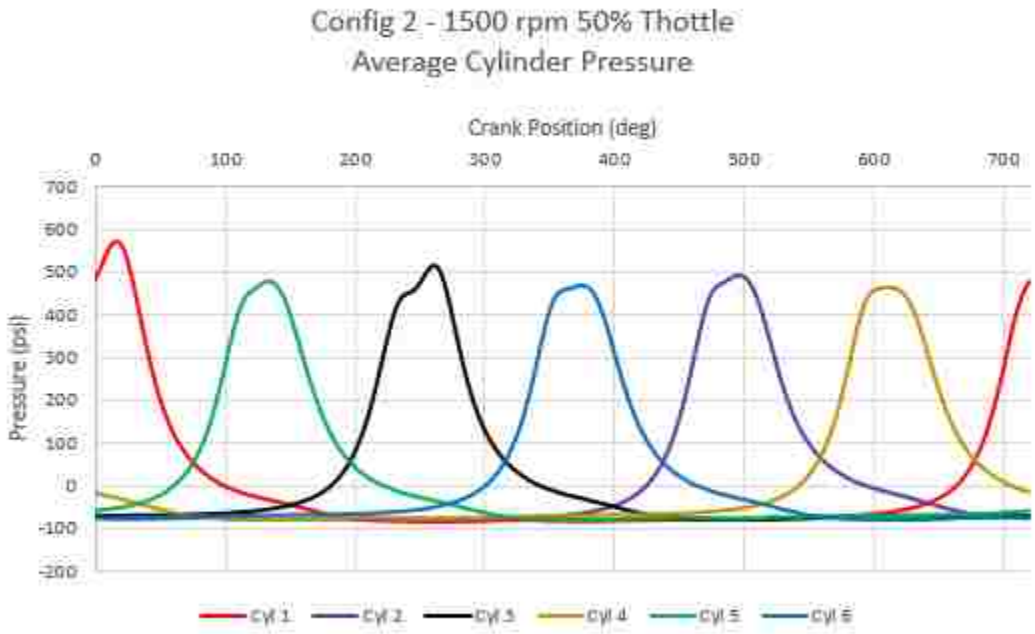
Config 2 - 1500 rpm 50% Thottle
Average Cylinder Pressure
Crank Position (deg)
0
100
200
300
400
500
600
700
Pressure (psi)
700
600
500
400
300
200
100
0
-100
-200
Cyl 1
Cyl 2
Cyl 3
Cyl 4
Cyl 5
Cyl 6

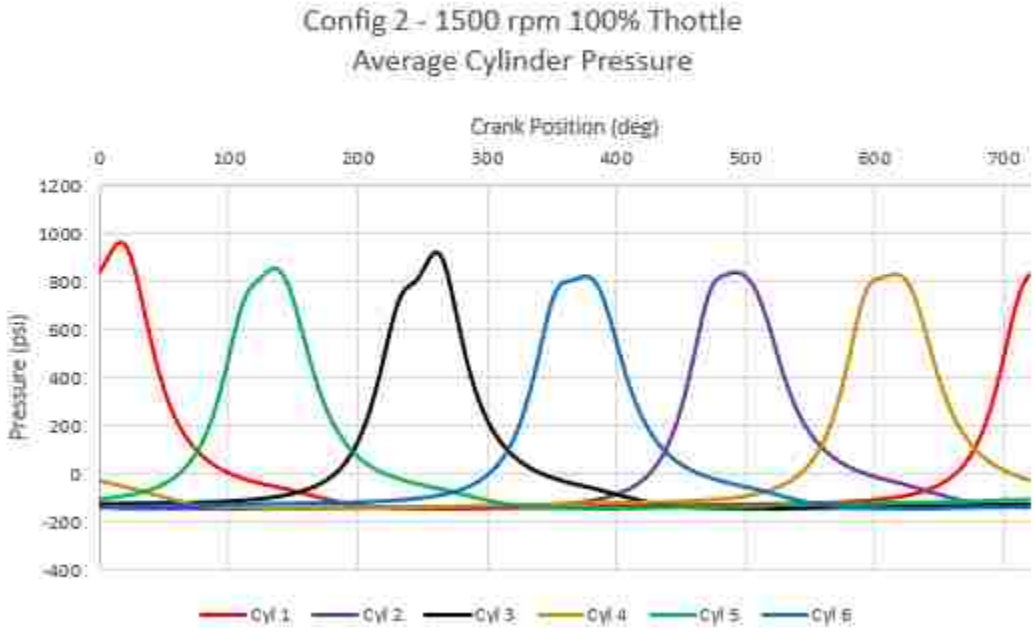
Config 2 - 1500 rpm 100% Thottle
Average Cylinder Pressure
Crank Position (deg)
0
100
200
300
400
500
600
700
Pressure (psi)
1200
1000
800
600
400
200
0
-200
-400
Cyl 1
Cyl 2
Cyl 3
Cyl 4
Cyl 5
Cyl 6

Config 3 - 750 rpm Idle
Average Cylinder Pressure

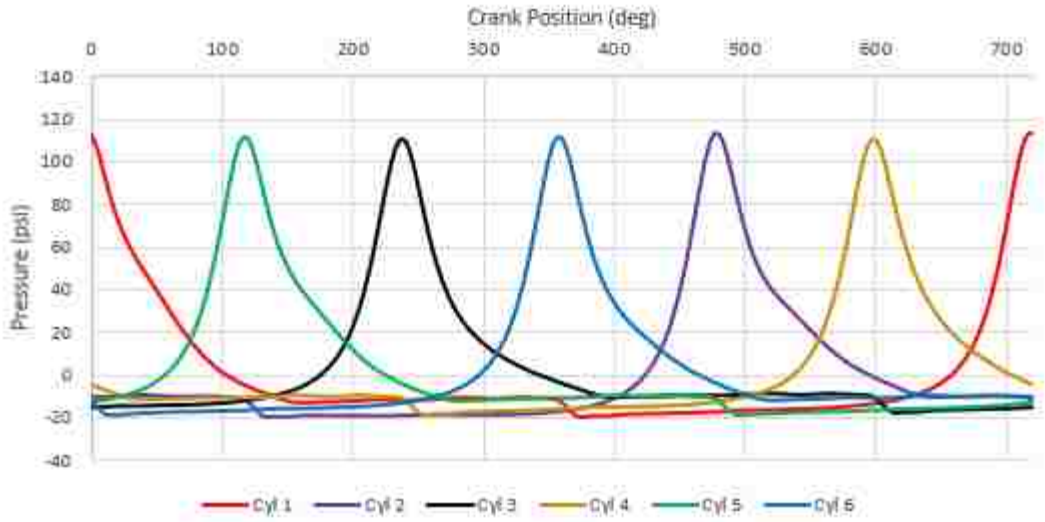

Config 3 - 1500 rpm 15% Thottle
Average Cylinder Pressure

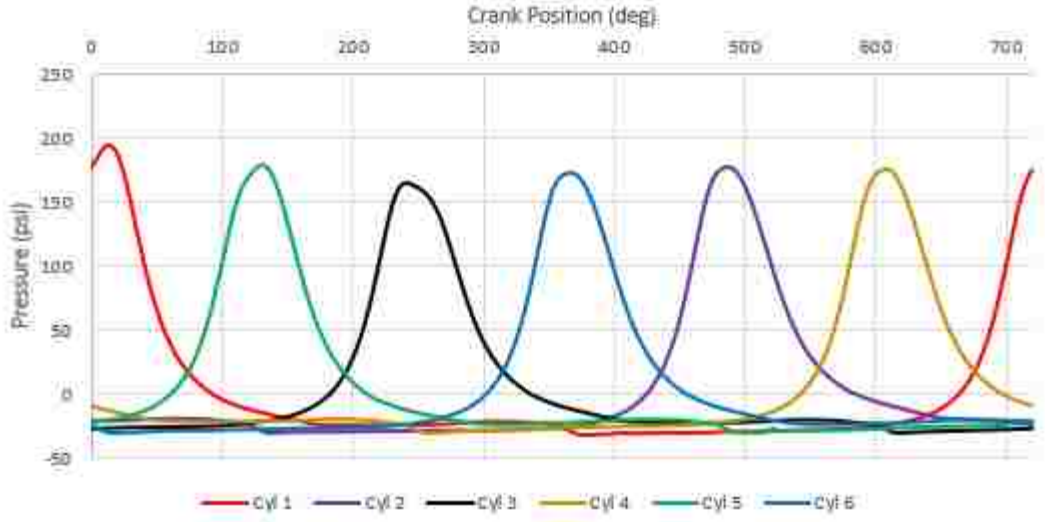

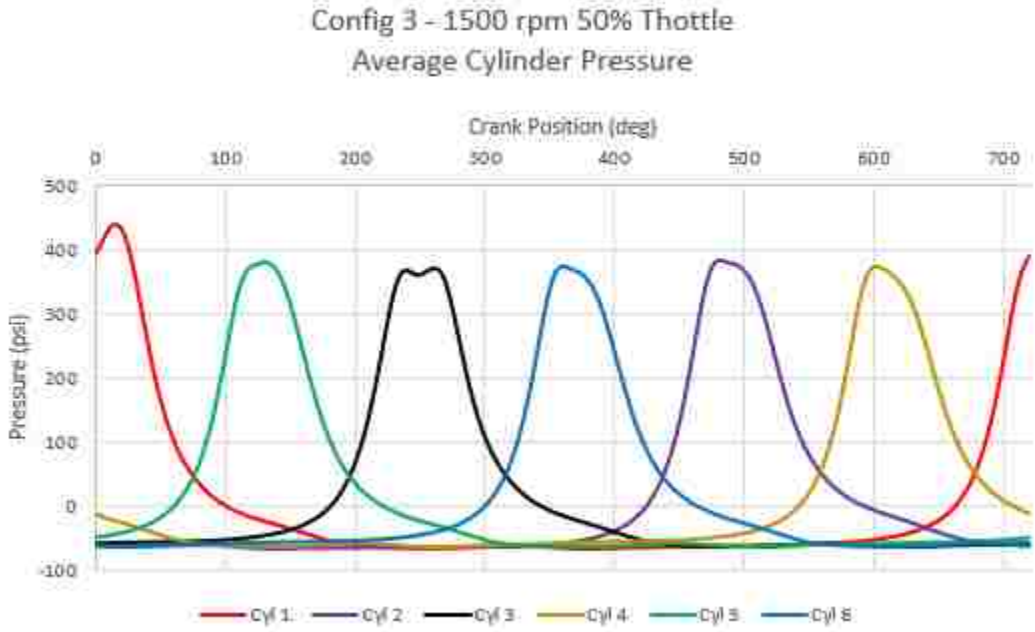
Config 3 - 1500 rpm 50% Thottle
Average Cylinder Pressure
Crank Position (deg)
0
100
200
300
400
500
600
700
Pressure (psi)
500
400
300
200
100
0
-100
Cyl 1
Cyl 2
Cyl 3
Cyl 4
Cyl 5
Cyl 6

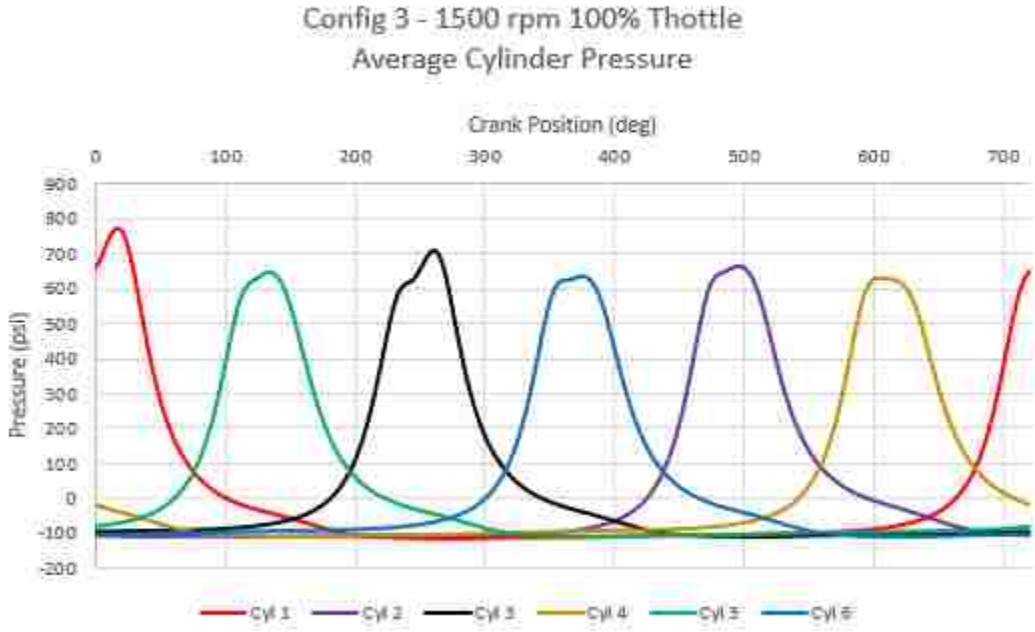
Config 3 - 1500 rpm 100% Thottle
Average Cylinder Pressure
Crank Position (deg)
0
100
200
300
400
500
600
700
Pressure (psi)
900
800
700
600
500
400
300
200
100
0
-100
-200
Cyl 1
Cyl 2
Cyl 3
Cyl 4
Cyl 5
Cyl 6

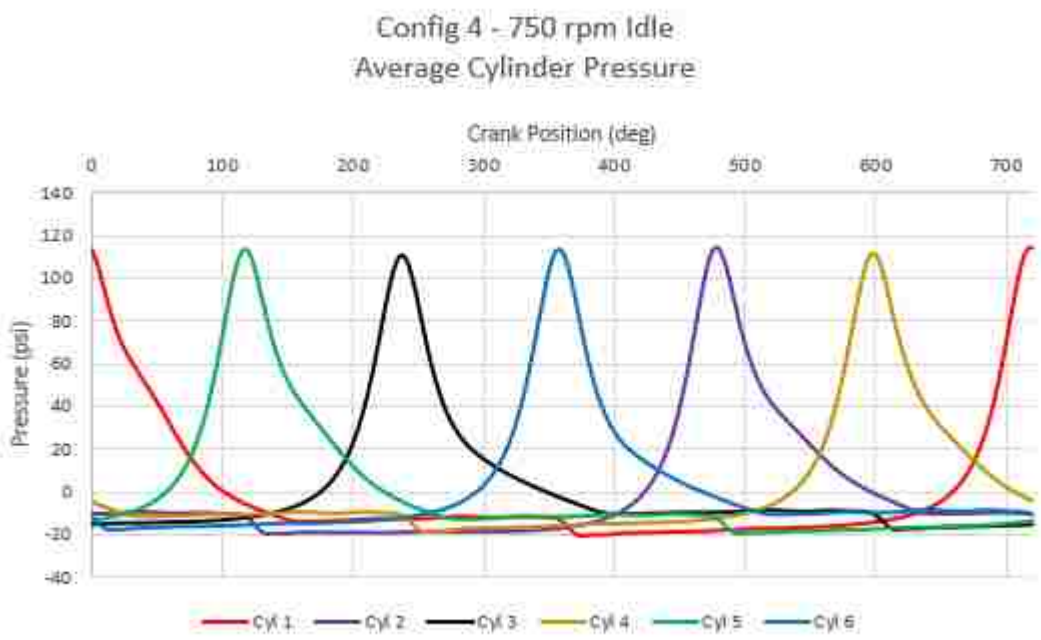
Config 4 - 750 rpm Idle
Average Cylinder Pressure
Crank Position (deg)
0
100
200
300
400
500
600
700
140
120
100
80
60
40
20
0
-20
-40
Pressure (psi)
Cyl 1
Cyl 2
Cyl 3
Cyl 4
Cyl 5
Cyl 6

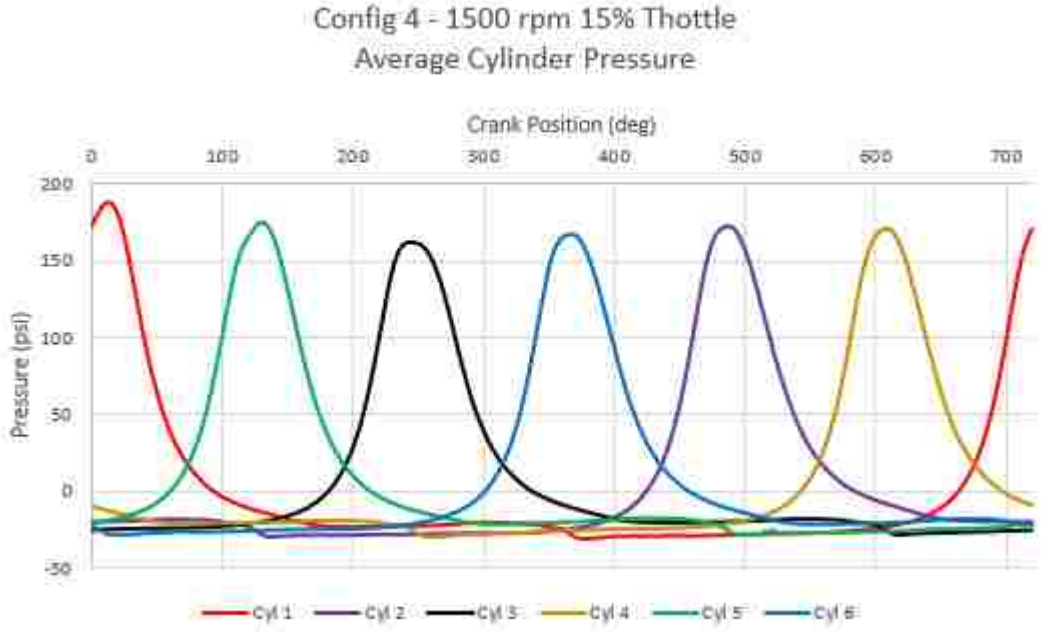
Config 4 - 1500 rpm 15% Thottle
Average Cylinder Pressure
Crank Position (deg)
0
100
200
300
400
500
600
700
200
150
100
50
0
-50
Pressure (psi)
Cyl 1
Cyl 2
Cyl 3
Cyl 4
Cyl 5
Cyl 6

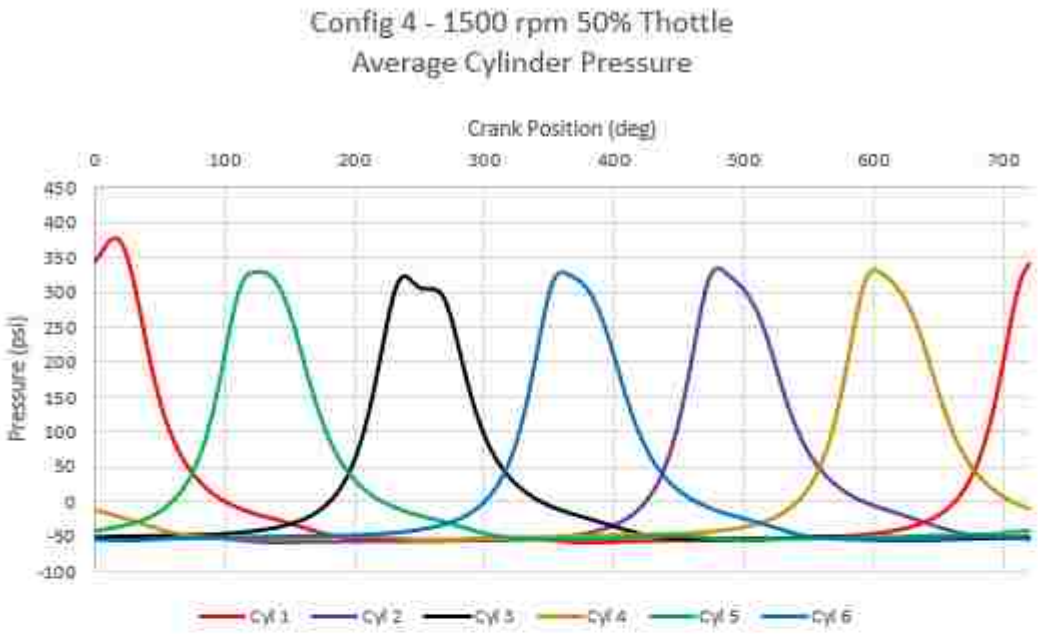
Config 4 - 1500 rpm 50% Thottle
Average Cylinder Pressure
Crank Position (deg)
0
100
200
300
400
500
600
700
Pressure (psi)
450
400
350
300
250
200
150
100
50
0
-50
-100
Cyl 1
Cyl 2
Cyl 3
Cyl 4
Cyl 5
Cyl 6

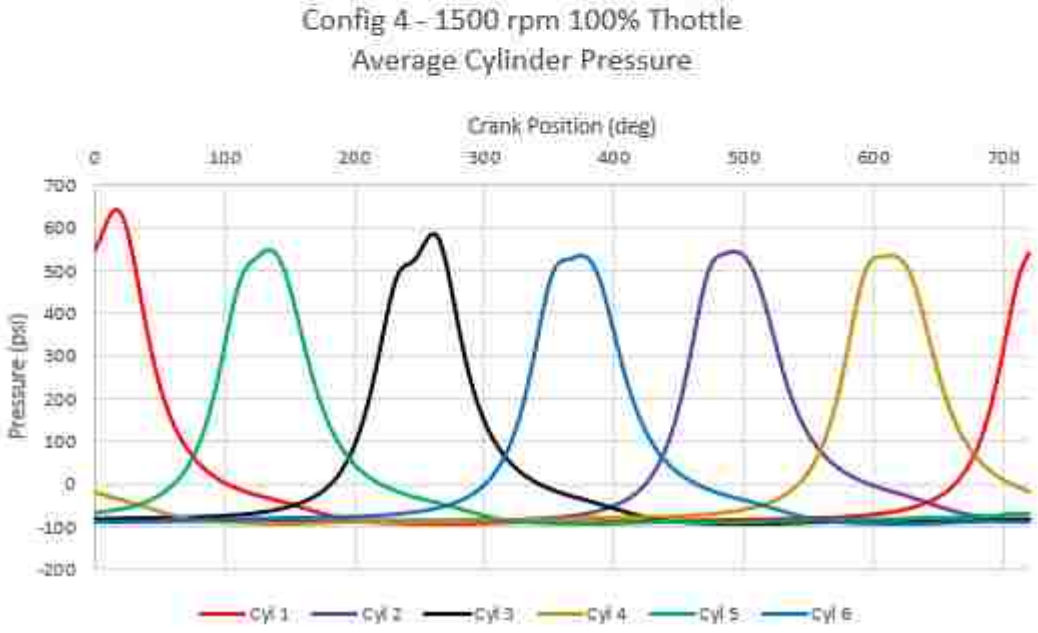
Config 4 - 1500 rpm 100% Thottle
Average Cylinder Pressure
Crank Position (deg)
0
100
200
300
400
500
600
700
Pressure (psi)
700
600
500
400
300
200
100
0
-100
-200
Cyl 1
Cyl 2
Cyl 3
Cyl 4
Cyl 5
Cyl 6

Appendix F: Pressure Rise Rate, Cylinder Pressure

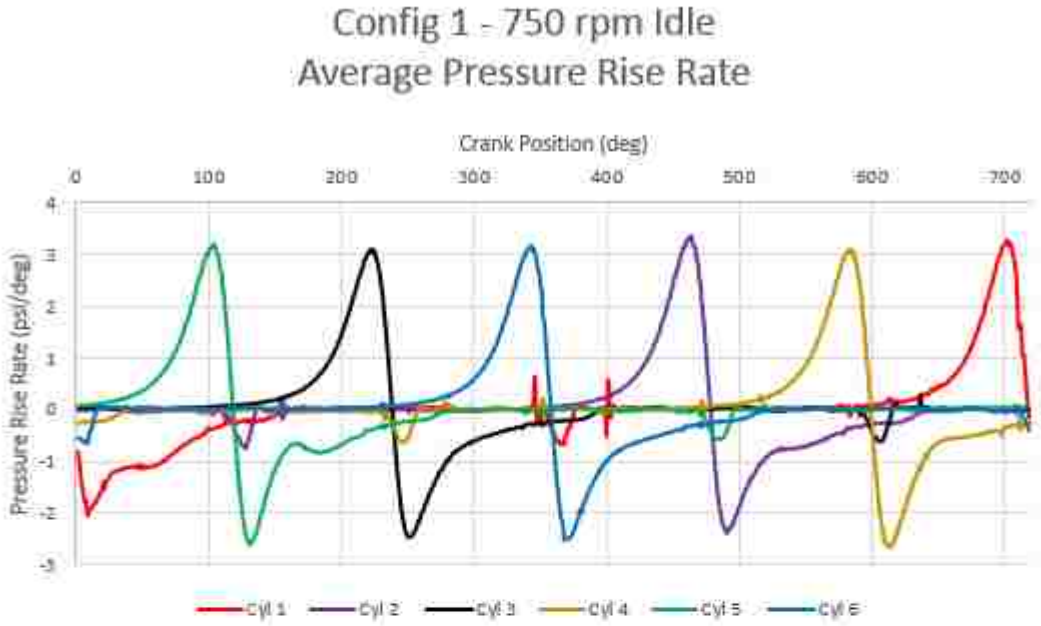

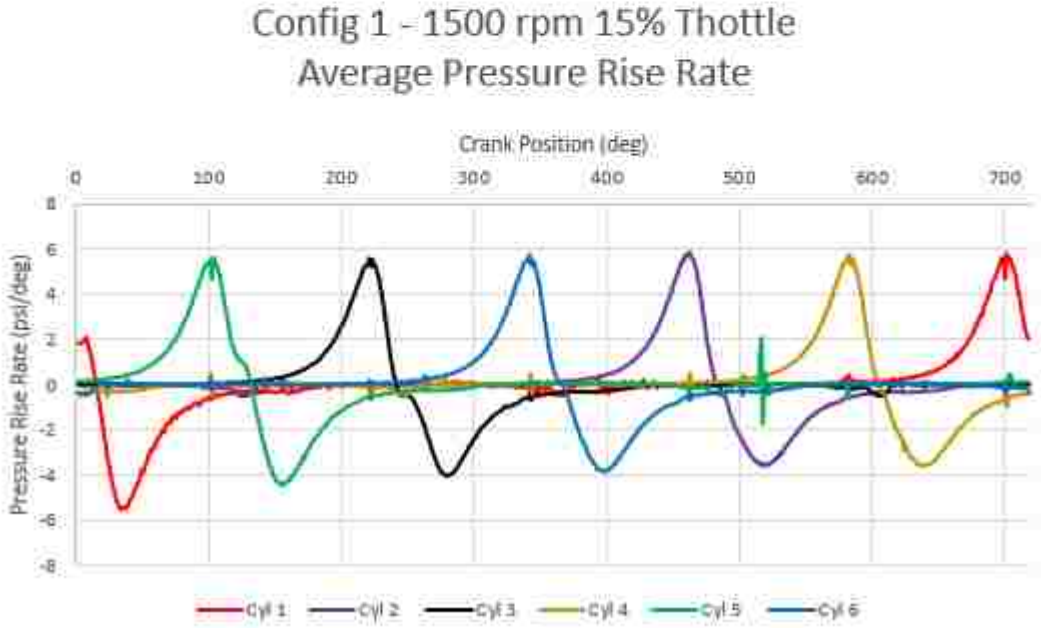

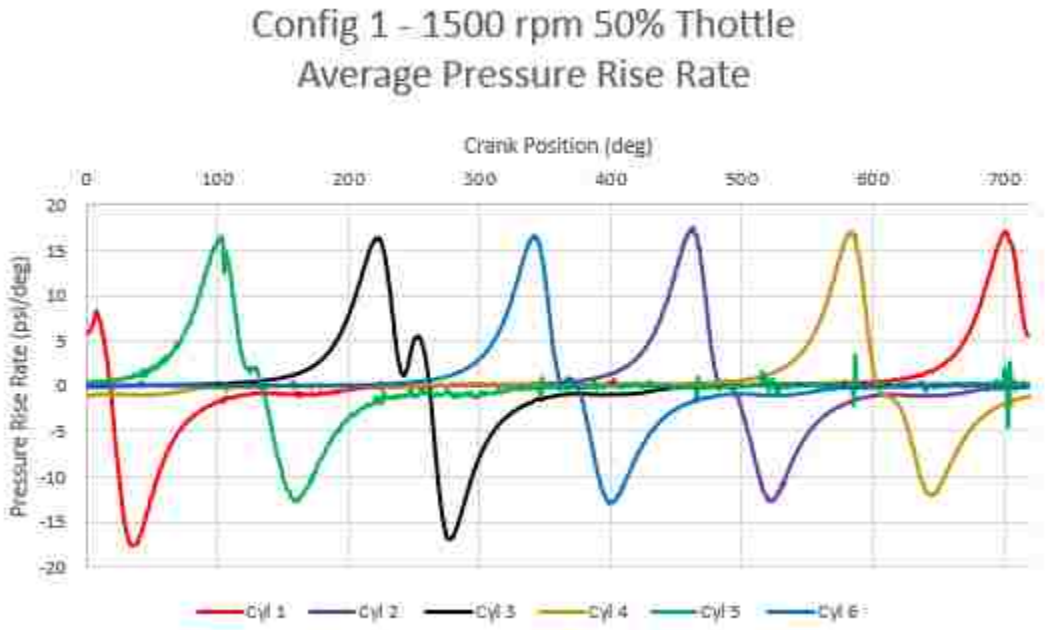
Config 1 - 1500 rpm 50% Thottle
Average Pressure Rise Rate
Crank Position (deg)
0
100
200
300
400
500
600
700
Pressure Rise Rate (psi/deg)
20
15
10
5
0
-5
-10
-15
-20
Cyl 1
Cyl 2
Cyl 3
Cyl 4
Cyl 5
Cyl 6

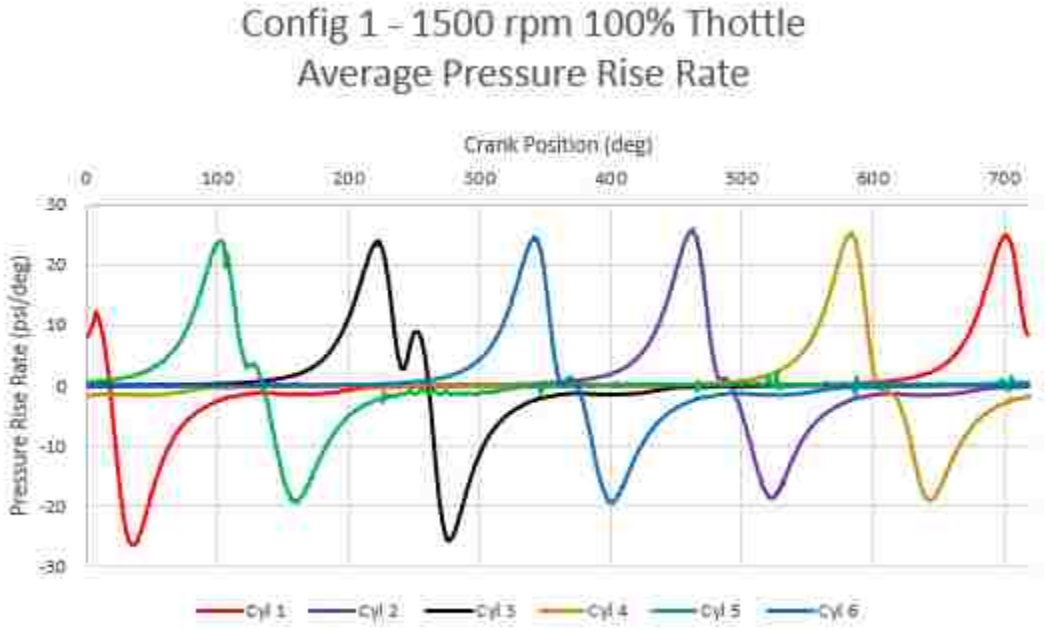
Config 1 - 1500 rpm 100% Thottle
Average Pressure Rise Rate
Crank Position (deg)
0
100
200
300
400
500
600
700
Pressure Rise Rate (psi/deg)
30
20
10
0
-10
-20
-30
Cyl 1
Cyl 2
Cyl 3
Cyl 4
Cyl 5
Cyl 6

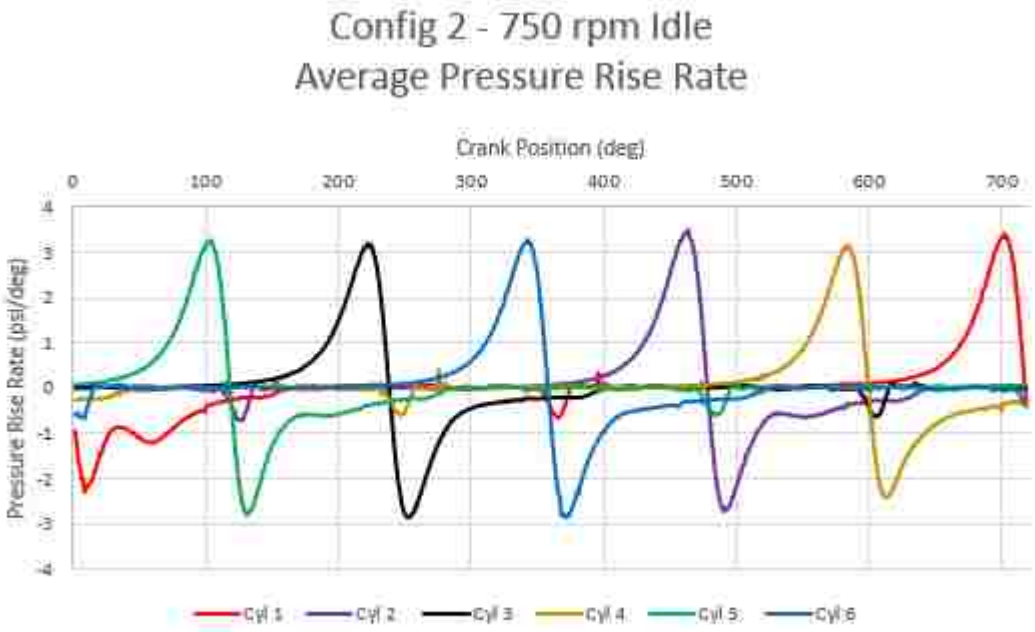
Config 2 - 750 rpm Idle
Average Pressure Rise Rate
Crank Position (deg)
0
100
200
300
400
500
600
700
Pressure Rise Rate (psi/deg)
Cyl 1
Cyl 2
Cyl 3
Cyl 4
Cyl 5
Cyl 6

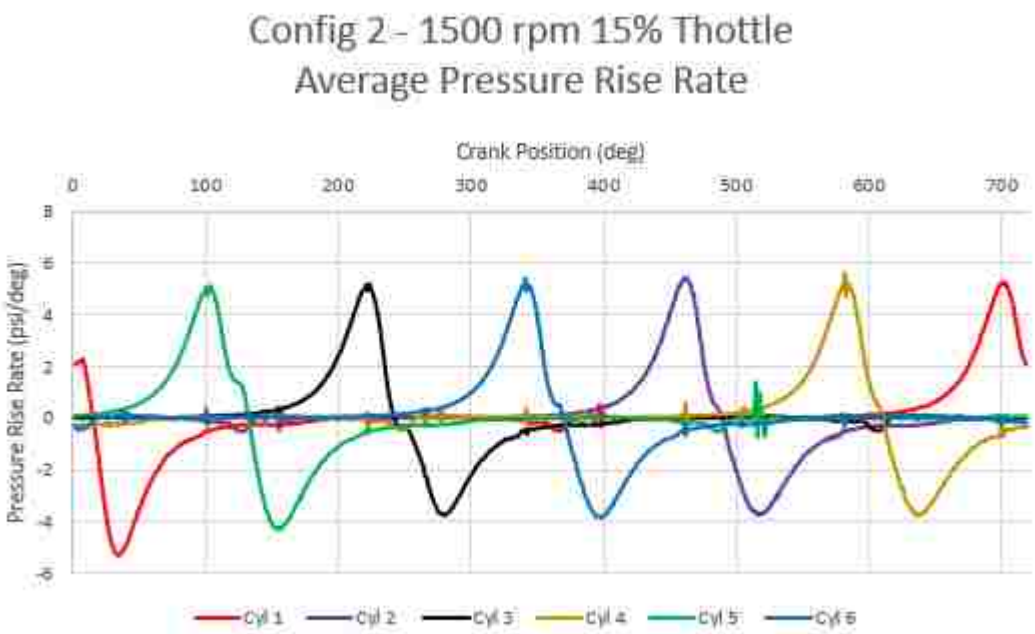
Config 2 - 1500 rpm 15% Thottle
Average Pressure Rise Rate
Crank Position (deg)
0
100
200
300
400
500
600
700
Pressure Rise Rate (psi/deg)
Cyl 1
Cyl 2
Cyl 3
Cyl 4
Cyl 5
Cyl 6

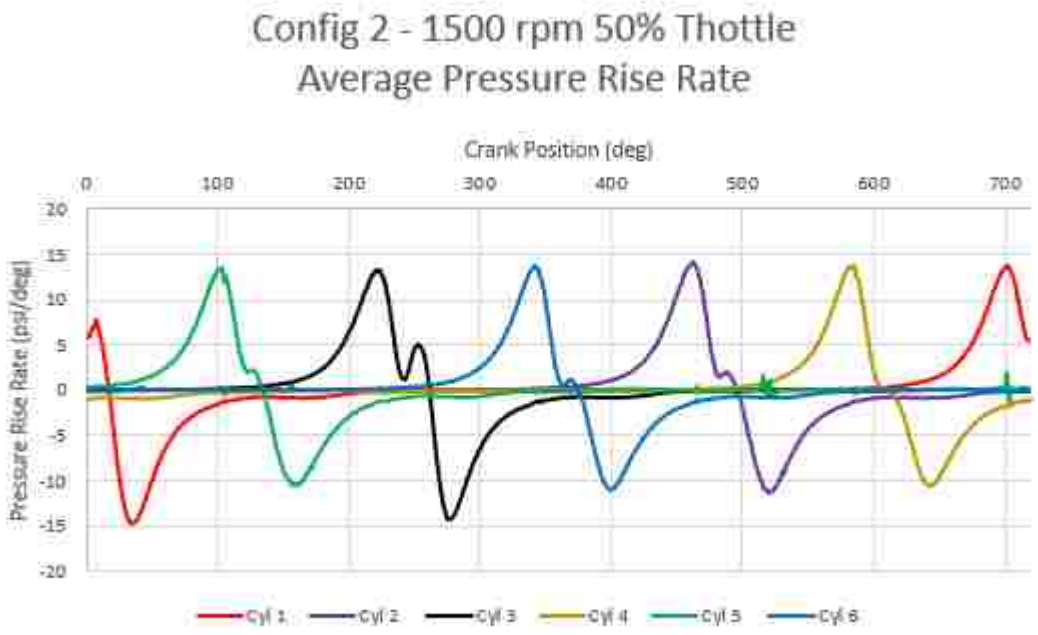
Config 2 - 1500 rpm 50% Thottle
Average Pressure Rise Rate
Crank Position (deg)
0
100
200
300
400
500
600
700
Pressure Rise Rate (psi/deg)
20
15
10
5
0
-5
-10
-15
-20
Cyl 1
Cyl 2
Cyl 3
Cyl 4
Cyl 5
Cyl 6

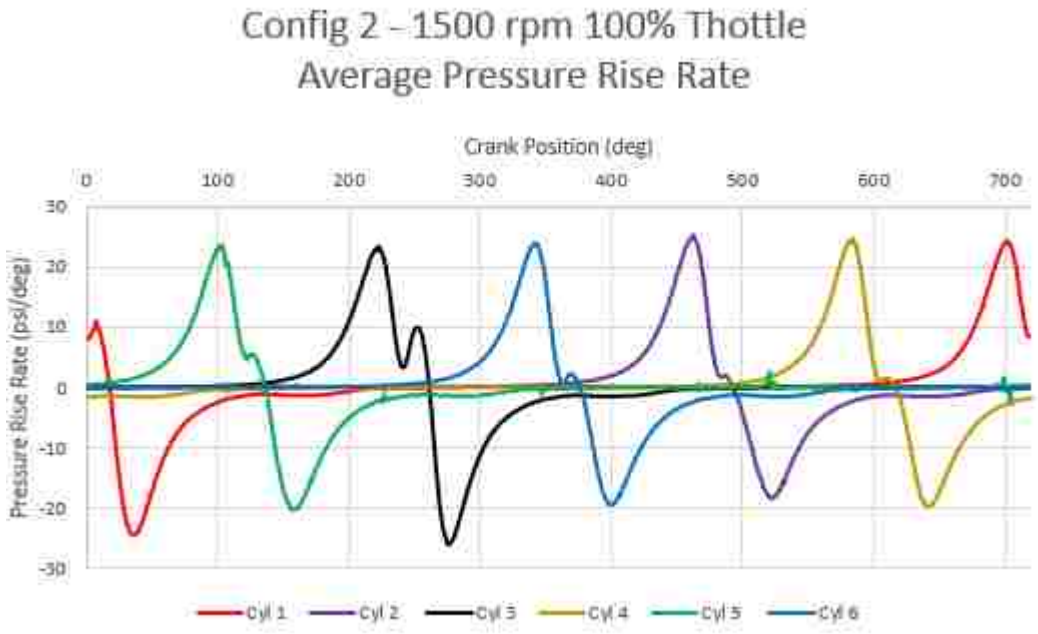
Config 2 - 1500 rpm 100% Thottle
Average Pressure Rise Rate
Crank Position (deg)
0
100
200
300
400
500
600
700
Pressure Rise Rate (psi/deg)
30
20
10
0
-10
-20
-30
Cyl 1
Cyl 2
Cyl 3
Cyl 4
Cyl 5
Cyl 6

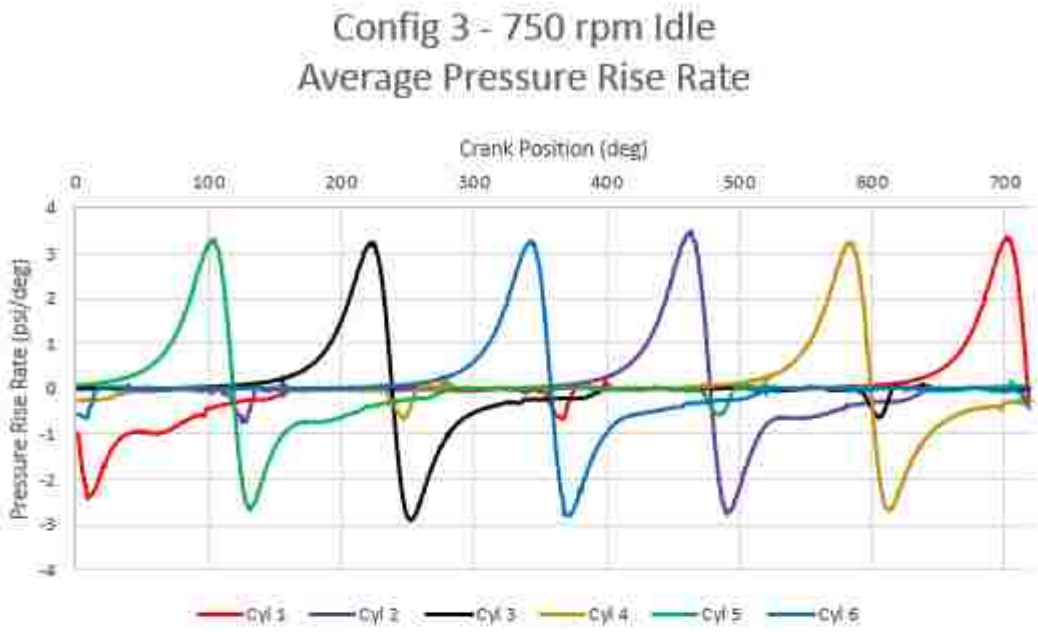
Config 3 - 750 rpm Idle
Average Pressure Rise Rate
Crank Position (deg)
0
100
200
300
400
500
600
700
Pressure Rise Rate (psi/deg)
Cyl 1
Cyl 2
Cyl 3
Cyl 4
Cyl 5
Cyl 6

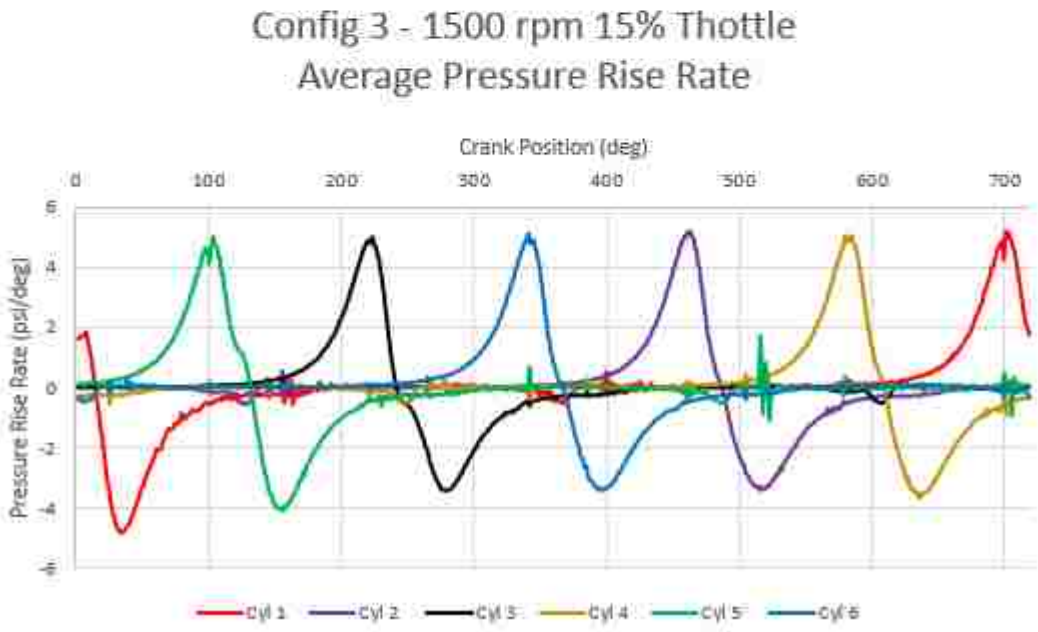
Config 3 - 1500 rpm 15% Thottle
Average Pressure Rise Rate
Crank Position (deg)
0
100
200
300
400
500
600
700
Pressure Rise Rate (psi/deg)
Cyl 1
Cyl 2
Cyl 3
Cyl 4
Cyl 5
Cyl 6

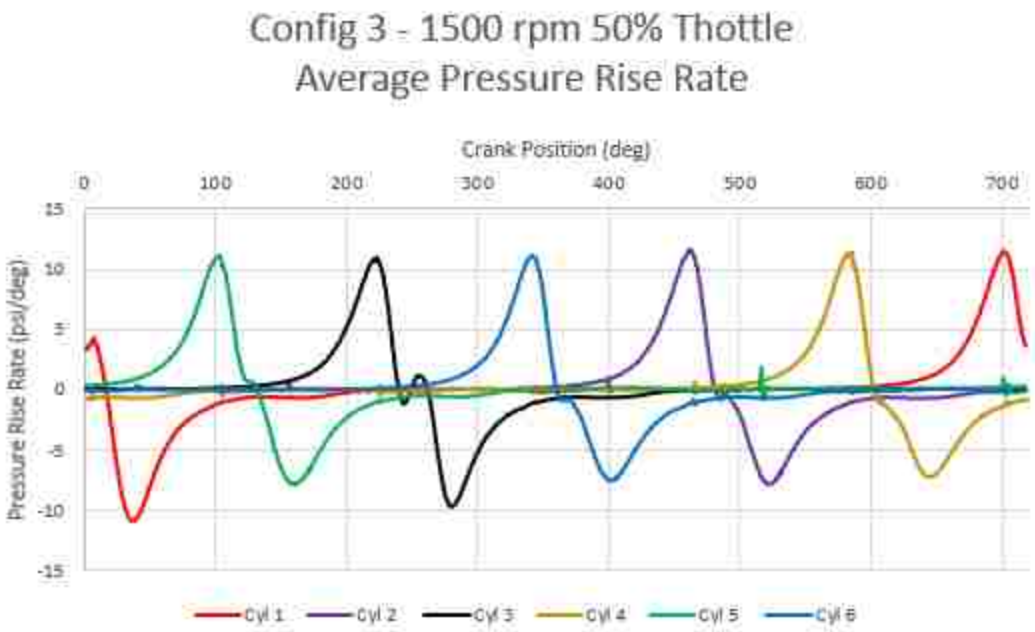
Config 3 - 1500 rpm 50% Thottle
Average Pressure Rise Rate
Crank Position (deg)
0
100
200
300
400
500
600
700
Pressure Rise Rate (psi/deg)
15
10
5
0
-5
-10
-15
Cyl 1
Cyl 2
Cyl 3
Cyl 4
Cyl 5
Cyl 6

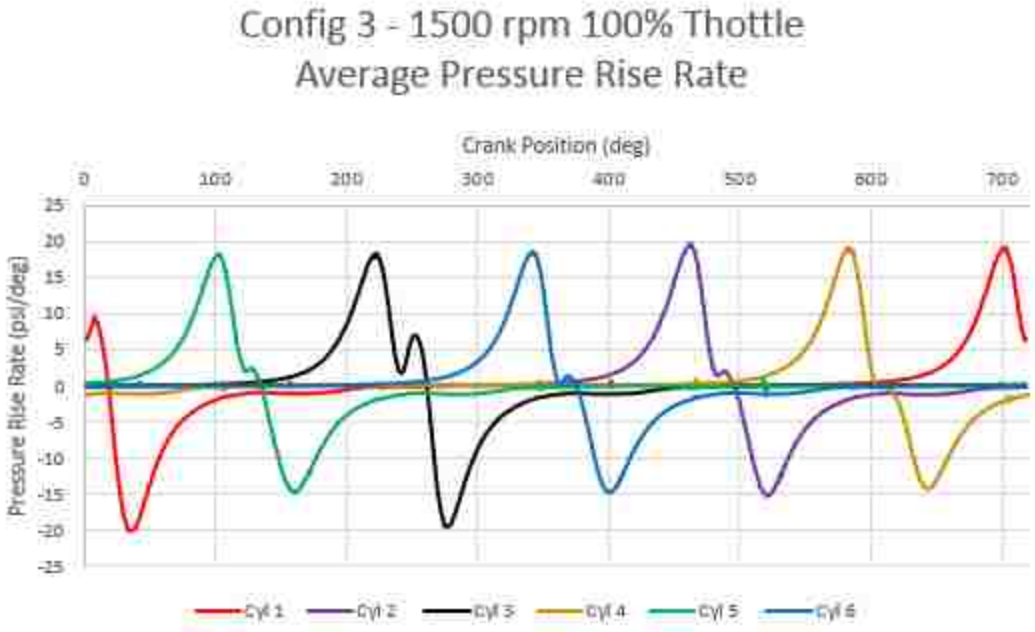
Config 3 - 1500 rpm 100% Thottle
Average Pressure Rise Rate
Crank Position (deg)
0
100
200
300
400
500
600
700
Pressure Rise Rate (psi/deg)
25
20
15
10
5
0
-5
-10
-15
-20
-25
Cyl 1
Cyl 2
Cyl 3
Cyl 4
Cyl 5
Cyl 6

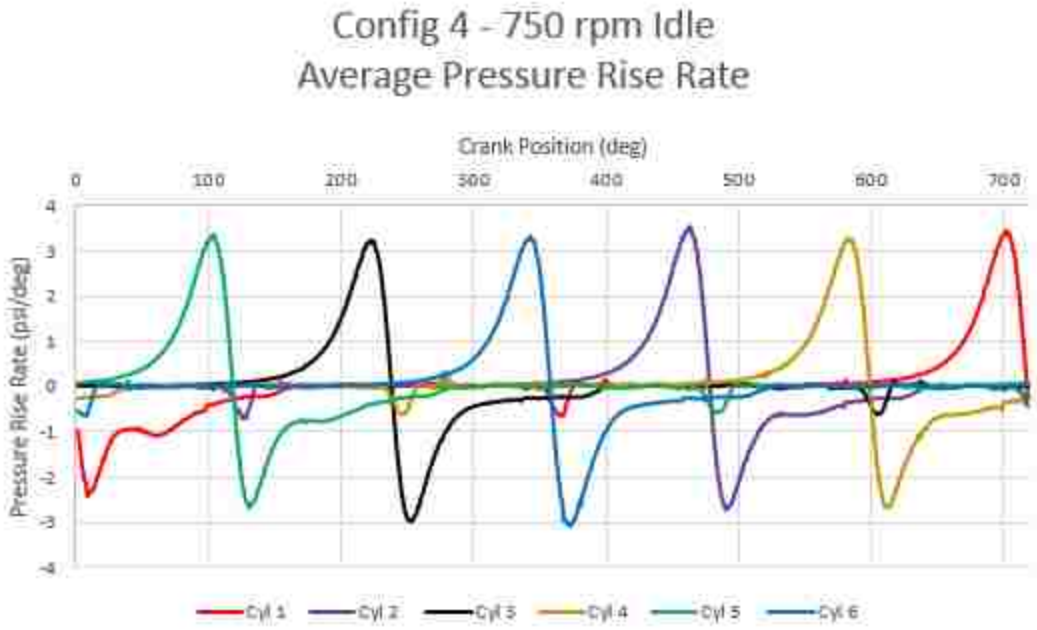
Config 4 - 750 rpm Idle
Average Pressure Rise Rate
Crank Position (deg)
0
100
200
300
400
500
600
700
Pressure Rise Rate (psi/deg)
4
3
2
1
0
-1
-2
-3
-4
Cyl 1
Cyl 2
Cyl 3
Cyl 4
Cyl 5
Cyl 6

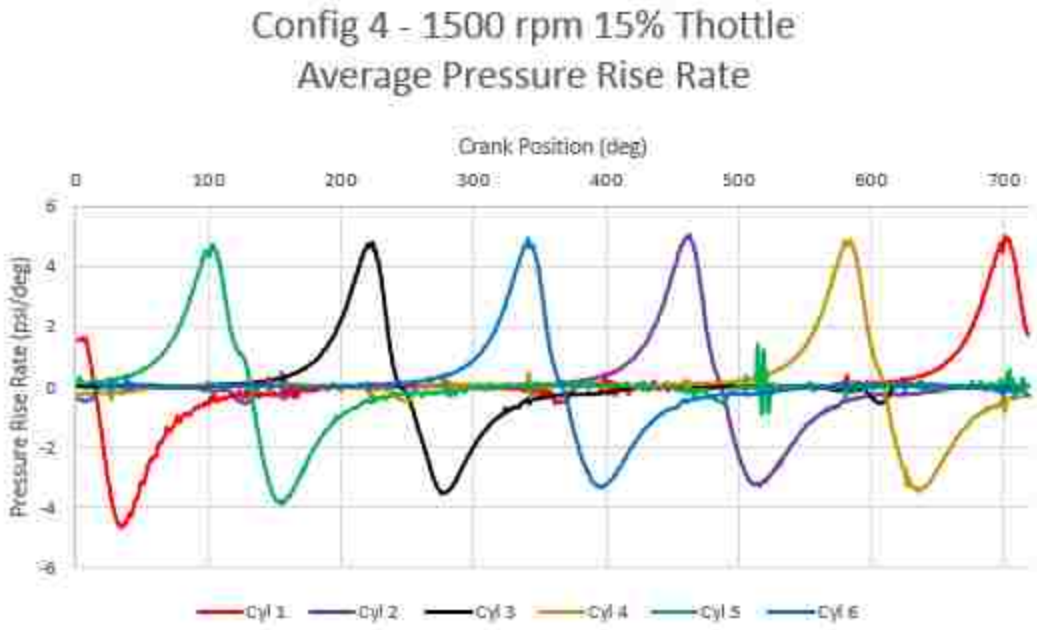
Config 4 - 1500 rpm 15% Thottle
Average Pressure Rise Rate
Crank Position (deg)
0
100
200
300
400
500
600
700
Pressure Rise Rate (psi/deg)
6
4
2
0
-2
-4
-6
Cyl 1
Cyl 2
Cyl 3
Cyl 4
Cyl 5
Cyl 6

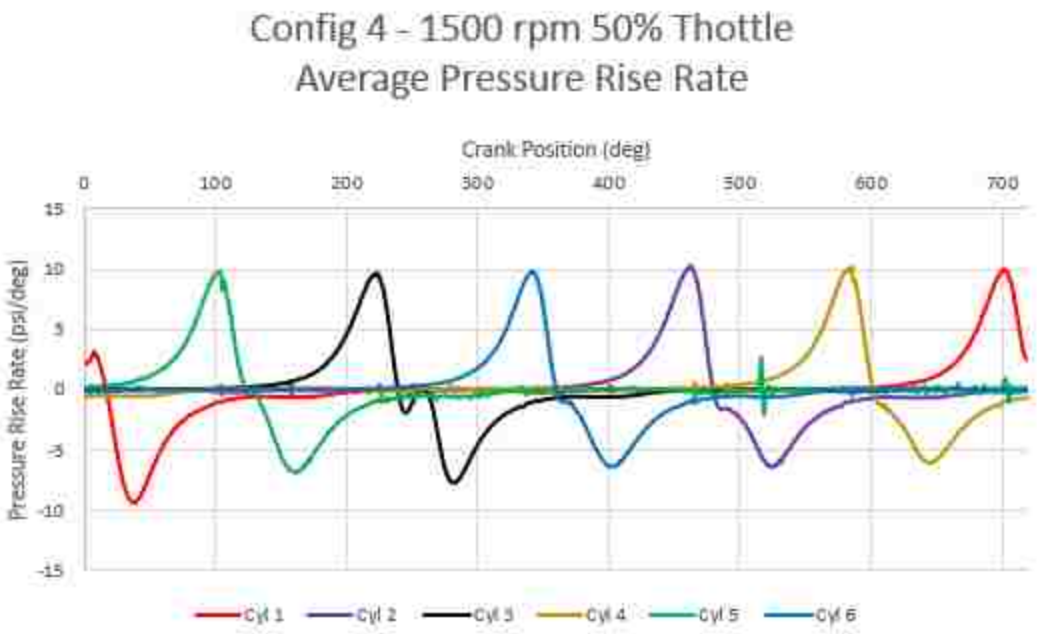
Config 4 - 1500 rpm 50% Thottle
Average Pressure Rise Rate
Crank Position (deg)
0
100
200
300
400
500
600
700
15
10
5
0
-5
-10
-15
Pressure Rise Rate (psi/deg)
Cyl 1
Cyl 2
Cyl 3
Cyl 4
Cyl 5
Cyl 6

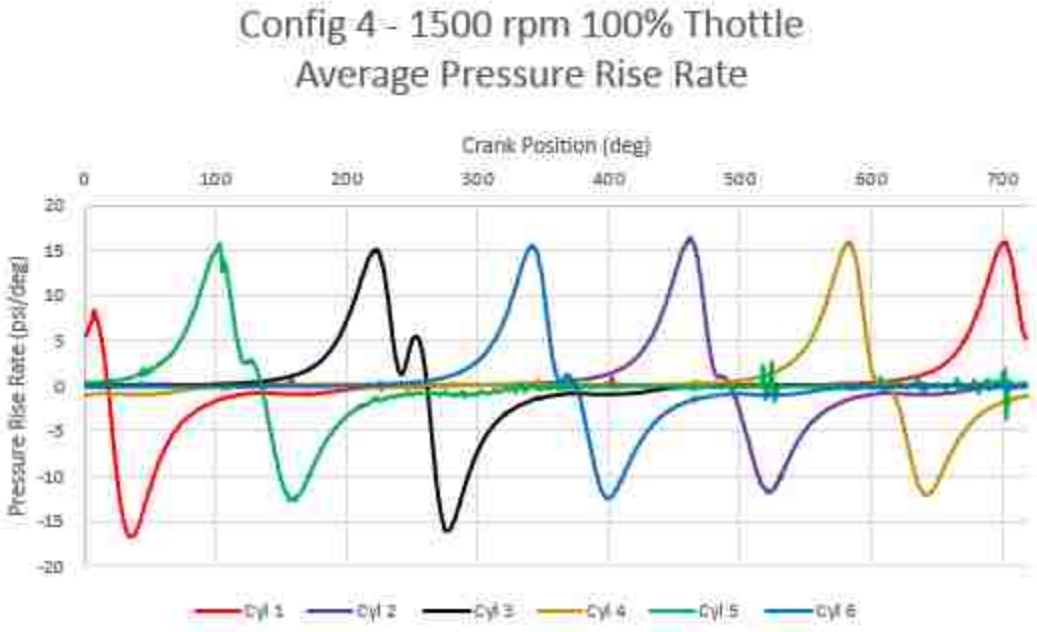
Config 4 - 1500 rpm 100% Thottle
Average Pressure Rise Rate
Crank Position (deg)
0
100
200
300
400
500
600
700
20
15
10
5
0
-5
-10
-15
-20
Pressure Rise Rate (psi/deg)
Cyl 1
Cyl 2
Cyl 3
Cyl 4
Cyl 5
Cyl 6

Appendix G: Vibration Results, 1/3 Octave

Engine Mount LF, 750, Idle

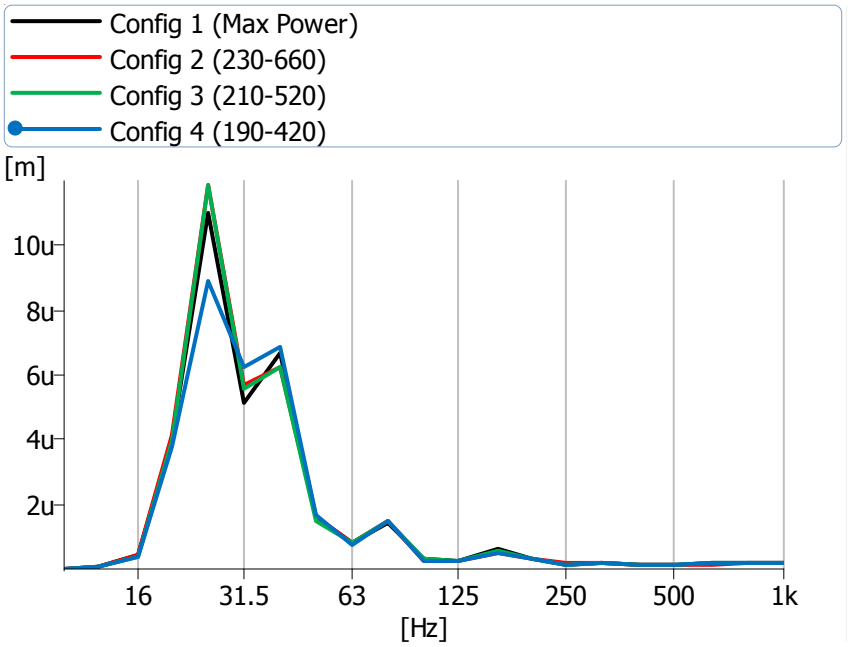

Engine Mount LR, 750, Idle

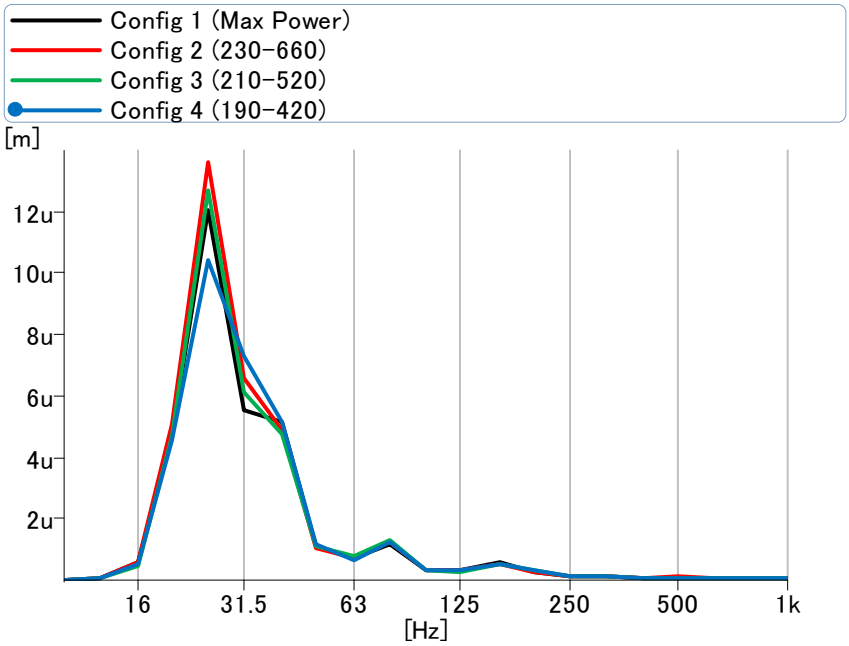

Engine Mount RF, 750, Idle

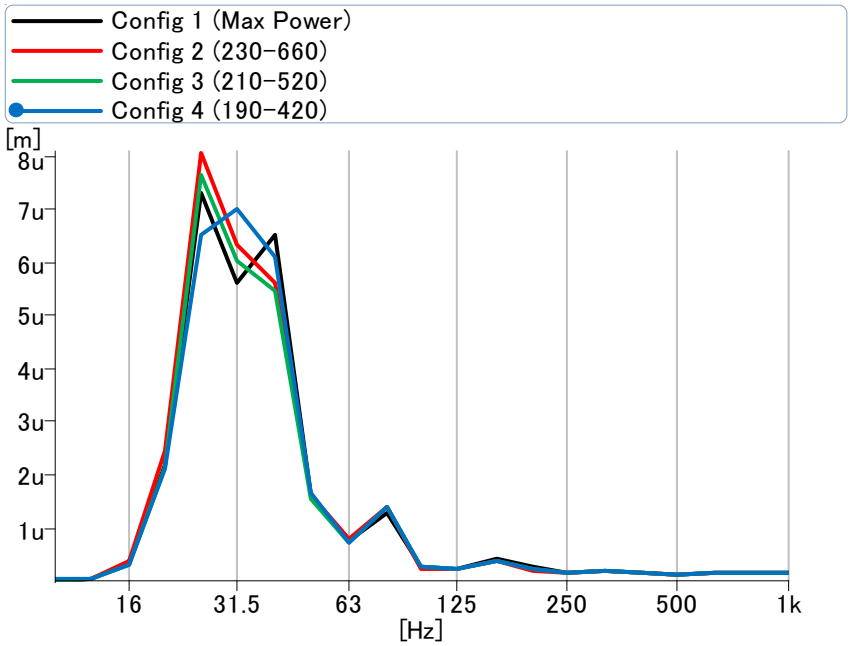

Engine Mount RR, 750, Idle

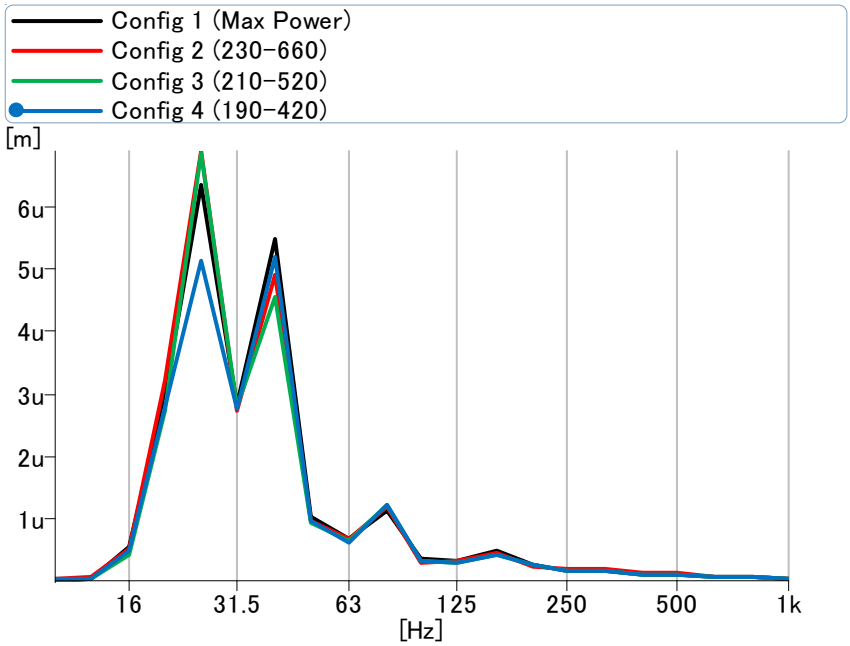

Engine Mount LF, 1500, 15%

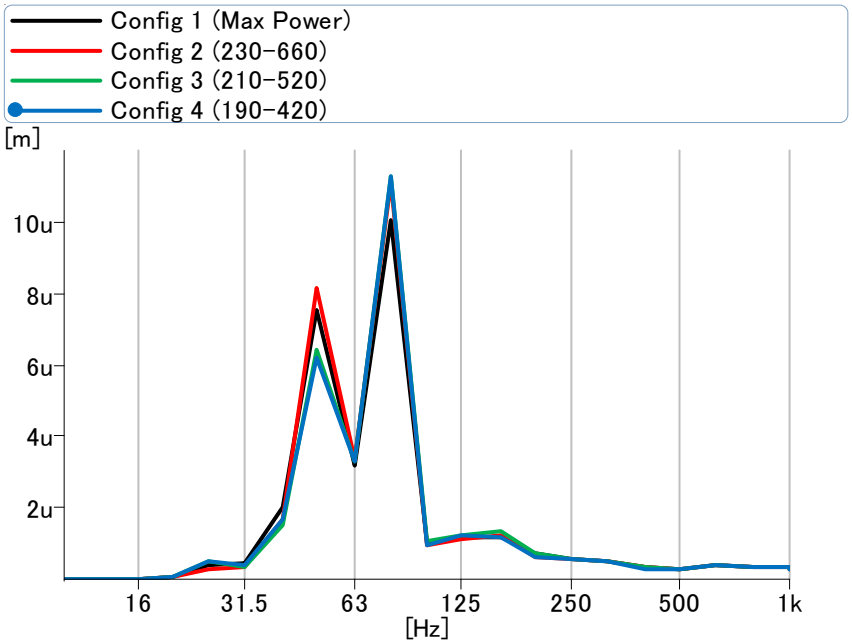

Engine Mount LR, 1500, 15%

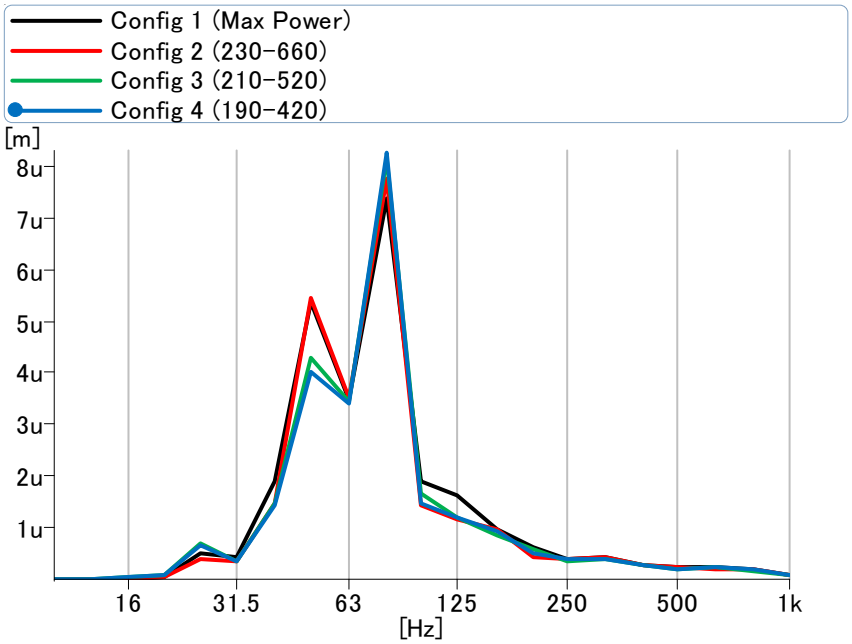

Engine Mount RF, 1500, 15%

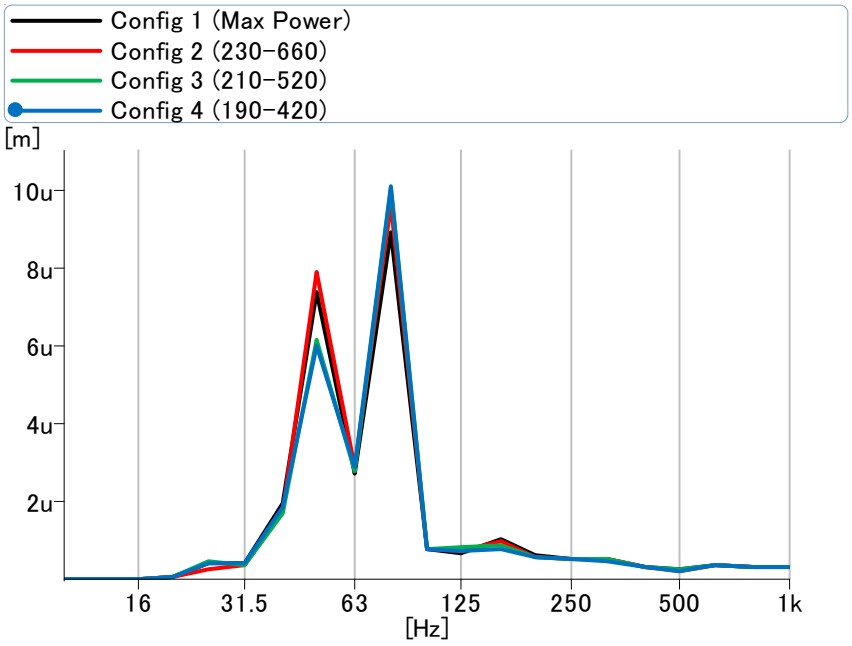

Engine Mount RR, 1500, 15%

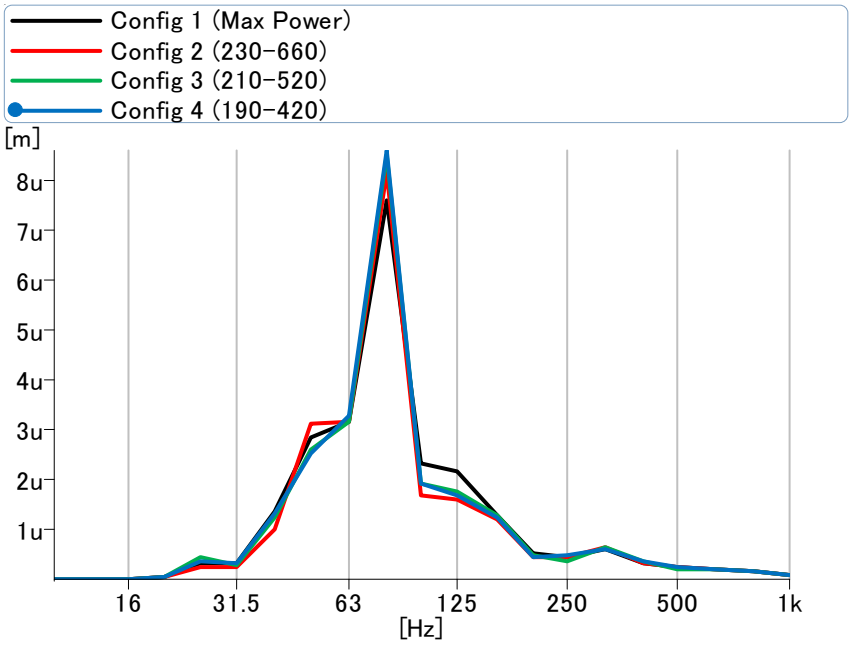

Engine Mount LF, 1500, 50%

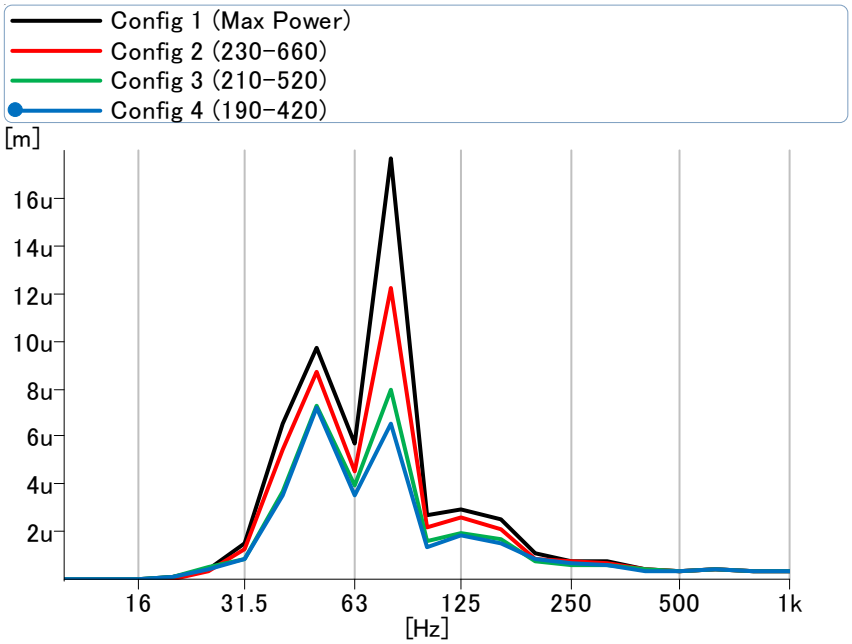

Engine Mount LR, 1500, 50%

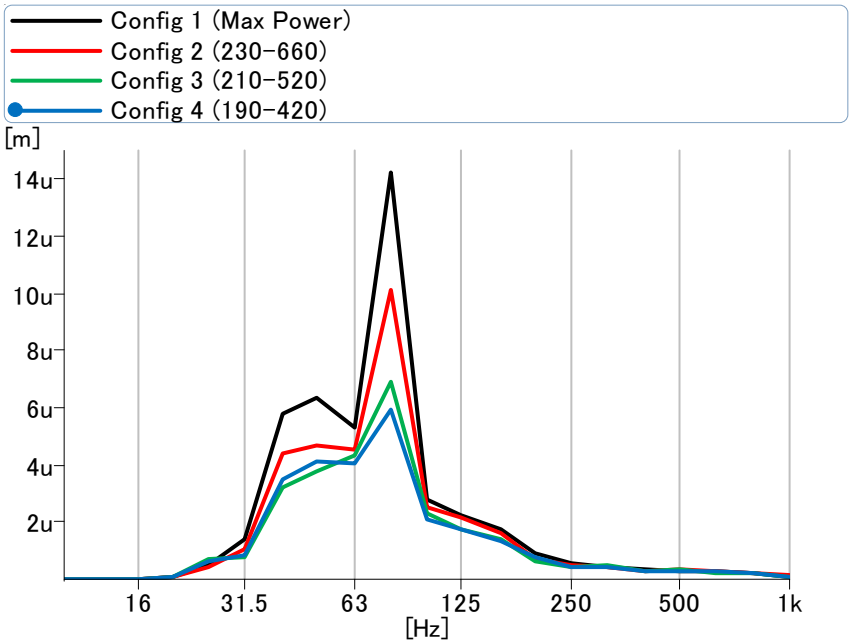

Engine Mount RF, 1500, 50%

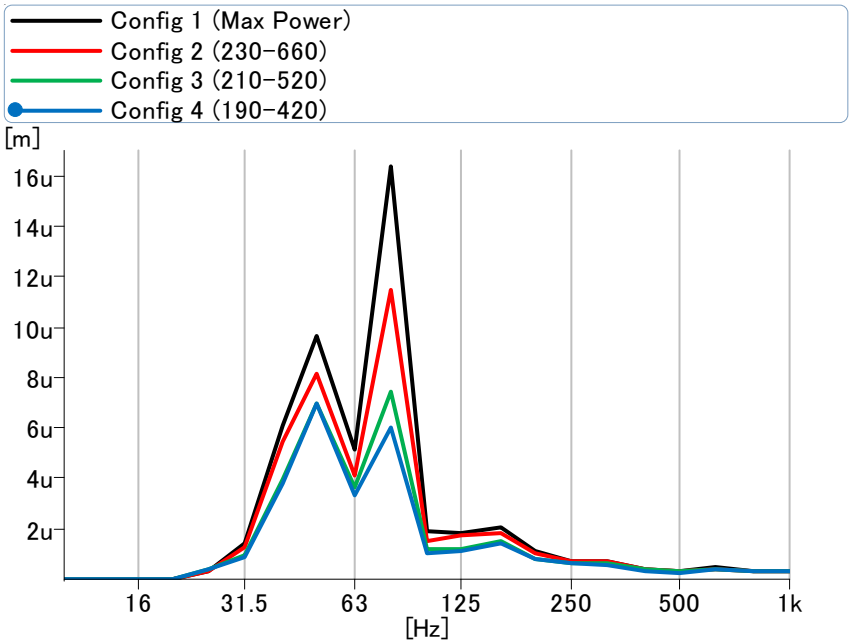

Engine Mount RR, 1500, 50%

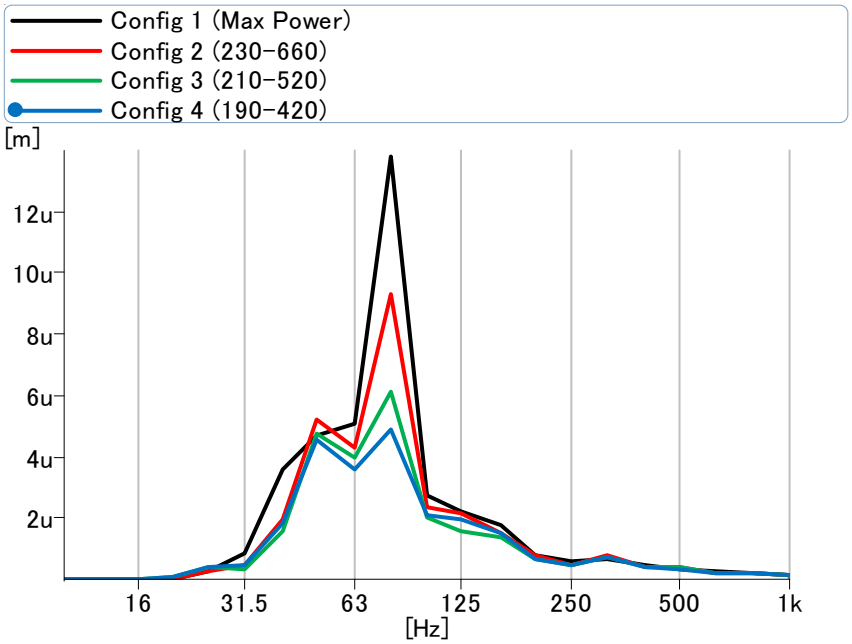

Engine Mount LF, 1500, 100%

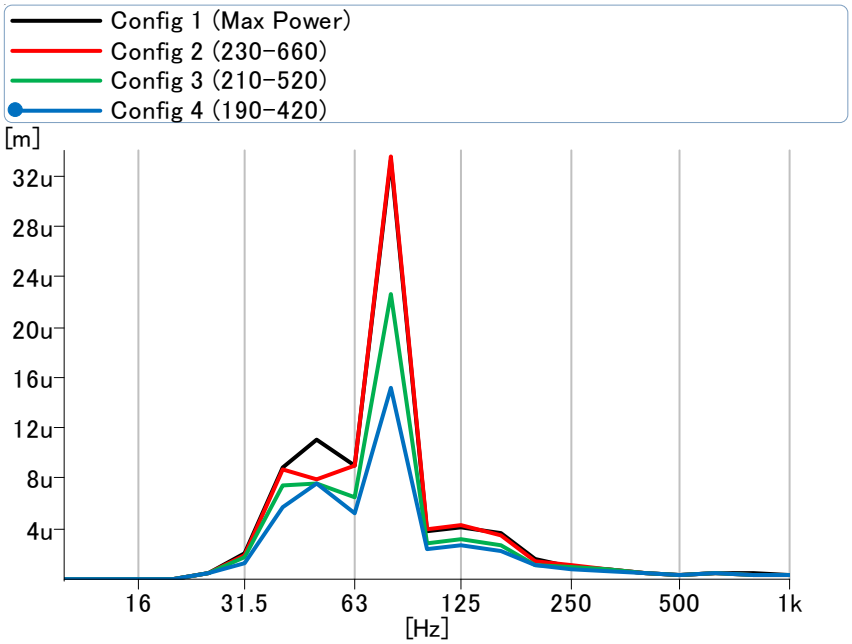

Engine Mount LR, 1500, 100%

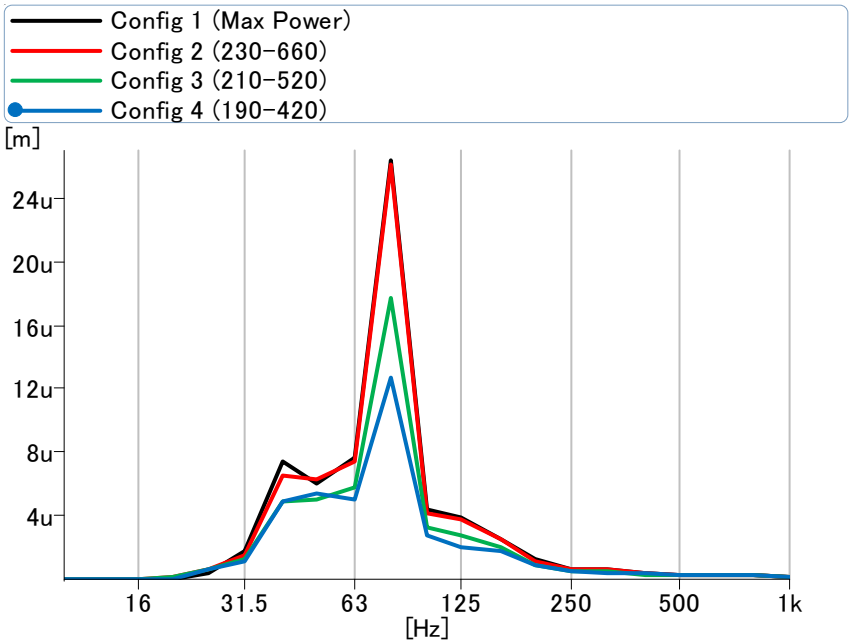

Engine Mount RF, 1500, 100%

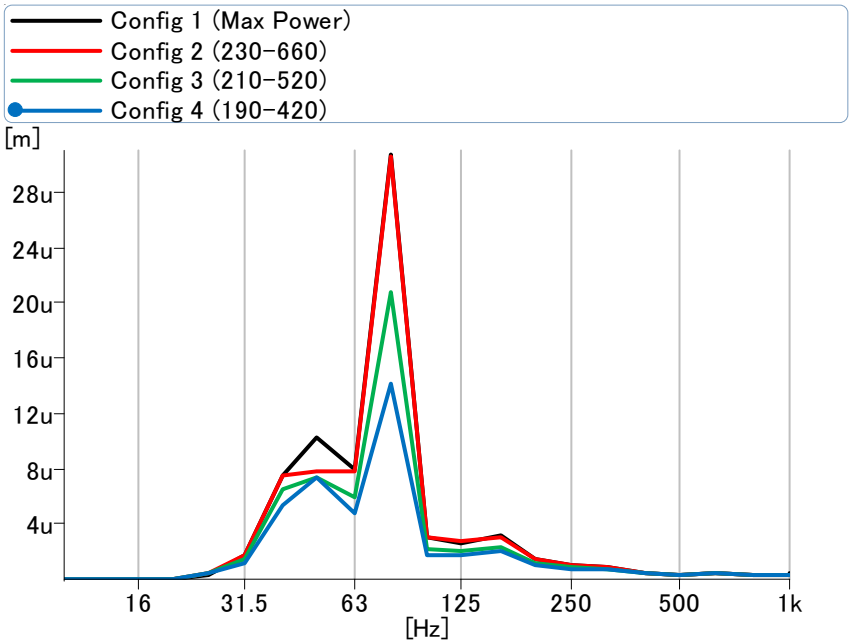

Engine Mount RR, 1500, 100%

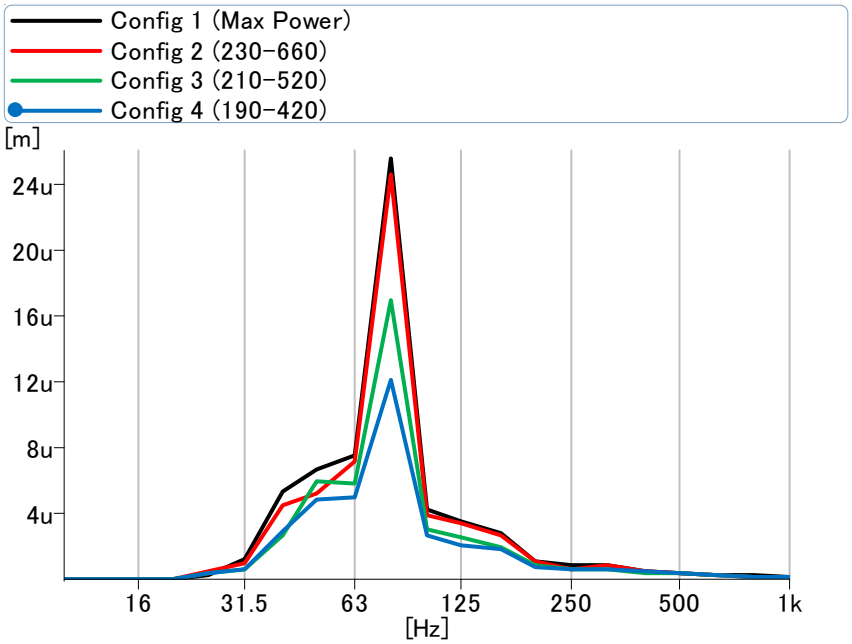

Appendix H: Vibration Results, Order

Engine Mount LF, 750, Idle

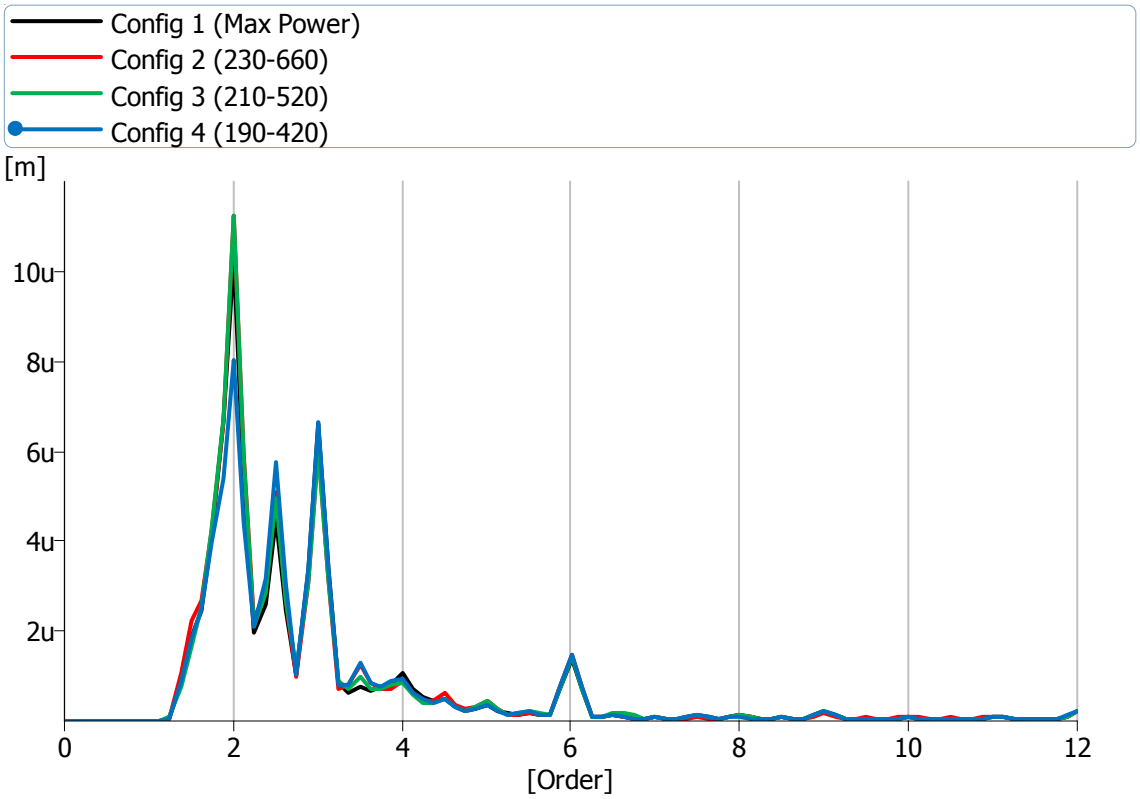

Engine Mount LR, 750, Idle

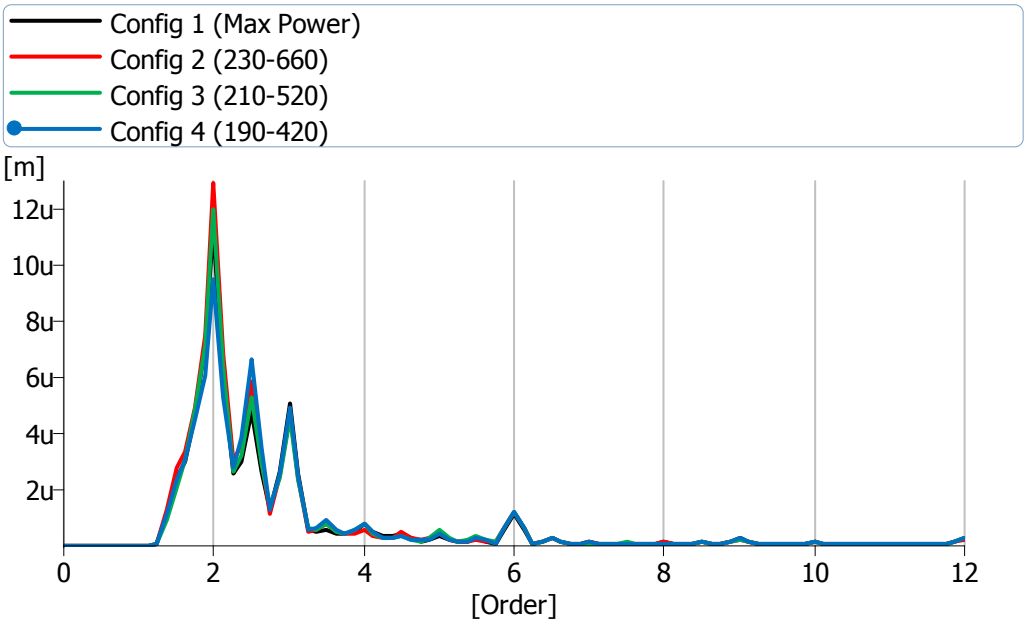

Engine Mount RF, 750, Idle

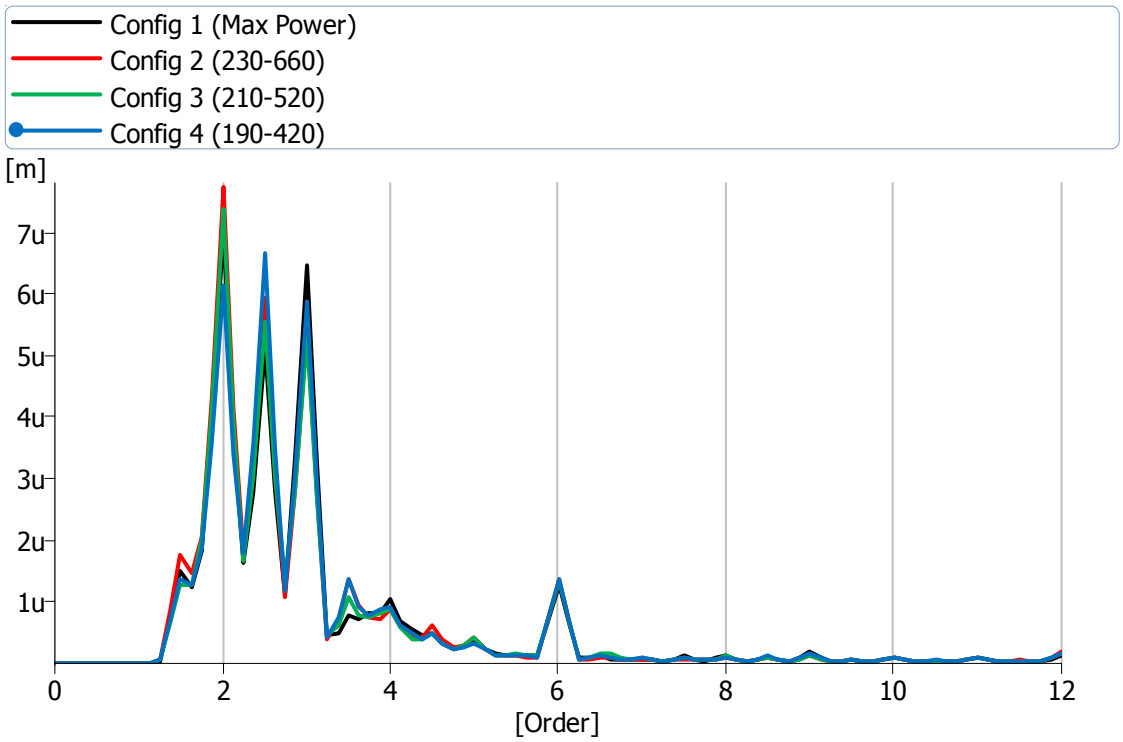

Engine Mount RR, 750, Idle

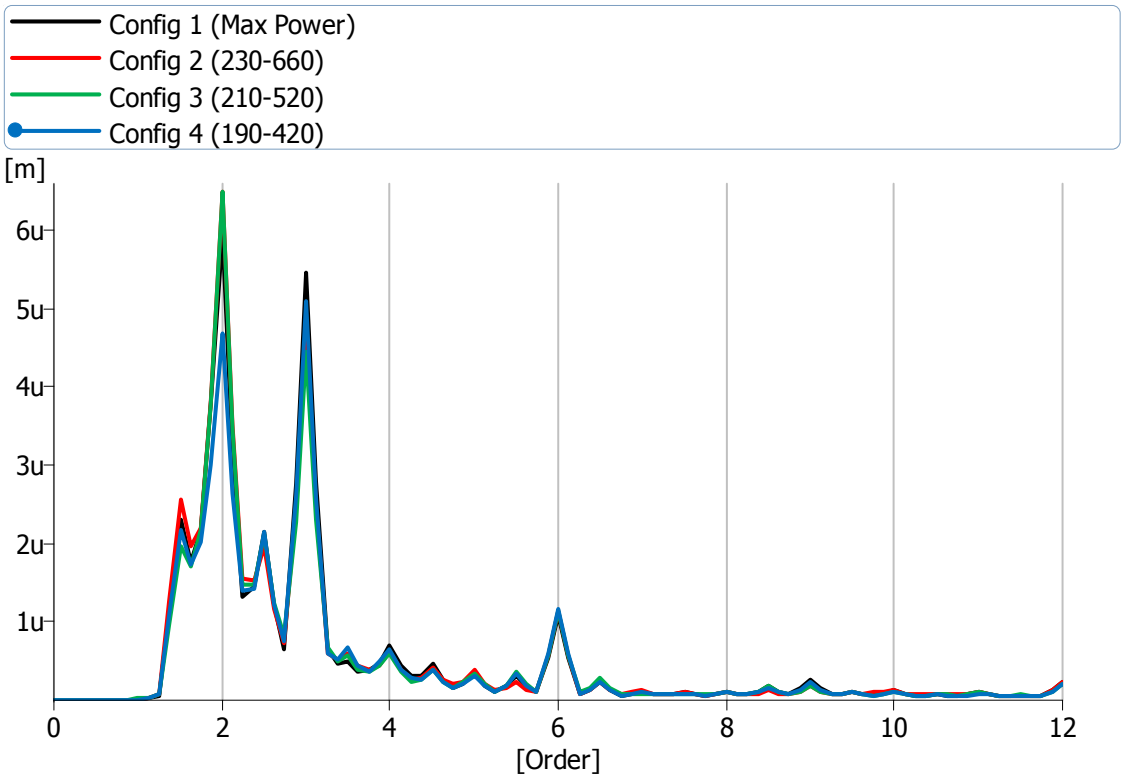

Engine Mount LF, 1500, 15%

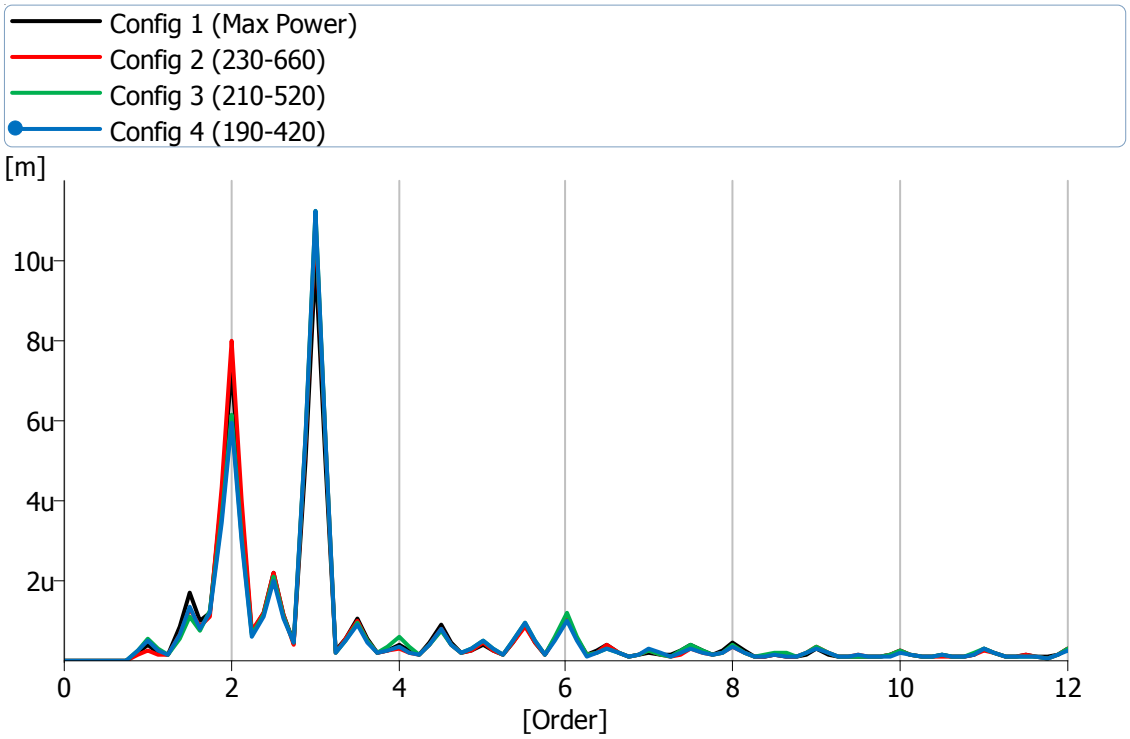

Engine Mount LR, 1500, 15%

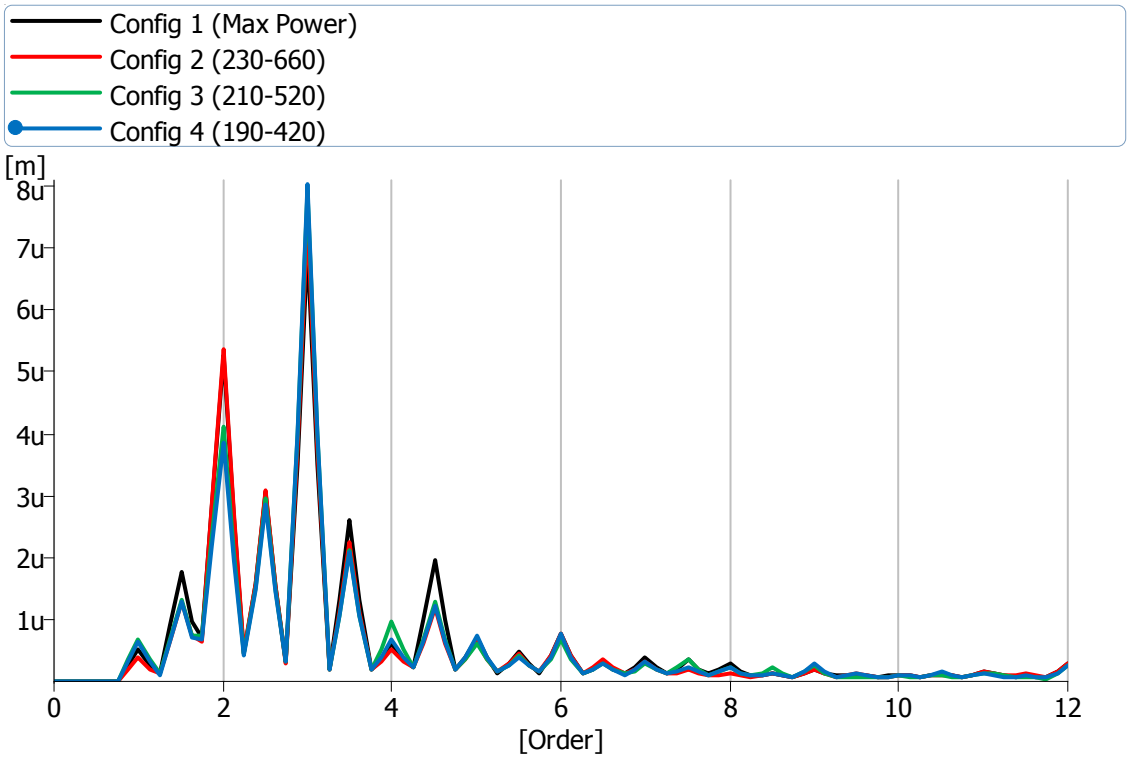

Engine Mount RF, 1500, 15%

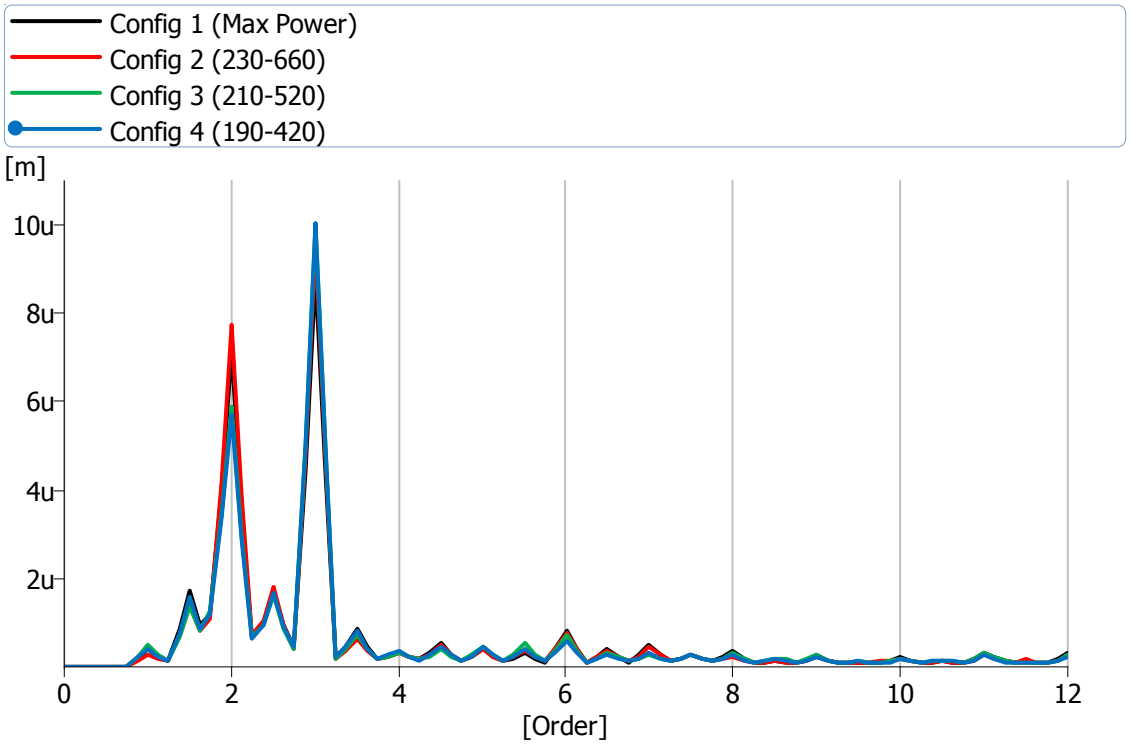

Engine Mount RR, 1500, 15%

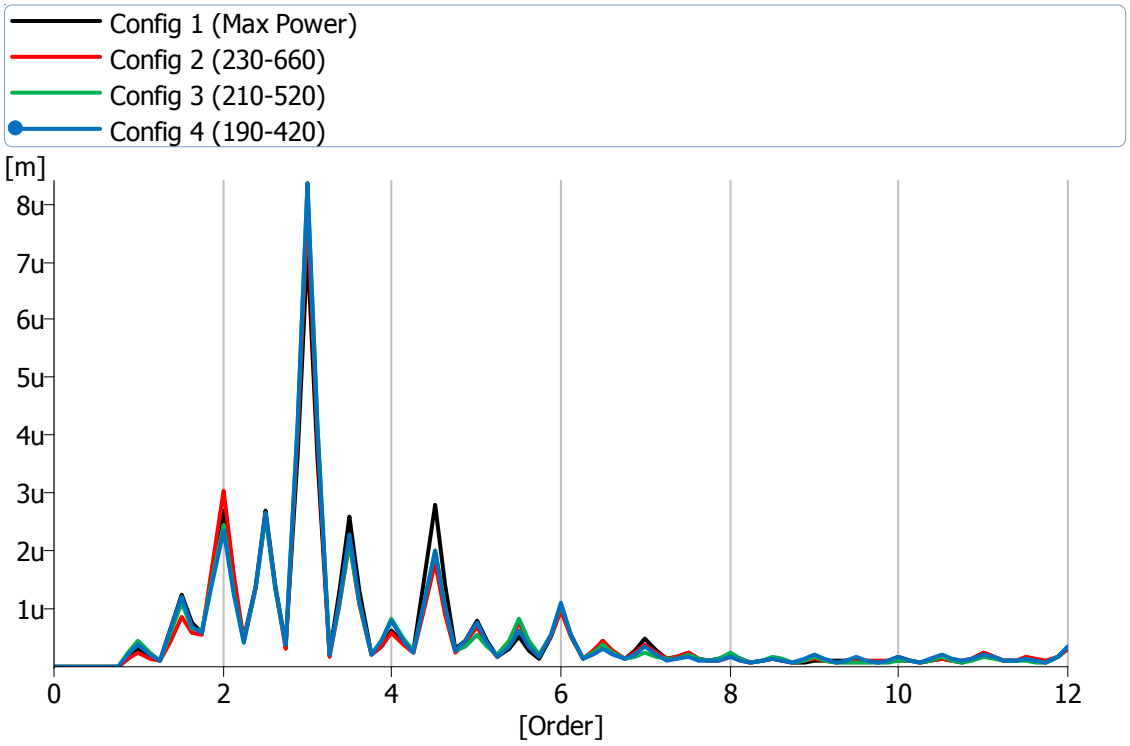

Engine Mount LF, 1500, 50%

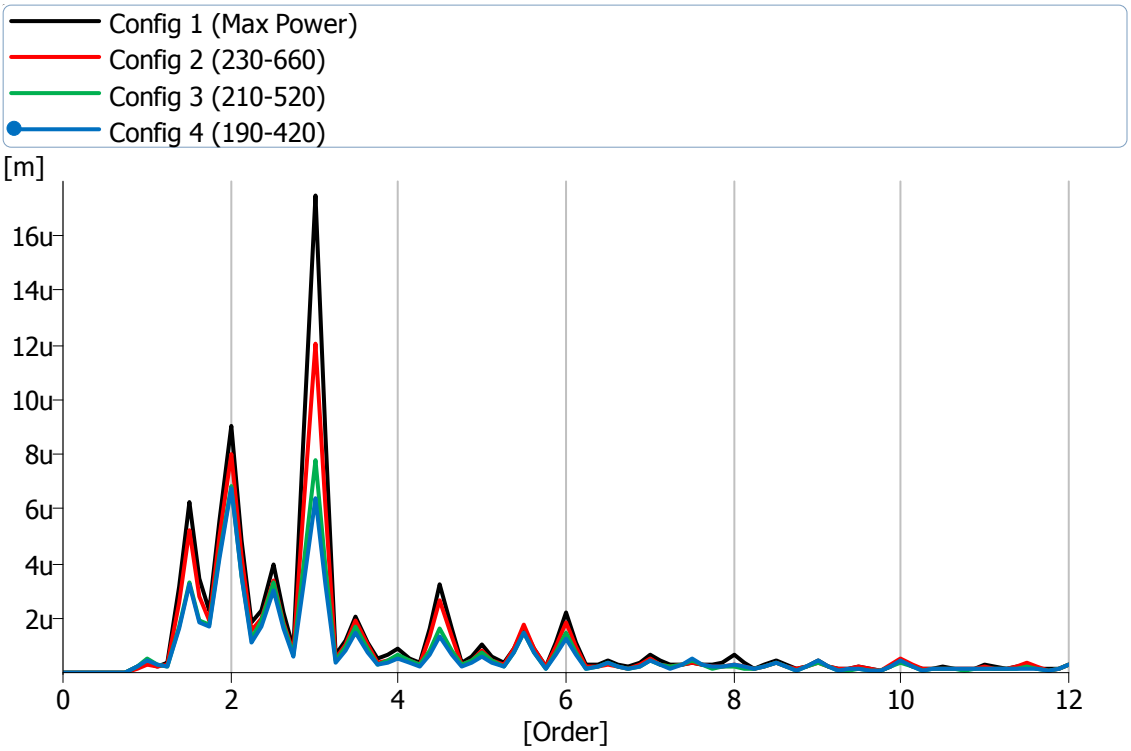

Engine Mount LR, 1500, 50%

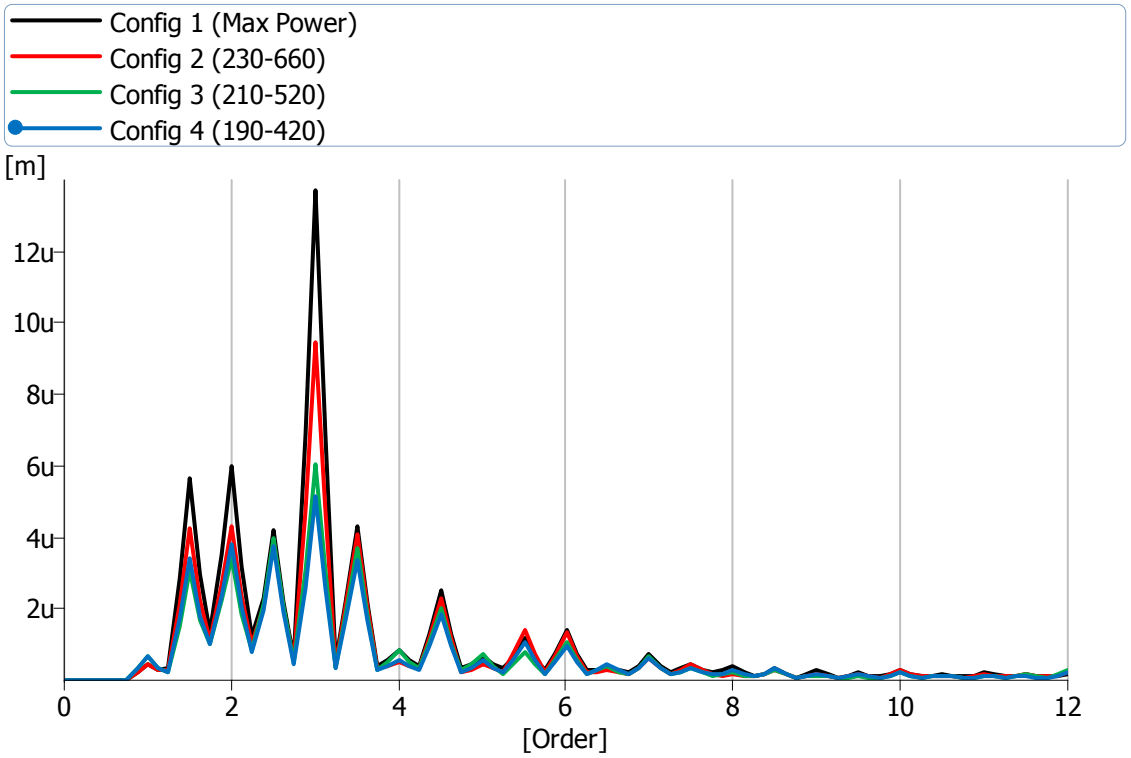

Engine Mount RF, 1500, 50%

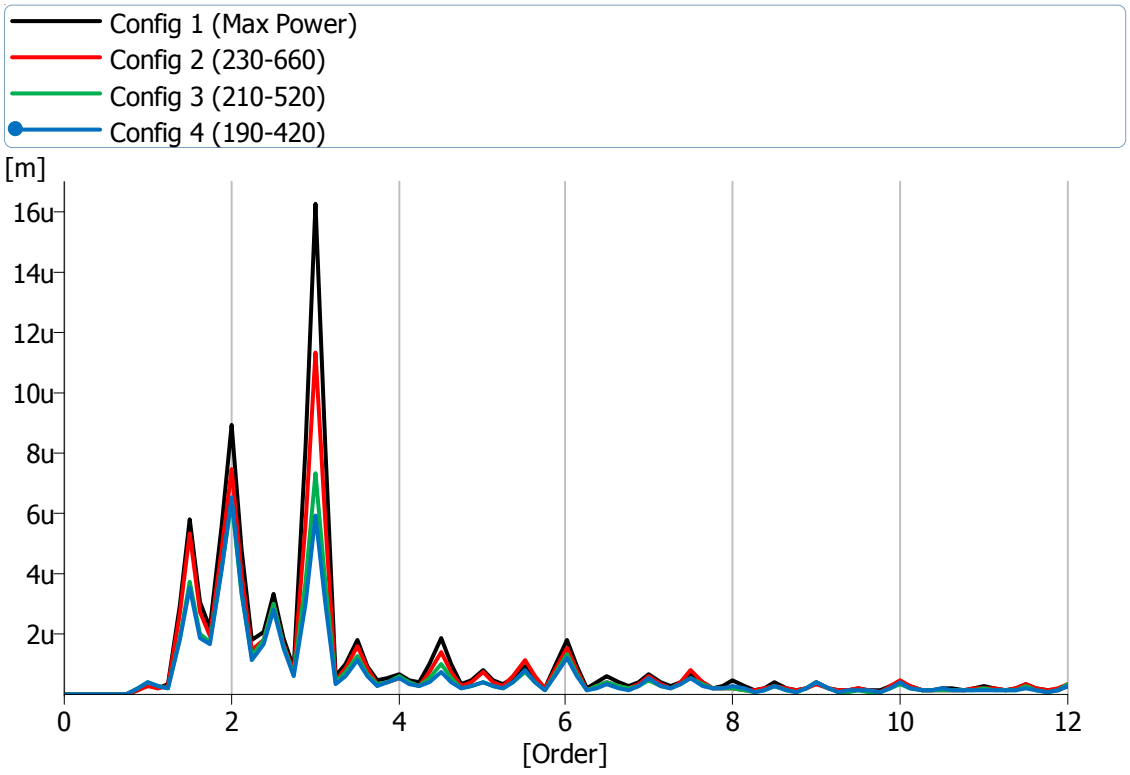

Engine Mount RR, 1500, 50%

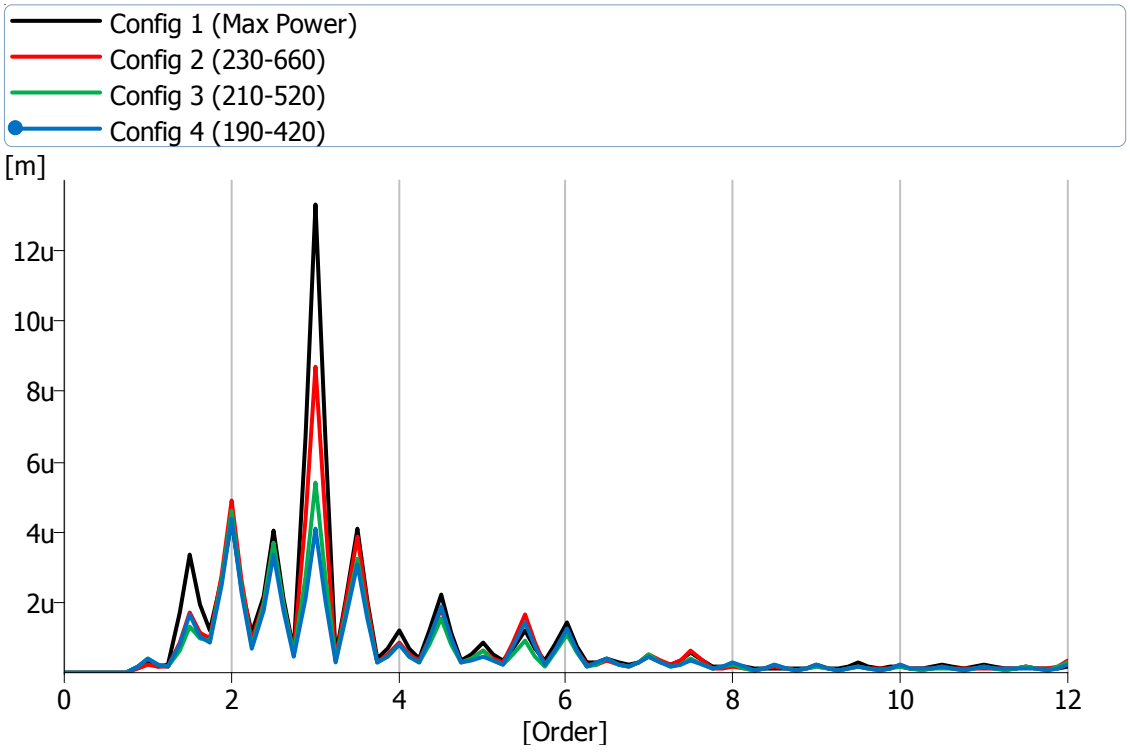

Engine Mount LF, 1500, 100%

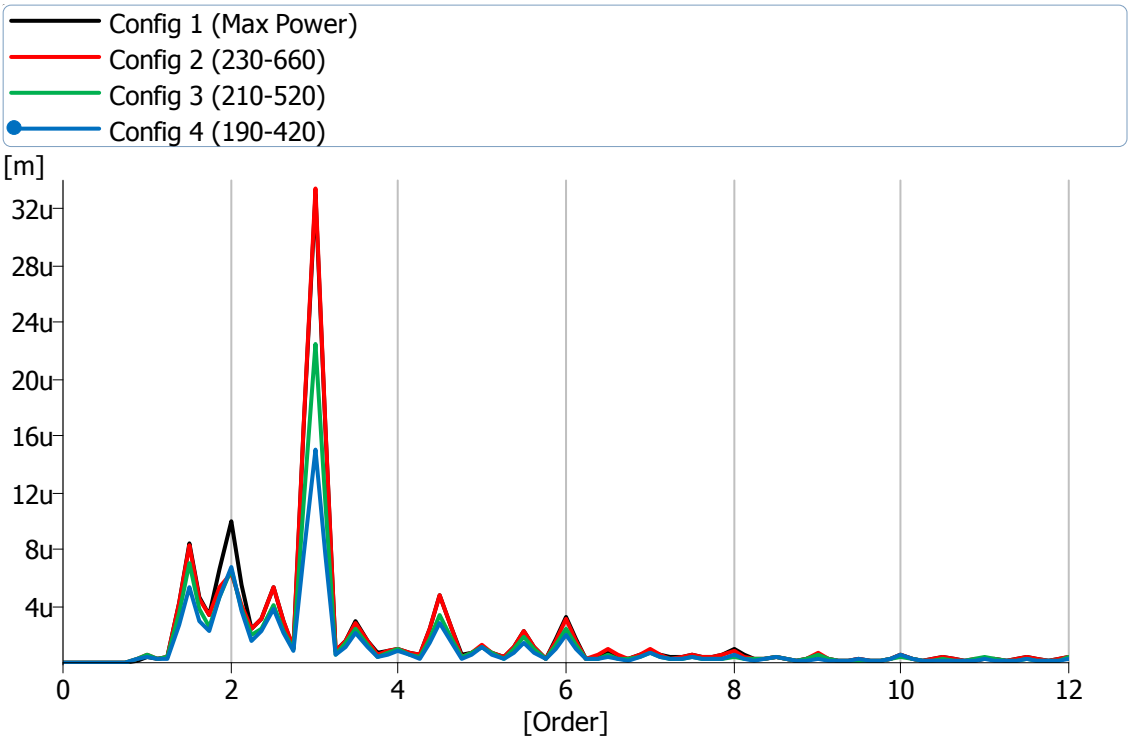

Engine Mount LR, 1500, 100%

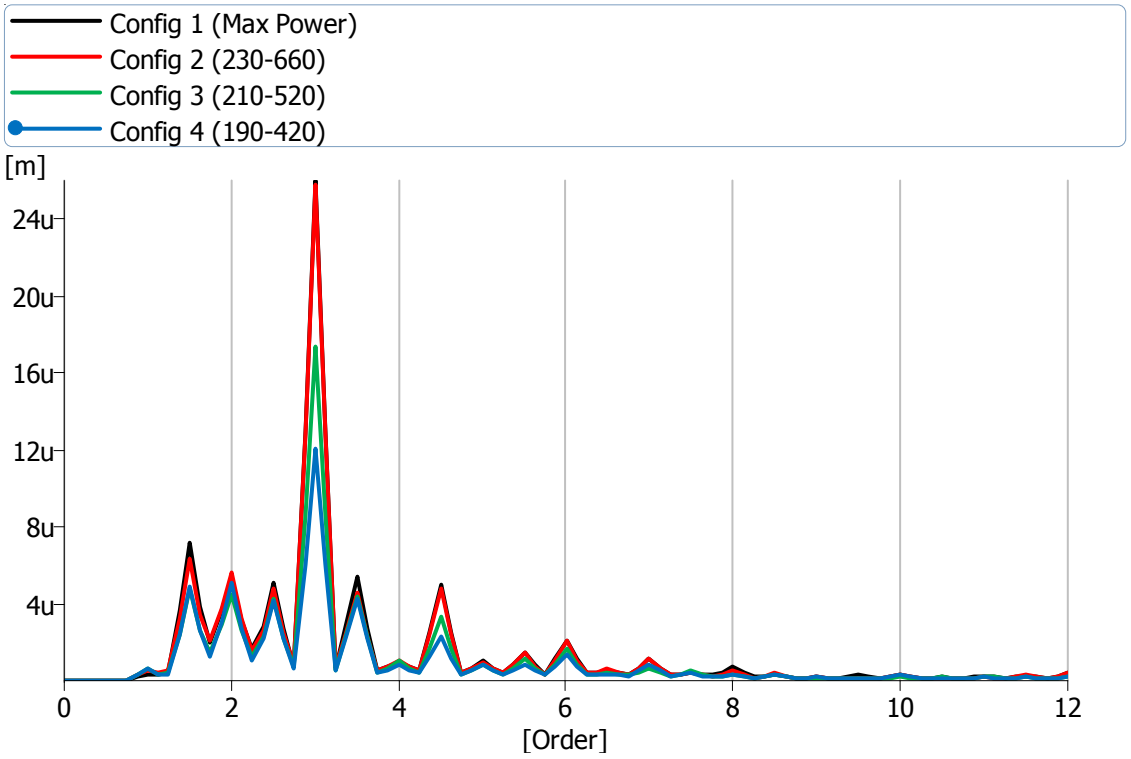

Engine Mount RF, 1500, 100%

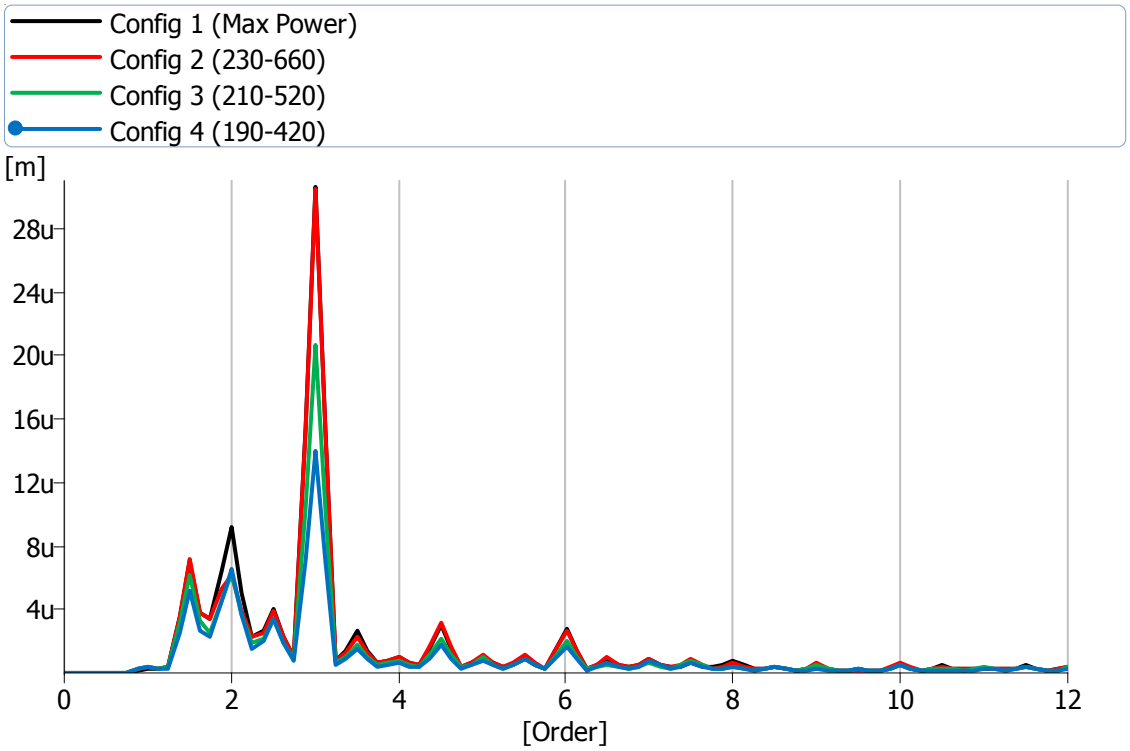

Engine Mount RR, 1500, 100%

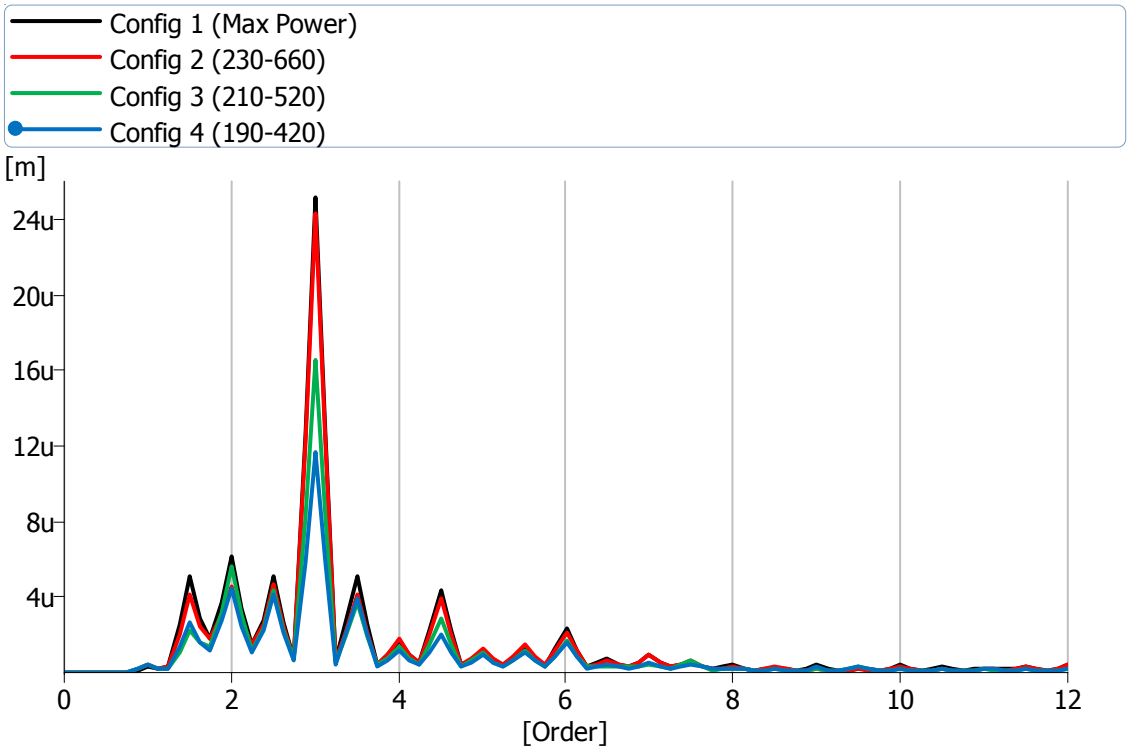

Appendix I: Vibration Results, FFT

Engine Mount LF, 750, Idle

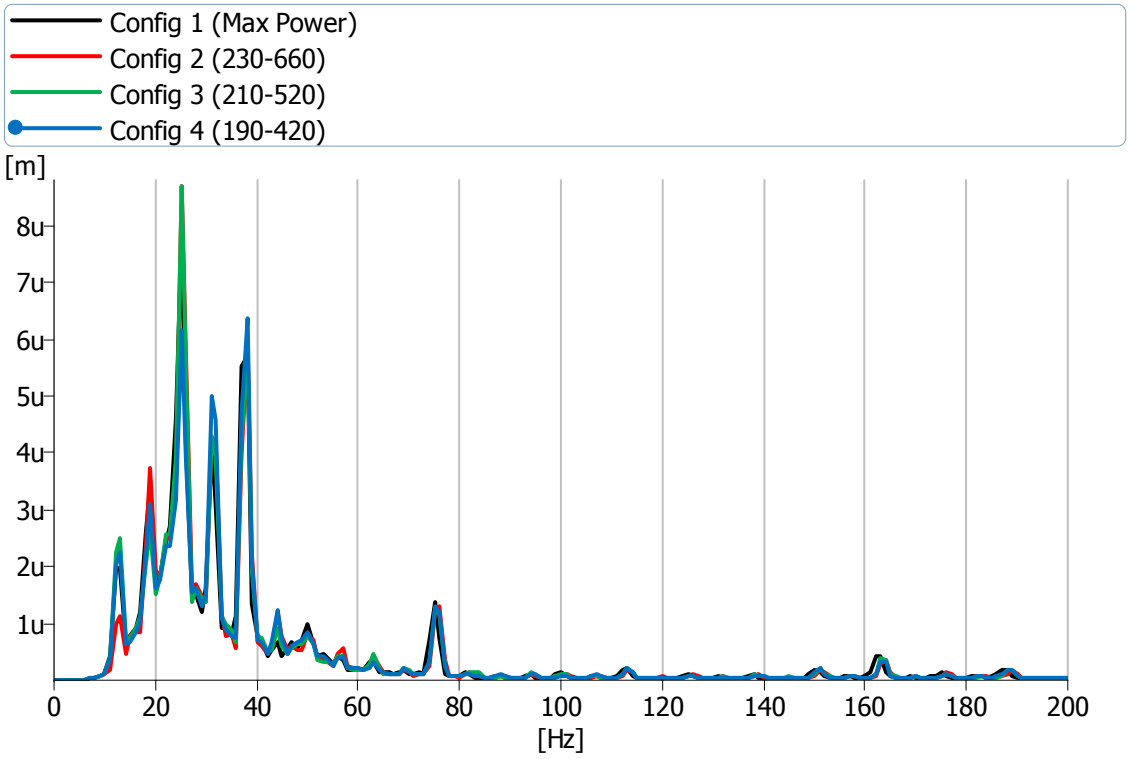

Engine Mount LR, 750, Idle

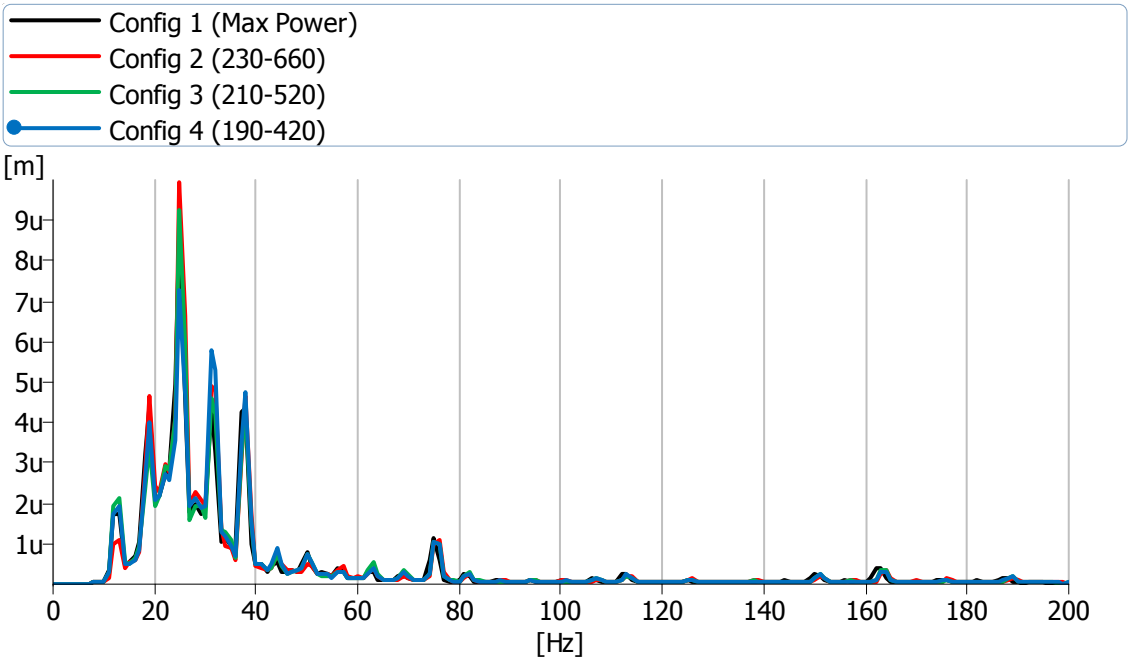

Engine Mount RF, 750, Idle

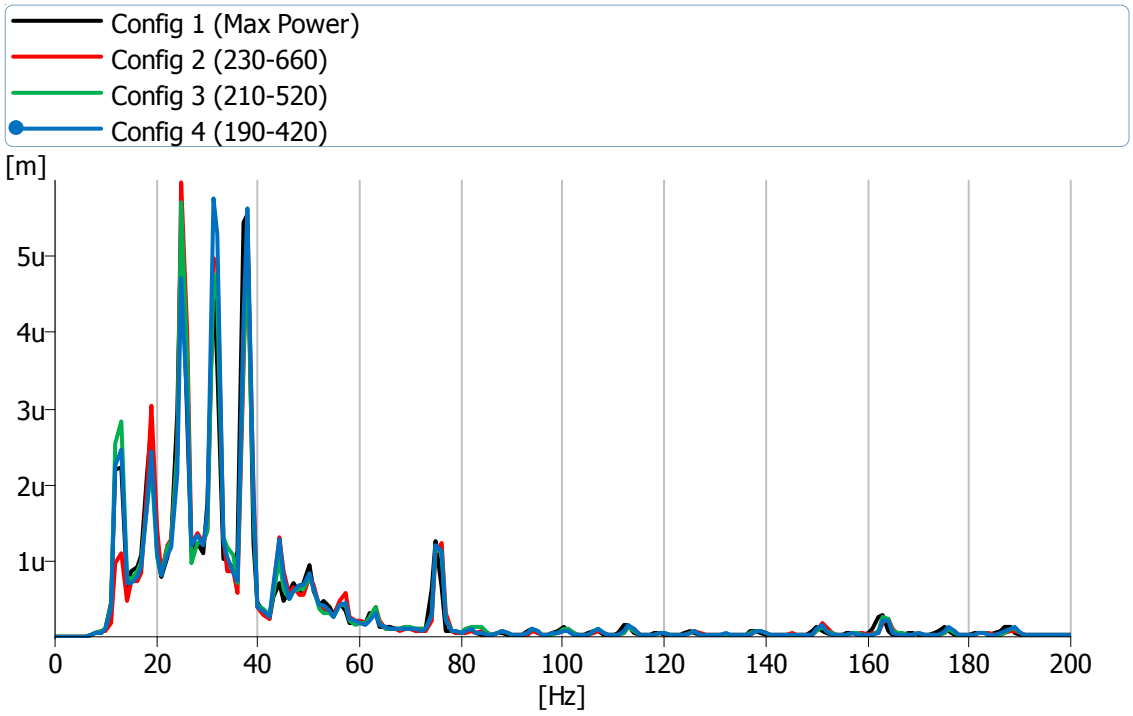

Engine Mount RR, 750, Idle

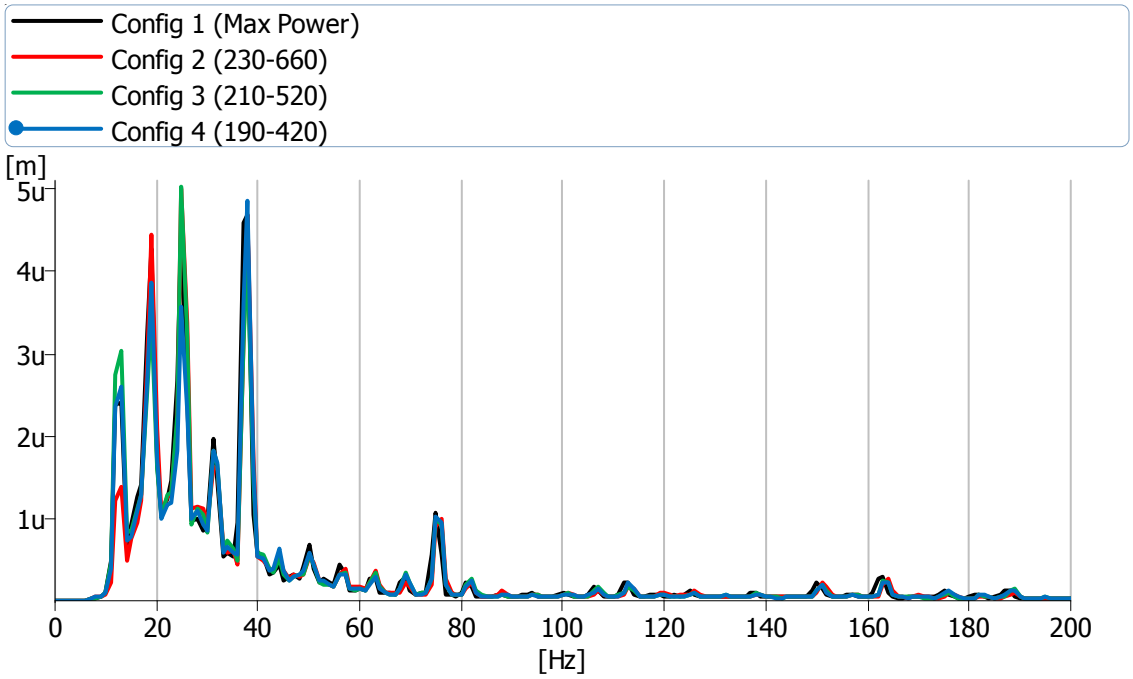

Engine Mount LF, 1500, 15%

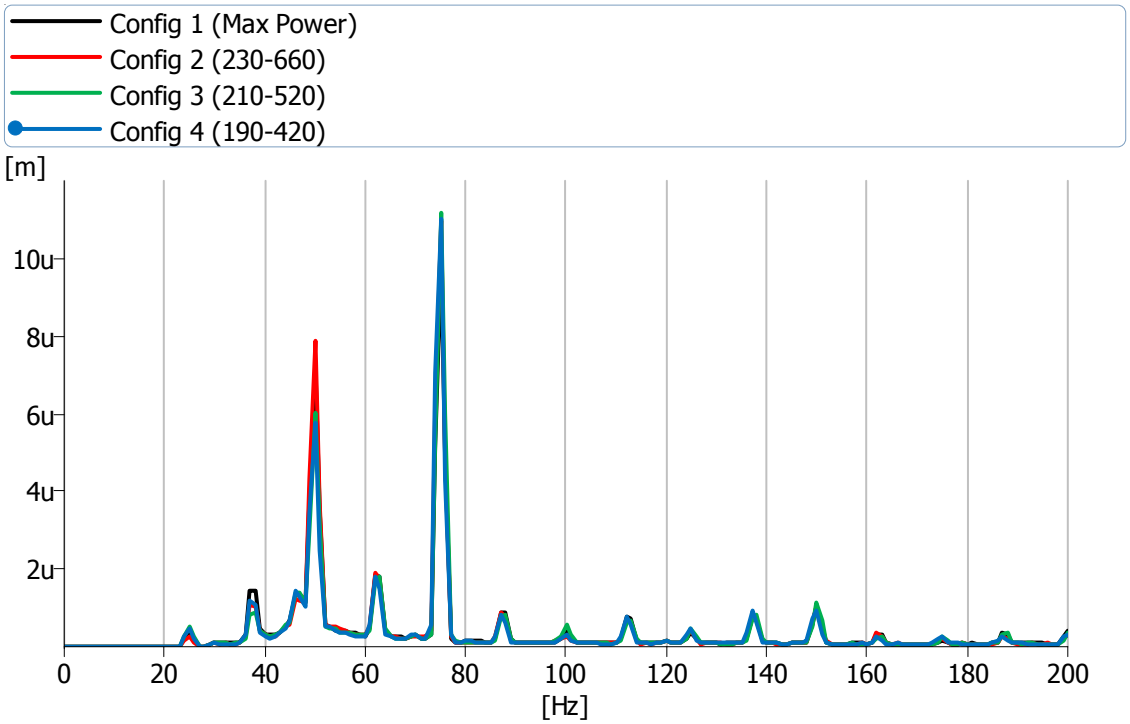

Engine Mount LR, 1500, 15%

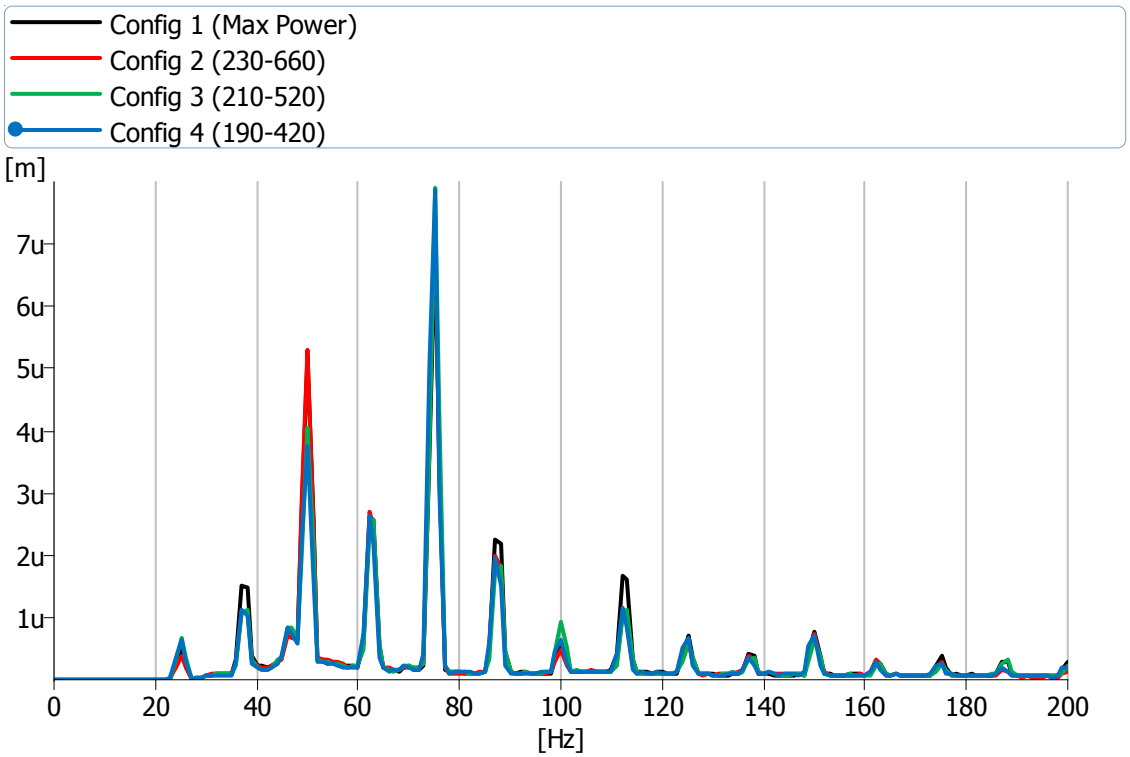

Engine Mount RF, 1500, 15%

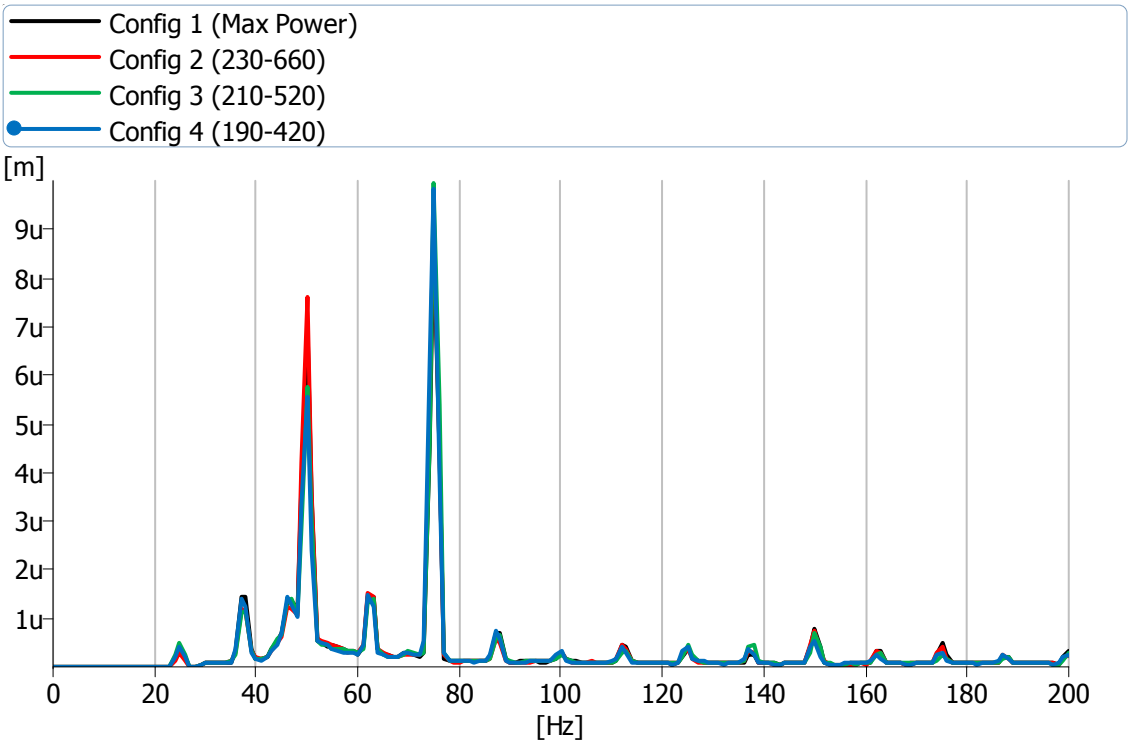

Engine Mount RR, 1500, 15%

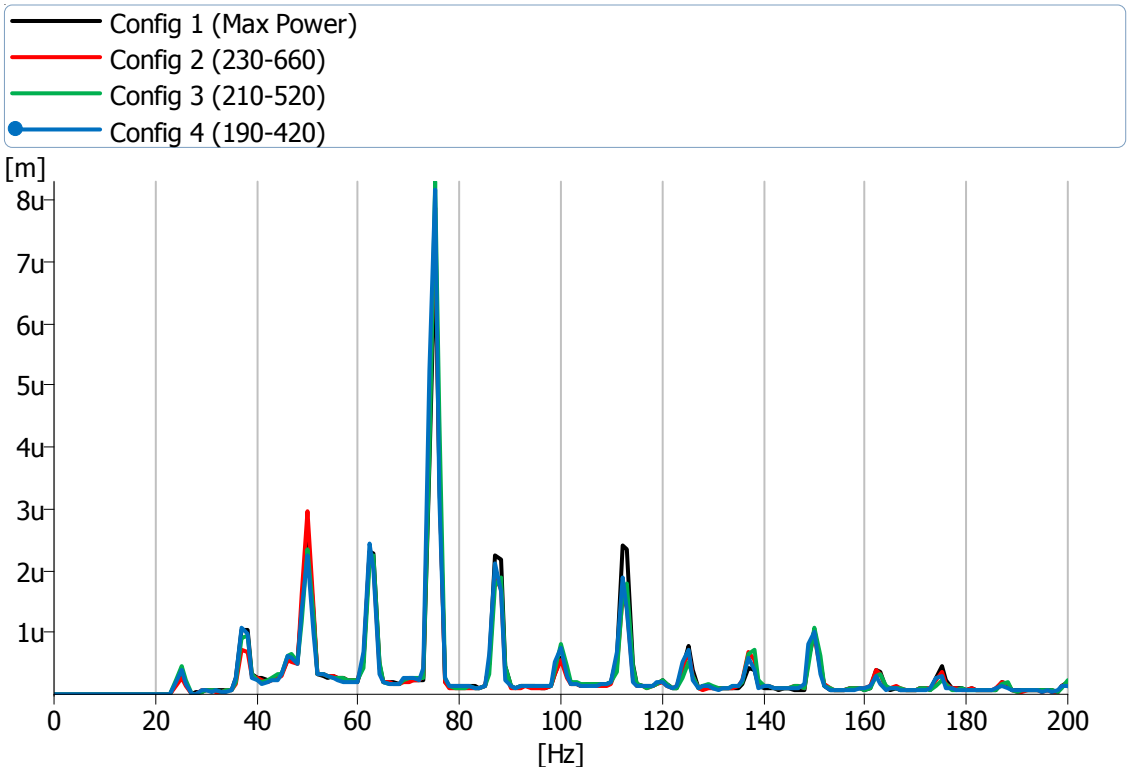

Engine Mount LF, 1500, 50%

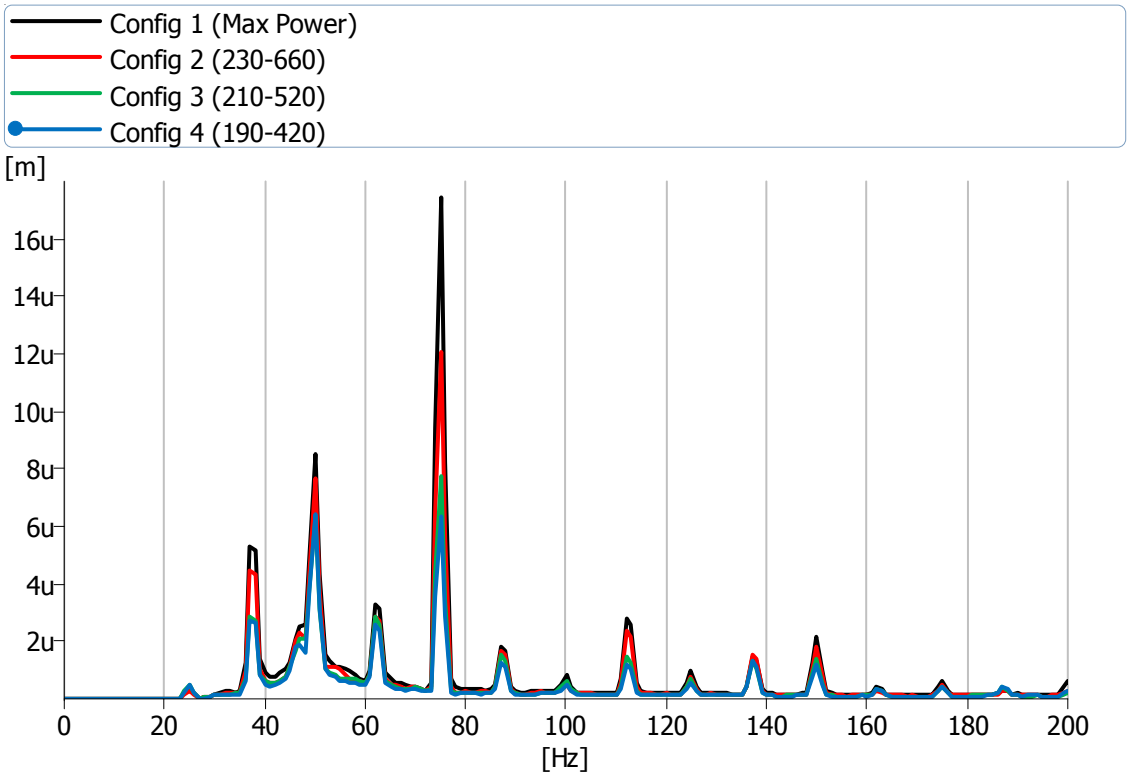

Engine Mount LR, 1500, 50%

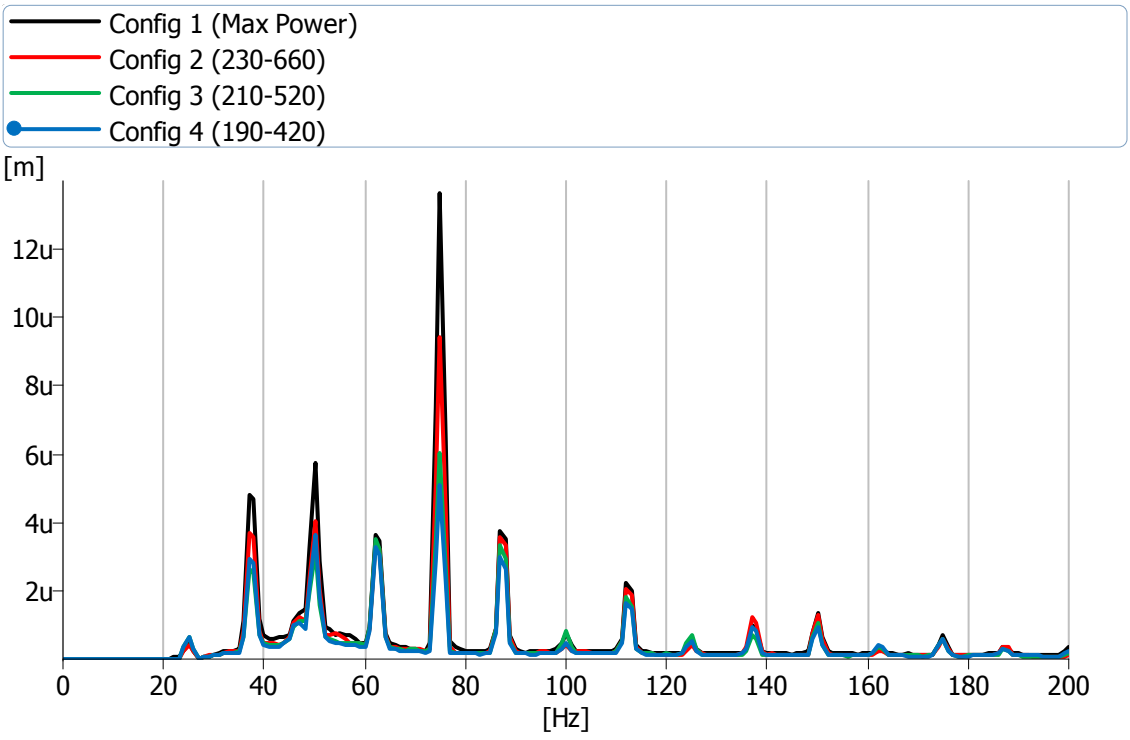

Engine Mount RF, 1500, 50%

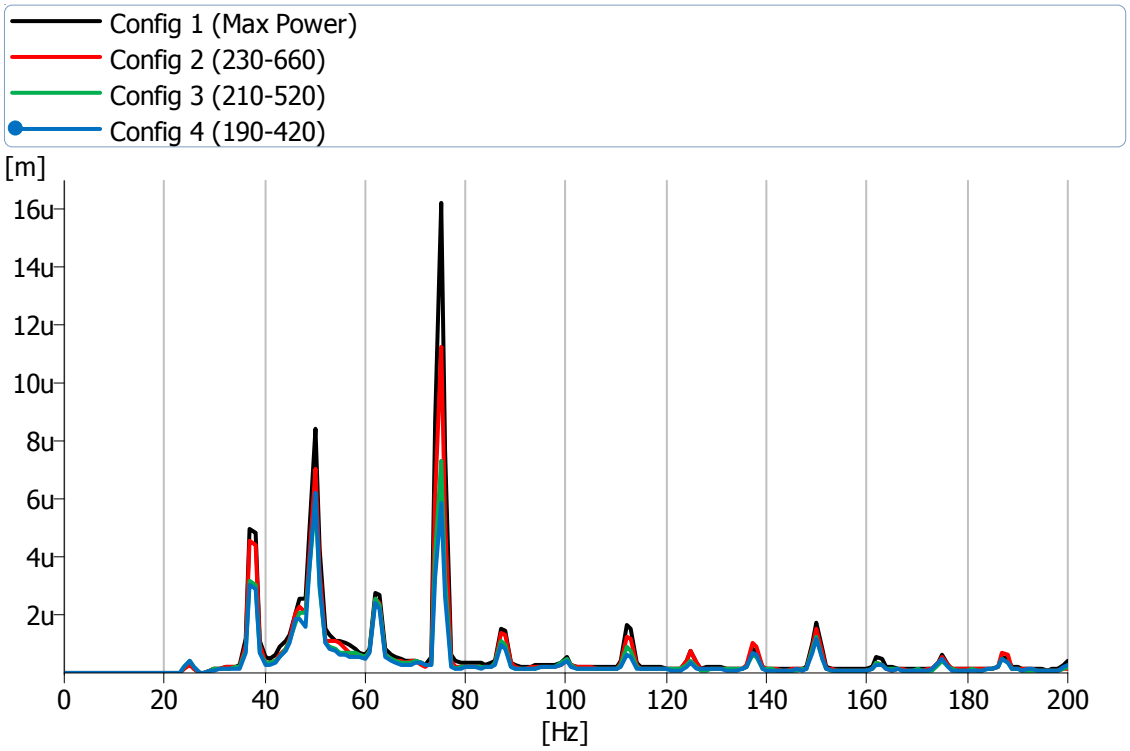

Engine Mount RR, 1500, 50%

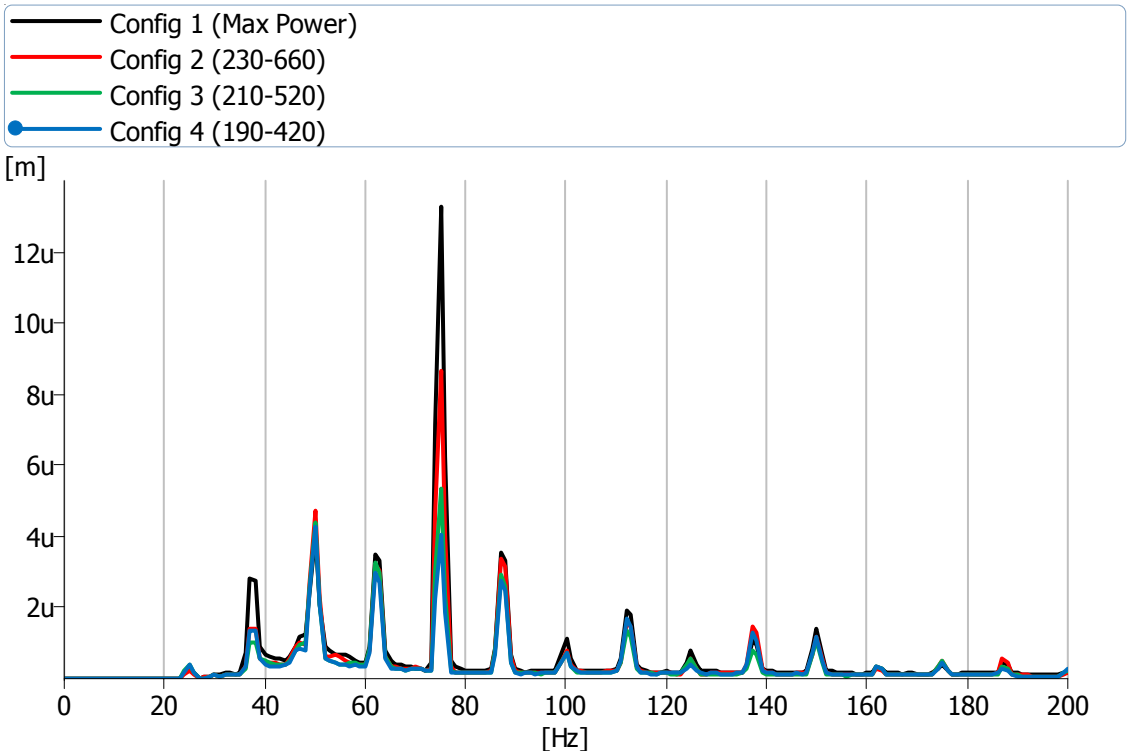

Engine Mount LF, 1500, 100%

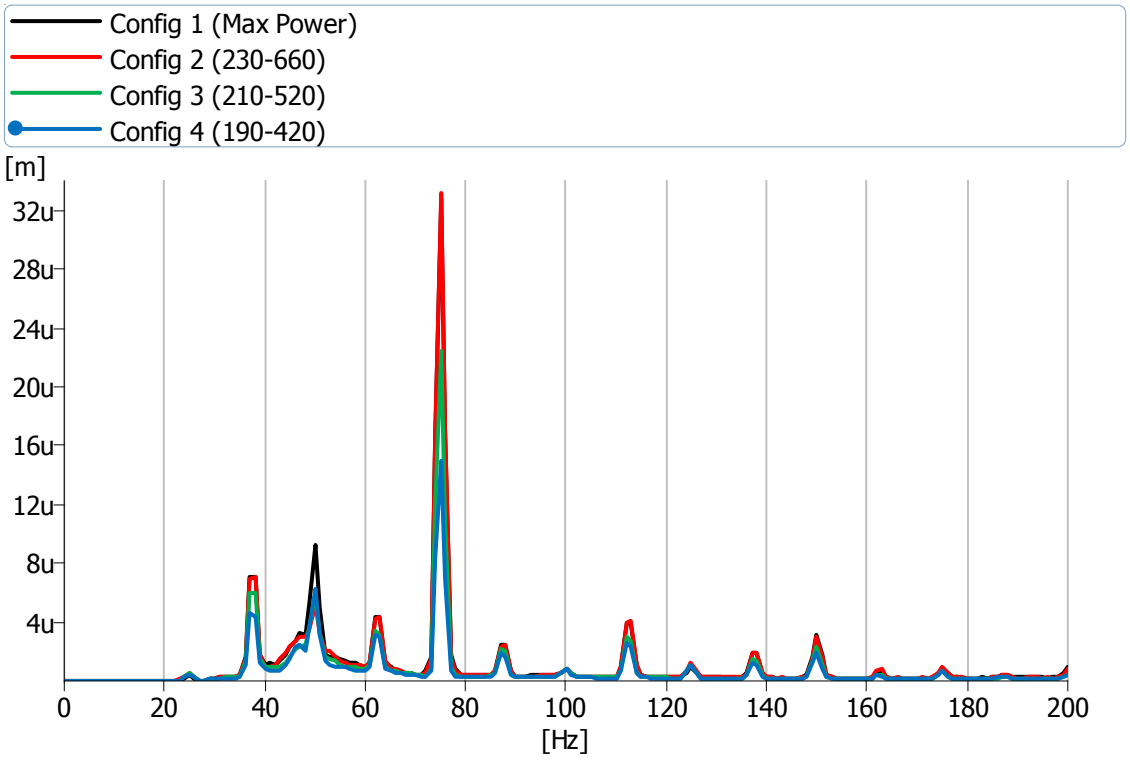

Engine Mount LR, 1500, 100%

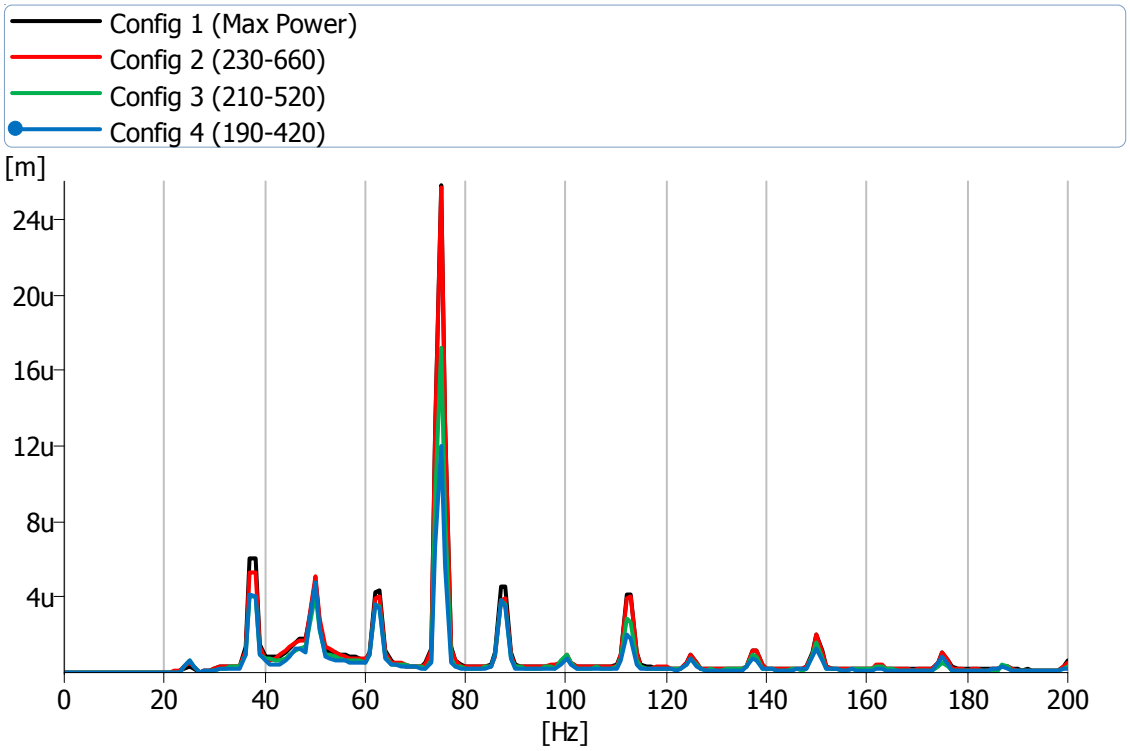

Engine Mount RF, 1500, 100%

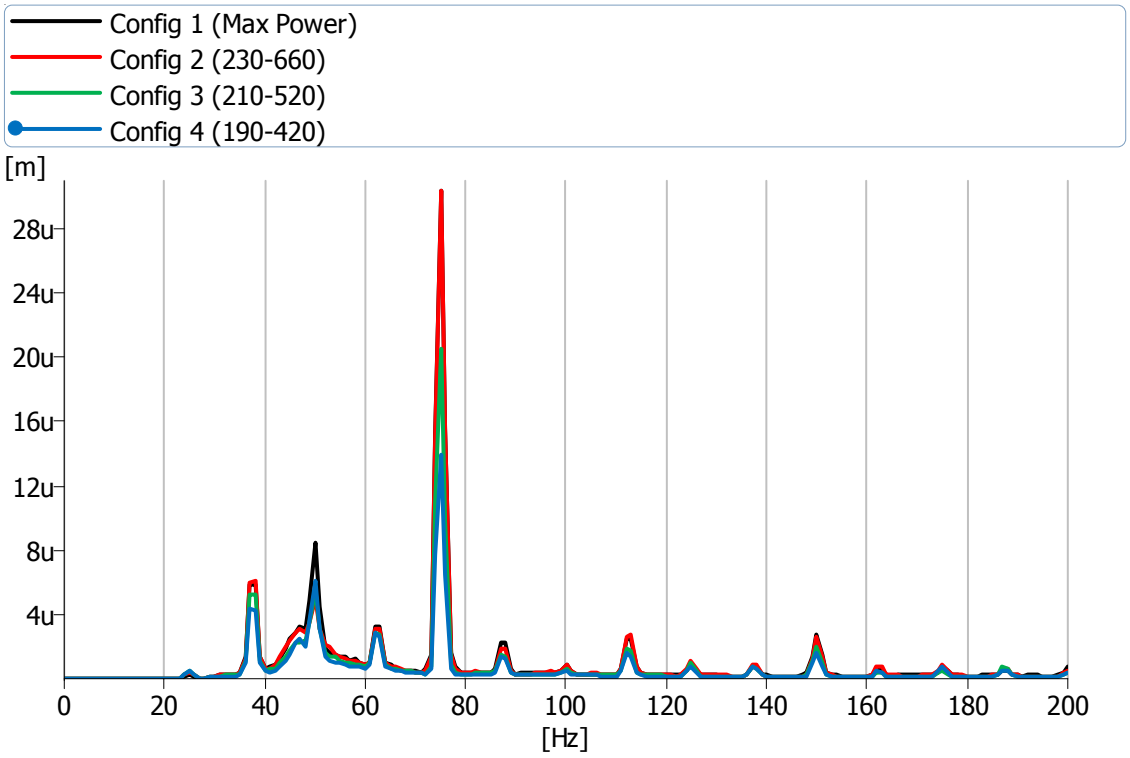

Engine Mount RR, 1500, 100%

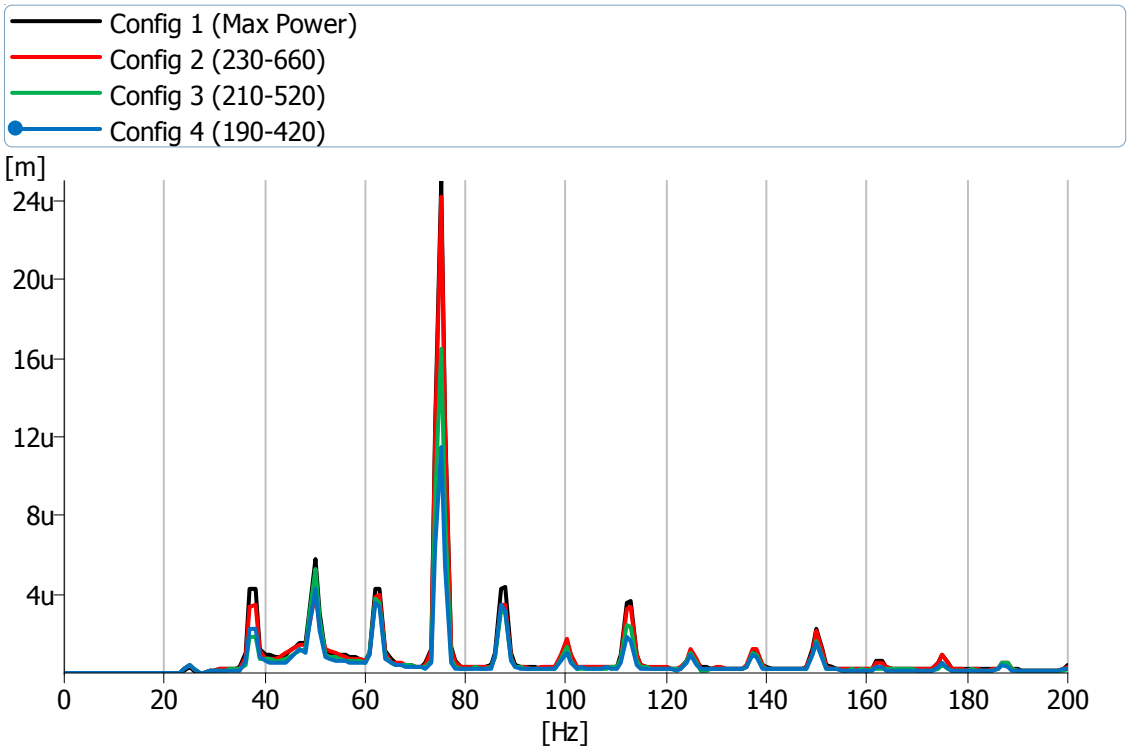

Appendix J: Mount Vibration vs Cylinder Pressure

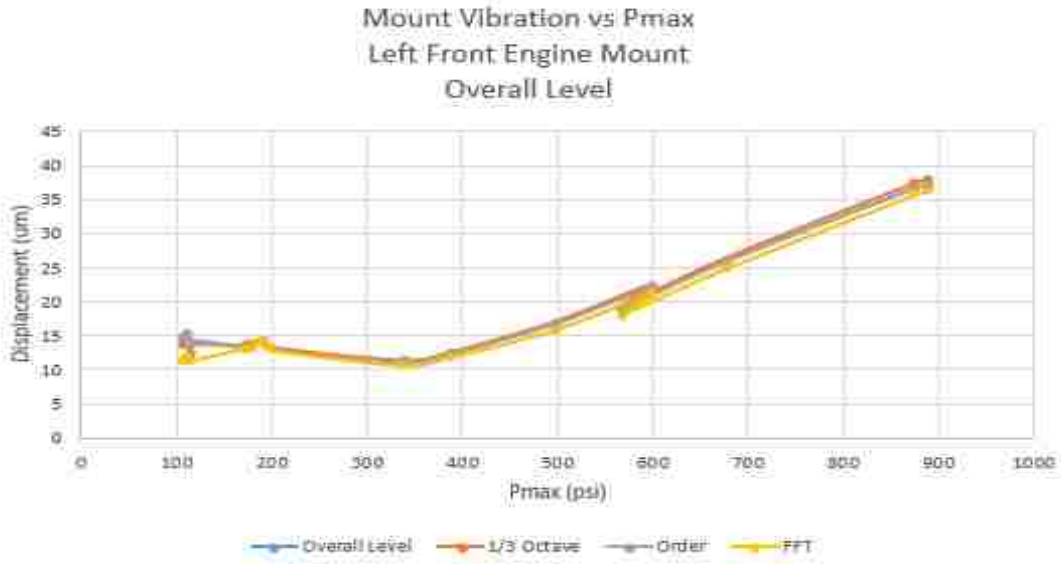

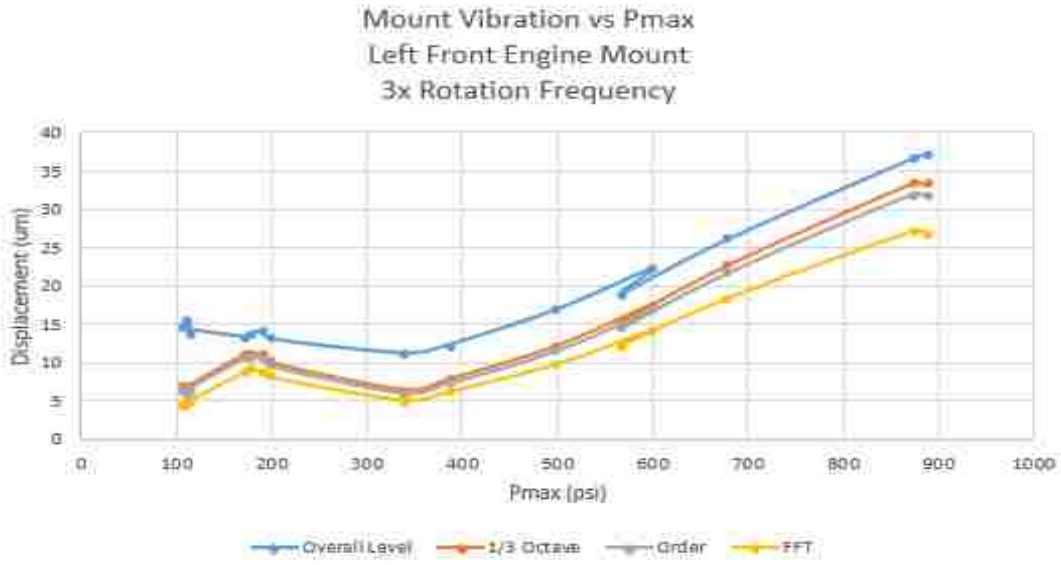

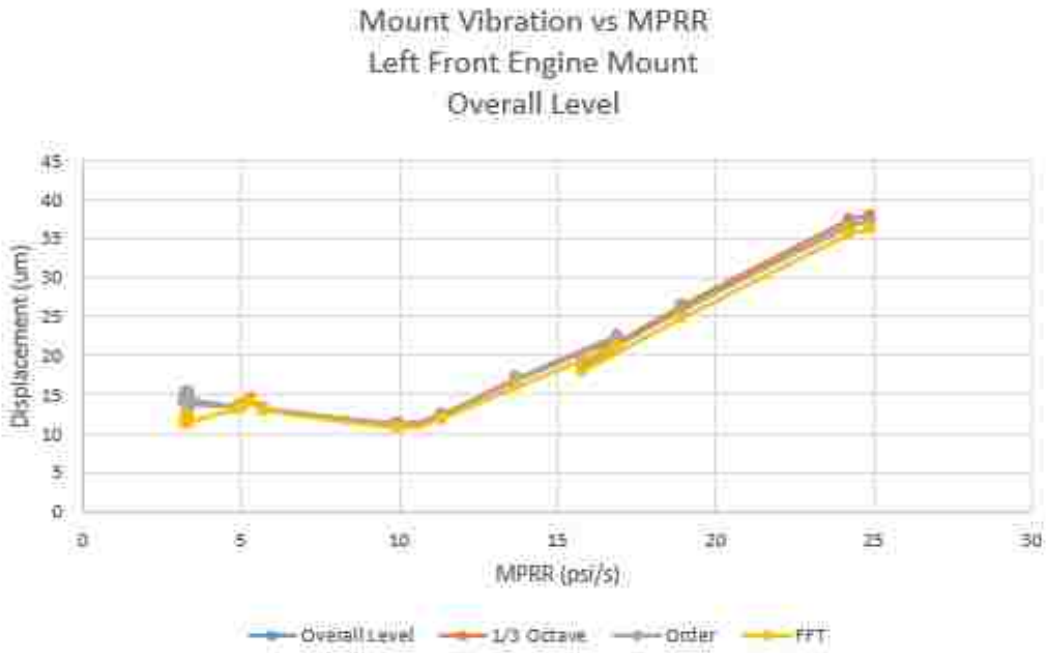
Mount Vibration vs MPRR
Left Front Engine Mount
Overall Level
Displacement (um)
MPRR (psi/s)
Overall Level
1/3 Octave
Order
FFT

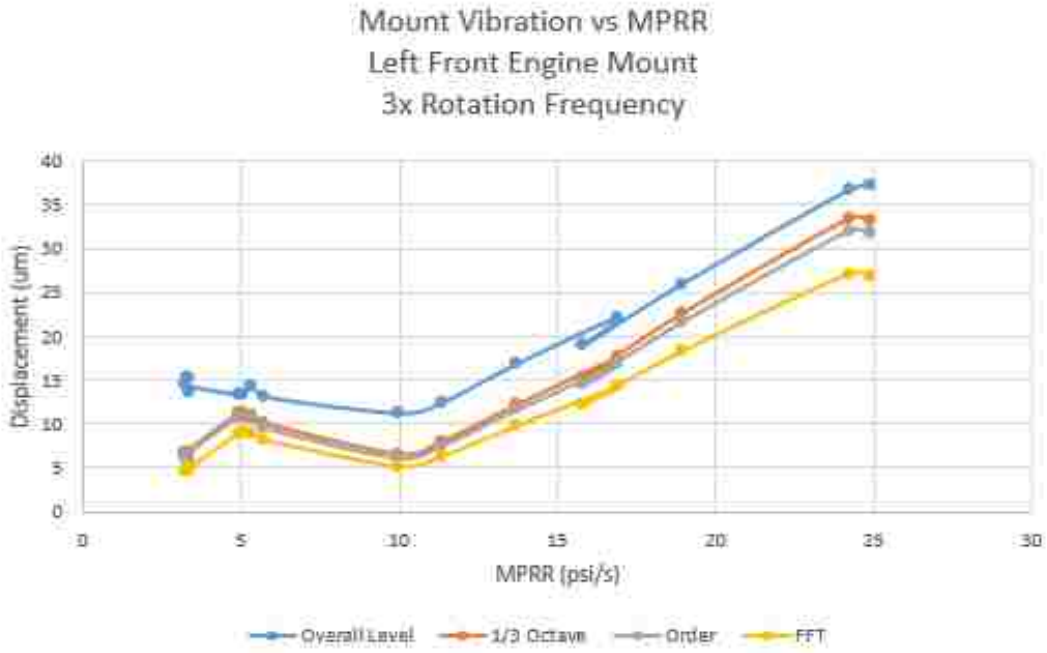
Mount Vibration vs MPRR
Left Front Engine Mount
3x Rotation Frequency
Displacement (um)
MPRR (psi/s)
Overall Level
1/3 Octave
Order
FFT

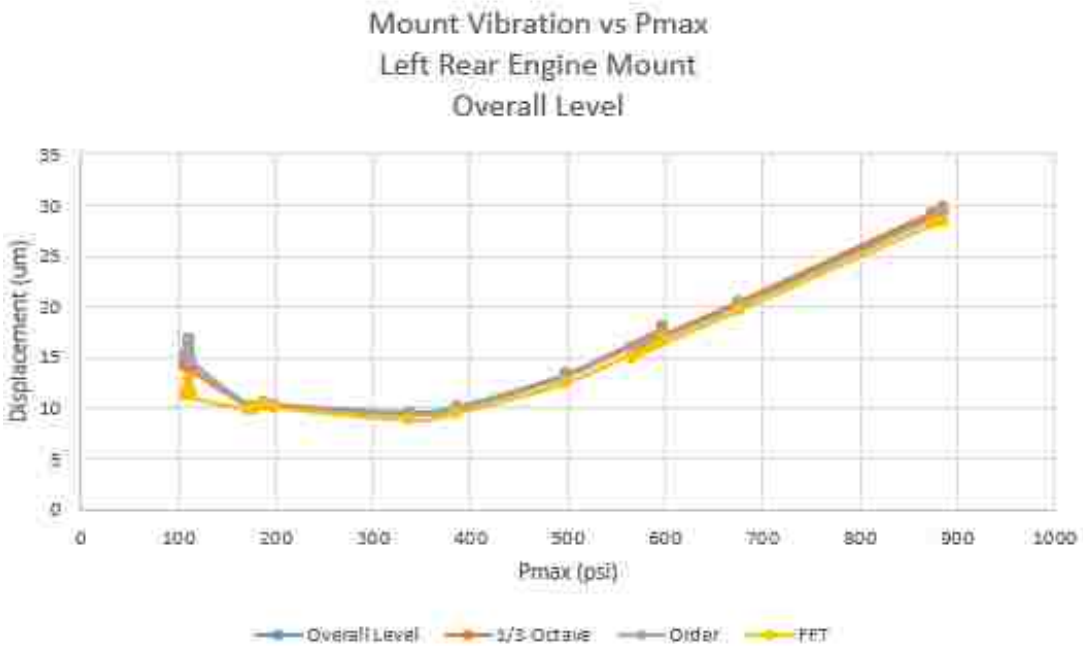
Mount Vibration vs Pmax
Left Rear Engine Mount
Overall Level
Displacement (um)
Pmax (psi)
Overall Level
1/3 Octave
Order
FFT

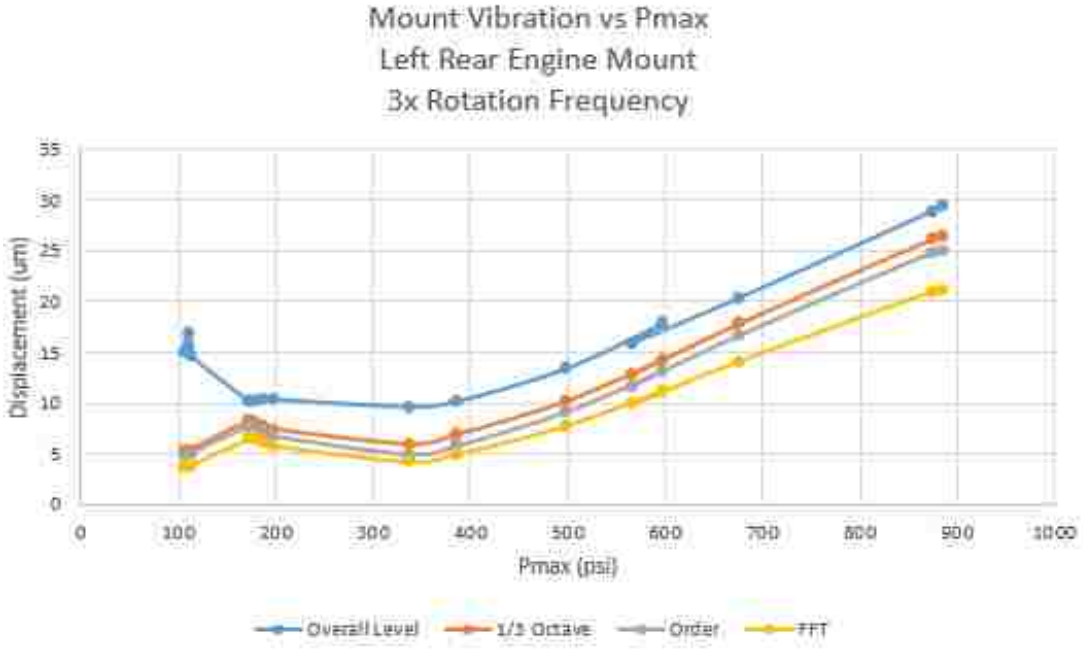
Mount Vibration vs Pmax
Left Rear Engine Mount
3x Rotation Frequency
Displacement (um)
Pmax (psi)
Overall Level
1/3 Octave
Order
FFT

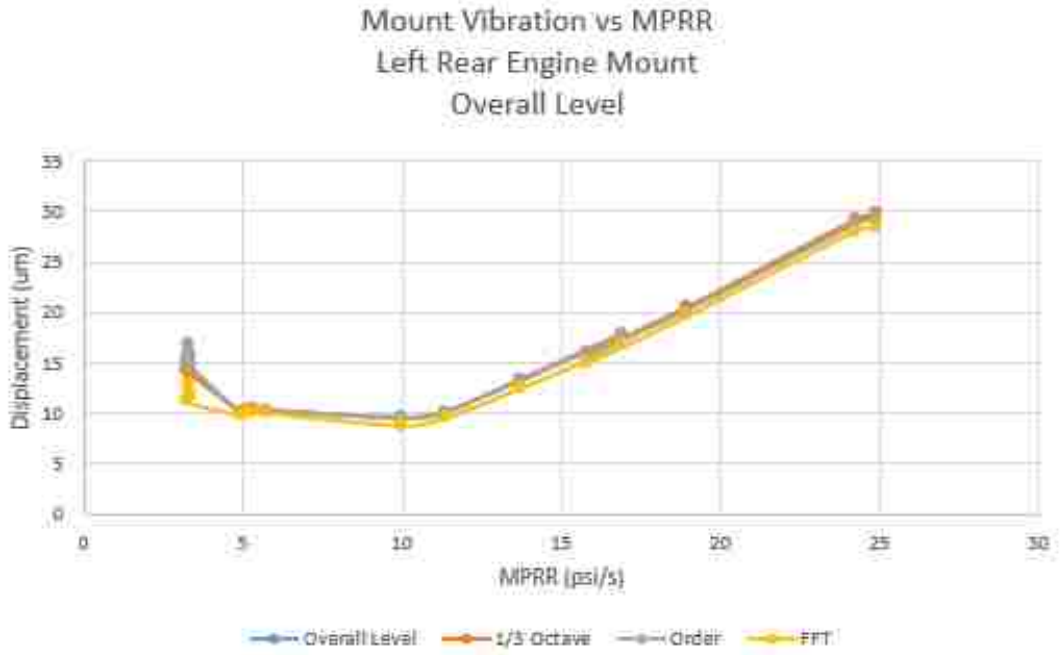
Mount Vibration vs MPRR
Left Rear Engine Mount
Overall Level
Displacement (um)
MPRR (psi/s)
Overall Level
1/3 Octave
Order
FFT

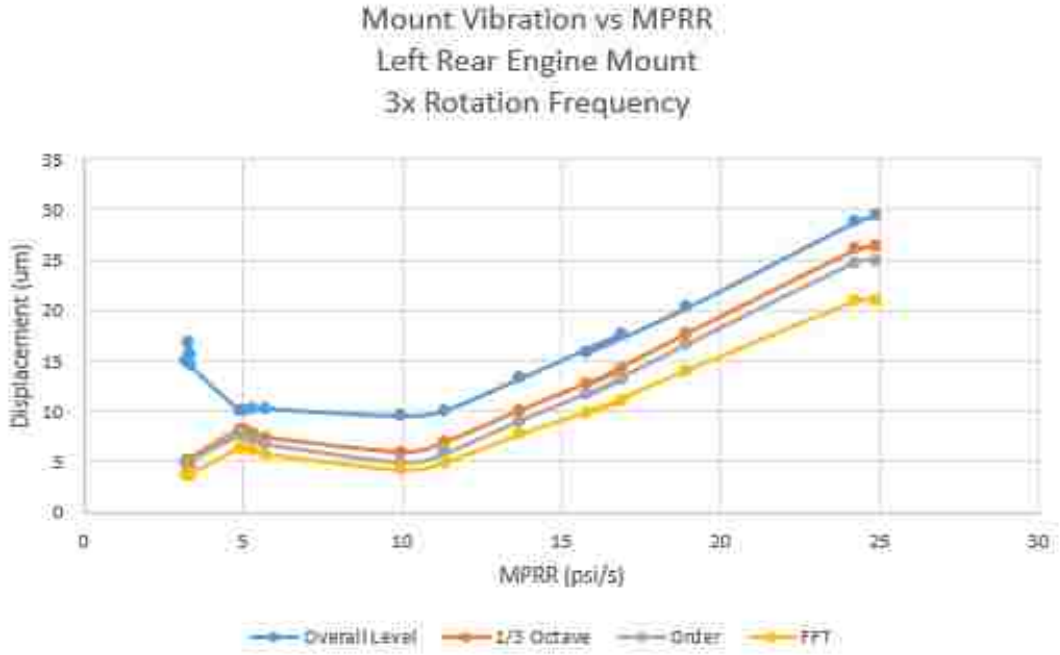
Mount Vibration vs MPRR
Left Rear Engine Mount
3x Rotation Frequency
Displacement (um)
MPRR (psi/s)
Overall Level
1/3 Octave
Order
FFT

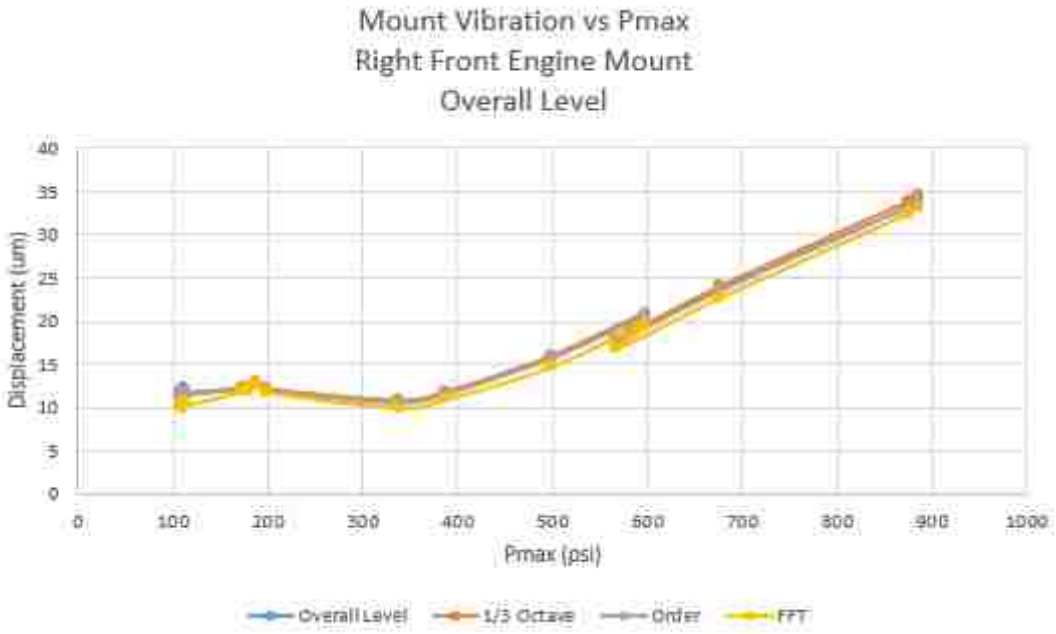
Mount Vibration vs Pmax
Right Front Engine Mount
Overall Level
Displacement (um)
Pmax (psi)
Overall Level
1/3 Octave
Order
FFT

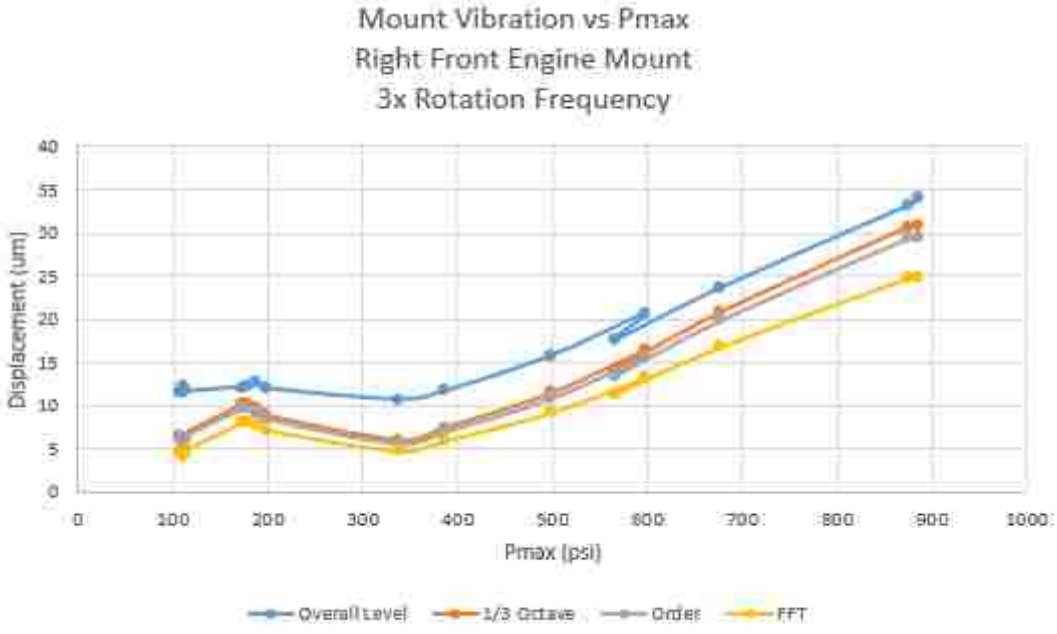
Mount Vibration vs Pmax
Right Front Engine Mount
3x Rotation Frequency
Displacement (um)
Pmax (psi)
Overall Level
1/3 Octave
Order
FFT

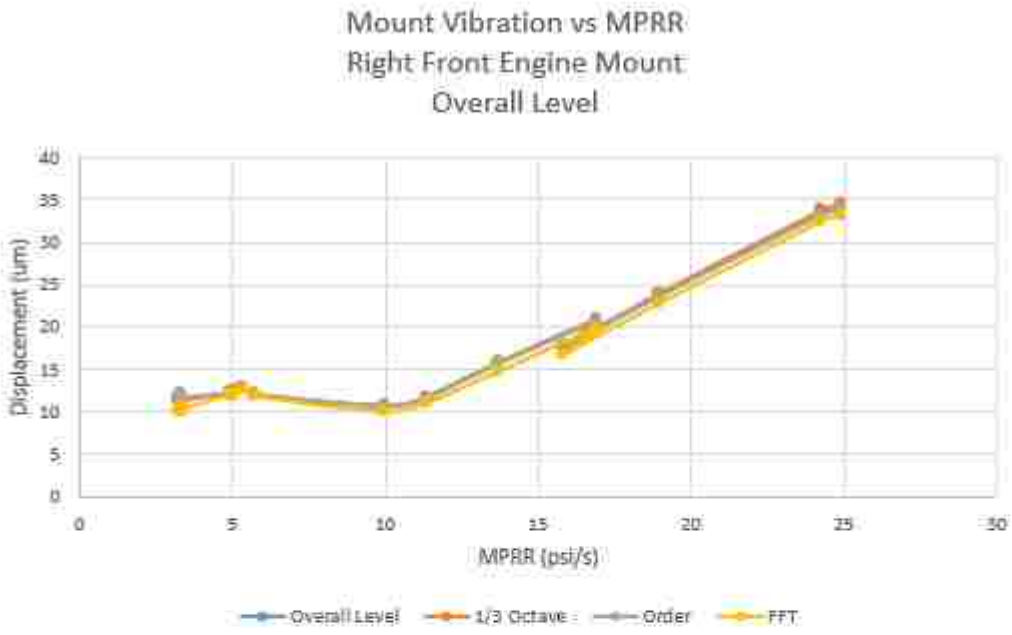
Mount Vibration vs MPRR
Right Front Engine Mount
Overall Level
Displacement (um)
MPRR (psi/s)
Overall Level
1/3 Octave
Order
FFT

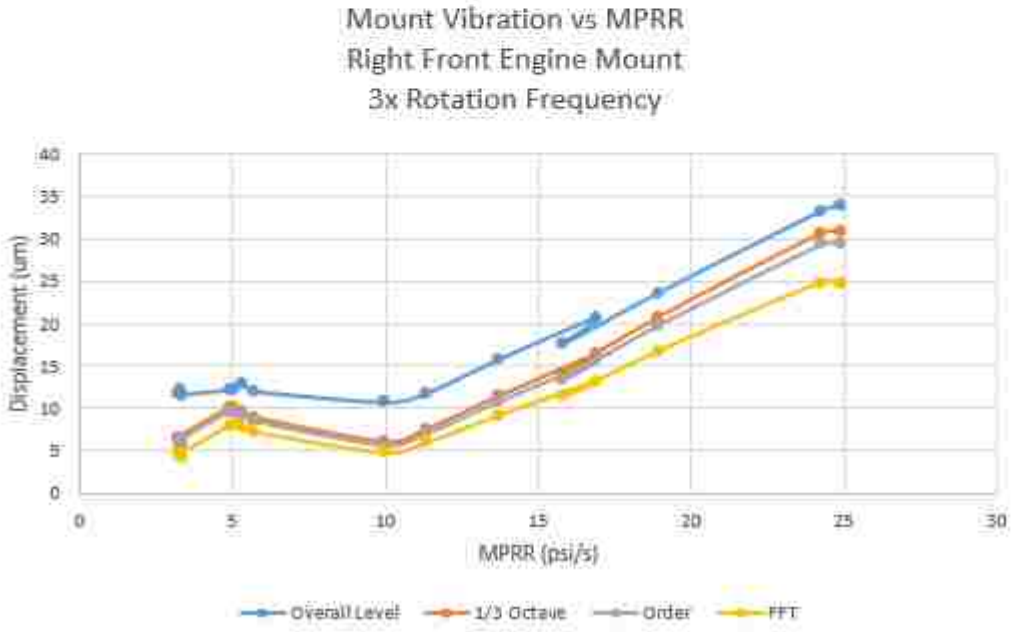
Mount Vibration vs MPRR
Right Front Engine Mount
3x Rotation Frequency
Displacement (um)
MPRR (psi/s)
Overall Level
1/3 Octave
Order
FFT

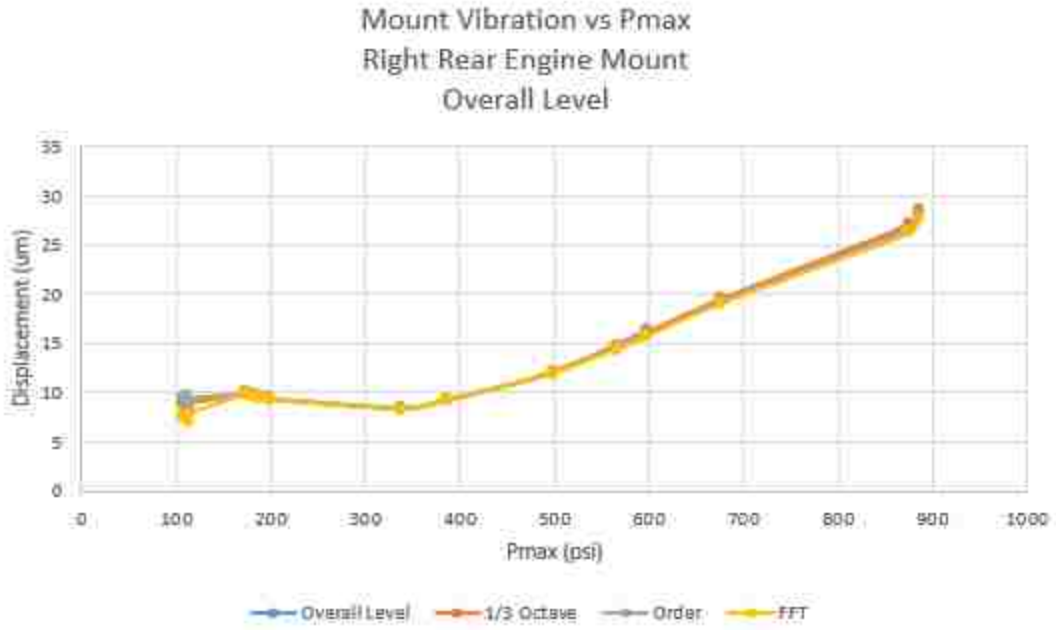
Mount Vibration vs Pmax
Right Rear Engine Mount
Overall Level
Displacement (um)
Pmax (psi)
Overall Level
1/3 Octave
Order
FFT

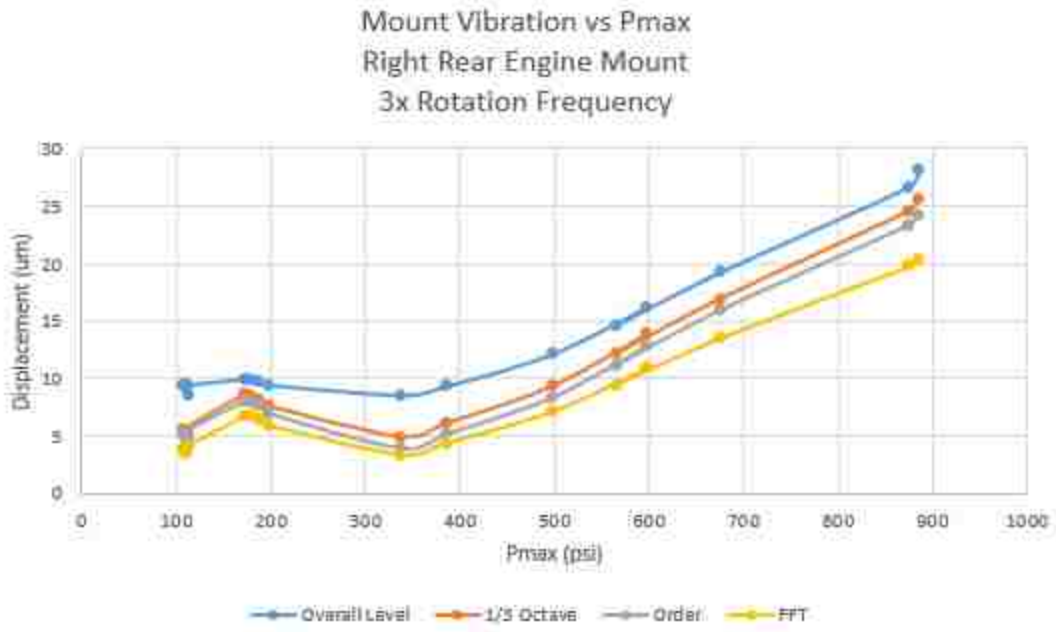
Mount Vibration vs Pmax
Right Rear Engine Mount
3x Rotation Frequency
Displacement (um)
Pmax (psi)
Overall Level
1/3 Octave
Order
FFT

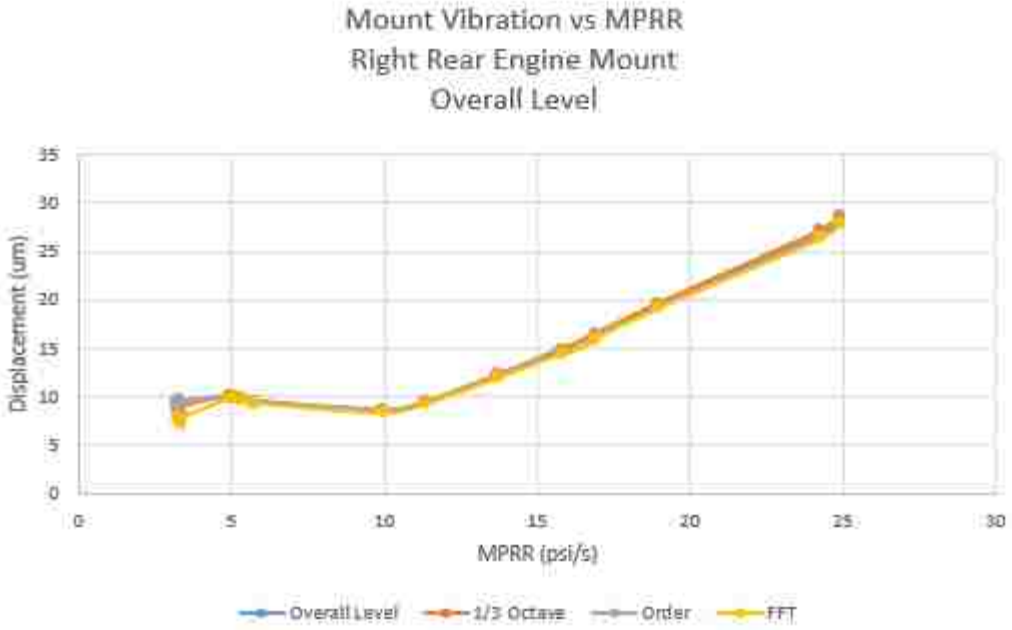
Mount Vibration vs MPRR
Right Rear Engine Mount
Overall Level
Displacement (um)
MPRR (psi/s)
Overall Level
1/3 Octave
Order
FFT

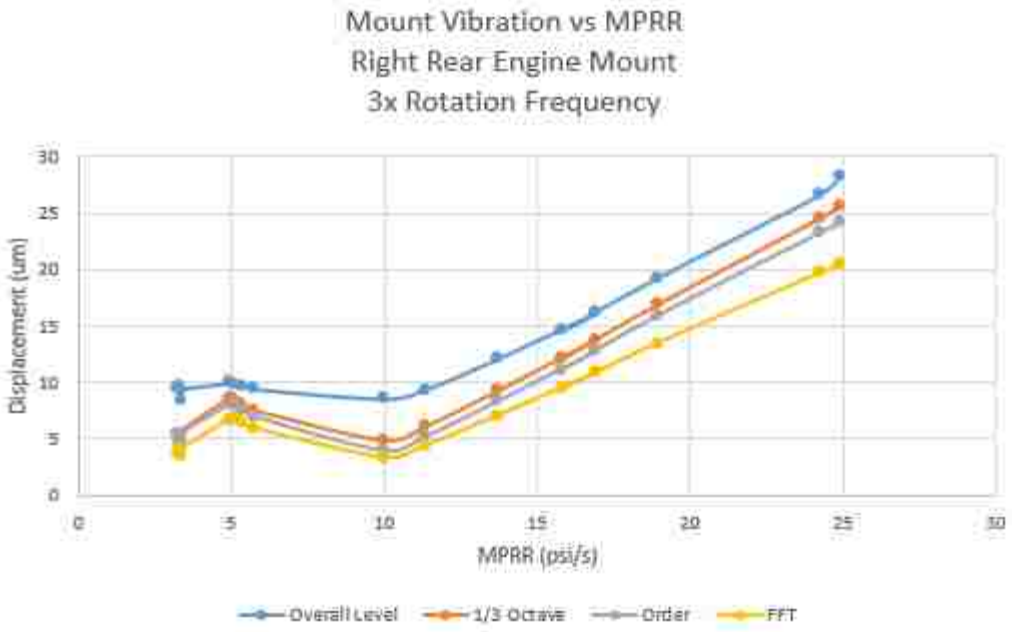
Mount Vibration vs MPRR
Right Rear Engine Mount
3x Rotation Frequency
Displacement (um)
MPRR (psi/s)
Overall Level
1/3 Octave
Order
FFT

VITA AUCTORIS

NAME:	Scott Hunt
PLACE OF BIRTH:	Santa Clara, California, USA
YEAR OF BIRTH:	1976
EDUCATION:	Center Grove High School, Greenwood, IN, 1994
	Purdue University, B.Sc., West Lafayette, IN, 1999
	University of Windsor, M.Sc., Candidate, Windsor, ON, 2016